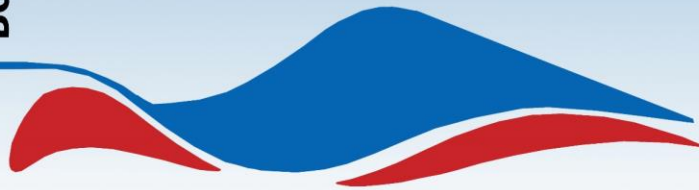


Bologna, 9-13 September, 2024

30th EWG-IE & 5th EWG-OOE Meetings



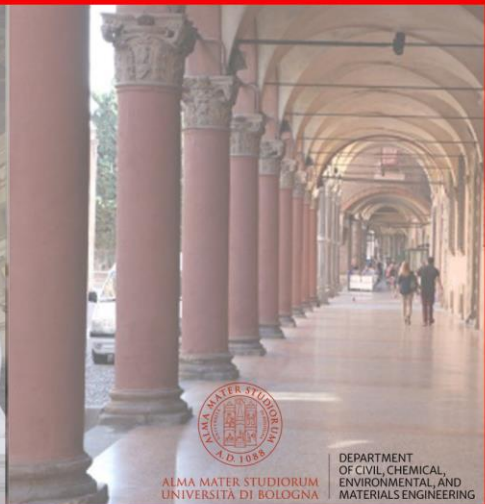
Book of Abstracts

30th Meeting of the European Working Group on
Internal Erosion in Embankment Dams, Levees and Dikes, and
their Foundations

5th Meeting of the European Working Group on
Overflow and Overtopping Erosion



Hercolani Palace, Bologna



ALMA MATER STUDIORUM
UNIVERSITÀ DI BOLOGNA

DEPARTMENT
OF CIVIL, CHEMICAL,
ENVIRONMENTAL, AND
MATERIALS ENGINEERING

This *Book of Abstracts* was printed by the University of Bologna, Italy

The information contained in this publication regarding commercial projects or firms may not be used for advertising or promotional purposes and may not be construed as an endorsement of any product or firm by the organizing committee of the 30th Meeting of the European Working Group on Internal Erosion in Embankment Dams, Levees and Dikes, and their Foundations (EWG-IE) and of the 5th Meeting of the European Working Group on Overflow and Overtopping Erosion (EWG-OOE). The Organizing Committee does not accept any responsibility for the statements made or the opinions expressed in this publication.

Book of Abstracts of the 30th Meeting of the European Working Group on Internal Erosion in Embankment Dams, Levees and Dikes, and their Foundations and of the 5th Meeting of the European Working Group on Overflow and Overtopping Erosion

Editors

Laura Tonni

Department of Civil,
Chemical,
Environmental and
Materials Engineering
University of Bologna
Bologna, Italy

Stéphane Bonelli

UMR RECOVER,
INRAE-Aix-Marseille
University
Aix-en-Provence, France

Jean-Robert Courivaud

EDF-CIH, Centre
d'Ingénierie Hydraulique
La Motte Servolex,
France

Michela Marchi

Department of Civil,
Chemical,
Environmental and
Materials Engineering
University of Bologna
Bologna, Italy

Graphic design layout

Ilaria Bertolini and Elena Dodaro

Department of Civil, Chemical, Environmental and Materials Engineering, University of Bologna, Italy

Arrangement of the printed text

Ilaria Bertolini, Elena Dodaro, Emanuele Tumedei and Luca Vignali

Department of Civil, Chemical, Environmental and Materials Engineering, University of Bologna, Italy

Scientific Committee of the 30th EWG-IE Meeting

Stéphane Bonelli, France (*Chair*)

Vera Van Beek, the Netherlands

Rodney Bridle, UK

Jonathan Fannin, Canada

Guido Gottardi, Italy

Henk van Hemert, the Netherlands

Michela Marchi, Italy

Didier Marot, France

Catherine O' Sullivan, United Kingdom

Jaromir Riha, Czech Republic

Bryant Robbins, United States

Alexander Scheuermann, Australia

Akihiro Takahashi, Japan

Laura Tonni, Italy

Eric Vincens, France

Scientific Committee of the 5th EWG-OOE Meeting

Jean-Robert Courivaud, France (*Chair*)

Benoît Blancher, France

Stéphane Bonelli, France

Myron van Damme, The Netherlands

Mike George, United States

Michela Marchi, Italy

Rafael Moran, Spain

Mark Morris, United Kingdom

Laura Tonni, Italy

Miguel Angel Toledo, Spain

Éric Vincens, France

Local Organizing Committee

Prof. Laura Tonni (Chair)

Prof. Michela Marchi (Co-Chair)

Prof. Guido Gottardi

Dr. Ilaria Bertolini

Dr. Elena Dodaro

Eng. Luca Vignali

Eng. Emanuele Tumedei



ALMA MATER STUDIORUM
UNIVERSITÀ DI BOLOGNA

DEPARTMENT
OF CIVIL, CHEMICAL,
ENVIRONMENTAL, AND
MATERIALS ENGINEERING



The event is organized under the auspices of



Silver sponsor



Table of Contents

30th EWG-IE Meeting

SESSION 1, PART 1: LABORATORY TESTING AND PHYSICAL MODELLING

Small-scale tests on a semi-permeable barrier against backward erosion piping.....	1
<i>S. Bersan, A. Van der Brug, R. Servais, V. van Beek</i>	
Prediction of the critical secant gradient function	4
<i>B.A. Robbins</i>	
Representative grain diameter in backward erosion.....	7
<i>S. Ramezanifouladi, J. Côté</i>	
Experimental study on the process behaviour of backward erosion piping in levee and dam foundations.....	10
<i>M. Wewer, J. Stamm, J.P. Aguilar-López</i>	

SESSION 1, PART 2: LABORATORY TESTING AND PHYSICAL MODELLING

Sand erodibility at backward erosion piping	13
<i>J. Riha, L. Petruła</i>	
Backward erosion piping with point outflow and semi-permeable polder blankets: experiments, modelling and research program	16
<i>J. Pol, V. Van Beek, H. Van Hemert, K. Dorst, M. Hijma, R. Koopmans, E. Rosenbrand</i>	
Disaggregation susceptibility of clayey silt mixture subjected to drying-wetting cycles observed by automated crumb test.....	19
<i>D. Ayssami, C. Chevalier, Y. Boussafir, S. Hemmati, P. Reiffsteck</i>	
Comprehensive study of suction bucket foundations and the associated risk of piping.....	22
<i>A. Farhat, L.-H. Luu, A. Doghmane, P. Cuéllar, P. Philippe</i>	
Stress-controlled suffusion testing of crushed dam material.....	25
<i>E. Bergliv, J. Laue, P. Viklander</i>	

SESSION 1, PART 3: LABORATORY TESTING AND PHYSICAL MODELLING

Onset of internal instability in gap-graded BSM sands.....	28
<i>S. Ataii, J. Fannin</i>	
Experimental assessment of the mechanical stability of erodible soils injected with fines.....	31
<i>A. Hegde, N. Benahmed, A. Wautier, P. Philippe, A. Doghmane</i>	
Effects of initial fines content and repeated seepage on suffusion-induced heterogeneity in gap-graded soils.....	34
<i>S. Ruangchai, A. Takahashi</i>	
Study of development of internal erosion by use of transparent materials.....	37
<i>S. Aulestia, P. Viklander, J. Toromanovic, J. Laue</i>	

SESSION 2, PART 1: INTERNAL EROSION MECHANISMS AND MODELLING

Injecting fine grains into 3D spherical packing-numerical and experimental implications	40
<i>F. Chen, A. Hegde, A. Wautier, N. Benahmed, P. Philippe</i>	
Filtration in granular materials: anisotropy induced effects due to ellipsoidal filter particle shapes	43
<i>A. Abdallah, E. Vincens, H. Magoariec, C. Picault</i>	
Impact of stress path on fabric evolution and erodibility of fine particles in gap-graded granular soils.....	46
<i>R. Dhamne, M. Disfani</i>	
Analysis of particle migration phenomena. Micro-mechanical modelling and interpretation of lab tests	49
<i>F. Federico, C. Cesali</i>	

SESSION 2, PART 2: INTERNAL EROSION MECHANISMS AND MODELLING

Numerical analysis of bearing capacity factors for uplift mechanism.....	52
<i>F. Pilati, F. Gabrieli, F. Zarattini</i>	
On the identification of the saturation line in the earthen levees: a comparison between a physically-based model and a practical approach	55
<i>B. Bonaccorsi, S. Barbetta, T. Moramarco, G.T. Aronica</i>	
Conclusions from the performance assessment of industry applicable IE initiated breach prediction models	58
<i>M.W. Morris, J.-R. Courivaud</i>	
Numerical modeling of internal erosion in the foundation of Agly river dikes (France).....	60
<i>S. Bonelli, L. Girolami</i>	
Numerical simulation of erosion mechanisms in Agly dike.....	63
<i>Z. Deng, S. Bonelli, L. Girolami, N. Benahmed, P. Philippe, G. Wang</i>	

SESSION 3, PART 1: MONITORING AND FIELD CASES

Detection of the paleo-environment of a diked river: implications for the erosion of foundation soils.....	66
<i>L. Girolami, E.J. Fogueng-Wafo, S. Bonelli, J.-M. Carozza, C. Camerlynck</i>	
Underseepage analysis on the Szigetköz floodplain area	69
<i>E. Koch, R. Ray, M. Maller, G. Bartal, M. Mayassah</i>	
Internal erosion within CNR earth structures: a review of field cases on the Rhône River from the 1950's to the present.....	72
<i>F. Seblany, R. Fellag, H. Chapuis, C. Picault, R. Béguin, C. Guidoux</i>	
On the triggering mechanism and evolution of concentrated erosion causing the failure of the levee of Panaro River (Italy) on the 6 th december 2020.....	75
<i>F. Ceccato, P. Simonini</i>	
A forward simulation and data driven approach in fusing geophysical data for subsurface characterization.	78
<i>C. Bremmer, J. King, E. Obando Hernandez, E. Leentvaar, J. van Engelen, A. Wiersma, M. Karaoulis</i>	
Analysis of case studies of canal embankment failures.....	81
<i>J.R. Courivaud, O. Bory, A. Vogel, K. Jarecka</i>	

SESSION 3, PART 2: MONITORING AND FIELD CASES

Commissioning of the world's first Fibre Optics monitoring system installed along a flood protection dike, in the Arles region, France: first data and setting up of the detection thresholds..... 84
C. Guidoux, R. Béguin, M. Boucher, P. Pinettes, J.-R. Courivaud, L. Salvan, T. Mallet

Thermal and mechanical resistance mapping of a hydraulic structure: detection and quantification of an internal flow before, during and after reinforcement work 87
M. Boucher, P. Pinettes, J.-R. Courivaud

FIBRADIKE project: preliminary test results 90
A. Höttges, C. Rabaiotti, A. Rosso

Internal erosion identification and quantification using vadose zone monitoring technologies..... 93
A. Ran

SESSION 4: RISK ASSESSMENT AND MANAGEMENT

Evaluation of the decision support framework on backward erosion piping 96
V. van Beek, B. Robbins, L. van der Linde, W. Kanning, E. Rosenbrand, T. O'Leary, A. Hill, H. Knoeff, H. van Hemert

Towards fragility curves: the case of Adige River levees 99
V. Mangraviti, L. Pinter, N. Fabbian, S. Cola

Updated "Piping Toolbox" – significant changes to concentrated leak erosion methodology in vertical cracks and impacts on practice 102
T.M. O'Leary

Lessons learnt for safety analysis from internal erosion accidents and incidents on embankment dams, based on a 3000 documents database.....105
N. Lebrun, J.-R. Courivaud, A. Vogel

USACE levee internal erosion incidents and failures..... 108
T.M. O'Leary, D.M. Schaaf

30th EWG-IE & 5th EWG-OOE Meetings - Common Session

Emergency reconstruction and safety enhancement project for the Idice torrent embankment breach 111
D. Mingozzi, M. Bentini, R. Paciolla, S. Tozzi, A. Zamagni, S. Saccà (ENSER srl, Italy)

A novel medium-scale experimental setup to investigate backward erosion piping..... 117
E. Dodaro, E. Tumedei, M. Marchi, G. Gottardi, L. Tonni

5th EWG-OOE Meeting

SESSION 1, PART 1: CASE STUDIES AND BREACH MODELLING

Climate change and embankment dam overtopping: lessons from the Libyan dam disaster in September 2023	120
<i>N. Kafashan, M. Aufleger</i>	
Estimation of breach hydrograph resulting from dam embankment failure due to internal erosion or overtopping: comparison of simplified methods with real-case break data and recommendations	123
<i>L. Del Gatto, Y. El Badaoui, J.-R. Courivaud</i>	
USACE levee overtopping incidents and failures	126
<i>T.M. O'Leary, D.M. Schaaf</i>	
Two historical cases of dam overtopping in the Czech Republic	129
<i>J. Riha, S. Kotaska</i>	
Testing empirical criteria for breach geometry estimation to recent embankment failure datasets	132
<i>A. Domeneghetti, M. Vaccari, I. Bertolini, M. Marchi</i>	

SESSION 2: REHABILITATION & STRENGTHENING METHODS

High pressure jet testing on soil-cement	135
<i>D. Zumofen</i>	
Lime treatment for erosion resistant levees in Belgium	138
<i>K. Verelst, F. Bertola, S. Nicaise, B. Vandevoorde</i>	
Calcium aluminate concrete - a unique protective material against erosion & cavitation damages	141
<i>D. Niepmann, A. Aboulela, C. Dowds</i>	
RCC and soil cement overtopping protection of embankments	144
<i>S. Todaro, B.A. Robbins, E. Friend, M. Dirdal</i>	

SESSION 3: EROSION DOWNSTREAM DAMS AND SPILLWAYS EROSION

Modelling of fractured rock erosion in open channels	147
<i>P. Teng, J. Gunnar I. Hellström, F. Johansson, C.-O. Nilsson</i>	

SESSION 4, PART 1: OVERFLOW AND OVERTOPPING EROSION MODELLING

The EU Interreg BONSAI project proposal	150
<i>M. van Damme, K. Verelst</i>	
Eight years of research into rockfill dams in HydroCen	153
<i>F.G. Sigtryggsdóttir</i>	

SESSION 4, PART 2: OVERFLOW AND OVERTOPPING EROSION MODELLING

The OVERCOME project: developing the Laverné field test facility	156
<i>M.W. Morris, J.-R. Courivaud, C. Picault, R. Morán</i>	
The OVERCOME project: advances in experimental research on the macro erosion of coarse-grained embankments in overflow scenarios.....	158
<i>R. Monteiro-Alves, R. Morán, M.Á. Toledo, M. Morris, J.-R. Courivaud, C. Picault</i>	
Resistance to overflow of earth-fill dams: laboratory tests and numerical modelling to characterize erosion processes.....	161
<i>H. Haddad, M. Hassan, L. Montabonnet, H. Stoter, C. Picault, M. Morris</i>	
Rhone dike overflow: comparison of field test measurements with different numerical modelling results .	164
<i>H. Umdenstock, C. Picault, F. Golay, S. Bonelli</i>	
Simulation of headcut breach dynamics using the two-dimensional depth averaged hydraulic model TELEMAC-2D	167
<i>Z. Amama, S.E. Bourban, J.-R. Courivaud, M. Morris, K. El Kadi Abderrazzak</i>	
A dataset on the breaches caused by the flood events that affected Emilia-Romagna in May 2023.....	170
<i>M. Marchi, I. Bertolini, A. Colombo, G. Gottardi, L. Morreale, T. Simonelli, L. Tonni</i>	

Small-scale tests on a semi-permeable barrier against backward erosion piping

S. Bersan¹, W.A. van der Brug², R. Servais², V.M. van Beek³

1. Hoogheemraadschap De Stichtse Rijnlanden, Houten, The Netherlands, silvia.bersan@hdsr.nl

2. Heijmans infra, Rosmalen, The Netherlands

3. Deltares, Delft, The Netherlands

ABSTRACT: SoSEAL, an injection technique inspired by the natural process of podzolisation, has been suggested as a measure against backward erosion piping in river dikes. Small-scale tests have been carried out where the piping process is simulated in a sand sample with a vertical barrier made of a SoSEAL-sand mixture. The sample with barrier has proven to be able to survive much higher horizontal hydraulic gradients than the reference test. The effect of the barrier on piping is illustrated in this document. The comparison with results from a finite element software is also discussed.

Keywords: podzolisation; BEP; pipe length; seepage barrier; D-Geo Flow

1 INTRODUCTION

The dike at the north side of the river Lek in the Netherlands is being reinforced between Amerongen and Schoonhoven to meet the safety standards. The water authority has signed with contractors an “innovation partnership” to develop new calculation and reinforcement techniques. Among the innovations features SoSEAL, an injection technique that aims for the reduction of hydraulic conductivity of aquifers. Inspired by the natural process of podzolisation, a suspension of flakes consisting of humic acid and aluminum salt is injected into the aquifer. The flakes block the pores forming a vertical barrier against groundwater flow. The barrier can be considered semi-permeable, since the hydraulic conductivity of the aquifer is reduced by a factor that depends on the amount of flocs, with a maximum of a factor 100. A SoSEAL barrier has been successfully applied to reduce seepage through an embankment of a drink-water basin (Zhou, 2020). For the river Lek the application against backward erosion piping is investigated.

The first development step consisted of a failure path analysis, to outline the potential applications of a SoSEAL barrier, and to define potential threats (Van Beek et al., 2023). From the analysis emerged that the biggest threat is the presence of holes in the barrier, either due to poor compenetration of the injected columns or to a poor connection with the blanket. The development team has therefore concluded that, with the current state of knowledge, a SoSEAL barrier should be designed in order to stop erosion at a safe distance from the barrier itself. In this way the presence of small holes in the barrier will not negatively affect the erosion process, as a numerical analysis suggests.

The design of a SoSEAL barrier requires therefore a model that can predict the pipe length given a certain head drop across a dike. The finite element software D-Geo Flow (Van Esch et al., 2013) is able to do that, but has been calibrated for a horizontal seepage path. In order to validate the software for the case of a vertical barrier small-scale piping tests including SoSEAL barriers of different length and hydraulic conductivity have been carried out, which have been compared to results of numerical simulations.

2 SMALL-SCALE PIPING TESTS

The sand sample in the physical model (Figure 1) has a size of 50x10x30cm (length x width x depth). The distance between inlet and exit point is 33,7 cm and the distance between the barrier and the exit point is 10,3 cm. The sample consists of uniform fine sand ($D_{50}=150\mu\text{m}$). During the test the hydraulic head at the inlet is kept constant and the head at the outlet is decreased in steps.

An overview of the test results is presented in Figure 2. The test IDs indicate the tested variation: barrier material (S=SoSEAL), reduction of hydraulic conductivity (25 or 100 times), length of the barrier in cm. Most tests have been repeated twice to verify the reproducibility of the results. In the graph only the second test (b) of each series is reported, except for the tests that were not repeated. The tests indicated with (Li) belong to a first set, which results will be published soon (Li et al., t.b.p.). The test indicated with L refers to an upside-down-L-shaped barrier, a barrier with a thicker upper portion. In practice this can be obtained with a second row of shorter injected columns and aims at reducing the chance of holes in the most sensitive part of the barrier, that is at the top of the aquifer.

The graph shows that the pipe length increases less with each head increment as the pipe approaches the barrier. This is visible as a change in slope of all lines as they approach the barrier. The zone where the barrier significantly influences the erosion process has been named “shadow zone”: here the horizontal groundwater flow is strongly reduced as well as erosion. For the long barriers, that close off at least half of the aquifer, the erosion process is influenced nearly from the beginning. For a short barrier the effect is visible only close to the barrier.

After the pipe(s) has reached the barrier, it stops growing in length but keeps growing in width. Moreover new pipes develop. In only two series of tests - the shortest barrier (5 cm) and the L-shaped barrier – the barrier was brought to collapse. In all the other tests the barrier survived the maximum applicable head difference, which was larger than 5 times the critical head difference in the reference test without barrier.

Before failure, the pipes transformed in a large eroded area and sand kept flushing out for 10 minutes under a constant head difference. Eventually it seems that the barrier translated horizontally and a pipe grew in the created space above the barrier. The fact that only the shortest barrier and the L-barrier failed supports the hypothesis that seepage gradients downstream of the barrier where high enough to cause geotechnical failure.

3 SOFTWARE VALIDATION

Comparison between laboratory and numerical results shows that the software D-Geo Flow strongly underestimates the pipe length for all tests. Two main reasons could explain what observed. In the numerical model erosion progresses when the groundwater flow is sufficient to transport the particles horizontally inside the pipe; the vertical force that can affect the detachment of the grains from the bottom is not included in the erosion criteria of the model; this component could become dominant when a barrier forces the flow to bend upwards. The second reason is that the 3-d aspect is neglected in the software, which assumes 2-dimensional flow. It is well known that 3-d effects cause longer pipes by equal load (Allan, 2018).

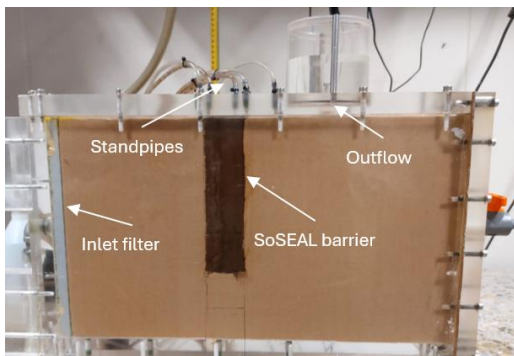


Figure 1. Side view small-scale model.

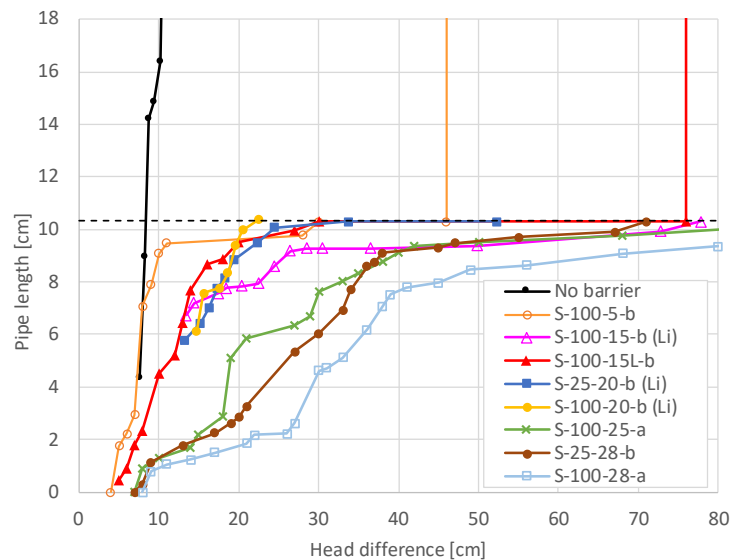


Figure 2. Overview results piping tests

ACKNOWLEDGMENTS

We thank the partners involved in the project: the water authority Hoogheemraadschap De Stichtse Rijnlanden, Heijmans Infra, GMB Civiel, de Vries & van de Wiel, Tauw, Delft University of Technology and Deltares. The research is financed by the national Flood Protection Program (HWBP).

REFERENCES

- Allan, R.J. (2018). Backward erosion piping. PhD thesis, University of New South Wales, Australia
- van Beek, V.M. et al. (2023). Failure path analysis for a SoSEAL barrier as a backward erosion piping measure. 29th Meeting of European Working Group on Internal Erosion, Lyon, France.
- van Esch, J.M., Sellmeijer, J.B., Stolle, D. (2013). Modeling transient groundwater flow and piping under dikes and dams. Computational Geomechanics (ComGeo III), Krakow, Poland.
- Li, L. et al. (to be published). Potential of low-permeability barriers to mitigate backward erosion piping. Géotechnique.
- Zhou, J. (2020). Development of a nature-based geo-engineering solution to reduce soil permeability in-situ. Master thesis, Delft University of Technology, The Netherlands.

Prediction of the Critical Secant Gradient Function

B.A. Robbins¹

1. U.S. Army Corps of Engineers Risk Management Center, Lakewood, Colorado, USA, bryant.a.robbins@usace.army.mil

ABSTRACT: Backward erosion piping is an internal erosion failure mode that threatens the integrity of dams and levees. Reliable prediction of backward erosion piping has remained difficult due to the lack of a primary erosion criterion for the progression of the erosion pipes. The concept of the critical secant gradient function (CSGF) was recently developed to be a spatially dependent primary erosion criterion for backward erosion piping. This study presents a method for predicting the CSGF based on statistical regression of laboratory measurements. Results demonstrate that the CSGF can be reliably predicted as a function of the grain size, void ratio, and coefficient of uniformity of the soil.

Keywords: backward erosion; internal erosion; primary erosion; progression

1 INTRODUCTION

Backward erosion piping is a type of internal erosion that undermines dams and levees as shown in Figure 1. The pipes progress when the head profile upstream of the pipe tip exceeds a critical head profile (Figure 2). Robbins (2022) developed the concept of the critical secant gradient function (CSGF) to spatially describe the secant gradient in front of the pipe tip. The CSGF can be used as a primary erosion criterion to predict pipe progression. This study presents a means for predicting the CSGF as a function of soil properties.

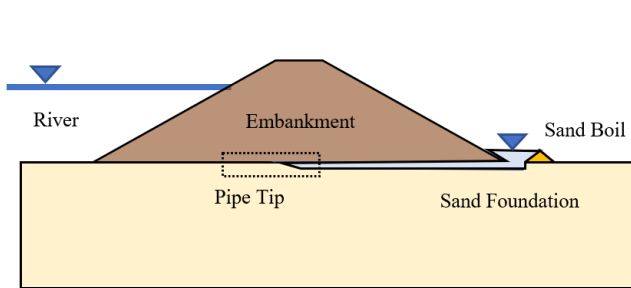


Figure 1. Backward erosion piping progressing beneath an embankment (Robbins 2023).

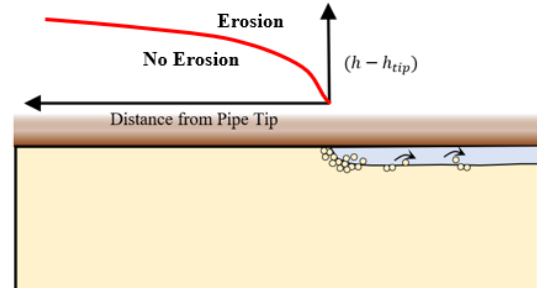


Figure 2. Critical head profile near the pipe tip (Robbins 2023).

2 THE CRITICAL SECANT GRADIENT FUNCTION

The critical secant gradient is the average hydraulic gradient between the pipe tip and some point in front of the pipe at the critical conditions for pipe progression. The secant gradient varies with distance in front of the pipe tip due to the nonlinear head profile in front of the pipe (Figure 1a). The CSGF describes the value of the critical secant gradient as a function of the distance, x , in front of the pipe tip. The critical secant gradient is given by (Robbins 2022)

$$i_{cs}(x) = Cx^{-0.5} \quad (1)$$

where i_{cs} is the critical secant gradient over distance x (m) in front of the pipe tip, and C ($m^{0.5}$) is a scalar coefficient given by

$$C = H_0 x_0^{-0.5} \quad (2)$$

where H_0 (m) is the head measured at any distance x_0 (m) in front of the pipe tip. By measuring the critical head profile at any distance in front of the pipe tip, the value of C can be determined such that the full CSGF is known.

3 MEASUREMENTS AND PREDICTION

The CSGF was measured for 7 soils in the laboratory using experiments as shown in Figure 2. Additional details regarding the experimental configuration and results can be found in Robbins (2022). The CSGF was measured for 7 soils with median grain sizes ranging from 0.15 mm to 1.4 mm and coefficients of uniformity ranging from 1.3 to 3.7. A total of 24 experiments was conducted to measure the CSGF at various densities for each soil. For each test, the differential head across the sample was increased until the pipe began to progress. When the pipe reached the pressure transducers spaced at 2 cm, the head was lowered to stop the pipe. The head was then gradually increased again until the pipe began to progress. The head measurements at various distances in front of the pipe were used to calculate the value of C to determine the CSGF. A regression on the results resulted in Equation 3 for predicting the coefficient C in Equation 1. A comparison of the predicted values of C to the measured values of C is provided in Figure 3.

$$C = 0.019 \left(\frac{d_{50}}{0.58} \right) + 0.115 \left(\frac{C_u}{2.02} \right) + 0.006 \left(\frac{e}{0.58} \right)^{-19.8} \quad (3)$$

In Equation 3, d_{50} (mm) is the median grain size, C_u is the soil coefficient of uniformity, and e is the soil void ratio.

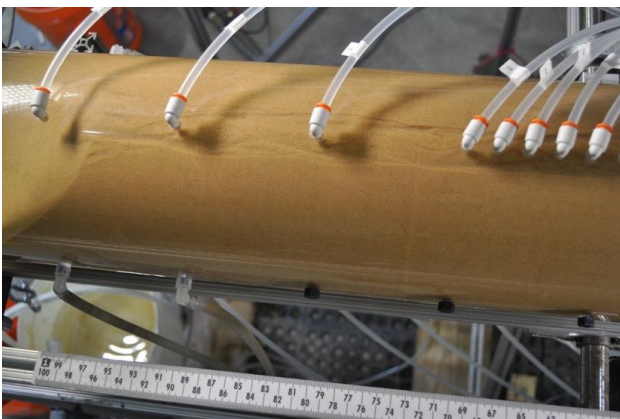


Figure 3. Laboratory measurements of the CSGF.

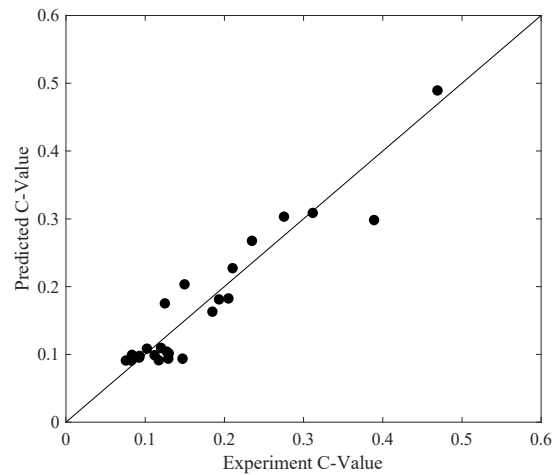


Figure 4. Comparison of predicted and measured c -values.

4 CONCLUSIONS

Backward erosion piping is a type of internal erosion that threatens the integrity of many dams and levees. As one of the main contributors to failure risks, prediction of backward erosion piping is critical for reliably assessing infrastructure risks and reliability. One of the primary obstacles to reliably predicting piping has been the lack of a primary erosion criterion for the progression of the erosion pipes (Robbins, 2022; Van Beek, 2015). Robbins (2022) developed the concept of the CSGF as a primary erosion criterion for backward erosion piping. This study presents a predictive relationship for the CSGF that predicts the value of C in Equation 1 as a function of the soils grain size, void ratio, and coefficient of uniformity. The results can be used as a primary erosion criterion for backward erosion piping modelling to assess risks of failure due to backward erosion piping.

REFERENCES

- Robbins, B.A. (2022). *Finite Element Modeling of Backward Erosion Piping*. Ph.D. Dissertation. Colorado School of Mines.
- Robbins, B.A. (2023). "A new approach for predicting progression of backward erosion piping." Presented at *Geo-Risk 2023*. Arlington, VA, July 23-26, 2023.
- Van Beek, V.M. 2015. *Backward Erosion Piping: Initiation and Progression*. PhD Dissertation. Technische Universiteit Delft.

Representative grain diameter in backward erosion

Sina Ramezanifouladi¹, Jean Côté²

1. Université Laval/Département de génie civil et de génie des eaux, Québec, Canada, sina.ramezanifouladi.1@ulaval.ca

2. Université Laval/Département de génie civil et de génie des eaux, Québec, Canada, jean.cote@gci.ulaval.ca

ABSTRACT: Global criteria, e.g. Sellmeijer et al. (2011) and Hoffmans and Van Rijn (2018) are widely used for dam safety assessment against backward erosion piping in the foundation. The representative grain diameters of d_{70} and d_{15} were used in these criteria, respectively. This paper presents the outcomes of 17 erosion tests in the improved small-scale cell developed by Ramezanifouladi and Côté (2024a). The results reveal that representative grain diameter with a smaller percentage passing may be used for prediction of the critical gradient for finer materials. It is speculated that for these materials, finer particles first set to move as a result of erosion, leading to piping.

Keywords: Backward erosion; Global criterion; critical gradient; representative grain diameter.

1 INTRODUCTION

Backward erosion piping (BEP) is one of the common mechanisms of internal erosion that endangers dam safety by leaving a progressing pipe in the foundation. Critical global gradient across the dam is usually used to assess the possibility of pipe progression. Ramezanifouladi and Côté (2024b) recently proposed a concise criterion (eq. 1) for predicting the critical gradient, in terms of the Sellmeijer's scale factor parameter and based on the slope-type exit data. In the equation, $i_{G,cr}$ is the critical global gradient, k is the hydraulic conductivity (m/s), K is the intrinsic permeability (m^2), and L is the length of erosion (m). Ramezanifouladi and Côté (2024a) also validated this model for hole-type exit using the improved small-scale test setup shown in figure 1. Automatic load application, horizontal compaction, more precise measurement equipment, and freely meandering pipe progression are among the improvements added to the setup. Table 1 summarizes the main information about soil grain size distribution. The critical global gradients range from 0.25 to 0.65 as measured for 17 BEP tests conducted on these soils, with relative densities varying from 12% to 64%. It was found out that the predicted gradients tend to deviate from the measured ones as the tested soils become finer. It is speculated that incipient motion and then progressive phase are governed by erosion of the finer particles existing in a soil.

$$i_{G,cr} = e^{-1.174} \cdot \left(\frac{k}{k_m}\right)^{-0.303} \cdot \left(\frac{d_{70}}{\sqrt[3]{KL}}\right)^{0.733} \quad (1)$$

Table 1. Soil grain size information.

Soil	Soil type	d_{100} (mm)	d_{70} (mm)	d_{10} (mm)	C_u	d_{50}/d_{15}	d_{90}/d_{10}
S1	Fine sand	0.850	0.395	0.160	2.02	1.69	3.63
S2	Fine sand	0.850	0.300	0.128	2.03	1.64	3.91
S3	Fine sand	0.180	0.164	0.131	1.21	1.15	1.34
S4	Fine sand	0.250	0.218	0.139	1.49	1.25	1.73
S5	Silty sand	0.315	0.150	0.060	2.70	1.85	3.50

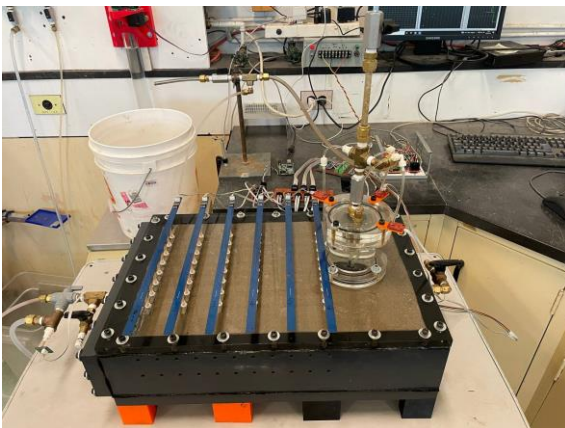


Figure 1. The improved rectangular cell with hole-type exit.

2 DISCUSSION

Figure 3 shows the predicted gradient using eq. 1 as a function of measured gradient during a BEP test. The performance of eq. 1 in prediction is acceptable, except for some samples, especially test 17 (soil S5, green dot) that is overestimated. It is speculated that the representative grain diameter used for prediction in eq. 1 might not always be d_{70} , depending on the soil type. Hoffmans and Van Rijn (2018) proposed a piping model according to the Shields criterion to determine the critical bed shear stress required for incipient motion of particles. They adopted the effect of non-uniformity of sand mixture by including d_{15} instead of d_{50} in their new definition of shear resistance. As opposed to in-mass transportation of particles in laminar flow, fine particles will move first if the pipe flow is considered turbulent, thus, they believed d_{15} is a better representative for nearly uniform sands ($4/3 < d_{50}/d_{15} < 2$). This agrees with Van Beek et al.'s (2013) observation on a dike located in Vuren, Netherlands where finer particles were found in the samples collected in the exit sand mound compared to the sands present under the dike. However, according to Van Rijn (2014), d_{15} cannot be the representative particle diameter for material with d_{90}/d_{10} ratios larger than 4-5, as the fine particles may be locked between the coarser particles.

For all the samples in this study, the retaining d_{90}/d_{10} ratio is smaller than 4-5, indicating that if erosion occurs, the coarser particles cannot retain the eroded materials. The ratio d_{50}/d_{15} of S1, S2, and S5 are in the range of nearly uniform materials, while soils S3 and S4 are even more uniform. Figure 4 is plotted showing the prediction of eq. 1 by simply considering different representative diameters without re-optimizing the fitting coefficient for now. Brown, red and green circles represent predicted gradients based on d_{70} , d_{50} , and d_{15} , respectively and blue triangles represent measured gradients. The figure shows the critical gradients for the tested soil organized in decreasing particle size from S1 to S5 (x-axis). As expected, for S1, the representative grain size to calculate the critical gradients appear to be well described by d_{70} . Physically speaking, fine particles may have been eroded during tests on soil S1, however, it did not lead to the progressive phase until coarser particles (d_{70}) were eroded. While for the finer soil S2, the representative diameter seems to be between d_{70} and d_{50} . Similarly, the critical gradients for soils S3 and S4 are fairly well predicted by finer diameter, i.e., d_{50} to d_{15} . However, as these soils are more uniform compared to the other, predictions are good in all cases. The measured gradient for soil S5 is clearly closer to the prediction with d_{15} . So far, no practical criterion exists for the assessment of backward erosion considering the full soil grain size distribution. This study draws attention to the need for further research on this aspect before using the existing criteria in numerical modelling. To further investigate this aspect, the grain size of the previously existing data will be studied and more experimental tests with the improved cell will be conducted.

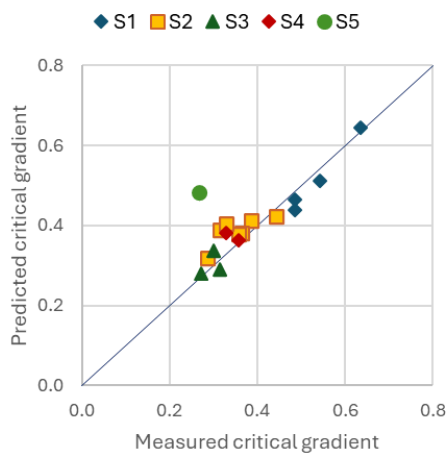


Figure 3. Predicted gradient as a function of measured one.

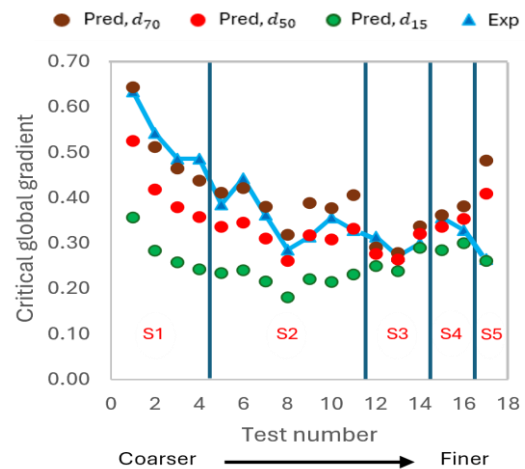


Figure 4. Comparison of the critical gradients.

REFERENCES

- Hoffmans, G. J. C. M. and Van Rijn, L. C. (2018). Hydraulic approach for predicting piping in dikes. *Journal of hydraulic research*, 56(2).
- Ramezanifouladi, S. and Côté, J. (2024a). An improved small-scale test setup for assessing backward erosion piping. *Submitted to Canadian Geotechnical Journal*.
- Ramezanifouladi, S. and Côté, J. (2024b). A novel criterion to assess the progression of backward erosion piping. *In preparation*.
- Sellmeijer, H., Lopez de la Cruz, J., Van Beek, V. M. and Knoeff, H. (2011). Fine-tuning of the backward erosion piping model through small-scale, medium scale and IJkdijk experiments. *European journal of environmental and civil engineering*, 15(8): pp. 1139-1154.
- Van Beek, V. M., Yao, Q. L. and Van, M. A. (2013). Backward erosion piping model verification using cases in China and the Netherlands. *International conference on case histories in geotechnical engineering*, Wheeling, IL.

Experimental study on the process behaviour of Backward Erosion Piping in levee and dam foundations

M. Wewer¹, J. Stamm¹, J.P. Aguilar-López²

1. Dresden University of Technology/Hydraulic Engineering, Dresden, Germany, manuel.wewer@tu-dresden.de

2. Delft University of Technology/Hydraulic Engineering, Delft, The Netherlands

ABSTRACT: Backward Erosion Piping (BEP) is one of the critical failure mechanisms for levees. Current assessment methods of BEP are either empirical or simplistic, leading to conservative and potentially costly flood protection designs. This study aims to improve the understanding of BEP through scale model experiments that focus on the role of vertical seepage forces on erosion criteria. The study will include experimental and numerical modelling to refine BEP erosion descriptions and to contribute to the development of reliable prediction methods.

Keywords: Backward Erosion Piping; Scale-model testing; Groundwater; Levee foundation.

1 INTRODUCTION

Inundations are a natural hazard with a major impact on society. Unless additional mitigation measures are taken, flood risks are expected to increase. Flood risk reduction strategies are diverse, a common mitigation measure is the use of structural flood protection systems such as levees (also called dikes or embankments) and dams. Failure of these flood defenses can be caused by a number of failure mechanisms such as overtopping, slope instability or internal erosion (Morris, et al., 2008). Backward erosion piping (BEP) is a specific internal erosion type of failure, which has accounted for 15 % of the historic levee and dam failures worldwide until year 2015 (Danka, et al., 2015). In 2013 floods in Germany, it was also one of the dominant failure mechanisms of the multiple levee breaches (Heyer, et al., 2015).

The reliable prediction of BEP has not been possible to date, as the erosion processes that describe the formation and progression of piping erosion are not sufficiently understood yet. The methods used in practice for assessing and dimensioning the structural stability against BEP are either empirical (Bligh, 1910) (Lane, 1935) or highly simplified representations of the groundwater flow coupling with the erosion process (Sellmeijer, et al., 2011) (Schmertmann, 2000). A validated prediction method for BEP has remained elusive to the hydraulic engineering profession, which leads to conservative dimensioning of flood protection structures against this failure mechanism (Robbins, 2022). To manage BEP in a safe, climate-adapted and cost-effective manner, the understanding of the physical process behavior including definitions of the critical hydraulic gradients for piping erosion needs to be further investigated.

2 EXPERIMENTAL SETUP

The aim of the present study is to improve the understanding of the most relevant BEP seepage induced erosion processes through the use of a scale model test. This will allow us to draw conclusions about the role of vertical seepage forces on the erosion criteria and their importance in the BEP prediction. The experimental BEP model is built entirely of acrylic glass material with screw based reinforcements along the joints. The upstream water level can be controlled by an elevated tank, which is connected via communicating tubes. The water enters the granular phase without requiring a filter and leaves the rectangular piping box through the pre-defined exit hole. At this location, the eroded sand mass can be collected and the water level is kept constant. The discharged water is subsequently weighed on a precision scale to determine the flow rate.

The model has internal dimensions of 800 mm in length, 500 mm in width and 170 mm in depth. The height is adjustable and can be decreased or increased. The height-adjustable cover allows vertical inflow into the pipe to vary, as it is expected that a greater aquifer thickness will provide more vertical inflow into the pipe. The actual levee or dam body is not represented in the planned experiments as it is generally assumed that the seepage flow there can be considered negligible. The flood protection structure is therefore replaced by an acrylic cover so that the erosion process can be visualized. While in most BEP models the sand is deposited and compacted from the side to ensure a sufficient contact with the cover, a conscious decision has been made to fill the setup from above to ensure a better representation of the horizontal layering of the sand. The cover is therefore removable and can be reinstalled once the sand has been installed. In addition, a thin layer of agar was applied to the cover. Agar is a galactose polymer that can be processed into a transparent, elastic

and sufficiently mechanically stable gel, which ensures adequate contact between the sand and the acrylic cover. The completed model setup with installed sand is shown in Figure 1.

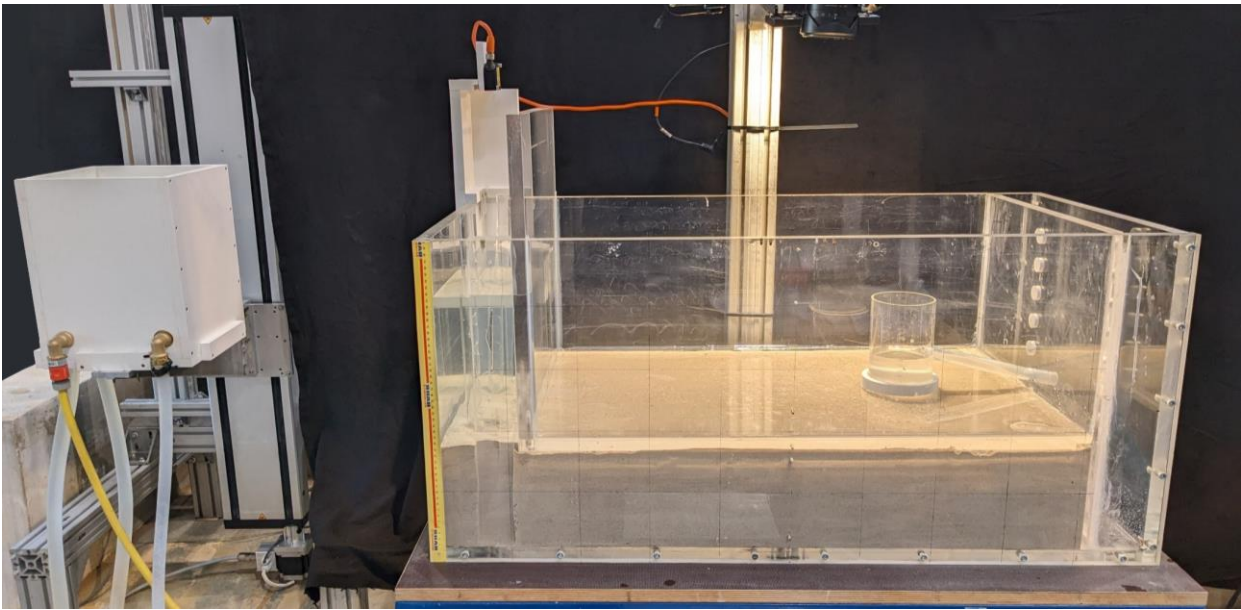


Figure 1. Photo of the experimental BEP setup in the hydraulic laboratory of the TU Dresden

3 WORK PROGRAMME

The main objective of the study is to improve the description of the BEP erosion process and to derive erosion criteria for primary and secondary erosion that can be used in reliable prediction methods. In order to answer this, different work packages have been created. Three of four work packages will deal with the experimental study of BEP (1. Free development of pipe; 2. Pre-defined pipe path; 3. Implementation of a cut-off wall). In work packages 4, a numerical study is added in order to acquire further hydraulically relevant parameters. The objective is to calculate further hydraulically relevant parameters such as 3D pore pressure and velocity fields in addition to the monitored values. The numerical model is based on the 2D FEM model developed at TU Dresden and TU Delft (Wewer, et al., 2021) and has already been extended by the third dimension in order to improve the representation of the flow behavior.

REFERENCES

- Bligh, W. G. 1910. Dams, barrages and weirs on porous foundations. Chicago: Engineering News, 1910.
- Danka, J. und Zhang, L. 2015. Dike failure mechanisms and breaching parameters. Hong Kong: *Journal of Geotechnical and Geoenvironmental Engineering*, [https://doi.org/10.1061/\(ASCE\)GT.1943-5606.0001335](https://doi.org/10.1061/(ASCE)GT.1943-5606.0001335), 2015.
- Heyer, T. und Stamm, J. 2015. Investigations and Analysis of Levee Failures during recent Floods in Saxony and Saxony-Anhalt (Germany). Brno: *Water Management and Hydraulic Engineering*, https://vst.fce.vutbr.cz/wp-content/uploads/2017/04/WMHE_2015_text.pdf, 2015.
- Lane, E. W. 1935. Security from underseepage: Masonry dams on earth foundations. Iowa: *Transactions of the American Society of Civil Engineers*, <https://doi.org/10.1061/TACEAT.0004655>, 1935.
- Morris, M.W., et al. 2008. Failure modes and mechanisms for flood defence structures. In: P. Samuels, S. Huntington, W. Allsop, and J. Harrop, eds., *FloodRisk2008*, pp. 693–701. s.l.: Taylor and Francis, <https://www.taylorfrancis.com/chapters/edit/10.1201/9780203883020-85/failure-modes-mechanisms-flood-defence-structures-morris-allsop-buijs-kortenhaus-doorn-lesniewska>, 2008.
- Robbins, B. A. 2022. Finite element modelling of backward erosion piping (PhD Thesis). Colorado: *Colorado School of Mines*, <https://repository.mines.edu/handle/11124/176610>, 2022.
- Schmertmann, J. H. 2000. The no-filter factor of safety against piping through sands. Florida: Judgment and innovation: the heritage and future of the geotechnical engineering, <https://doi.org/10.1061/9780784405376.006>, 2000.
- Sellmeijer, H., et al. 2011. Fine-tuning of the backward erosion piping model through small-scale, medium-scale and IJkdijk experiments. Delft: *European Journal of Environmental and Civil Engineering*, <https://doi.org/10.1080/19648189.2011.9714845>, 2011.
- Wewer, M., et al. 2021. A transient backward erosion piping model based on laminar flow transport equations.

Sand Erodibility at Backward Erosion Piping

J. Riha¹, L. Petrula²

1. Brno University of Technology, Faculty of Civil engineering, Brno, Czech Republic, riha.j@vutbr.cz

2. HBH Projekt spol. s r.o., Brno, Czech Republic, l.petrula@hbh.cz

ABSTRACT: Backward erosion piping is driven by seepage forces acting on the soil grains at the downstream end of a seepage path. Three types of sand with grain sizes of 0/2, 0.25/2 and 0.25/1 were tested in the new experimental device. During 42 tests the progression of the seepage path, the piezometric heads and the eroded material were observed by two synchronous cameras, set of piezometers and pressure cells. An empirical formula for the rate of backward erosion piping was proposed. Comparison of lateral erosion characteristics with the available literature provided quite a good fit.

Keywords: backward erosion piping; seepage; experimental research; critical hydraulic gradient; soil erodibility.

1 INTRODUCTION, CONTEXT, MOTIVATION

Research on the mechanics of backward erosion piping (BEP) shows that the pipe initiates at its downstream tip, where the pressure gradient reaches the maximum value. The erosion progresses in the backward direction by detachment of soil grains at the pipe tip. Robbins et al. (2020) revealed that the pipe erosion rate depends on the hydraulic gradient, on the grain size and void ratio of the material. However, prediction models often still fail due to the complexity of the phenomena involved, which proceed differently in soils with different geomechanical and seepage properties.

In order to provide more experimental data on BEP initiation and progression, a small scale experimental device was proposed, constructed (Petrula, Říha, 2022), tested and used for the research on both backward and lateral erosion.

2 MATERIALS, METHODS

42 tests on three types of the sand with properties according to Tab. 1 were carried out. The testing procedure started with sample preparation. Given the dimensions of the testing box, and in order to eliminate the scale effect as much as possible, maximum sand grains were 2 mm. Then sample was placed into the box, was saturated and subjected to seepage with fixed downstream and variable stepwise increasing upstream boundary condition governed by the movable tank position. During the initial phase no erosion occurred. The tank was gradually raised step by step, and the piezometric heads along the sample were measured. After a certain critical elevation of the tank was exceeded, erosion occurred. Finally, after an intensive erosion, a total failure occurred, and the experiment finished.

Table 1. Performed experiments and sample properties.

Material grain size	Number of tests	Uniformity coefficient C_u	Grain density ρ_d	Porosity n	
				Min.	Max.
	[-]	[-]	[kg/m ³]	[-]	
0/2 mm	26	2.98	2638	0.286	0.381
0.25/2 mm	8	2.08	2638	0.319	0.341
0.25/1 mm	8	1.84	2638	0.331	0.346

3 RESULTS AND DISCUSSION

The analysis of the results focused on the both local and average critical hydraulic gradient and both the backward and lateral erosion rates. The piezometric head along the shortest seepage path, the mass of eroded material and pipe dimensions were observed during the erosion phase by the camera and finally evaluated (Fig. 1). The eroded pipe was divided into sections washed away due to backward erosion and lateral erosion (Fig. 2).

It was found that the local gradients at the tip of the pipe were about 2.4 times higher than the mean gradients in the soil sample. However this ratio will be really higher as measured gradients at the tip were determined using the piezometric heads measured in the standpipes with the span of 2 cm.

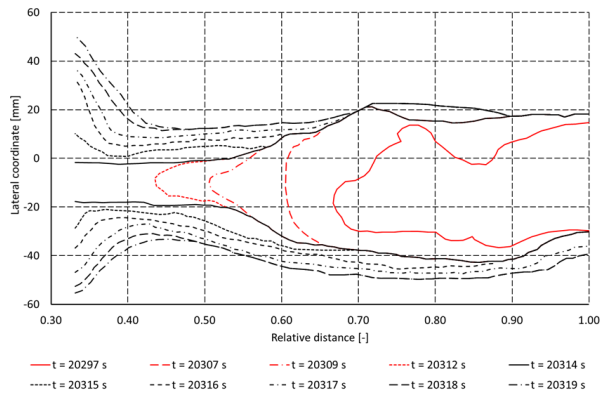


Figure 1. Changes in pipe shape during BEP.

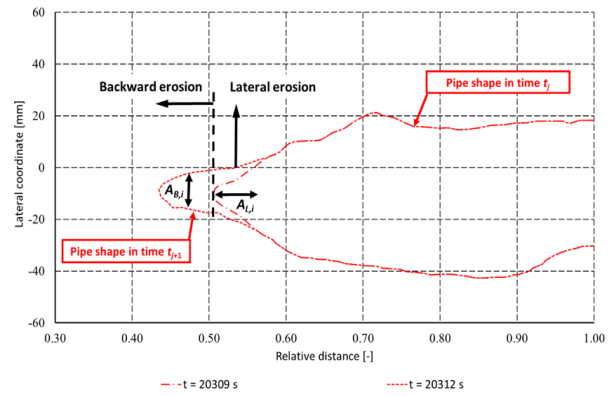


Figure 2. Scheme of separation of backward and lateral erosion.

Based on the trend analysis for the mean hydraulic gradient, an exponential relation was chosen when expressing the backward erosion rate. For the porosity, and grain size linear dependence was used. The beginning of the BEP was expressed via the mean critical hydraulic gradient. The final formula holds:

$$\dot{\epsilon}_B = 0.94[-1 + e^{0.83(J_{mean} - J_{c,mean})}] \cdot \frac{0.35}{d_{50}} \cdot \frac{0.476}{n}, \quad \text{for } J_{mean} > J_{c,mean} \quad (1)$$

where $\dot{\epsilon}_B$ is the backward erosion rate [kg/s/m²], d_{50} is the grain size corresponding to 50% passing [mm], J_{mean} is the mean hydraulic gradient during the BEP, $J_{c,mean}$ is the critical mean gradient and n is porosity. The obtained results suffer from considerable scatter, which can be attributed to the randomness of the not utterly continuous erosion progression, and to uncertainties and inaccuracies in the evaluation of experimental erosion rates (reading of the erosion pipe dimensions from the video logs, determination of the pipe "depth", and time step errors in the case of very fast erosion). As the the erosion pipe widened during the tests, the characteristics of lateral erosion during the BEP were evaluated using methodology similar to that used by (Wan, Fell 2004), who expressed the lateral erosion rate as follows:

$$\dot{\epsilon}_L = C_e(\tau - \tau_c) \quad \text{for } \tau > \tau_c \quad (2)$$

where τ is the shear stress along the erosion pipe. The critical shear stress τ_c dropped with increasing porosity and increased with increasing sand uniformity with values from 1.2 to 5 Pa. The values of C_e ranged from 0.022 to 1.7 (with 80 % of values less than 0.4). These values correspond to the range obtained by Wan and Fell (2004) for loose soils ($\tau_c < 6.4$ Pa, C_e from 0.02 to 0.25).

4 CONCLUSIONS

The comparison of hydraulic gradients shows that in this study determined the local gradients at the pipe tip are about 2.4 times higher than the average ones. Both local and average hydraulic gradients provide approximately linear relation to the sample porosity. The mean hydraulic gradients range from 0.5 to 1.8 depending on sample compaction (porosity), they in some cases exceed values published in previous studies (Robbins et al. 2018), though the gradients from previous studies were derived for rather higher porosities. The rates of backward and lateral erosion were derived from experiments. The Eq. (1) for the estimation of backward erosion rate was derived to be applied for uniform sand ($C_u < 3$) with the mean grain size $d_{50} < 0.35$ mm. The characteristics of lateral erosion, namely critical shear stress and coefficient of soil erosion, comply with values derived by Wan and Fell (2004).

ACKNOWLEDGMENTS

FAST-S-24-8513 „Analysis of the influence of input variables on the results of numerical models used in the safety assessment of water structures“ and TACR SS07010401 "Water management analysis to support natural flooding and the transformation effect of the floodplain".

REFERENCES

Petrula, L. and Říha, J. (2022). A new small scale experimental device for testing backward erosion piping. Journal of Hydrology and Hydromechanics, vol. 70, no. 3, pp. 376 384. DOI: <https://doi.org/10.2478/johh-2022-0023>.

Backward Erosion Piping with point outflow and semi-permeable polder blankets: experiments, modelling and research program

J.C. Pol¹, V.M. van Beek², H. van Hemert³, K. Dorst⁴, M. Hijma², R. Koopmans⁵, E. Rosenbrand²

1. HKV, Lelystad, Netherlands, pol@hkv.nl

2. Deltares, Delft, Netherlands, Vera.vanBeek@deltares.nl

3. Rijkswaterstaat, Lelystad, Netherlands, henk.van.hemert@rws.nl

4. Waterschap Limburg, Roermond, Netherlands, k.dorst@waterschaplimburg.nl

5. Arcadis, Arnhem, Netherlands, rimmer.koopmans@arcadis.com

ABSTRACT: In the field, Backward Erosion Piping (BEP) often appears as single sand boil, associated with strongly 3D groundwater flow. This abstract describes a new research project focused on scale effects and 3D-effects. In addition, small-scale experiments with point outflow and leakage to the polder and their numerical modeling are presented. The results show that leakage through a semi-permeable blanket significantly increases the critical head in comparison to an impermeable blanket, and the process tends to become initiation-dominated. Model predictions improve when primary erosion is included in the numerical model.

Keywords: Backward Erosion Piping; 3D, leakage; experimental program.

1 INTRODUCTION

Most physics-based BEP design models (e.g. Sellmeijer model) are essentially 2D representations of the piping process. However, many field situations have concentrated outflow to a single point (3D), where a sand boil appears. Previous research shows that 3D situations simulating impermeable blankets may lead to significantly lower critical head compared to 2D situations (Vandenboer et al., 2018; Van Beek et al., 2022). Also, leakage through a semi-permeable polder blanket may positively impact the critical head (Bezuijen, 2017). Thirdly, recent studies show that different models may perform equally well at laboratory scale, but yield strongly deviating results when applied to field scale (Hoffmans, 2021; Pol, 2022). Currently, there is limited understanding of the combined effect of 3D flow concentration and leakage on BEP, especially for field scale ($L \sim 100$ m). To address these questions, recently, a research program has been initiated on scale effects for BEP in 3D situations, which is described here. In addition, results of a first series of small-scale experiments with point outflow and leakage to the polder and their numerical modeling are presented.

2 RESEARCH PROJECT OUTLINE

The initiated research project aims to address the research questions above in order to provide updated design methods for dike assessment and design in The Netherlands. It is funded by the Dutch Flood Protection Programme and Rijkswaterstaat, and carried out by a consortium of a water authority, knowledge institute and private parties. Figure 1 shows the main project components. As the final testing programme will be established mid 2025, the programme can still be updated based on new insights and expert judgement.

Experiments will have a configuration with 3D point outflow, similar to Vandenboer et al. (2018). Exact dimensions and soil types of the small, medium and large scale experiments are to be determined. Depending on the outcomes of the exploration phase, the large-scale experiments will be focused at studying the influence of polder side boundary (closed or semi-permeable) and/or material properties (coarse sand, sandy gravel) on the scale effects.

Modelling of the experiments as well as parametric studies will be done using the 3D numerical model DgFlow (Van Esch et al., 2013) and simpler existing design methods. An international model comparison will be held to compare how different types of BEP models perform in predicting the planned experiments. Based on the modelling results, numerical model improvements are included if needed, and findings are translated into design guidelines for dikes.

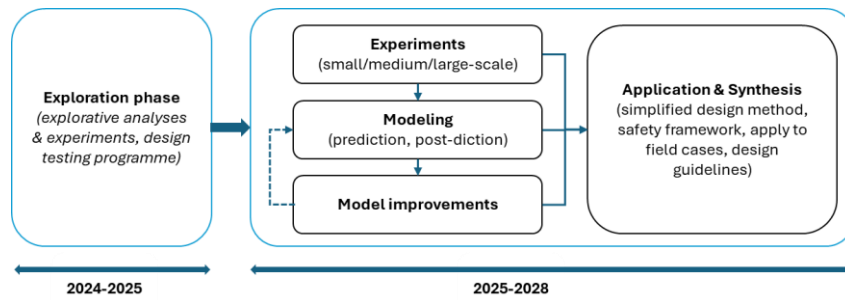


Figure 1. Research project components.

3 EXPERIMENTS AND MODELLING

Leakage to the hinterland (polderside behind the exit) is expected to be an important factor in the 3D effect. The more leakage, the less flow concentrates to the pipe and the more limited the 3D effect is. Leakage depends on transmissivity of the aquifer and the resistance of the blanket. We have executed preliminary small-scale experiments (Figure 2) in which we vary the head at the polderside boundary with +/- 1 cm relative to the exit head (h_{exit}), and investigated whether the 3D model DgFlow (Van Esch et al., 2013, Van Beek et al., 2022) can properly simulate it.

Both the model calculations and experiments show that leakage to the hinterland in 3D situations has a clear influence on the piping process: the critical head (inflow head relative to the exit head at which piping occurs) increases and the critical pipe length decreases. Figure 3 shows the experimental and modelled critical head for different degrees of leakage (no leakage in closed case, most leakage in $h_{\text{exit}} - 1\text{cm}$ case). A model without primary erosion underestimated the critical head, especially for the cases with the strongest leakage (which also become initiation-dominated). Adding primary erosion with a prior best guess value of 1.4 for the local critical hydraulic gradient over the 5 mm pipe-element at the pipe tip (i_c) improved the agreement. However, reproducing the case with strongest leakage, where primary erosion plays a greater role due to the shorter critical pipe length, required a higher value of 1.8 for i_c . The 2D version of DgFlow yields a rather constant $H_{\text{crit}}=0.145\text{-}0.150$ cm depending on the polder head boundary. Hence, the findings suggest that the 3D effect decreases with increasing leakage to the hinterland. The research program will investigate whether the 3D model can predict tests at larger scales, and to what extent the 3D effect reduces with leakage at larger scale.

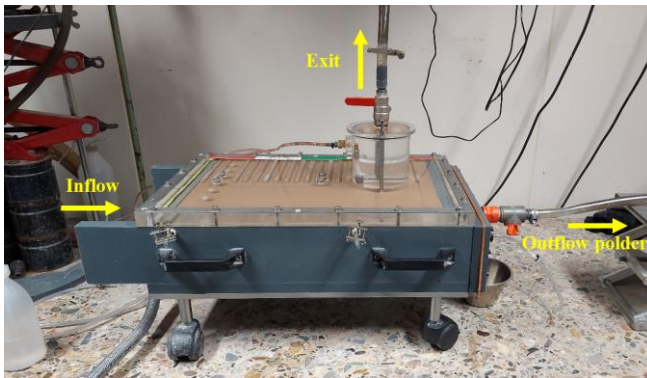


Figure 2. Experimental setup.

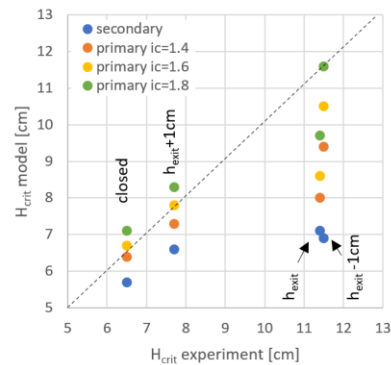


Figure 3. Results for critical head H_{crit} .

REFERENCES

- Bezuijen, A. (2017). The influence of the leakage length on the initiation of backward erosion piping. *Proc. 25th Meeting of the European Working Group on Internal Erosion*, VM van Beek and AR Koelewijn (Eds), pp. 88-96.
- Hoffmans, G. (2021). Influence of erosion on piping in terms of field conditions. *Journal of Hydraulic Research*, 59(3), 512-522.
- Pol, J. (2023). Discussion of: Influence of erosion on piping in terms of field conditions By G. Hoffmans, *Journal of Hydraulic Research*, 61(1), 162-164.
- Van Beek, V., Robbins, B., Rosenbrand, E., & van Esch, J. (2022). 3D modelling of backward erosion piping experiments. *Geomechanics for Energy and the Environment*, 31, 100375.
- Vandenboer, K., Van Beek, V. M., & Bezuijen, A. (2018). 3D character of backward erosion piping. *Géotechnique*, 68(1), 86-90.
- Van Esch, J.M., Sellmeijer, J.B., & Stolle, D. (2013). Modeling transient groundwater flow and piping under dikes and dams. *Proc. 3rd International Symposium on Computational Geomechanics (ComGeo III)*, S. Pietruszczak & G. Pande (Eds.), Taylor & Francis.

Disaggregation susceptibility of clayey silt mixture subjected to drying-wetting cycles observed by automated crumb test

D. Ayssami¹, C. Chevalier¹, Y. Boussafir¹, S. Hemmati¹ and Ph. Reiffsteck¹

1. GERS/SRO, Champs-sur-Marne, France, dalia.ayssami@univ-eiffel.fr

ABSTRACT: This study focuses on a soil mixture composed of 90% of silt and 10% of kaolinite, subjected to 1, 3, 6 and 12 of drying and wetting cycles. Using the Automated Crumb Test (ACT), the results show that disaggregation time decreases with the number of cycles due to reduced permeability and cohesion. On the dry side, specimens initially resist but eventually disaggregate from the mid-height from the 6th cycle onwards. On the wet side, crack formation accelerates, leading to faster disaggregation by the 12th cycle. Initial swelling prior to disintegration was observed in both cases.

Keywords: Crumb test; drying-wetting cycles; disaggregation; erosion.

1 GENERAL CONTEXT

Soil dispersion refers to the ability of the particles constituting the material to be deflocculated into still water. When affected by this phenomenon, the material disperses into a colloidal suspension of extremely fine particles in water without movement (Van Olphen, 1963). This phenomenon is closely linked to the erosion process and ultimately to the failure of dams and embankment dykes (Moore and Masch, 1962; Sherard et al., 1977; Bell and Maud, 1994), especially in the case of internal erosion, where dispersion is often recognized as a cause of particle tearing. Laboratory studies of the erosive behavior of compacted soils (Wan and Fell, 2004; Briaud, 2008; Haghghi et al., 2013; Fattahi et al., 2017; Haghghi et al., 2020), have shown that erosion, depends on soil texture, clay type, water content, compaction state, temperature and the composition of the erosive fluid. This sensitivity can be linked to "dispersive properties" and/or "disaggregation properties" under the action of water. The Automated Crumb Test (ACT) is one of the tests used to study the susceptibility of soil to disaggregate in contact with water. Initially developed by Emerson in 1964, this standardized test (ASTM D 6572-00), was improved by several researchers, in order to obtain quantitative rather than qualitative results (Pham et al., 2008; Haghghi et al., 2020). The aim of this paper is to use ACT quantitative results to study the influence of ageing of the material over seasons, by applying several drying-wetting cycles, on its susceptibility to disaggregate in contact with water, and forecast internal erosion mechanism.

2 EXPERIMENTAL STUDY AND FIRST RESULTS

The material used in this study is a mixture of 90% of silt and 10% of kaolinite. The soil is initially prepared in a wet state ($w = w_{OPN} + 3\%$). The specimens were prepared in a cylindrical mould 3 cm diameter and 4 cm high and compacted at 95% of the Normal Proctor optimum. The number of hydric cycles selected for study is 1, 3, 6 and 12. Each cycle begins with drying and ends with wetting. The water content varies between $w_{OPN} + 3\%$ (wet side) and $w_{OPN} - 6\%$ (dry side). Three repeatability tests were carried out for each case study to ensure the reliability of the results. Drying will take place in the open air, at a temperature of 20°C and a relative humidity of 50%. For wetting, the capillary rise method was used. The ACT is a quick and easy test: simply dip the soil specimen into a small container filled with water and follow the behavior and evolution of the specimen's shape and size over time, thanks to a camera placed in front of it. A software programmed with the Python language extracts three parameters over time: top, base diameter and its height.

The results obtained show that the disaggregation time of the specimen decreases with the number of cycles. The soil therefore loses its strength in the end, which implies a degradation of the permeability and cohesion over time.

Figure 1-a gives an example of the specimen's behavior in its initial state, after 1 and 12 hydric cycles for both dry and wet part of the cycle. The times shown below each photo are the average for the 3 repeatability tests. A) Compared with the initial disaggregation time, the 1st cycle has the greatest impact on the material, with an increase in the resistance time to immersion in water, due to the fact that permeability decreases during drying and cohesion increases (Ayssami et al., 2024). After this 1st cycle, it takes less time for disaggregation and there is a kind of stabilisation of this time. B) The disaggregation mechanism is very different depending on whether a sample is immersed at the end of a drying stage or at the end of a wetting stage. When the soil is dry, disaggregation takes the form of decohesion of small aggregates or

particles. From 1 to 6 cycles, specimens disaggregate from the top. After 6 cycles, it disaggregates from the middle and breaks into two parts. On the wet side, the behavior of the soil changes completely. Cracks are formed until they intersect and break the specimen. The velocities of formation and propagation of these cracks quickly increase with the number of cycles.

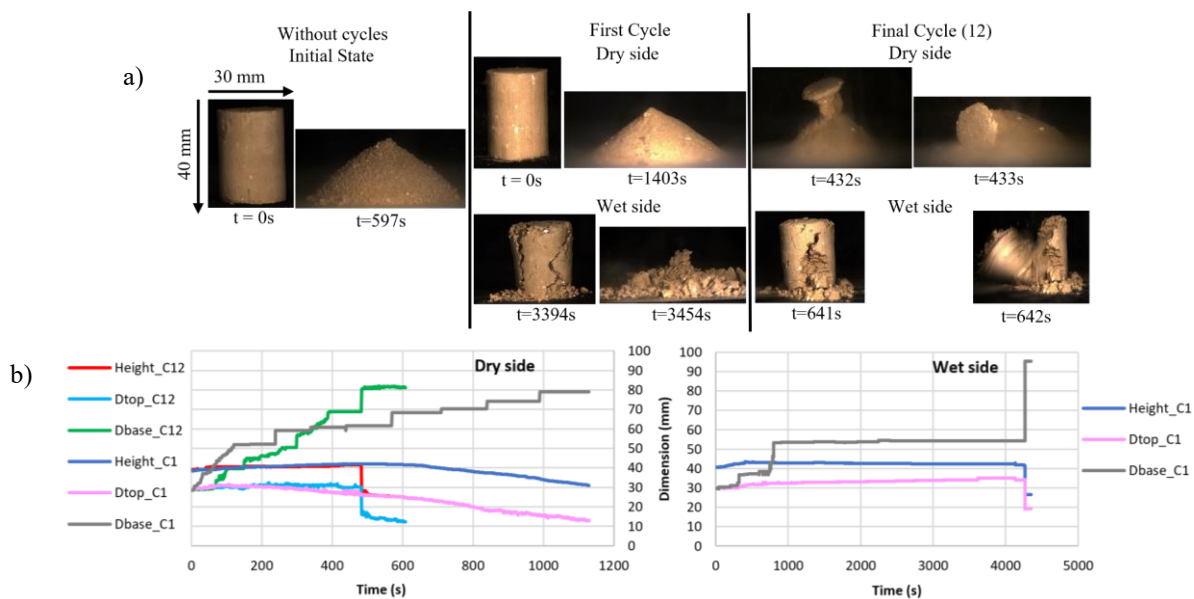


Figure 1. (a) Example of the evolution of soil behavior in the initial state, first and last cycle for both dry and wet cases. (b) Example of the variation in specimen dimensions during the first and twelfth cycle.

Figure 1-b shows the results of the image processing curves, of cycle 1 on the dry side and cycle 12 on both sides. According to these curves, in both cases, the specimens initially swell before they begin to disaggregate. The start of the swelling phase for the wet side describes the appearance of the first cracks. The amplitude and time of swelling decrease with the number of cycles. According to the two dimensions, top diameter and height, the sharp drop marks that the specimen has broken into two parts at the end of the twelfth dry and wet cycle.

REFERENCES

- Ayssami, D., Chevalier, C., Boussafir, Y., Hemmati, S. and Reiffsteck, Ph. 2024. «Effect of varying hydric cycles on the different properties of a kaolinite-treated silt ». (To be submitted).
- Bell, F. G. and Maud, R. R. 1994. « Dispersive soils: A review from a South African perspective. » *Quarterly Journal of Engineering Geology and Hydrogeology*, 27:195-210. <https://doi.org/10.1144/GSL.QJEGH.1994.027.P3.02>
- Briaud, J.-L. 2008. « Case Histories in Soil and Rock Erosion: Woodrow Wilson Bridge, Brazos River Meander, Normandy Cliffs, and New Orleans Levees ». *Journal of Geotechnical and Geoenvironmental Engineering* 134 (10): 1425-47. [https://doi.org/10.1061/\(ASCE\)1090-0241\(2008\)134:10\(1425\)](https://doi.org/10.1061/(ASCE)1090-0241(2008)134:10(1425))
- Fattahi, S. M., Soroush, A. and Shourijeh, P. T. 2017. « The hole erosion test: A comparison of interpretation methods. » *Geotechnical Testing Journal* 40 (3): 20160069-505. <https://doi.org/10.1520/GTJ20160069>
- Haghighi, I., Chevalier, C., Duc, M., Reiffsteck, Ph. and Guédon, S. (2013). Improvement of hole erosion test and results on reference soils. *Journal of Geotechnical & Geoenvironmental Engineering*, 139(2), 330–339. [https://doi.org/10.1061/\(ASCE\)GT.1943-5606.0000747](https://doi.org/10.1061/(ASCE)GT.1943-5606.0000747)
- Haghighi, I., Martin, Th., Reiffsteck, Ph., Duc, M., Szymkiewicz, F. and Chevalier, C. 2020. « An Automated Crumb Test Procedure to Estimate the Soil Disaggregation Properties in Contact with Water ». *European Journal of Environmental and Civil Engineering* 26 (10): 4416-31. <https://doi.org/10.1080/19648189.2020.1854123>
- Moore, W. L. and Masch, F.D. 1962. « Experiments on the Scour Resistance of Cohesive Sediments ». *Journal of Geophysical Research* 67 (4): 1437-46. <https://doi.org/10.1029/JZ067i004p01437>
- Pham, T. L., Chevalier, C., Duc, M., Reiffsteck, Ph. and Guedon, S. 2008. « Developpement of a new test to characterize dispersion of soil », Fourth International Conference on Scour and Erosion, 436-41.
- Sherard, J. L., Dunnigan, L. P. and Decker, R. S. 1977. « Some Engineering Problems with Dispersive Clays. », Dispersive clays, Related Piping, and Erosion in Geotechnical Projects, ASTM STP 623, 3-12.
- Van Olphen, H. 1963. *An Introduction to Clay Colloid Chemistry*. John Wiley; 2nd Edition. New York.
- Wan, C. F. and Fell, R. 2004. « Investigation of Rate of Erosion of Soils in Embankment Dams ». *Journal of Geotechnical and Geoenvironmental Engineering* 130 (4): 373-80. [https://doi.org/10.1061/\(ASCE\)1090-0241\(2004\)130:4\(373\)](https://doi.org/10.1061/(ASCE)1090-0241(2004)130:4(373))

Comprehensive study of suction bucket foundations and the associated risk of piping

Abbas Farhat¹, Li-Hua Luu¹, Alexis Doghmane¹, Pablo Cuellar², Pierre Philippe¹

1. *RECOVER, INRAE-Aix Marseille univ., 3275 Rte C'ezanne, Aix en Provence, 13100, France abbas.farhat@inrae.fr; li-hua.luu@inrae.fr; alexis.doghmane@inrae.fr; Pierre.philippe@inrae.fr

2. BAM Bundesanstalt für Materialforschung und-prüfung, Unter den Eichen 87, Berlin, 12205, Germany. Pablo.cuellar@bam.de

ABSTRACT: The suction bucket foundation is increasingly recognized as a reliable and cost-effective option for offshore wind turbines. However, while the installation of a suction bucket is relatively straightforward in sandy soil, there remains limited understanding of soil state. Piping erosion challenges have been encountered on sites during the installation process, stemming from various factors including bucket size, soil properties beneath the cylindrical tip of the bucket, as well as soil layering and cementation. This paper outlines the various difficulties encountered in the installation process. To address these challenges, we have constructed a small-scale physical model to replicate field installation with different configurations and protocols. The bucket was either fixed at a set depth or mobile with vertical guidance, being embedded deeper into the soil layer solely by suction. Several types of soil were used: fully granular, fully cemented, and mixed in two layers (granular and cemented). The findings demonstrate systematic results for the granular tests, yet this consistency was not fully observed in the cemented ones.

Keywords: Suction bucket foundation; Piping erosion; Internal erosion; suction installation.

1 INTRODUCTION, CONTEXT, MOTIVATION

The rising demand for renewable energy, especially from offshore wind turbines, has spurred research into cost-effective foundation designs (Koterias and Ibsen, 2019). Among these, the suction bucket foundation has emerged as a particularly promising option (Xiaoni et al., 2019; Bienen et al., 2017; Ragni et al., 2020). There are many advantages for using this type of foundation: reduced installation costs and duration, low noise emission, high bearing capacity, retrieval and reuse in various locations, and potential to be installed at an extend water depth (Wang and Yin 2020). A suction bucket consists of a steel cylinder that is open at one end and closed at the other, with a water extraction hole or metallic pipes (Tasan and Yilmaz, 2019). The bucket is installed into the seabed in two phases. Initially, it embeds into the seabed due to its own weight, forming a seal between the inner bucket and the water above the soil. Once the bucket stops moving, suction pressure is applied inside the bucket through the water extraction hole. This creates a differential pressure between the inside and outside of the bucket, allowing it to embed further without additional force. The installation process is significantly influenced by the soil layer beneath the bucket walls and the bucket's dimensions and lacks understanding about how it can be affected by changes in soil state, such as the expansion of the soil bed inside the bucket or the introduction of cementation (Ragni et al., 2020). Locally, the differential pressure across the bucket wall fluidizes the soil just beneath the wall, causing it to lose its bearing capacity and thereby facilitating the installation process by the moving the grains beneath the walls. In the case of sandy soil, this differential pressure will cause the soil inside the bucket to partially fluidize. However, the suction bucket installation can come to a complete halt for two reasons (Chen et al., 2019; Kim et al., 2019; Harireche et al., 2013): Firstly, as the suction rate increases, the soil inside the bucket begins to heave and mound up, which increases seepage flow. This mounding can eventually form a soil plug that reaches the top surface of the bucket before it achieves the desired embedded depth. Secondly, excessive suction pressure can lead to issues such as localized piping failure or rat hole formation. These issues create preferential seepage flow paths along zones close to the bucket wall, resulting in a significant drop in differential pressure and compromising the continuation of the process.

2 EXPERIMENTAL RESULTS

To tackle this problem, we have constructed a small-scale physical model that mimics on-site installation scenarios. In our setup, both the bucket and reservoir are crafted from plexiglass, enabling direct observation inside using a camera (refer to Figure 1). Our aim is to gain a deeper understanding of the underlying processes. To simplify the physics of the experiment, we have used artificial soil composed of spherical glass beads. For the case of a granular soil, two sets of parametric study were conducted, either by varying the self-weight of the bucket (0 N, 10 N, 20 N) and the particle size

(1.4 mm, 2.54 mm, and 3 mm), and by fixing the bucket vertical position and varying the particle size (1.4 mm, 2.54 mm, and 3 mm). The results are quite systematic and repeatable for both set of studies. For the case of cemented soil, the sample is constructed by adding paraffin to the granular beads using the method explained in (Farhat et al,2024). A parametric study was conducted by varying the self-weight of the bucket (0 N, 10 N, 20 N) and the particle size (1.4 mm, 2.54 mm, and 3 mm) with three different paraffin contents (0.1%, 0.2% and 0.3%).

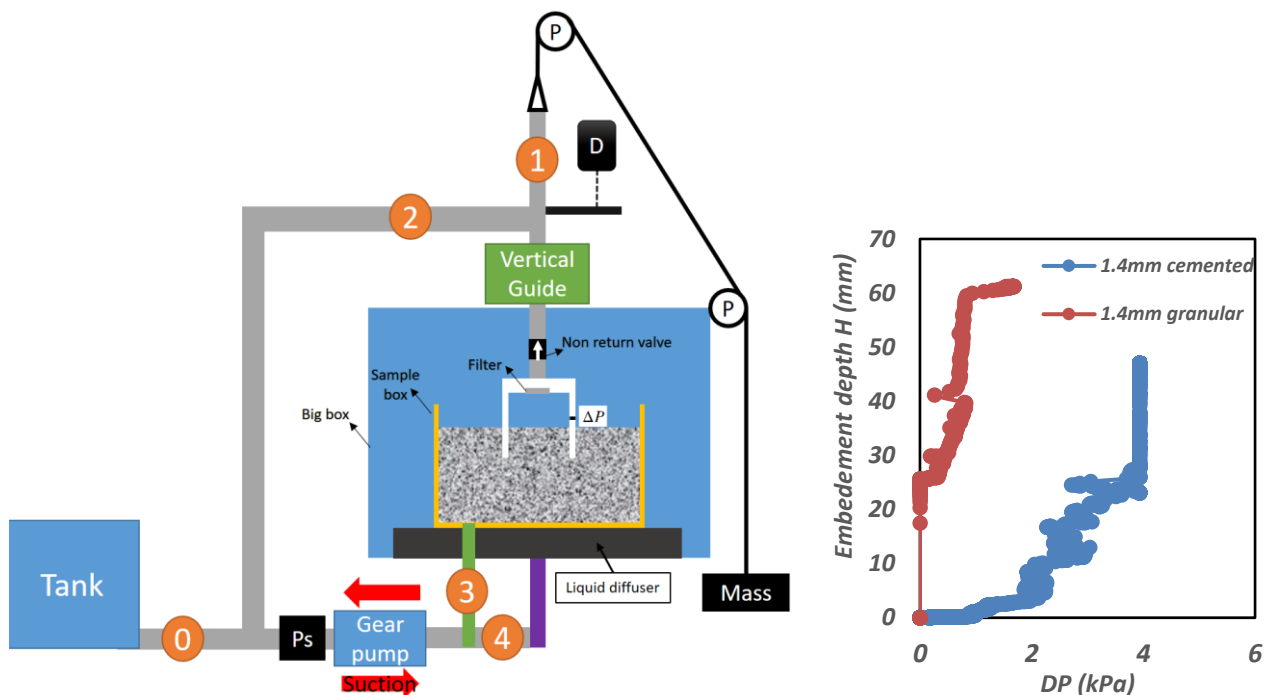


Figure 1. (left) Suction bucket physical model, (right) experimental findings of 1.4mm of the embedment depth versus differential results for fully granular and fully cemented soil.

Figure 1 presents findings on the differences between granular and cemented soil samples. It is evident that in granular soil, there is an initial embedment due to the self-weight of the bucket, which is not observed in the cemented soil. Additionally, the cemented soil requires a higher flow rate, i.e., differential pressure, to achieve substantial embedment of the bucket, although lower than in the granular soil.

REFERENCES

- Koteras, A.K., 2019, L.B.I.: Medium-scale laboratory model of mono-bucket foundation for installation tests in sand, <https://cdnscepub.com/doi/abs/10.1139/cgj-2018-0134>. *Can. Geotech. J.* 56 (8): 1142–1153 (2019)
- Wu, X., Hu, Y., Li, Y., Yang, J., Duan, L., Wang, T., Adcock, T., Jiang, Z., Gao, Z., Lin, Z., Borthwick, A., Liao, S.: Foundations of offshore wind turbines: A review. *Renewable and Sustainable Energy Reviews* 104, 379–393 (2019) <https://doi.org/10.1016/j.rser.2019.01.012>
- Bienen, O.C.D.Z.F.Y.. B.: Physical modelling of suction bucket installation and response under long-term cyclic loading, <https://doi.org/10.3723/osig17.524>. *Off-shore Site Investigation Geotechnics 8th International Conference* Proceeding, pp. 524-531(8) (2017)
- Ragni, R., Bienen, B., Stanier, S., O’Loughlin, C., Cassidy, M.: Observations during suction bucket installation in sand. *International Journal of Physical Modelling in Geotechnics* 20(3), 132–149 (2020) <https://doi.org/10.1680/jphmg.18.00071>
- Wang, P., Yin, Z.-Y.: Micro-mechanical analysis of caisson foundation in sand using dem. *Ocean Engineering* 203, 107240 (2020) <https://doi.org/10.1016/j.oceaneng.2020.107240>
- Tasan, H.E., Yilmaz, S.A.: Effects of installation on the cyclic axial behaviour of suction buckets in sandy soils. *Applied Ocean Research* 91, 101905 (2019) <https://doi.org/10.1016/j.apor.2019.101905>
- Kim, J., Manspecker, M.P., Thomas, S.N.: Augmenting the synergies of chemotherapy and immunotherapy through drug delivery. *Acta Biomaterialia* 88, 1–14 (2019) <https://doi.org/10.1016/j.actbio.2019.02.012>
- Chen, B.-F., Huang, T.-t.: On fluid-filled mixture model for suction pile foundation analysis. *Ocean Engineering* 188, 106306 (2019) <https://doi.org/10.1016/j.oceaneng.2019.106306>
- Farhat, A., Luu, L.H., Doghmane, A., Cuéllar, P., Benahmed, N., Wichtmann, T. and Philippe, P., 2024. Micro and macro mechanical characterization of artificial cemented granular materials. *Granular Matter*, 26(3), 65 (2024) <https://doi.org/10.1007/s10035-024-01426-2>

Stress-controlled suffusion testing of crushed dam material

Elin Bergliv¹, Jan Laue², Peter Viklander³

1. Luleå University of Technology, Luleå, Sweden, elin.bergliv@ltu.se

2 Luleå University of Technology, Luleå, Sweden

3 Luleå University of Technology, Luleå, Sweden and Hydroresearch AB, Täby, Sweden

ABSTRACT: The stresses induced in a dam caused by its self weight affects suffusion processes inside a dam. Research has shown that adding this external stress on a suffusive soil specimen influence the internal stability. Environmental legislation prohibits the use of naturally rounded sands and gravels for construction projects in Sweden. Therefore, crushed or blasted soil and rock are to be used, having particles that are angular in shape. When loading, angular particles break more easily compared to naturally rounded particles, which might impact particle size distribution, permeability, or porosity. This in turn can potentially impact the internal stability.

A flexible wall, stress-controlled suffusion device is described in this paper to study the impact of confining stress and particle breakage on suffusion of an angular filter material. The migrated particles are collected, and their weight, particle size distribution, and particle angularity recorded.

Keywords: Suffusion; stress-controlled test; internal erosion; particle degradation, angular particles

1 INTRODUCTION

Suffusion tests are performed to evaluate the susceptibility of internal erosion of a soil material. By adding confining stress to a sample, the resistance to internal erosion increases (Wang et al, 2022; Chen et al, 2021; Silva, 2022). The stress state in a dam might also include shear stresses (Chang and Zhang, 2013). Adding shear stresses to a suffusion test gives a more complex internal erosion behaviour (Chang and Zhang, 2013; Liang et al, 2019; Luo et al, 2020). Naturally rounded material has been used in filters and shoulder materials of dams in Sweden historically. Due to environmental aspects, natural materials are nowadays prohibited to be used by Swedish authorities, which leads to the use of crushed and blasted soils as an alternative. This material is in general more angular compared to naturally rounded materials. Angular shaped materials have shown to have higher resistance to internal erosion compared to rounded materials (Marot et al, 2012; Maroof et al, 2021).

Confining and shear stress might cause particle breakage, which in turn can impact the resistance to internal erosion by changed particle size distribution, fines content, porosity, permeability etc. Due to stress concentration and possible larger amount of defects, angular particles tend to break more easily compared to rounded particles (Alaei and Mahboubi, 2012). For an angular material subjected to stress it is important to take the particle breakage into consideration. The aim of this study by using a flexible wall device is to combine suffusion tests and map out effects of particle angularity under different confining stresses to increase the knowledge in the interaction of particle breakage and suffusion.

2 STRESS-CONTROLLED SUFFUSION DEVICE

A stress-controlled suffusion device was made of an existing triaxial apparatus (Figure 1). The cell and two controllers were used to create confining stress for a 50 mm diameter sample. The downwards water seepage was created from gravitational flow, where the vertical position of the water reservoir was adjusted to vary hydraulic gradients. A custom-made bottom cap with an internal funnel allowed for continued migration of particles from the sample to the particle collection outside of the cell. The weight of the collected migrated particles will be recorded at intervals as well as the seepage water.

The planned testing includes confining stresses between 100-500kPa and hydraulic gradients up to 10. The tested material will be an angular filter material. The collected migrated fines will be analysed regarding shape using image analysis. If the shape of the migrated particles deviates from the shape of the particles of the main sample, it can be concluded that breakage has occurred.

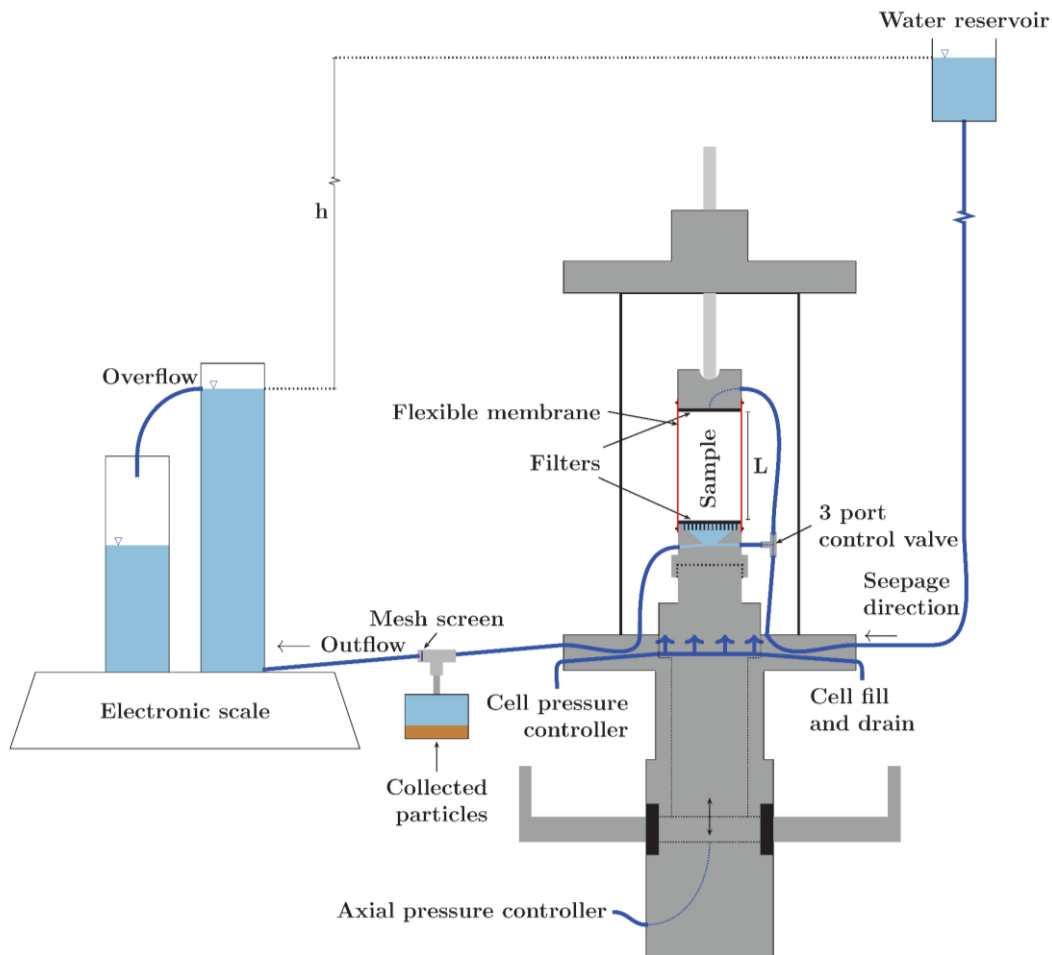


Figure 1. Stress-controlled suffusion device for 50 mm samples with collection of migrated particles.

REFERENCES

- Alaei, E. and Mahboubi, A. (2012). A discrete model for simulating shear strength and deformation behaviour of rockfill material, considering the particle breakage phenomenon. *Granular Matter*, 14(6):707-717. <https://doi.org/10.1007/s10035-012-0367-7>
- Chang, D. S. and Zhang, L. M. (2013). Critical hydraulic gradients of internal erosion under complex stress states. *Journal of Geotechnical and Geoenvironmental Engineering*, 139(9):1454-1467. [https://doi.org/10.1061/\(ASCE\)GT.1943-5606.0000871](https://doi.org/10.1061/(ASCE)GT.1943-5606.0000871)
- Chen, R., Liu, L., Li, Z., Deng, G., Zhang, Y., and Zhang, Y. (2021). A novel vertical stress-controlled apparatus for studying suffusion along horizontal seepage through soils. *Acta Geotechnica*, 16(7):2217-2230 - 2230. <https://doi.org/10.1007/s11440-021-01164-2>
- Liang, Y., Wang, J., Liu, M., Yeh, T.-C., Hao, Y., and Zha, Y. (2019). Onset of suffusion in upward seepage under isotropic and anisotropic stress conditions. *European Journal of Environmental and Civil Engineering*, 23(12):1520-1534 - 1534. <https://doi.org/10.1080/19648189.2017.1359110>
- Luo, Y., Luo, B., and Xiao, M. (2020). Effect of deviator stress on the initiation of suffusion. *Acta Geotechnica*, 15(6):1607-1617 - 1617. <https://doi.org/10.1007/s11440-019-00859-x>
- Maroof, M. A., Mahboubi, A., and Noorzad, A. (2021). Effects of grain morphology on suffusion susceptibility of cohesionless soils. *Granular Matter*, 23(8). <https://doi.org/10.1007/s10035-020-01075-1>
- Marot, D., Bendahmane, F., and Nguyen, H. H. (2012a). Influence of angularity of coarse fraction grains on internal erosion process. *International Conference on Scour and Erosion (ICSE6)*. <https://doi.org/10.1051/ihb/2012040>
- Silva, I. (2022). *Investigation of Suffusion in Glacial Till Dam Cores – Testing methods and critical hydraulic gradients*. PhD thesis, Luleå University of Technology, Luleå, Sweden.
- Wang, G., Deng, Z., Yang, J., Chen, X., and Jin, W. (2022). A large-scale high-pressure erosion apparatus for studying internal erosion in gravelly soils under horizontal seepage flow. *Geotechnical Testing Journal*, 45(6):1037-1053. <https://doi.org/10.1520/GTJ20220045>

Onset of Internal Instability in Gap-Graded BSM Sands

Sara Ataii^{1,2}, Jonathan Fannin³

1. University of British Columbia/Department of Civil Engineering, Vancouver, Canada, sara.ataii@gmail.com

2. BGC Engineering Inc., Vancouver, Canada, SAtaii@bgcengineering.ca

3. University of British Columbia/Department of Civil Engineering, Vancouver, Canada, fannin@civil.ubc.ca

1 INTRODUCTION

In laboratory permeameter testing of a potentially unstable soil gradation, the onset of internal instability is evidenced by any resulting mass loss, change in hydraulic conductivity, and volume change of the test specimen. Ideally, the design of the permeameter device enables all three parameters to be measured in real-time. The erosion response of two gap-graded Bennett South Moraine (BSM) sands is reported herein, using a newly developed triaxial permeameter (TXP) device with this capacity for real-time measurement (Ataii and Fannin, 2022). Analysis of the test results examines the onset of instability with reference rate of mass loss, and the subsequent change in hydraulic conductivity with increased hydraulic loading and mean effective stress, as reported in Figure 1.

2 METHODOLOGY AND RESULTS

The two gap-graded BSM sands had a nominal gap ratio (D'_{15}/d'_{85}) of 10, and an initial finer fraction content (S_f) of approximately 20 % or 25 %, respectively. The size range of the coarser and finer fractions was 1.40 – 3.35 mm and 0.11 – 0.21 mm, respectively. Three specimens of each gap-graded sand were tested in the TXP device. All six specimens were reconstituted to a loose state, using the moist tamping technique, on a base (outflow) wire mesh with 1.37 mm square openings and percent open area of 73 %. After saturation, the gradations were isotropically consolidated to an initial mean effective stress $p'_c \approx 100$ kPa, 150 kPa, or 200 kPa, respectively. Following consolidation, each was subjected to head-controlled multistage downward seepage flow. The magnitude and duration of the hydraulic gradient increments were similar, but not identical, in each test (see Figure 1a): they were selected with the objectives of (i) identifying the onset of mass loss, and (ii) maximizing mass loss. The largest value of applied hydraulic gradient varied between tests, and was governed by the specimen response and the capacity of the TXP device. Upon completion of the seepage stage, the eroded specimens were axially compressed at a displacement rate of 0.25 mm/min, with the objective of characterizing the stress-strain response for analysis with respect to the principles of critical state soil mechanics.

During the seepage stage, hydraulic gradient was calculated using a differential pressure transducer connected across the top (inflow) and bottom (outflow) boundaries of the specimen; mass loss was measured in a back-pressurized chamber located below the base pedestal of the triaxial cell, following the method of Ke and Takahashi (2014); volume change was monitored with reference to change in volume of the cell fluid surrounding the specimen within a double-wall triaxial cell, following the method of Slangen (2015); flow rate was determined using a high-precision weigh-scale under the inflow reservoir supplying water to the top of the specimen.

Results of the six tests are summarized in Table. 1. All specimens exhibited a suffusive response associated with mass loss and insignificant axial and volumetric strains ($\epsilon_{a, \max} = 0.04$ % and $\epsilon_{v, \max} = 0.17$ %). As internal erosion progressed with each increment of hydraulic gradient, the finer fraction content decreased (see Figure 1a) and hydraulic conductivity increased (see Figure 1b). For descriptive purposes herein, the hydraulic gradient at which the mass loss rate exceeded 0.1 g/min for a period of 5 min defines a reference point termed “onset of mass loss” (i_{c-m}), for which values are reported in Figure 1a. The hydraulic gradient at which the hydraulic conductivity increased by more than 5% relative to that of the previous stage, and did not decrease in the next two stages, defines a reference point termed “onset of conductivity increase” (i_{c-k}), for which values are reported in Figure 1b. The 0.1 g/min threshold for the onset of mass loss represents the minimum sensitivity of the TXP mass loss measurement unit. This value represents the observed fluctuation range in mass loss rate in the absence of actual mass loss. These fluctuations were induced by the control system's performance as it tried to maintain constant backpressure at the bottom of the specimen and in the mass loss measurement chamber in a feedback loop.

The relative position and magnitude of the i_{c-m} and i_{c-k} reference points (see Figure 1) distinguishes between the onset of mass loss and change in hydraulic conductivity. It appears the difference is more pronounced in the sand with relatively larger finer fraction content. The difference is tentatively attributed to the competing effects of particle removal and

clogging prior to the development of erosion paths within the sand. Once these paths are established by seepage forces, the specimen experiences significant mass loss accompanied by consistent increase in hydraulic conductivity.

Table 1. Summary of test results

Test ID	Post-Consolidation			Onset		Hydraulic Conductivity			End of Seepage			
	S_{f-c} (%)	e_c	p'_c (kPa)	i_{c-m}	i_{c-k}	k_i (cm/s)	k_f (cm/s)	k_f/k_i	ϵ_{a-EOS} (%)	ϵ_{v-EOS} (%)	e_{EOS}	S_{f-EOS} (%)
E-BSM-10:20-MT-100-D	20.0	0.538	99.7	0.7	1.0	0.184	0.276	1.5	0.02	0.08	0.593	17.0
E-BSM-10:20-MT-150-D	20.2	0.527	149.3	1.0	1.5	0.142	0.163	1.2	0.03	0.09	0.562	18.1
E-BSM-10:20-MT-200-D	20.1	0.514	199.4	1.2	1.5	0.113	0.164	1.5	0.02	0.11	0.558	17.4
E-BSM-10:25-MT-100-D	25.0	0.474	100.0	1.6	1.4	0.029	0.297	10.2	0.01	0.17	0.585	19.2
E-BSM-10:25-MT-150-D	25.0	0.467	150.2	3.0	4.0	0.056	0.201	3.6	0.03	0.12	0.560	20.0
E-BSM-10:25-MT-200-D	25.1	0.466	199.0	6.0	12.0	0.023	0.116	5.0	0.04	0.11	0.523	21.9

S_{f-c} , e_c , p'_c : finer fraction content, void ratio, and mean effective stress at the end of consolidation, i_{c-m} : mass loss-based critical hydraulic gradient, i_{c-k} : hydraulic conductivity-based critical hydraulic gradient, k_i : initial hydraulic conductivity, k_f : last reliably measured hydraulic conductivity, ϵ_{a-EOS} and ϵ_{v-EOS} : axial and volumetric strains at the end of seepage, e_{EOS} and S_{f-EOS} : void ratio and finer fraction content at the end of seepage

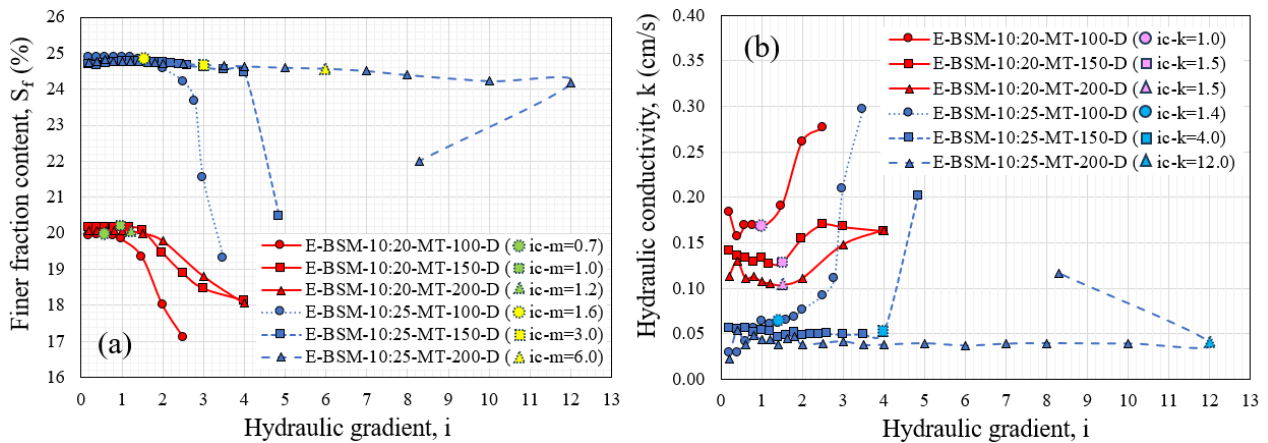


Figure 1. Suffusion response of the gap-graded sands with multistage downward seepage: (a) S_f - i and (b) k - i

3 SUMMARY REMARKS

1. The TXP device enables a real-time determination of any change in mass, volume, and hydraulic conductivity.
2. Mass loss is detected in advance of a small increase in hydraulic conductivity in each gap-graded sand.
3. In the absence of significant volume change, internal erosion took the form of suffusion.
4. The hydraulic gradient to trigger suffusion increases with mean effective stress.
5. Suffusion initiates at a higher hydraulic gradient in the gap-graded sand with greater finer fraction content.

ACKNOWLEDGMENTS

Funding for the university-industry research project was provided by the Natural Sciences and Engineering Research Council of Canada (NSERC) and BC Hydro & Power Authority.

REFERENCES

- Ataï, S. and Fannin, J. (2022). A triaxial permeameter to study the mechanical consequences of internal erosion. Proc. GeoCalgary2022, Can. Geotech. Society, 6p.
- Ke, L. and Takahashi, A. (2014). Triaxial erosion test for evaluation of mechanical consequences of internal erosion. ASTM Geotech. Testing J., 37(2): 347-364.
- Slangen, P. (2015). On the influence of effective stress and micro-structure on suffusion and suffusion. Ph.D. thesis, University of British Columbia, Vancouver, Canada.

Experimental assessment of the mechanical stability of erodible soils injected with fines

Abhijit Hegde¹, Nadia Benahmed¹, Antoine Wautier¹, Pierre Philippe¹, Alexis Doghmane¹

1. INRAE, Aix Marseille Université, RECOVER, Aix-en-Provence, France

ABSTRACT: With the aim of improving the mechanical stability of loose, erodible granular materials, a novel re-enforcement technique, which involves filling the voids of coarse granular material with fine grains, has been explored. An eroded coarse Hostun sand is injected with sieved Fontainebleau fine sand. The size ratio between the two materials ($R = D_{15}$ of coarse/ d_{85} of fines) was varied from 4.6 to 11.3. The concentration profile of fines inside the sample is observed to change from a non-homogenous distribution to a homogenous distribution with increasing size ratio and the maximum amount of fines that we were able to inject does not exceed 4-5% of fine content. Post injection, samples with size ratio of 11.3 are subjected to undrained triaxial tests and the impact of fines is assessed by comparing the mechanical behavior with non-injected samples prepared at similar inter-granular void ratio. It is found that at small strains, the injected fines make the soil less contractive and improve the undrained shear strength of the soil.

Keywords: Suffusion, Fine grains injection, re-enforcement, mechanical behaviour.

1 INTRODUCTION

Internal erosion process such as suffusion occur due to the detachment of fines from the coarse soil skeleton as water seeps through the voids. Eventually, the loss of a significant amount of fines can lead to an overall loss of mechanical stability of the eroded material, which can lead to higher chances to observe the sudden liquefaction of hydraulic structures such as embankments and dykes. A possible strategy for preventing the onset of such mechanical instabilities would consist in injecting fine grains into the coarse, loosen matrix in a way that these fines clog and provide lateral support to the load bearing skeleton of the material. This idea is motivated from recent numerical results (Wautier et al., 2019). Therefore, through this experimental campaign we intend to find further support to the above-mentioned numerical results.

2 INJECTION EXPERIMENTS AND RESULTS

Injection experiments are performed on a coarse, sub-angular Hostun sand 1/2.5 having a D_{15} of 1.37 mm and C_u of 1.4, which has been used previously to study suffusion (Nguyen et al., 2019). Samples are prepared inside a suffusion permeameter (Figure 1) using the moist tamping method in 7 layers of 2 cm each, at a relative density of 20%. The final dimensions of the sample are 140 mm in height and 70 mm in diameter. Next, Fontainebleau sand, NE34, was sieved to obtain fines corresponding to size ratios of 4.6, 4.9, 7, 8.8 and 11.3. After preparation, samples are initially flushed with CO_2 in-order to improve saturation, and then deaerated water is passed through the sample in the upward direction at a very small flow rate of 50 ml/min. After saturation, an air-tight reservoir filled with water and a predetermined amount of fines (40g) is connected to the permeameter. A magnetic agitator is put inside the reservoir to fluidize the fines and prevent sedimentation before injection. Injection is then performed by applying a downward flow on the samples using a pump, at a constant flow rate of 2500 ml/min. After the completion of injection, the concentration of fines in each layer is obtained by, first, gradually slicing 2 cm thick sections along the height of the specimen. Then, the slices are oven-dried and sieved to determine the quantity of fines. The Fines Concentration, F_c , defined as $m_f / (m_f + m_c)$, where m_f is mass of fines and m_c is the mass of coarse fraction, is computed for each layer to obtain the concentration profile, which is shown in Figure 2 for the different size ratios used in our current study. As can be observed, the concentration profile decays exponentially for the smaller size ratios, 4.6 and 4.9, and hence is very non-homogenous. However, by the time we go to 7, the exponential trend turns linear, and at a size ratio of 11.3, the profile gets closer to homogeneity. The measured fine content was 4.3%, 4.2% and 4.2% for $R=4.6$, 4.9 and 7 respectively, and this dropped to 3.3% for 8.8, and 2.5% for $R=11.3$. For $R=11.3$, multiple rounds of injection were performed and after 3 rounds, we were able to achieve a F_c value of 4.4% at which stage the injection was stopped and the sample was subjected to triaxial tests.

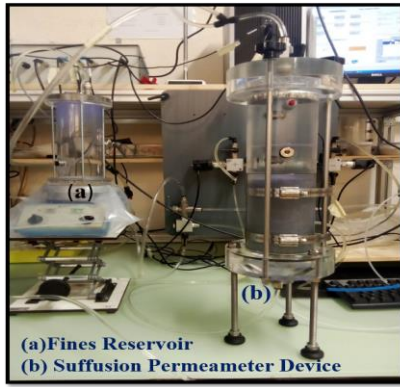


Figure 1. Illustration of the experimental setup used for fines injection.

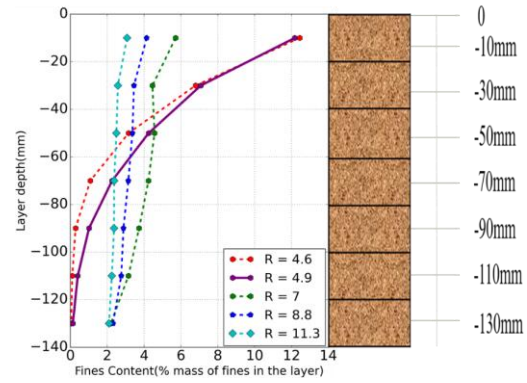


Figure 2. Profile of fines concentration inside the injected sample for different size ratios.

3 MECHANICAL BEHAVIOR

For investigating the effect of the injected fines on the mechanical behaviour, undrained compression triaxial tests are performed on the injected samples as well as on the non-injected ones. For comparison, two set of samples, having a size ratio of 11.3 were chosen. To perform triaxial tests on the injected sample, the sample is first de-saturated and frozen. Then, it is carefully transferred to the triaxial device where it is allowed to thaw under a confining stress of 100 kPa. Next, undrained compression loading is applied under fully saturated conditions ($B \geq 96\%$), effective confining stress of 100 kPa, and a vertical strain rate of 1% per minute. The non-injected and injected samples have the same initial inter-granular void ratio of 0.778. The results of triaxial tests are depicted in Figure 3 and Figure 4. In Figure 3, one can see that the addition of fines has resulted in a significant increase in the undrained shear strength of the injected sample (by ~ 30 kPa). The examination of stress path (Figure 4) shows that the addition of fine grains suppress the existence of a point with q -constant incremental evolution and the subsequent risk of (transient) liquefaction. For large axial strain, both materials (injected and non-injected one) reach the same critical state line, which is probably linked to the fact the mass of injected fine grains remains limited.

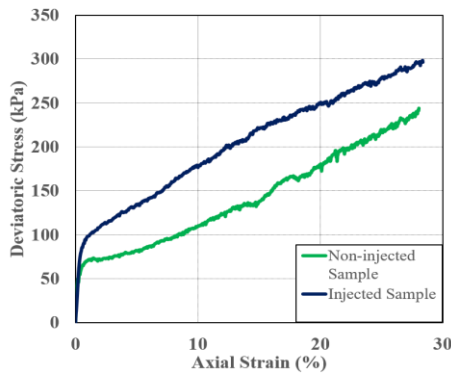


Figure 3. Comparison of the undrained mechanical behavior between injected and non-injected samples in the q - ϵ_a space.

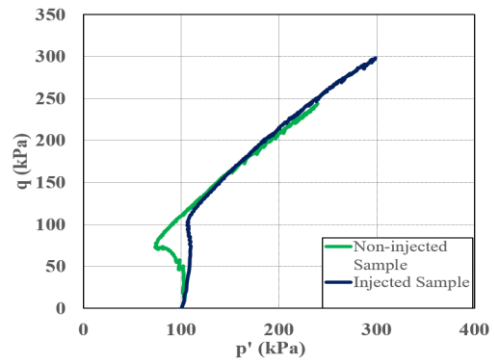


Figure 4. Undrained stress path of injected and non-injected samples.

REFERENCES

Antoine Wautier, Stéphane Bonelli, and François Nicot. (2019). Rattlers contribution to granular plasticity and mechanical stability. *International Journal of Plasticity*, 112:172–193.

Nguyen, C. D., Benahmed, N., Andò, E., Sibille, L., & Philippe, P. (2019). Experimental investigation of microstructural changes in soils eroded by suffusion using X-ray tomography. *Acta Geotechnica*, 14, 749-765

NSSGA (2013). *The Aggregates Handbook*, 2nd ed., National Stone, Sand, and Gravel Association. Alexandria, Virginia.

Effects of initial fines content and repeated seepage on suffusion-induced heterogeneity in gap-graded soils

S. Ruangchai¹, A. Takahashi²

1. Tokyo Institute of Technology, Tokyo, Japan, ruangchai.s.aa@m.titech.ac.jp

2. Tokyo Institute of Technology, Tokyo, Japan, takahashi.a.al@m.titech.ac.jp

ABSTRACT: Seepage-induced erosion tests are performed to investigate the effects of initial fines content and repeated seepage on suffusion-induced heterogeneity in gap-graded soils using a triaxial erosion apparatus. After the erosion tests, spatial variations of the fine fraction are examined by cross-sectional images taken at various depths using a digital microscope with the help of image processing. The observations and measurements indicate that the initial fines content significantly affects the post-erosion heterogeneity of the soils. It is also found that the distribution of fines becomes more uniform in the middle of the specimen as the number of cycles increases.

Keywords: suffusion; triaxial erosion test; spatial fines content distribution; heterogeneity; image processing

1 INTRODUCTION

Many researchers have reported that suffusion/suffosion-type internal erosion significantly influences the mechanical behaviour of soils. However, somewhat contradictory findings have been reported depending on test conditions or researcher and lead to differing conclusions. As for the undrained strength of gap-graded soils, Ouyang and Takahashi (2015) and Mehdizadeh *et al.* (2017) reported an increase in the undrained shear strength due to suffusion/suffusion, while Prasomsri and Takahashi (2020) observed the opposite effect of suffusion on the strength. This discrepancy may potentially be attributed to the suffusion-induced heterogeneity of the soils. Several attempts have been made to examine such a soil heterogeneity induced by suffusion. Deng and Wang (2022) quantified the three-dimensional state of the soils by scanning a transparent soil specimen using a laser sheet during seepage. Nguyen *et al.* (2019) used X-ray CT to investigate changes in the microstructure of granular soil during a suffusion test. In this study, seepage erosion tests are performed to investigate the effects of initial fines content and repeated seepage on suffusion-induced heterogeneity in gap-graded soils using a triaxial erosion apparatus. After the erosion tests, spatial variations of the fine fraction are examined by cross-sectional images taken at various depths using a digital microscope with the help of image processing.

2 OUTLINE AND RESULTS OF EXPERIMENTS

The apparatus used was initially developed by Ke and Takahashi (2014) and was modified by Prasomsri and Takahashi (2020), which allows the seepage flow controlled by pressure. Gap-graded soils (mixtures of Silica No. 3 whose $D_{50} = 1.62$ mm and Silica No. 8 whose $D_{50} = 0.140$ mm) are used in the tests. The specimens are prepared by the moist tamping method to achieve a relative density of 50% with initial fines content (FC) of 10%, 15%, 20% and 25%. The initial effective confining pressure is 50 kPa for all the cases. In the seepage stage, the difference between the inlet tank pressure and base back pressure is gradually increased in ten minutes and maintained at 30 kPa for 30 minutes. Subsequently, the pressure is decreased at the same rate, completing one seepage cycle in around 50 minutes. For the cases with multiple seepage cycles, this process is repeated. The maximum hydraulic gradient during the pressure-maintained period is around seven for initial $FC = 25\%$, while the minimum value is around 0.3 for initial $FC = 10\%$.

Distributions of survived fines obtained from the image analysis for different initial fines contents are shown in Fig. 1. It is observed that larger initial fines content leads to a larger accumulation of fines in the middle part of the sample, which agrees with the observation by Nguyen *et al.* (2019). This may be attributed to the downward flow causes the fines at the top to migrate downward and accumulate in the middle section. The accumulation of fines in this region may result in particle clogging, which can increase the hydraulic gradient and reduce the permeability of the soil. In contrast, specimens with smaller initial fines content exhibit less significant accumulation of fines in the middle part. In the $FC = 10\%$ case, the survived fines distribution appears more uniform, indicating that fines can flow more easily without encountering significant obstructions.

Distributions of the coefficient of variation of fines content after seepage for different initial fines contents are shown in Fig. 2, which provides insights into the heterogeneity of fines distribution within the soil specimen. The

coefficient of variation of fines content ranges from 0.07 to 0.1 before seepage. The larger initial fines content leads to a smaller variation, i.e., relatively uniform, in the middle section. This may be attributed to the larger abundance of fines available for erosion and rearrangement, resulting in a more consistent distribution throughout the middle section. This may hold for the underfilled microstructure but not for the overfilled and filled states, since preferential flow is expected when the fines are more dominant. On the other hand, except for the $FC = 10\%$ case, the smaller initial fines content exhibits more variation in the middle section. This indicates that the distribution of fines is more heterogeneous after erosion. The limited amount of fines available for erosion and rearrangement may lead to more uneven distribution and increased variation. However, when the fines content is very low as in the case with $FC = 10\%$, the variation becomes less in the middle section. This may be attributed to the easy transportation of fines because of the limited presence of fines in the pore spaces, resulting in less variation across the specimen. Regardless of the initial fines content, the variation at the top and bottom of the specimen is large probably because of non-uniform seepage flow around the inlet/outlet.

Histogram and density functions of the survived fines for the whole specimen for different initial fines contents are shown in Fig. 3. The larger initial fines content cases appear to be approximated by a normal distribution. On the other hand, as the initial fines content decreases, the distribution exhibits a bimodal or multi-modal pattern. This indicates a more heterogeneous distribution of survived fines within the specimen.

Similar plots for the cases with different seepage cycles are shown in Figs. 4-6. With the increase in the seepage cycles, more erosion occurs and the distribution of survived fines becomes more uniform in the middle of the specimen.

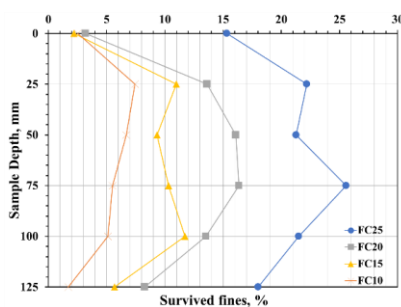


Figure 1. Distributions of survived fines for different initial fines contents.

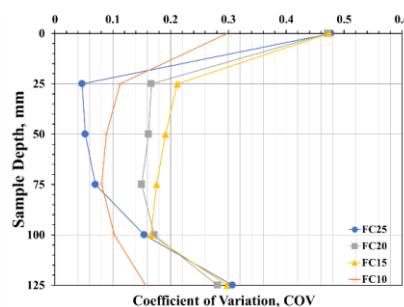


Figure 2. Variation of survived fines for different initial fines contents.

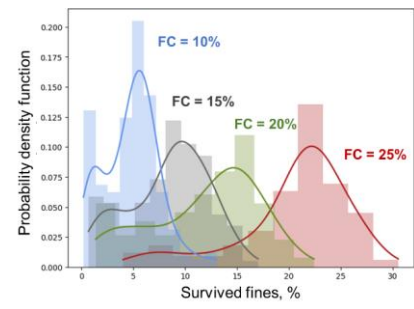


Figure 3. Histograms and density functions for the whole specimen for different initial fines contents.

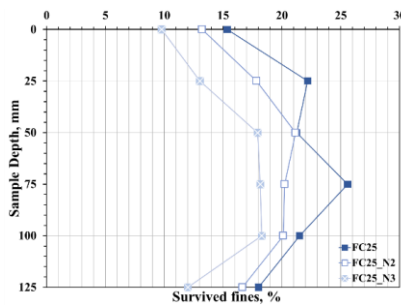


Figure 4. Distributions of survived fines for different seepage cycles.

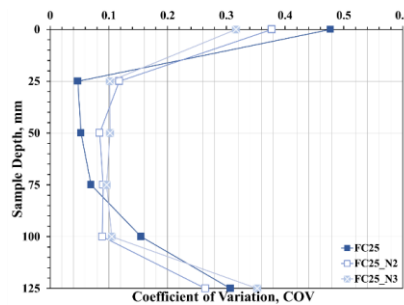


Figure 5. Variation of survived fines for different seepage cycles.

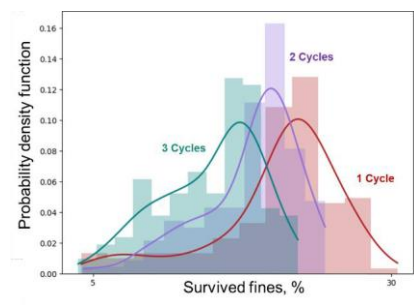


Figure 6. Histograms and density functions for the whole specimen for different seepage cycles.

REFERENCES

- Deng, Z. and Wang, G. (2022). A 3D visualization method for identifying fabric characteristics during suffusion using transparent soil. *Canadian Geotechnical Journal*, 59(10), 1833-1843. <https://doi.org/10.1139/cgj-2021-0191>
- Ke, L., and Takahashi, A. (2014). Triaxial erosion test for evaluation of mechanical consequences of internal erosion. *Geotechnical Testing Journal*, 37(2), 347-364. <https://doi.org/10.1520/GTJ20130049>
- Mehdizadeh, A., Disfani, M. M., Evans, R., Arulrajah, A., and Ong, D. E. L. (2017). Mechanical consequences of suffusion on undrained behaviour of a gap-graded cohesionless soil-an experimental approach. *Geotechnical Testing Journal*, 40(6), 1026-1042. <https://doi.org/10.1520/GTJ20160145>
- Nguyen, C.D., Benahmed, N., Andò, E., Sibille, L. and Philippe, P. (2019). Experimental investigation of microstructural changes in soils eroded by suffusion using X-ray tomography. *Acta Geotechnica*, 14(3), 749-765. <https://doi.org/10.1007/s11440-019-00787-w>
- Ouyang, M., and Takahashi, A. (2015). Influence of initial fines content on fabric of soils subjected to internal erosion. *Canadian Geotechnical Journal*, 53(2), 299-313. <https://doi.org/10.1139/cgj-2014-0344>
- Prasomsri, J., and Takahashi, A. (2020). The role of fines on internal instability and its impact on undrained mechanical response of gap-graded soils. *Soils and Foundations*, 60(6), 1468-1488. <https://doi.org/10.1016/j.sandf.2020.09.008>

Study of development of internal erosion by use of transparent materials

Shane Aulestia¹, Peter Viklander^{1,2}, Jasmina Toromanovic¹, Jan Laue¹

1. Luleå University of Technology, Luleå, Sweden, shane.aulestia@ltu.se

2. HydroResearch AB, Täby, Sweden

ABSTRACT: In this research project, internal erosion, with a focus on suffusion, using transparent soils and image analysis techniques is investigated. The study aims to understand the initiation and progression mechanisms of suffusion by simulating particle size distributions equivalent to ones used in dam cores under different hydraulic conditions. Comparative testing on transparent soils and natural graded moraines will validate the approach for studying internal erosion. The project targets are to understand particle migration within the soil matrix and to provide data for enhanced modelling and rehabilitation practices in dam safety. Insights gained could significantly improve the safety and lifespan evaluation of embankment dams globally, with particular relevance to Swedish dams.

Keywords: Internal erosion; transparent soils; suffusion; silica.

1 INTRODUCTION

Ensuring the safety and lifespan of embankment dams are critical, especially as they age and face increasing environmental and dam safety challenges. Internal erosion is a major concern for embankment dams with soil cores and natural filters. Initiation mechanisms of internal erosion are due to e.g. material properties as particle size distribution and void ratio; hydraulic load and stress conditions. In addition, quality, construction and design of filters are of importance. Suffusion is one type of internal erosion observed in embankment dams having gap-grading particle size distribution in core and/or filter materials, causing washing out of fine-grained particles. Thus, causing increased seepage, and eventually, depending on local conditions, extensive erosion endangering the safety of a dam when passing a critical level. Graded moraines, such as glacial tills, exhibit an increased susceptibility to suffusion when compared to other soil types used in dam construction when one or several fraction sizes are lacking. In Sweden, most of hydropower embankment dams were built more than 50 years ago, therefore aging is a safety concern.

Previous research aimed to enhance dam safety by exploring the susceptibility of glacial tills to suffusion. Silva (2022) reviewed existing methods for assessing soil susceptibility, comparing testing conditions, and presents an experimental study on critical hydraulic gradients for suffusion initiation in glacial till soils. Results indicate that the critical hydraulic gradient depends upon testing conditions, including axial loading, the rate of gradient increase, and time intervals of exposure. Furthermore, it underscores the efficiency of Kenney and Lau (1985, 1986) empirical method adapted by Li and Fannin (2008) and Rönnqvist (2015) for assessing suffusion susceptibility. These insights offer valuable contributions to the assessment and mitigation of internal erosion in embankment dams, thereby addressing a significant safety concern within dams.

Building on Silva's (2022) findings, this study aims to use techniques such as transparent soils and image analysis to investigate the migration of fine particles and the movement of coarse particle clusters under seepage forces. Transparent soils, which have similar properties to natural sands (Sadek et al., 2002; Liu et al., 2003) or clays (Iskander et al., 1994; Iskander et al., 2002), consist of a two-phase medium where refractive index-matching allows solids to represent the soil skeleton and a fluid solution to mimic pore fluids. Various solids, i.e., amorphous silica, silica gel, hydrogel, fused quartz, and laponite, have been employed in conjunction with fluid solutions, depending on the solid, as mineral oil and paraffinic solvent, calcium bromide brine, sucrose solution, or water (Iskander et al., 2015). The project aims to provide deeper insights into how internal erosion processes develop and may affect geotechnical and hydraulic properties on dams.

2 METHODOLOGY

This research investigates the use of silica gels and silica powder combined with the liquid calcium bromide brine to simulate the soil fabric and fluid conditions in embankment dams. The particle size distribution to create transparent soils will use the adapted Kenney and Lau (1985, 1986) empirical method, using different gradations for core materials in embankment dams. Initial experiments will involve oedometer and failing head permeability test to compare the

compressibility and hydraulic conductivity of transparent soils with those of natural graded moraines. This comparison aims to validate the feasibility of using transparent soils for studying internal erosion. Samples will then be subjected to various hydraulic loading conditions to determine the critical hydraulic gradients for gap-graded mixtures, drawing parallels with experimental data from gap-graded moraines.

The use of specific fine grain sizes of moraine mixed with silica will facilitate the tracking of fine particles under seepage forces. Dark grains will enhance visibility through the transparent medium, making it easier to monitor particle movement using image analysis. Maintaining the translucency of the sample mixtures and employing transparent containers will be crucial for effective observation. The insights gained from these experiments may provide valuable data for numerical modelling at a particle level using distinct element methods, which in a later stage of the project will be used to simulate suffusion development in embankment dams, contributing to improved assessment and mitigation strategies for dam safety.

3 OUTLOOK

This research aims to provide better understanding of internal erosion processes, particularly suffusion, in aging embankment dams. Utilizing transparent soil techniques and image analysis, this project aims to visualize and analyze on the migration of fines and the movement of coarse clusters under varying hydraulic conditions. By simulating in the lab environment, the particle size distribution and hydraulic environments similar to conditions found in dam cores, the research work will expose how different gradations and compositions impact the initiation and progression of suffusion. This methodology not only facilitates a direct observation of particle dynamics but also allows a comparison between the experimental data and natural conditions seen in moraines.

Transparent soils offer the potential to replicate the behavior of glacial till cores employed in embankments, particularly those designed for the storage of tailings material in the mining industry, and water retention dams for hydropower. Utilizing transparent soil techniques and image analysis, this project aims into visualization and analysis on the migration of fines and the movement of coarse clusters under varying hydraulic conditions. While there is potential to extrapolate these findings to larger scales, this remains an area for future research. Additionally, the transparency of these soil mixtures is temperature-dependent, needing controlled conditions for optimal results. Despite these challenges, the applicability of these findings could enhance rehabilitation strategies for embankment dams, which are imperative to mitigate potential socio-economic and environmental implications in the event of failure. Given the escalating global demand for mining resources and renewable energy, proactive measures are essential to predict long-term issues, looking for a more sustainable and efficient construction methodologies to extend infrastructure lifespans.

ACKNOWLEDGMENTS

The research presented here was carried out as a part of Swedish Centre for Sustainable Hydropower - SVC. svc.energiforsk.se. Besides, we would like to acknowledge to PPG Industries Inc. for its contribution to this project.

REFERENCES

- Iskander, M., Lai, J., Oswald, C., and Mannheimer, R. (1994). Development of a transparent material to model the geotechnical properties of soils. ASTM International. *Geotech. Test. J.* 17(4): 425-433. <https://doi.org/10.1520/GTJ10303J>
- Iskander, M., Liu, J., and Sadek, S. (2002). Transparent amorphous silica to model clay. *Journal of Geotechnical and Geoenvironmental Engineering*. 128(3): 262-273. [https://doi.org/10.1061/\(ASCE\)1090-0241\(2002\)128:3\(262\)](https://doi.org/10.1061/(ASCE)1090-0241(2002)128:3(262))
- Iskander, M., Bathurst, R. J., and Omidvar, M. (2015). Past, present, and future of transparent soils. ASTM International. *Geotech. Test. J.* 38(5): 557-573. <https://doi.org/10.1520/GTJ20150079>
- Liu, J., Iskander, M., and Sadek, S. (2003). Consolidation and Permeability of Transparent Amorphous Silica. ASTM International. *Geotech. Test. J.* 26(4): 390-401. <https://doi.org/10.1520/GTJ11257J>
- Sadek S., Iskander M., and Liu J. (2002). Geotechnical properties of transparent silica. *Canadian Geotechnical Journal*. 39(1): 111-124. <https://doi.org/10.1139/t01-075>
- Silva, I. (2022). *Investigation of Suffusion in Glacial Till Dam Cores: Testing methods and critical hydraulic gradients*. PhD dissertation, Luleå University of Technology

Injecting Fine Grains into 3D Spherical Packing-Numerical and Experimental Implications

Fan Chen¹, Abhijit Hegde¹, Antoine Wautier¹, Nadia Benahmed¹, Pierre Philippe¹

NRAE, Aix-Marseille University, RECOVER, Aix-en-Provence, France

ABSTRACT: A conceptual countermeasure against suffusion-induced fine sand loss is by re-injecting fines from upstream to induce clogging in the soil matrix. This work attempts to study the infiltration mechanics of fine sand into granular columns combining numerical simulation and laboratory experiments. The base soil used in this work adopts the particle size distribution (PSD) of typical Hostun Sand and different governing factors, such as size ratios, base soil packing density are analysed. The results from numerical and experimental aspects on the fine retention distribution within coarse grain matrix are compared and a simple probabilistic model based on pore-constriction size statistics is put forward to interpret the characteristic infiltration depth L_0 .

Keywords: Suffusion; fine injection; PFV-DEM; micro-mechanics.

1 INTRODUCTION

Suffusion, a significant concern in geotechnical engineering, refers to the internal erosion process where fluid flow washes away finer soil particles, potentially leading to the loss of the soil's finer fraction (Seed et al. 2023; Bonelli, 2013). This process can severely compromise the soil's mechanical stability, posing risks of structural damage or failure over time. The phenomenon is primarily driven by the percolation of fines due to internal fluid flows. One mitigation strategy involves using hydraulic flow to reintroduce fine particles into the coarser soil matrix.

Effective remediation of internal erosion through fine particle infiltration requires a thorough understanding of the influencing factors. Research on grain infiltration has examined variables such as the size ratio of coarse and fine particles (R), the quantity of injected fine particles (affecting collective arching), the coefficient of restitution between particles, and the friction coefficient (Cooke et al. 1978; Gao et al, 2023). Traditionally, studies have simplified the infiltration process using mono-dispersed, gravity-driven infiltration, with particle size ratios limited to a narrow range.

Consequently, existing studies overlook the fluid-driven infiltration in poly-dispersed soils with varying packing densities, which are typical in remediation methods for internal erosion. In this study, a series of experiments and coupled Pore-scale Finite Volumes-Discrete Element Method (PFV-DEM) simulations are conducted to observe the gravity- and fluid-driven infiltration of fine particles into coarse-grain column. The influence of size ratio R is systematically measured via characteristic infiltration distances from both numerical and experimental work. A probabilistic model to interpret the infiltration distance of fines is derived based on the constriction size distribution given by either the numerical model, or a modified Rayleigh distribution from particle size distribution (PSD) of the granular material.

2 EXPERIMENTAL AND NUMERICAL SETUPS

In this experiment, the Hostun sand NH1/2.5 with sub-angular grains shape is selected as the eroded base soil and prepared at a relative density of 20 %. For the injected fine particles, the Fontainebleau sand NE34 with sub-rounded grains shape is adopted. The size ratio of R is calculated by D_{15}/d_{85} as a classic parameter introduced by the well-known Terzaghi retention criterion. To determine different values of R , the Fontainebleau sand was further sieved into different size ranges. An experimental apparatus (Figure 1(a)) of injecting fine-suspension into a coarse column is developed based on a conventional suffusion permeameter device (Nguyen et al, 2019). An air-tight reservoir filled with water and a predetermined amount of fines (40 g for all tests). A magnetic agitator is put inside the reservoir to uniformly disperse the fines in the water and prevent their sedimentation. Then, it is connected to the conventional suffusion permeameter to introduce the fine suspension into the coarse-sand column. The injected fine suspension would be either retained inside or percolate through the column.

In parallel, a PFV-DEM simulations were conducted. Numerical columns with the same PSD used in our experiments are generated. The fine particles of varying size d were randomly positioned above the column and then released under either gravity or hydraulic force resulting from an internal fluid flow (Figure 1(b)) for the two extreme densities (loosest and densest).

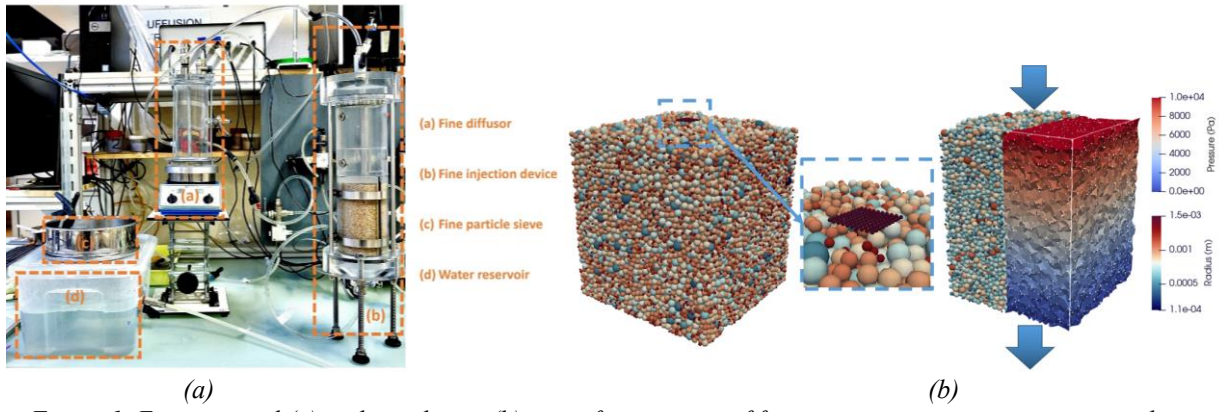


Figure 1. Experimental (a) and simulation (b) setup for injection of fine-suspension into coarse-grain column.

3 RESULTS AND CONCLUSIONS

The passing fraction of fines allows an exponential decaying fitting function to obtain a very crucial measure, the characteristic infiltration depth of fines L_0 , which would allow us to quantitatively compare and describe the efficiency of filters for different parameters of concern, such as relative density, size ratio, etc. The fitting results from experimental and numerical work were found quite consistent. Then, we propose a simple probabilistic model based on the size of the fine particles and the pore-constriction size statistics of the filter, to predict the average penetration distance of the fines within the filter. Knowing the probability density functions for constriction sizes, we can define the probability P_d that a fine particle of diameter d can pass through a constriction in the coarse matrix. Under assumptions of a homogeneity and equal spacing of constrictions, the distance ΔZ between two successive constrictions is related to the mode value of the pore size distribution D_{p50} as indicated in Figure 2(a). To obtain the pore/constriction size distribution, a modified Rayleigh distribution function is introduced based on the PSD of Hostun Sand. Finally, the model is described as below:

$$L_0 = \frac{-1}{(3 - \sqrt{6}) \ln(P_d)} D_{p50}$$

This simple probability model is then used to predict the characteristic infiltration depth L_0 under different packing density and size ratio R . Interestingly, this simple probabilistic model is found to predict quite well the L_0 , showing a linear trend for $\log(L_0)$ versus R in both dense and loose columns (Figure 2(b)). This consistency validates the idea that the average probability P_d of fine particles passing through constrictions in soil with a homogeneous pore-constriction network captures the key physics governing their infiltration.

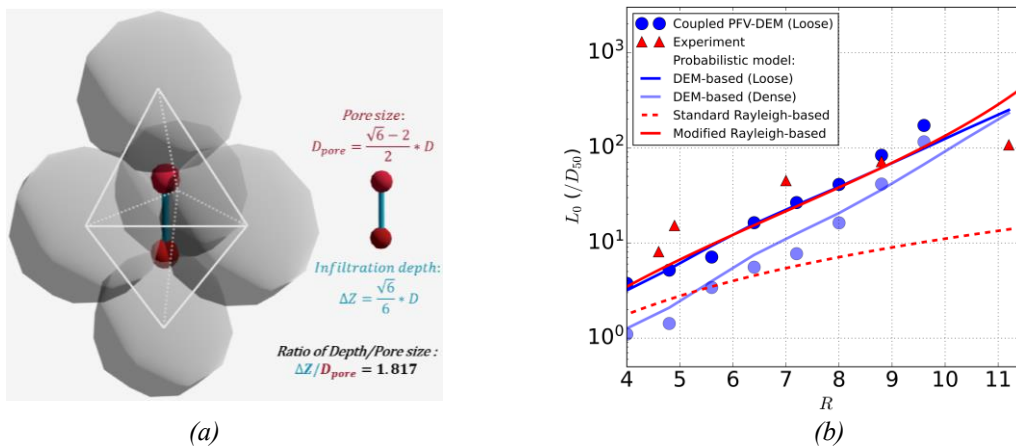


Figure 2. Probabilistic model predicting decaying length: (a) micro-mechanical configuration to calculate ΔZ via D_{p50} ; (b) predicted value of L_0 compared with experimental and numerical results.

REFERENCES

- Seed, H. B. and Duncan, J. M. (1987). The failure of teton dam. *Engineering Geology*, 24, 173–205.
 Bonelli, S. (2013). *Erosion in geomechanics applied to dams and levees*. John Wiley & Sons.

Filtration in granular materials: anisotropy induced effects due to ellipsoidal filter particle shapes

Ali Abdallah¹, Eric Vincens¹, H el ene Magoaric¹, Christophe Picault²

1. Univ Lyon, Ecole Centrale de Lyon, CNRS, ENTPE, LTDS, UMR5513, 36 Avenue Guy de Collongue, Ecully, 69134, France.

2. CACOH, Compagnie Nationale du Rh one, 4 Rue de Chalon-sur-Sa one, Lyon, 69007, France.

ABSTRACT: This work explores how fabric anisotropy mainly induced by anisotropic particle shapes in alluvial materials affects the filtration mechanisms. Using the discrete element method, various numerical samples involving ellipsoidal particles were created and subjected to directional filtration tests. The findings underscore the important role played by particle shapes on the obtained filtration properties in such materials.

Keywords: Particle shape, pore, constriction, connectivity, DEM

1 INTRODUCTION

Dikes along rivers are generally made of alluvial materials collected in the river banks. These anisotropic-shape materials may also be used as protective layers against internal erosion. Their efficiency to mitigate this hazard may be questioned depending of the orientation of flow with respect to the fabric anisotropy which may be pronounced in such materials. For example, in earth embankment dams, seepage flow tends to move parallel to gravity direction, while in filters that are installed on the downstream side of a dike to mitigate internal erosion, it typically follows a horizontal direction. Current design criteria for granular filters, such as particle-size and constriction-based criteria [1,2] do not take in account the direction of flow, assuming that their retention capacity is isotropic in nature. However, granular materials exhibit fabric anisotropy on-site due to deposition methods and applied loads but this latter may greatly be amplified if anisotropic particle shape is involved. Therefore, the main objective of this study is to thoroughly evaluate if and how the direction of flow in alluvial granular filters composed of anisotropic-shaped materials affects their retention capability.

2 METHODOLOGY

The discrete element method (DEM) was used to generate numerical samples with a same grading (coefficient of uniformity of 2.2) and porosity (0.41). To achieve a range of anisotropy levels, ellipsoidal particles with different aspect ratios were used. Table 1 gives the six different particle aspect ratios adopted and the resulting fabric anisotropy magnitudes of the generated samples. Then, using an enhanced dry filtration model [3] numerical filtration tests were conducted in vertical and horizontal directions to analyze the directional retention capacities of filters. Subsequently, an extraction algorithm [4] was employed to obtain the pore space data from the numerical samples, establishing a comprehensive relationship between the anisotropic filtration outcomes and the underlying anisotropic pore structure. In addition to determining the number and size of constrictions in each direction, the directional connectivity within samples was calculated. Specifically, the number of connected pores in a given direction with at least one input and one output constriction larger than the moving particle size was calculated.

Table 1: Aspect ratio of the particles and fabric anisotropy in studied samples.

Numerical sample	Aspect ratio	Fabric anisotropy
Flat	1 : 1 : 1/3	0.384
Partially Flat	1 : 1 : 1/2	0.207
Partially rounded	1.5 : 1 : 0.67	0.222
Spherical	1 : 1 : 1	0.032
Partially elongated	2 : 1 : 1	0.211
Elongated	3 : 1 : 1	0.319

3 RESULTS AND ANALYSIS

Starting with the filtration results, the analysis of directional filtration (vertical and horizontal) reveals that, regardless of particle shapes, filters exhibit distinct retention capacities based on the direction of filtration (Figure 1). Filters tend to retain more fines in the vertical (i.e. gravity) direction. Notably, the difference between the vertical and horizontal retention curves is greatest in samples with high anisotropy. Furthermore, the findings demonstrate the influence of particle shapes on filtration capacity.

The pore space extraction analysis indicated that while the size and number of constrictions could account for the different filtration results among various samples, they did not explain the directional differences observed in the filtration outcomes. However, the analysis of the directional connectivity of the pore space qualitatively demonstrated that horizontal connectivity is consistently greater than vertical connectivity in all samples (Figure 2). This finding may explain the higher retention coefficient observed in the vertical direction compared to the horizontal direction. High connectivity, which signifies a more interconnected pore structure, increases the likelihood of fine particles migrating more extensively within the filter before encountering a blockage.

In conclusion, particle shapes significantly alter the topological and morphological anisotropic properties of granular filters, thus affecting directional filtration processes more than the direction of flow itself. This study highlights the necessity for a comprehensive approach that considers particle shapes to derive filtration properties in order to achieve accurate results. However, this consideration may be oversized in engineering practice.

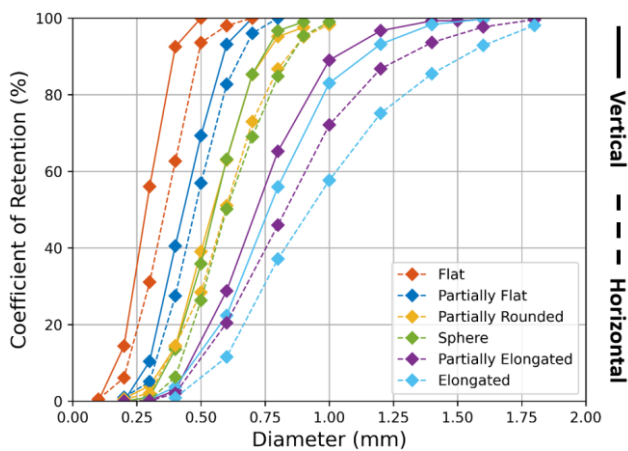


Figure 1: Retention coefficient of the filters with different particle shapes for vertical filtration and horizontal filtration

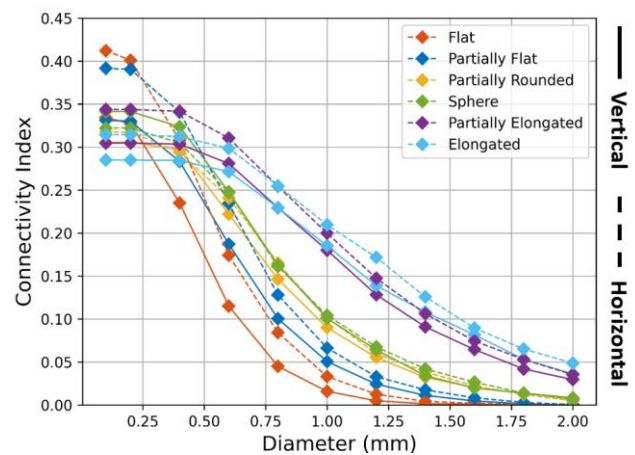


Figure 2: Connectivity index for the filters with different particle shapes in the case of a vertical filtration and horizontal filtration

ACKNOWLEDGMENTS

This work belongs to a project funded by Compagnie Nationale du Rhone (CNR). The authors acknowledge the support of CNR.

REFERENCES

- Terzaghi, K., Peck, R. B., & Mesri, G. (1996). Soil mechanics in engineering practice. John Wiley & sons.
- Indraratna, B., Raut, A. K., & Khabbaz, H. (2007). Constriction-based retention criterion for granular filter design. *Journal of Geotechnical and Geoenvironmental Engineering*, 133(3), 266-276.
- Abdallah, A., Vincens, E., Magoaric, H., & Picault, C. (2024). DEM filtration modelling for granular materials: Comparative analysis of dry and wet approaches. *International Journal for Numerical and Analytical Methods in Geomechanics*, 48(3), 870-886.
- Raeini, A. Q., Bijeljic, B., & Blunt, M. J. (2017). Generalized network modeling: Network extraction as a coarse-scale discretization of the void space of porous media. *Physical Review E*, 96(1), 013312.

Impact of Stress Path on Fabric Evolution and Erodibility of Fine Particles in Gap-Graded Granular Soils

R.R. Dhamne¹, M.M. Disfani¹

*1. Department of Infrastructure Engineering, The University of Melbourne, Melbourne, Australia,
r.dhamne@student.unimelb.edu.au, mmiri@unimelb.edu.au*

ABSTRACT: The mechanical behaviour of gap-graded soils susceptible to suffusion is significantly affected by soil fabric, which undergoes changes in particle arrangement, interparticle contacts, and the pore network. This study examines the impact of axial compression and extension stress paths on the susceptibility of cohesionless fines in gap-graded granular soils with various gap ratios, covering stable, transitional, and unstable soil assemblies using the Discrete Element Method (DEM). Fabric indicators such as variations in global void ratio (e), the formation of contact force chains, and the proportions of inactive, semi-active, and active fines based on the fine coordination number ($Z_{avg,f}$) during shearing were used to illustrate the evolving role of fines in the soil stress matrix under different stress paths. The results indicate that the changes are more significant for fine particles that play a semi-active role compared to those that are inactive or fully active. Consequently, the impact of stress paths on the susceptibility of fine particles is more pronounced for semi-active fine particles.

Keywords: Internal Erosion; Gap-Graded Cohesionless Soil; Stress Path; Fine Particle Contribution; Coordination Number; Discrete Element Modeling.

1 INTRODUCTION

Internal erosion contributes significantly to the instability and potential dysfunction of structures like foundations, dams, and levees. Over the past century, around 50% of dam failures have been caused by internal erosion in form of concentrated leak erosion, backward erosion, soil contact erosion, and suffusion (Richards and Reddy, 2012). Suffusion, a key focus of this study, involves the detachment and transport of fine particles through the soil matrix due to seepage flow. Soils that are susceptible to suffusion, referred to as "internally unstable," undergo detachment, transport, and migration of fine particles when geometrical, stress states and history (Shire et al., 2014), and hydraulic conditions are met. Recent studies on suffusion have increasingly focused on the impact of stress conditions due to their complexity and prevalence in earthen structures. In embankment dams, stress and hydraulic conditions vary by location, with soils typically experiencing anisotropic stress states. The maximum principal effective stress is oblique, forming angles between 0 and 90 degrees relative to the primary flow direction (Chang and Zhang, 2011). This process can result in modifications to the soil pore structure and, under specific conditions, alter its fabric and stress-bearing matrix. These fabric changes influence the soil's overall mechanical properties by causing a readjustment of its particles (Mehdizadeh et al., 2021).

2 DESIGN METHODOLOGY AND BASIC ASSUMPTIONS

Three-dimensional Discrete Element Method (DEM) simulations were conducted to evaluate the impact of stress paths on the erodibility of cohesionless fines in gap-graded granular soils. Cubical assemblies of spherical particles representing gap-graded soils were used in the simulations, employing Particle Flow Code (PFC3D) (Itasca, 2005). DEM samples were generated using non-overlapping spherical particles. Periodic boundary conditions were used to simulate infinite size and reduce boundary effects (Figure 1(b)). The Hertz-Mindlin contact model, which is ideal for non-cohesive interactions due to its nonlinear elastic properties, was used (Shire et al., 2014). The DEM replicated simulated samples with particle-size distributions for gap ratios (GR) of 2, 5, and 7, combined with a fine content (f_c) of 25% (Figure 1(a)). This approach aimed to encompass a range of stable, transitional, and unstable soil assemblies (Shire et al., 2014; Ahmadi et al., 2020). Power-law distribution functions were used to randomly distribute particles among fine and coarse fractions, excluding gravitational effects to prevent segregation and non-uniformity. During consolidation, all specimens were isotropically confined to a constant effective stress of $p' = 140$ kPa. To create dense specimen, the interparticle friction coefficient was set to $\mu_{f0} = 0.1$, respectively. Once equilibrium was reached, μ_{f0} was restored to 0.5, following common DEM practices (Thornton, 2000; Ahmadi et al., 2020).



Figure 1. (a) Particle-size distribution curve for varying gap-ratios, (b) DEM sample.

3 RESULTS AND DISCUSSION

DEM results show that void ratios decrease in gap-graded assemblies as GR increases from 2 to 7 (Figure 2(a)). Conversely, dense packings exhibit increased void ratios under axial compression and extension stress paths due to particle rearrangement. Motivated by findings that fines with zero or single contacts contribute no stress (Thornton, 2000), this study examined the effect of shearing on inactive fines, or rattlers, based on fabric indicator i.e., $Z_{avg,f}$. Semi-active fines (2 to 4 contacts) provide lateral support in the stress matrix, while active particles (>4 contacts) form a solid skeleton (Ahmadi et al., 2020). For soils with GR=2, fine particle types varied minimally under axial compression and extension (Figure 2(b)). However, higher hydraulic gradients may cause internal erosion due to increased semi-active particles and fewer inactive ones during large strains. In soils with GR=5, variations in inactive fines more noticeably change the soil fabric during initial shearing than compression. In soils with GR=7, inactive fines increase at large strains, resulting in more erodible particles. Axial compression shows that specimens with vertical contact normals are more dilative, stiffer, and less erodible (Figure 2(e)), whereas those with horizontal contact normals are more contractive, less stiff, and highly erodible (Figure 2(d)).

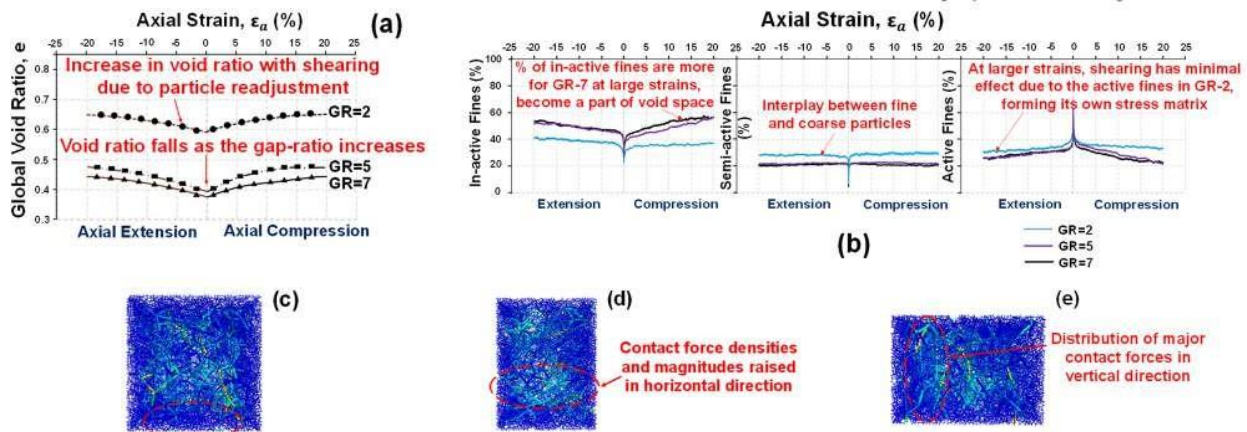


Figure 2. (a) Variation in void ratios across different gap-ratios, (b) Role of fine particle types during shearing based on $Z_{avg,f}$, (c) Contact force chains after confinement stage, (d) Extension, (e) Compression

REFERENCES

- Ahmadi, M., Shire, T., Mehdizadeh, A. and Disfani, M. (2020). DEM modelling to assess internal stability of gap-graded assemblies of spherical particles under various relative densities, fine contents and gap ratios. *Computers and Geotechnics*, 126: 103710. <https://doi.org/10.1016/j.compgeo.2020.103710>
- Chang, D.S. and Zhang, L.M. (2011). A stress-controlled erosion apparatus for studying internal erosion in soils. *Geotechnical Testing Journal*, 34(6): 579-589. <https://doi.org/10.1520/GTJ103889>
- Itasca Consulting Group (2005). PFC3D, v. 3.1. User Manual. Minneapolis, USA.
- Mehdizadeh, A., Disfani, M.M. and Shire, T. (2021). Post-erosion mechanical response of internally unstable soil of varying size and flow regime. *Canadian Geotechnical Journal*, 58(4): 531-539. <https://doi.org/10.1139/cgj-2019-0790>
- Richards, K.S. and Reddy, K.R. (2012). Experimental investigation of initiation of backward erosion piping in soils. *Géotechnique*, 62(10): 933-942. <https://doi.org/10.1680/geot.11.P.058>
- Shire, T., O'sullivan, C., Hanley, K.J. and Fannin, R.J. (2014). Fabric and effective stress distribution in internally unstable soils. *Journal of geotechnical and geoenvironmental engineering*, 140(12): 04014072. [https://doi.org/10.1061/\(ASCE\)GT.1943-5606.0001184](https://doi.org/10.1061/(ASCE)GT.1943-5606.0001184)
- Thornton, C. (2000). Numerical simulations of deviatoric shear deformation of granular media. *Geotechnique*, 50(1): 43-53. <https://doi.org/10.1680/geot.2000.50.1.43>

Analysis of particle migration phenomena. Micro-mechanical modelling and interpretation of lab tests

F. Federico¹, C. Cesali¹

1. Department of Civil Engineering and Computer Science Engineering, University of Rome Tor Vergata, Rome, Italy,
fdrfnc@gmail.com; cesali@ing.uniroma2.it

ABSTRACT: The granulometric compatibility between materials characterized by different grain size distribution (GSD) plays a key role in the safety of zoned embankment dams and levees. The possible migration of fine particles through voids larger than their size, at the contact between different materials due to seepage, has been thus analysed according to two different approaches: a “*traditional*” continuum model and an original numerical procedure, aiming to better highlight and identify the micro-mechanical aspects that govern the growth of the transition effective filtering zone.

Keywords: Particle migration; Granulometric stability; Grain size and volume void distributions.

1 INTRODUCTION

For a reliable simulation of particle migration phenomena at the contact between materials characterized by different grain size curves, the (space and time) variability of granulometric properties, voids volume, porosity (n), permeability (k), flow velocity and direction, local piezometric gradients, should be taken into account. “*Continuum*” approaches allow a partial description of the local variability of these variables, especially the voids volume distribution, VVD, and the related constriction size distribution, CSD. A numerical procedure to simulate coupled particle migration and seepage processes by considering the grain size curve, VVD, CSD, porosity of materials, rate of the suspension, piezometric gradients, drag forces associated with the seepage flow and contact forces induced by confining pressures, as well as their mutual dependency, has been recently developed to overcome these limits.

2 MODELLING APPROACHES

Continuum models. By considering a representative elementary volume of a granular material composed by the volume of particles in suspension, the fluid phase and the solid phase (stable and deposited particles) volumes, the particle migration process can be described, along space x and time t , by the following system of three partial differential equations (PDEs) (Vardoulakis, 2004):

$$\nabla \cdot [(1 - c_s) \cdot n \cdot \vec{v}_f] = - \frac{\partial[(1-c_s) \cdot n]}{\partial t} \quad (1) \quad [\text{fluid mass balance equation}]$$

$$\nabla \cdot (c_s \cdot n \cdot \vec{v}_{sp}) = \frac{\partial[(1-c_s) \cdot n]}{\partial t} \quad (2) \quad [\text{solid mass balance equation}]$$

$$\frac{\partial n(x,t)}{\partial t} = \lambda \cdot [1 - n(x,t)] \cdot c_s(x,t) \cdot n(x,t) \cdot v_{sp}(x,t) \quad (3) \quad [\text{kinetic equation}]$$

\vec{v}_f being the velocity vector of the fluid phase; c_s , the concentration of particles in suspension; n , volumetric porosity; \vec{v}_{sp} , the velocity vector of the suspended and transported particles ($\vec{v}_{sp} = \chi \cdot \vec{v}_f$, with $\chi \in (0; 1]$, Federico, 2017); λ , an experimentally calibrated parameter (Vardoulakis, 2004). If the following hypotheses: (i) $v_{sp} = v_f$ ($\chi=1$, Federico, 2017) and (ii) unidirectional flow (1-D case) are assumed (since $\vec{v}_D = n \cdot \vec{v}_f$, \vec{v}_D being Darcy’s velocity), the above system of PDEs may be solved by an explicit second order method Finite Difference Method (Δx , Δt are space and time integration intervals, respectively; $i = i$ -th element of the system composed by two different contacting materials):

$$c_{s,i}^t = \frac{\frac{1}{2}(c_{s,i+1}^{t-1} + c_{s,i-1}^{t-1}) \frac{n_i^{t-1}}{\Delta t} - v_{D,i,t-1} \cdot \frac{(c_{s,i+1}^{t-1} - c_{s,i-1}^{t-1})}{2\Delta x}}{\left[\frac{n_i^{t-1}}{\Delta t} - (1 - c_{s,i}^{t-1}) \cdot \lambda_i \cdot (1 - n_i^{t-1}) \cdot v_{D,i,t-1} \right]} \quad (4)$$

Proposed procedure. A numerical procedure to simulate coupled particle migration and seepage processes, previously developed by the Authors and based on the model proposed by Indraratna and Vafai (1997), is herein applied. The proposed procedure is thus founded on the fluid and solid mass balance equations, and on the concept of critical hydraulic gradient derived from limit equilibrium considerations, where the migration of particles is assumed to occur under applied

hydraulic gradients exceeding the critical value, this one depending on particle diameter and its confining conditions (plugged or unplugged particles), coupled to the effective “internal geometry” of the porous materials (i.e. Constriction Sizes Distribution, CSD, instead of an average diameter of voids) (for more details please see Federico and Cesali, 2018).

3 APPLICATION AND COMPARISON

The continuum approach and the proposed numerical procedure (PNP) have been applied to the lab experimental results obtained by Locke et al. (2001). Particularly, the effects of a downward seepage flow through a system *B-T* composed by a well-graded sand (150 mm thickness), as base soil (*B*), and a well-graded gravel (800 mm thickness), as transition (*T*), are measured. Transition material (*T*) is characterized by *D*15 (particles diameter corresponding to the 15% passing) = 10.1 mm; different base soils (*B*), characterized by *d*85 (particles diameter corresponding to the 85% passing) satisfying the values of the piping ratio *D*15/*d*85 = 4 and 7 (as from *Terzaghi* criterion limits) are tested. The main results provided by the “continuum approach” are “porosity vs distance”, “concentration of suspended particles vs distance”. The PNP, in addition to these “global” variables, also provides information at the micro (*particle*) scale, particularly the GSD and CSD curves. The comparison (Figure 1) between measured and numerical (according to both approaches) values of the “mass (M_{PT}) passing through the transition material [g/cm^2]” is carried out ($M_{PT} = c_s \cdot n \cdot \rho_s \cdot V/S$; ρ_s being the grains density/unit weight; *S*, the area of the sample cross section; *V*, the volume of the sample). The Figure 2 shows the additional results at the microscale provided by the PNP in terms of final GSD and CSD curves at different distances from B-T interface.

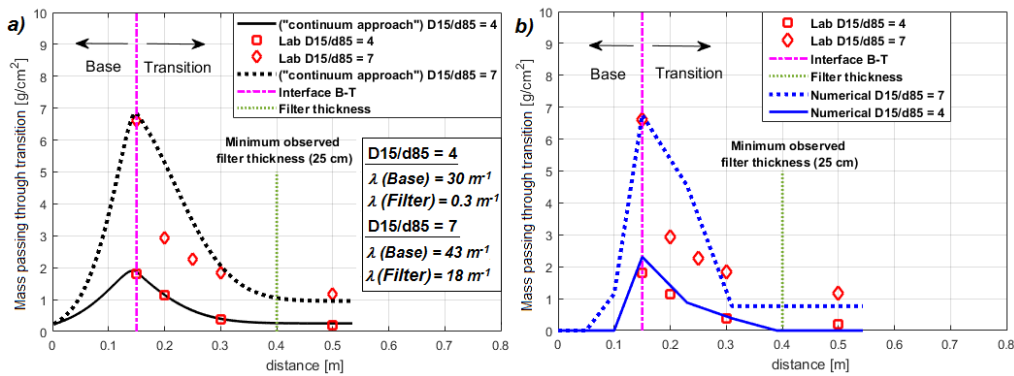


Figure 1. “Mass passing through transition” vs distance according to: a) “continuum” approach; b) PNP.

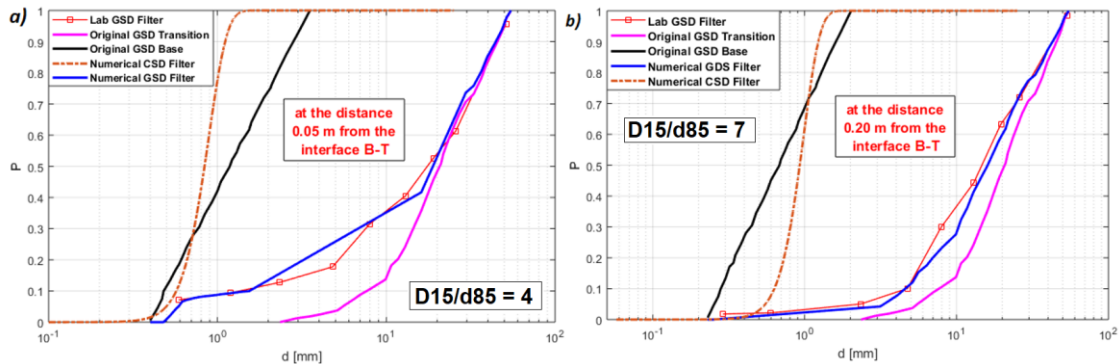


Figure 2. PNP: final GSD and CSD curves of transition (*T*): a) for $D15/d85 = 4$, at the distance from the interface B-T of 0.05 m, b) for $D15/d85 = 7$, at the distance from the interface B-T of 0.20 m.

4 MAIN CONCLUDING REMARKS

The combined application of the two approaches (*continuum* model and proposed numerical procedure, PNP) allowed firstly the validation of both methods as well as the simultaneous understanding of the macroscopic effects of the phenomenon due to aspects and processes at the microscopic level.

REFERENCES

Federico, F. (2017). Particle migration phenomena related to hydromechanical effects at contact between different materials in embankment dams. *GRANULAR MATERIALS*, ISBN 978-953-51-5423-5, INTECH.

Numerical analysis of bearing capacity factors for uplift mechanism

Federico Pilati¹, Fabio Gabrieli¹, Francesco Zarattini¹

1. University of Padua, Department of Civil, Environmental and Architectural Engineering, Padua
francesco.zarattini@unipd.it

ABSTRACT: The uplift failure mechanism in levees is triggered by the development of high pressures in foundation soil, at the interface between a shallow cohesive layer and an underlying sand layer, hydraulically connected to the riverside. The uplift mechanism has similarities with the failure mechanism of a strip anchor embedded in clay and subjected to pull-out forces. Upper and lower bound solutions of bearing capacity factor N_c of horizontal anchors were derived from numerical analyses by Merifield *et al.* (2001). In this work a numerical study of N_c was performed, based on numerical analyses of Merifield *et al.*, in order to simulate an uplift mechanism. At first, models were created with homogeneous undrained material and no self-weight. Then, the case with the introduction of a sand layer below the shallow clay layer was examined. Lastly, a unit weight was assigned to the material in the case of homogeneous clay. From these models the ultimate pull-out capacity q_{ult} was obtained by varying the embedment depth H , from which N_c is derived.

Keywords: Uplift; Bearing capacity factor; Soil unit weight; Anchors; Pull-out capacity.

1 INTRODUCTION

The uplift failure is an instability mechanism of levees triggered by the development of high pressures beneath the toe of the earth structure. This failure mechanism requires a specific stratigraphic condition, consisting of a shallow weak low-permeability layer, overlying a coarser and more permeable one, this latter acting as a hydraulic preferential flow path between riverside and landside. The behaviour of the interface between foundation layers, subjected to uplift pressures, is similar to that of a horizontal anchor embedded in soil and subjected to pull-out forces. In Merifield *et al.* (2001) the problem of pull-out resistance of anchors was examined by applying numerical analysis, in order to obtain rigorous bounds of the ultimate pull-out capacity, by using formulations of the upper and lower bound of limit analysis. The assumptions of this modelling are:

- The undrained shear strength c_u of clay is represented by the Tresca yield criterion;
- Material has no unit weight ($\gamma = 0$);
- An imposed displacement is applied to the nodes of the anchor base.

The purpose of this work is to study the uplift mechanism through FEM analysis, following the same geometry and geotechnical properties of the numerical model of Merifield *et al.*, but assigning a uniform pressure along the anchor size. Many models were analysed in order to determine the ultimate pull-out capacity for various cases. The ultimate anchor pull-out capacity q_u in undrained clay is expressed by this formulation:

$$q_u = c_u \cdot N_c \quad (1)$$

where N_c is the bearing capacity factor (or break-out factor). N_c consists in two terms: the first one is independent of soil weight, while the second depends on soil weight. Then, the expression of q_u becomes:

$$q_u = f(c_u, H, B) + f(\gamma, H) = c_u \cdot N_{co} + \gamma H \cdot N_q \quad (2)$$

where N_{co} is the bearing capacity factor independent of weight, B is the anchor size, H is the embedment depth and N_q is the contribution of the capacity factor dependent on the soil weight. The break-out factor N_{co} is a logarithmic function of the embedment ratio H/B .

2 RESULTS AND DISCUSSION

In this work finite element simulations were carried on, using the software *MIDAS FEA NX*, to study the value of N_c in relation to H/B for some combinations of parameters. At first, the model was created by applying an imposed

displacement along the anchor size B , in order to replicate the results of Merifield *et al.* Then, the same model was created, but applying an upward pressure along B in order to see the differences with the case of imposed displacement. The results of these two analyses are reported in the $H/B - N_{co}$ graph in Figure 1, compared with lower and upper bound solutions of Merifield *et al.* Both analyses are near to the lower bound solution and there are no big differences between them. The next step was to simulate the presence of a sand layer beneath the anchor. The sand was modelled using the Mohr-Coulomb yield criterion. Two cases were examined: one with a continuous sand layer below the clay layer and one with a sand layer interrupted at the end of anchor size B . The results of these two cases are reported in Figure 2, compared with lower and upper bound solutions. Both cases showed values N_c lower than lower bound solution due to loss of resistance contribution provided by clayey material.

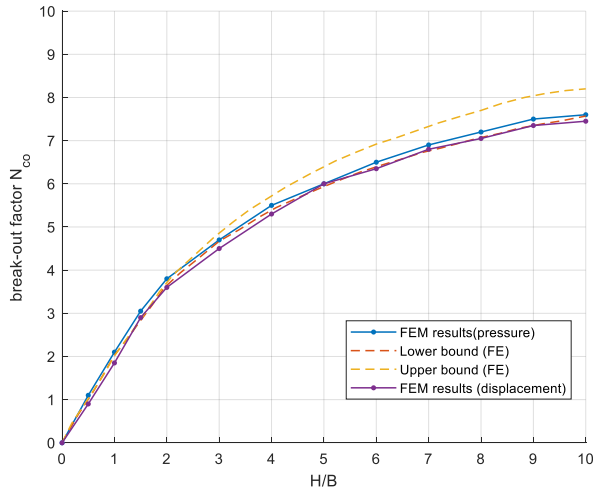


Figure 1. Comparison between homogeneous material FEM results and upper and lower bound solutions.

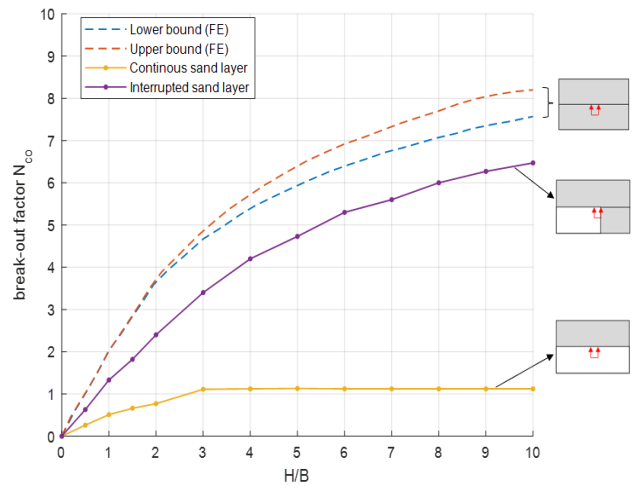


Figure 2. Comparison between continuous and interrupted sand layer FEM results and upper and lower bound solutions.

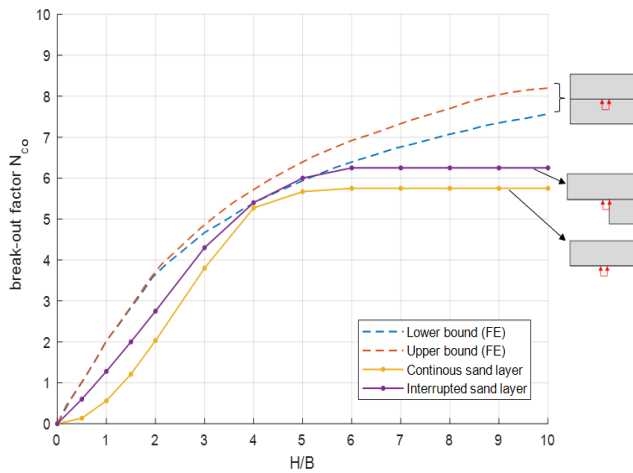


Figure 3. Comparison between continuous and interrupted sand layer FEM results (No sand mesh) and upper and lower bound solutions.

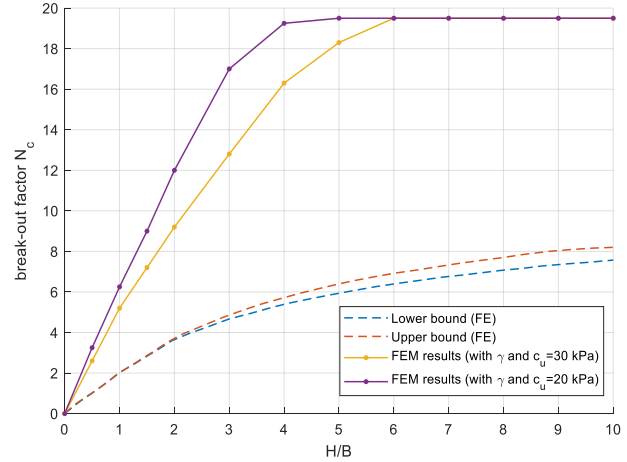


Figure 4. Comparison between homogeneous material FEM results (with unit weight) and upper and lower bound solutions.

Applying the same analyses but deleting sand mesh, the results are shown in Figure 3. Even in this case, the analyses provided values of N_c lower than the lower bound solution, and the curves reach a constant value of N_{co} after the value of H/B for which the failure mechanism does not involve the free surface and becomes localized near the anchor.

Lastly, the case of homogeneous clay with an assigned unit weight of 20 KN/m^3 was examined. In Figure 4 the results are presented, for the case with undrained shear stress $c_u = 30 \text{ kPa}$ and $c_u = 20 \text{ kPa}$. Both cases showed values of N_c much higher than upper and lower bound solutions and a constant stretch for high embedment ratios. In both cases it is derived, through Eq.2, that N_q is near to 1 where N_c is increasing, while it is lower than 1 where N_c is constant.

REFERENCES

Merifield, R. S., S. W. Sloan, and H. S. Yu. "Stability of plate anchors in undrained clay." *Geotechnique* 51.2 (2001): 141-153.

On the identification of the saturation line in the earthen levees: a comparison between a physically-based model and a practical approach

B. Bonaccorsi^{1,2}, S. Barbetta², T. Moramarco², G.T. Aronica¹

1. Dipartimento di Ingegneria, Università di Messina, 98158 Messina, Istituto di Ricerca per la Protezione Idro-geologica, Consiglio Nazionale delle Ricerche (IRPI-CNR), Perugia

ABSTRACT: Earthen levees are one of the main structural measures against flooding in floodplain areas. They basically reduce the flood hazard when remain undamaged during severe floods; however, they can collapse for different failure mechanisms, causing huge financial and social losses. The seepage-induced piping phenomenon has received much attention due to frequent occurrence in the recent past leading to significant damages. In this context, the present work investigates the seepage process in earthen embankments, applying and comparing the outcomes of: 1) a practical approach based on the Marchi's equation (Marchi, 1961) and 2) a two-dimensional (2D) numerical model (SEEP/W). The analysis is addressed to define the vulnerability to seepage and the impact of boundary/initial conditions and flood characteristics on the estimated vulnerability. To this end, with the comparison between the Marchi's equation and the numerical model, it is demonstrated that the approach of Marchi achieves results more in favour of safety. In addition, through SEEP/W can be confirmed that an initial condition of the soil more saturated increases the probability of failure.

Keywords: Risk, levee, seepage, failure.

1 INTRODUCTION, CONTEXT, MOTIVATION

Each year, the impact of flood events is very significant in terms of damage caused on infrastructures and, above all, loss of life. Earthen levees are one of the most widespread structural measures to protect people from flooding even if, frequently, these structures can failure due to different mechanisms. For this reason, an organization of six countries (France, Germany, Ireland, Netherland, United Kingdom and USA) published in 2013 the International Levee Handbook (ILH), providing a practical guidance for the design and management of embankments, with the aim of making acceptable also a possible collapse of these structures. Many mechanisms can cause the levee breaches formation, although the most common are overtopping and piping (Orlandini et al., 2015; Palladino et al., 2019). Piping is a very dangerous mechanism because it is not clearly visible and, for this reason, hard to identify in time.

In scientific literature, many authors studied this process with the aim of identify the saturation line, using both simple expeditious and physically-based models. The former can be applied in large scale analyses to investigate the vulnerability of extensive levee systems; the latter can be used for deeper investigation in selected case studies since their application requires the knowledge of hydraulic and geotechnical parameters.

In this study, the saturation lines identified through a practical procedure based on the Marchi's equation and the 2D finite element model SEEP/W are evaluated and compared. Moreover, SEEP/W is applied to investigate the impact of initial condition (i.e. saturation water content) and different characteristics of the material (i.e. residual water content, soil type, hydraulic conductivity) on the identification of the saturation line.

2 EQUATIONS

For the assessment of the saturation line, Barbetta et al. (2017) developed a practical procedure based on Marchi equation:

$$H(x) = (h'_0) \left[1 - \operatorname{erf} \left(\frac{x}{2} \sqrt{\frac{\varepsilon}{K_s H_0 D}} \right) \right] \quad (1)$$

where h'_0 = water head, H_0 = groundwater depth, D = duration of the flood event, K_s = hydraulic conductivity, ξ = soil porosity, erf = error function, i.e. twice the integral of the Gaussian distribution with zero mean and variance equal to

0.5. (Figure 1). To evaluate the saturation line location through physically-based approach, the numerical model SEEP/W was used in the present work. SEEP/W, part of GeoStudio software, is a finite element model (FEM) able to solve the simple saturated steady state problems and also saturated/unsaturated time dependent problems. There are three main parts to a finite element analysis: the first is the numerical domain, including the selection of an appropriate geometry and a discretized mesh; the second is the specification of material properties and the third is the definition of the appropriate boundary conditions. The comparison between the seepage lines evaluated with the two methods (Figure 2a) show that the lines are very similar, as it can see in the Table 1 where the performance through the Root Mean Square Error (RMSE) is summarized. Specifically, the saturation line estimated through Marchi's equation is more cautionary than the same one assessed with SEEP/W since it provides a higher maximum length of infiltration (x_{max}). However, SEEP/W simulates more accurately the seepage process, also setting the characteristics of the soil; Figure 2b shows the different lines obtained by assuming different residual volumetric water content values with a fixed saturated volumetric water content. The volumetric water content describes the capability of the soil to store water; therefore, when the residual volumetric water content increases, the soil is more saturated and the seepage line grows, while the maximum length of infiltration decreases. For this reason, a more saturated soil could rise the probability of failure.

3 TABLES AND FIGURES

Table 1. Assessment of the Root Mean Square Error for different water heads

water head (m)	RMSE
0.5	0.06
1	0.13
1.5	0.15
2	0.25
2.5	0.24
3	0.41

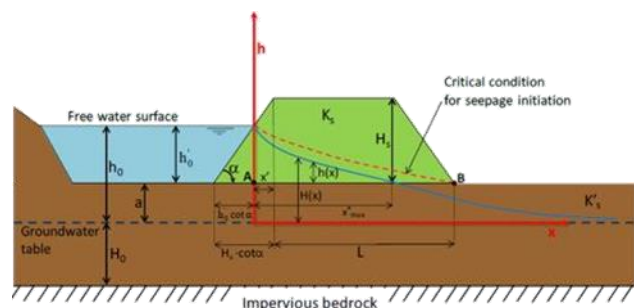


Figure 1. Saturation line for a levee with known geometry (for symbols see text).

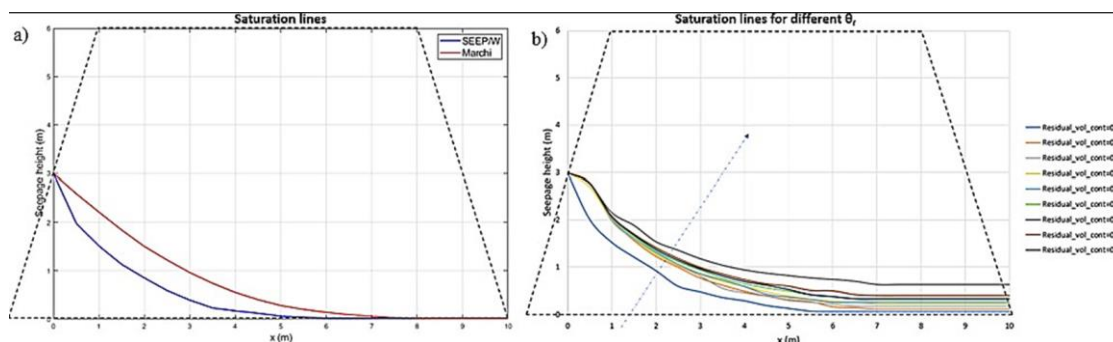


Figure 2. a) Saturation lines assessed with Marchi's equation and SEEP/W (fixing $\theta_r = 0.2$ and $\theta_s = 0.5$); b) Seepage lines considering different residual volumetric water content values θ_r and a fixed saturated water content equal θ_s to 0.5.

REFERENCES

Barbetta, S., Camici, S., Bertuccioli, P., Palladino, M.R., Moramarco, T., (2017). Refinement of seepage vulnerability assessment for different flood magnitude in National levee database of Italy. Hydrology Research - Special Issue Hydrology Days, IWA Publishing.

CIRIA, Ministry of Ecology, USACE. (2013). The International Levee Handbook.

Marchi, E. (1961). Sulla filtrazione attraverso gli argini fluviali (On the infiltration process within levees). In: Proceedings of VII Convegno di Idraulica e Costruzioni Idrauliche, Palermo, Italy.

Orlandini, S., Moretti, G. and Albertson, J. D. (2015): Evidence of an emerging levee failure mechanism causing disastrous floods in Italy, Water Resour. Res., 51, 7995–8011.

Palladino, M. R., Barbetta, S., Camici, S., Claps, P., & Moramarco, T. (2020). Impact of animal burrows on earthen levee body vulnerability to seepage. Journal of Flood Risk Management, 13 (Suppl. 1), e12559.

Conclusions from the Performance Assessment of Industry Applicable IE Initiated Breach Prediction Models

M.W. Morris¹, J-R. Courivaud²

1. HR Wallingford, Oxfordshire, UK; mark.morris@samuifrance.com

2. EDF-CIH, Bourget du Lac, France; jean-robert.courivaud@edf.fr

ABSTRACT: Progress with the EDF funded Performance Assessment of Industry Applicable IE Initiated Breach Prediction Models project was reported at previous meetings of the Internal Erosion Working Group. Since then, the project has concluded the performance analysis for the 3rd and final phase of the assessment programme, investigating the range of uncertainty in all aspects of the observed and modelled breach test cases. A brief overview of the project will be provided, followed by a summary of findings from each of the model assessment phases, along with overall conclusions.

Keywords: Dam and levee breach; breach modelling; internal erosion initiated breach.

Numerical modeling of internal erosion in the foundation of Agly river dikes (France)

S. Bonelli¹, L. Girolami^{1,2}

1. INRAE-Aix-Marseille University, UMR RECOVER, Aix-en-Provence, France, stephane.bonelli@inrae.fr

2. University of Tours, Laboratoire GÉHCO, Tours, France, laurence.girolami@inrae.fr

ABSTRACT: The subsurface soils beneath the river dikes and in the protected zone are mostly composed of permeable sediments. Flood-induced seepage flows can lead to internal erosion processes in these permeable layers. The issue addressed here concerns the influence of the shape of these permeable layers on the initiation and development of internal erosion, and its consequences. This analysis is carried out using a finite-element numerical model with several two dimensional geometries of a typical profile of Agly dike (France). Twenty successive floods are considered. The variations of two quantities of interest are analyzed: the artesian zone size, promoting leaks and sand boils, and the uplift zone size, promoting hydraulic fracturing and fluidisation.

Keywords: Flood protection dikes; foundation; internal erosion; suffusion; numerical modelling.

1 INTRODUCTION

The foundation soils of river dikes are often made up of permeable layers. These layers correspond to the history of the river, in terms of paleo-valley and paleo-channels (Girolami, 2023). These layers are not necessarily tabular. The question then arises as to whether the shape of these layers can have an influence on the initiation of internal erosion, and on its development. This paper takes up the modelling carried out in Girolami et al. (submitted) on the case of the Agly dikes, where numerous sinkholes and sand boils have been observed (Tourment et al., 2018).

2 FINITE ELEMENT MODELLING

The model is based upon on the mixtures theory initially introduced by Vardoulakis et al. (1996). The erosion law is based on Darcy velocity and a critical velocity (erosion threshold). The critical velocity is given by the empirical expression of Kovacs and Ujfaludi (1983) rewritten to have dimensional consistency similar to the expression of Patrashev and Pravedny (1965), in Radchenko et al. (2012). The erosion law is driven by an erosion coefficient similar to that of Wan and Fell in a similar way to Bonelli and Marot (2011). The increase in the specific permeability of sandy gravel due to suffusion is quantified by the Kozeny-Carman equation with a new description based on the bimodal character of the soil (Fig. 1a). Four two dimensionnal geometries were considered (Fig 1b): G1 corresponding to a classical tabular geometry; G2, G3 and G4 incorporating a reduction in the thickness of the permeable layer, from 10 m to 2 m, at different x-coordinate. The water level on the river side corresponds to twenty consecutive floods.

3 NUMERICAL MODELLING RESULTS

Fig. 2 shows the three locations where internal erosion is initiated, and the two areas where it develops. By studying the pore pressure at the base of the topsoil, we can quantify the size of the zone where this pressure is artesian (promoting leaks and sand boils), and the size where this pressure corresponds to an uplift condition (promoting hydraulic fracturing and fluidisation). Fig. 3 shows the evolution of the size of these two zones as a function of the number of floods. This set of results shows that the shape of the paleo-valleys has an influence on the initiation and development of internal erosion in the subsurface soil, beneath the dike and in the protected zone. To improve the description, the three-dimensional geometry of the paleo-valley should be taken into account, and it would be necessary to model possible contact erosion of the sandy silt layer beneath the gravelly sand layer, and contact erosion of the base of the dike or topsoil.

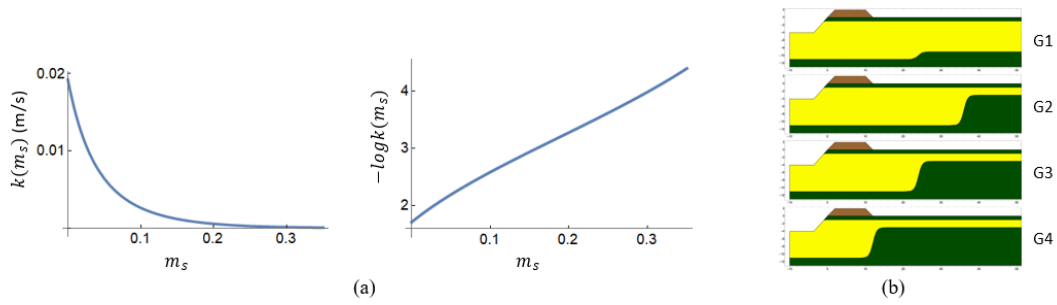


Figure 1. (a) Influence of the sand volume fraction m_s on hydraulic conductivity k of sandy gravel; (b) The four geometries studied deduced from geophysical measurements (Girolami et al., 2023), where the permeable sandy gravel is in yellow ($4 \times 10^{-5} \leq k \leq 2 \times 10^{-2}$), and the low permeability sandy silt is in green ($k=10^{-6}$ m/s).

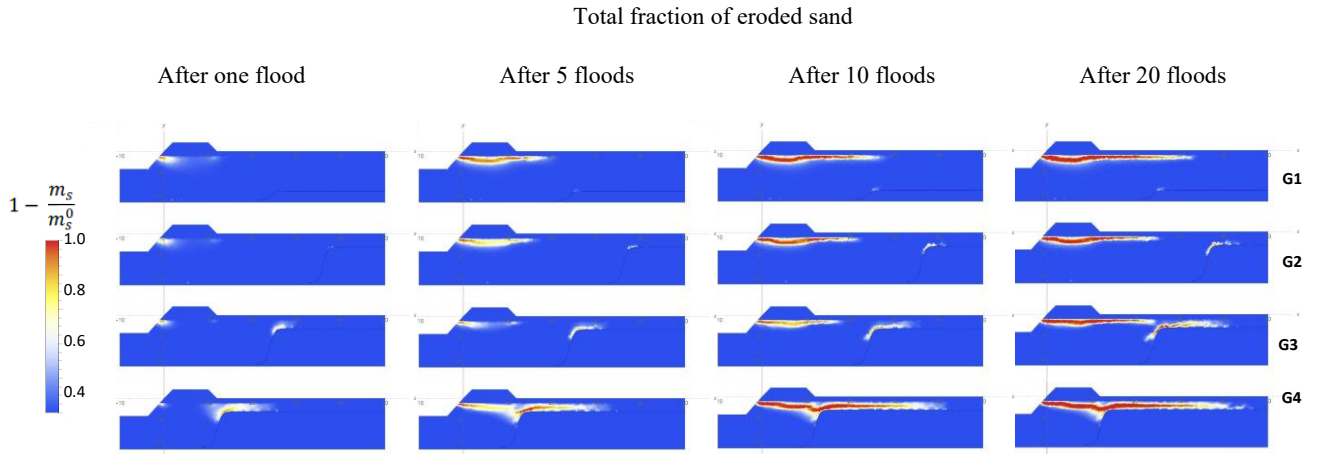


Figure 2. Volume fraction field of eroded sand $1 - m_s/m_s^0$ for the four geometries, at various times.

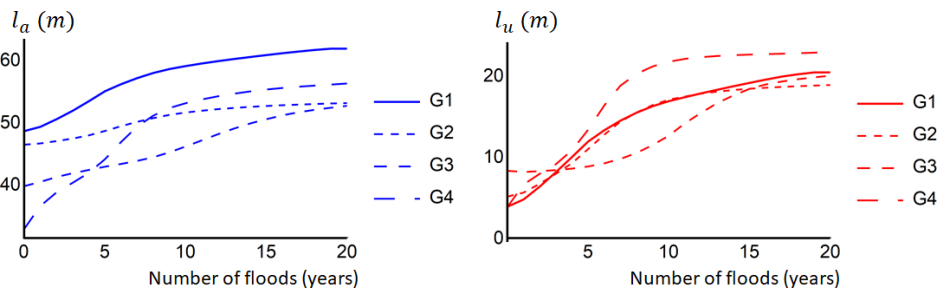


Figure 3. Artesian zone size l_a (promoting leaks and sand boils) and uplift zone size l_u (promoting hydraulic fracturing and fluidisation) in the protected area as a function of the number of floods (and according to time in years if there is one flood per year).

REFERENCES

- Bonelli, S. and Marot, D. (2011). Micromechanical modelling of internal erosion, *Eur. Journ. Env. Civil Eng.*, 15(8): 1207-1224.
- Girolami, L., Bonelli, S., Valois, R., Chaouch, N., Burgat, J. (2023). On Internal Erosion of the Pervious Foundation of Flood Protection Dikes, *Water*, 15(21), 3747.
- Girolami et al., On the origin and distribution of erosion signatures around flood protection dikes (submitted).
- Kovacs, G., Ujfaludi, L. (1983). Movement of fine grains in the vicinity of well screens, *Hydro. Sci. J.* 28(2): 247-260.
- Radchenko, V., Belkova, I., Rummyantsev, O. (2012). The Russian practice of earth dam seepage strength. *Proc. ICSE-6, 6th International Conference on Scour and Erosion*, SHF, Paris, Paper 281, pp. 577-584.
- Tourment, R., Benahmen, N., Nicaise, S., Meriaux, P., Salmi, A., Rougé, M. (2018). Lessons learned on the damages on the levees of the Agly River, analysis of the sand-boils phenomena. *Proceedings of the 26th ICOLD Congress*, Q.103 R.21, Vienna.
- Vardoulakis, I., Stavropoulou, M., Papanastasiou P. (1996). Hydro-mechanical aspects of the sand production problem. *Transport in porous media*. 22(2): 225-244.
- Yang, J., Yin, Z.Y., Laouafa, F., Hicher, P.Y. (2019). Internal erosion in dike-on-foundation modeled by a coupled hydromechanical approach. *Int. J. Numer. Anal. Methods Geomech.*, 43, pp. 663-683.

Numerical simulation of erosion mechanisms in Agly dike

Z. Deng^{1,2}, S. Bonelli¹, L. Girolami^{1,3}, N. Benahmed¹, P. Philippe¹, G. Wang²

1. RECOVER, INRAE Aix-Marseille Université, Aix-en-Provence, France

2. School of Civil Engineering, Chongqing University, Chongqing, China

3. GêHCO, Campus Grandmont, Université de Tours, Tours, France

ABSTRACT: This study aims to investigate the mechanism responsible for the numerous erosion signatures (sand boils, sinkholes, and leaks) observed at the Agly dike through numerical simulations. Numerical configurations were mapped according to stratigraphic structures revealed by geophysical measurements (EMI and ERT). A multi-species transport finite element method was employed to simulate the erosion process in the sandy gravel sediments. The evolution of seepage and erosion fields during periodic flood events was examined. The results indicate that suffusion and contact erosion at the paleo-channel throat might be responsible for the formation of sinkholes, while the emergence of the sand boils and leaks can be attributed to the high confined pore water pressure acting on the low-permeable surface layer.

Keywords: River dikes; internal erosion; geophysical observations; numerical simulations.

1 INTRODUCTION

Suffusion and contact erosion refer to the phenomenon of fine particles in the soil migrating within the intergranular pores of the coarse matrix for the first case, and at the interface of coarse and fine soil layers for the second case, under seepage flow. These phenomena have been extensively documented in earthen structures and natural sediments. Given their complex multi-phase coupling process and inherently unobservable nature, predicting and explaining their physical process and subsequent consequences remain a significant challenge.

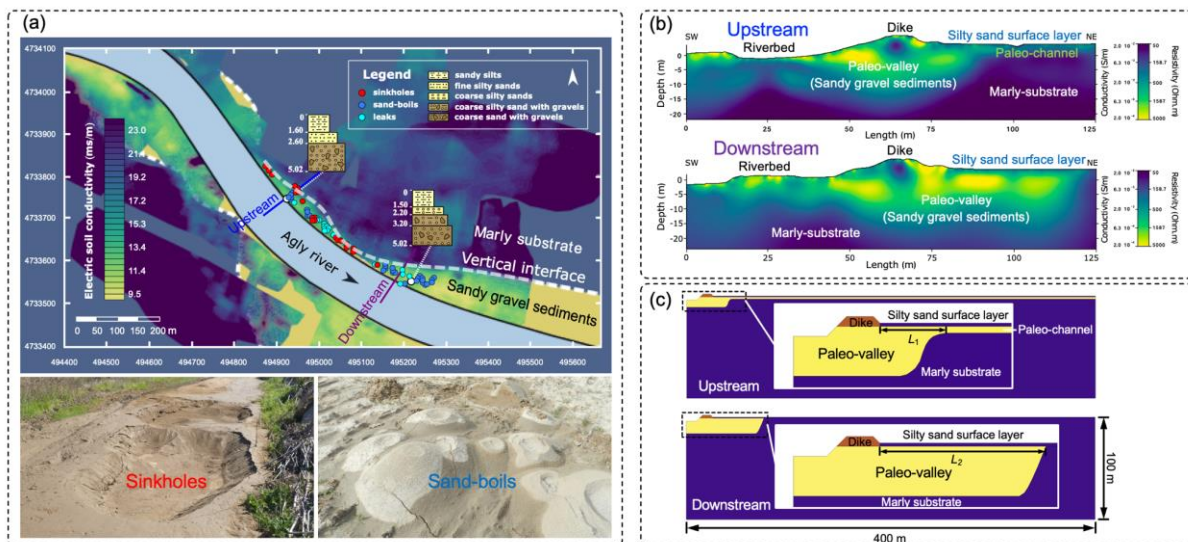


Figure 2. (a) distribution and photo of the erosion signatures, (b) geophysical results; and (c) numerical configurations.

In the field of Agly dike, three kinds of erosion signatures -sinkholes, sand boils, and leaks- were observed at the protected area on the side of the northern bank during each flood. Their distribution and photographs are presented in Figure 2 (a). The geophysical results (EMI and ERT) of the two typical profiles located upstream and downstream, respectively, from which two distinct stratigraphic structure configurations can be identified (Girolami et al. 2023) are shown in Figure 2 (b). In the upstream area, the sandy gravel paleo-valley of 15 m thick tapers into a paleo-channel of 1 m thick beyond a vertical interface between the sediments and substrate. The sandy gravels were overlaid by a low-permeable silty sand surface layer of approximately 1 m thick. In contrast, the vertical interface in the downstream area truncates the sandy gravel sediments. Moreover, from the plane view of the EMI results shown in Figure 2 (a), it can be deduced that the distance of the vertical interface from the dike varies along the river flow direction.

2 NUMERICAL MODELLING

Two simplified configurations representing the upstream and downstream areas of the dike were established to simulate and analyze erosion behaviors. In each configuration, scenarios with three different vertical interface locations were examined, as illustrated in Figure 2 (c). The numerical description of suffusion was formulated within a continuum four-constituent mixture framework. The erosion of fine particles was quantified by employing the erosion model for sandy gravels proposed by Deng et al. (2023). The governing equations were solved by the Multiphysics FEM program COMSOL Multiphysics.

3 NUMERICAL RESULTS AND CONCLUSIONS

Figure 3 presents the distribution of fines content in sandy gravel sediments and the distribution of hydraulic gradients in the silty sand surface layer in both upstream and downstream areas of the dike. In the upstream area, the constriction of the sandy gravel sediment creates a high-velocity zone at the paleo-channel throat, giving rise to intense suffusion and potential contact erosion (Figure 3 (a)). This can be responsible for the sinkholes observed on-site. Additionally, a considerable portion of the silty sand surface layer is subjected to a hydraulic gradient greater than one (Figure 3 (b)), which is valuable to local heave failure. Moreover, with the vertical interface approximating the dike, suffusion at the paleo-channel throat could be intensified, while the likelihood of local heave in the silty sand surface layer might be diminished.

In the downstream area, suffusion was primarily limited to the zones near the riverside (Figure 3 (c)), which explains the absence of sinkholes in the field. Notably, it can be seen in Figure 3 (d) that scenarios with closer vertical interfaces not only exhibit higher hydraulic gradients but also present larger areas susceptible to heave failure. These mechanisms help clarify why sand boils mainly occur in zones with a closer vertical interface.

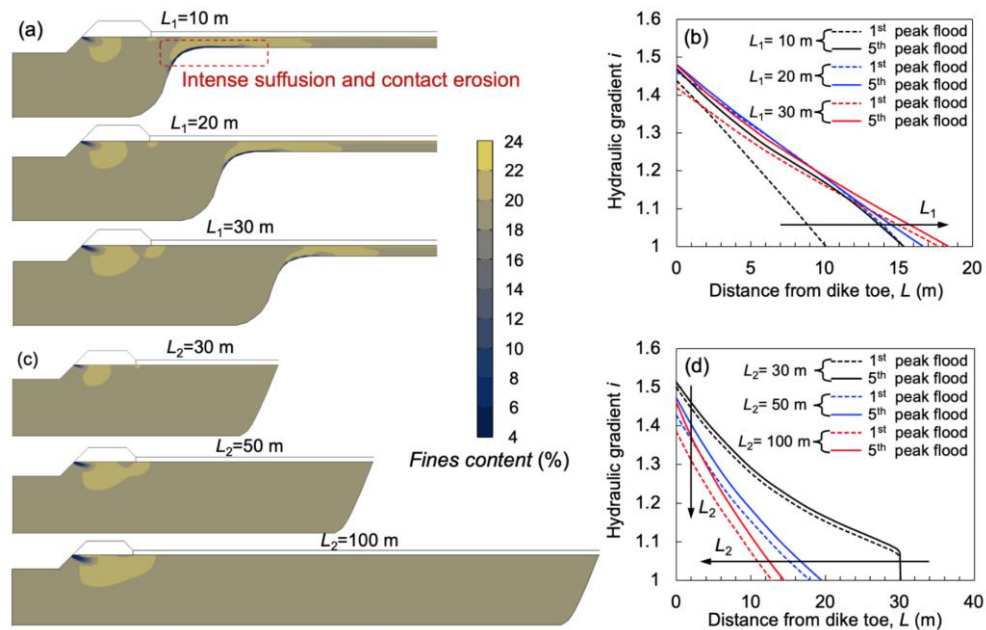


Figure 3. Fines content distribution in sandy gravel sediments and hydraulic gradient distribution in the silty sand surface layer in the upstream area (a-b), and the downstream area (c-d).

ACKNOWLEDGMENTS

The authors gratefully acknowledge the support of the China Scholarship Council (CSC No. 202306050130). The support provided by INRAE is also greatly acknowledged.

REFERENCES

- Deng, Z., Wang, G., Jin, W., Tang, N., Ren, H., Chen, X. (2023). Characteristics and quantification of fine particle loss in internally unstable sandy gravels induced by seepage flow. *Engineering Geology*, 321: 107150. <https://doi.org/10.1016/j.enggeo.2023.107150>.
- Girolami, L., Bonelli, S., Valois, R., Chaouch, N., Burgat, J. (2023). On Internal Erosion of the Pervious Foundation of Flood Protection Dikes. *Water*. 15: 3747. <https://doi.org/10.3390/w15213747>.

Detection of the paleo-environment of a diked river: implications for the erosion of foundation soils

L. Girolami^{1,2}, E.J. Fogueng-Wafo¹, S. Bonelli¹, J.-M. Carozza³, C. Camerlynck⁴

1. INRAe-Aix-Marseille University, UMR RECOVER, Aix-en-Provence, France, laurence.girolami@inrae.fr; edouardo-jovick.fogueng-wafo@inrae.fr; stephane.bonelli@inrae.fr

2. University of Tours, Laboratoire GêHCO, Tours, France

3. La Rochelle University, Laboratoire LIENSs, La Rochelle, France, jean-michel.carozza@univ-lr.fr

4. Sorbonne University, Laboratoire METIS, Paris, France, christian.camerlynck@sorbonne-universite.fr

ABSTRACT: Among internal erosion processes that affect fluvial protection dykes, erosion of natural soils located beneath and around protected plains is associated with the appearance of leaks, sand-boils, sinkholes during flooding events, near the dike toes, as a result of hydromorphodynamics phenomena induced by internal flows. We present here geophysical observations of the river paleo-morphology and their implications in term of the understanding of the origin and distribution of such internal erosion processes.

Keywords: Observation; internal erosion; electric and electromagnetic measurements; paleo-morphology of the river.

1 INTRODUCTION

In this work, we investigate processes of internal erosion that affect foundation soils located beneath and around protection dikes. During flooding events, many erosion signatures (leakages, sand-boils, sinkholes; Figure 1) are recorded near the dike toes, suggesting the development of physical phenomena (fluidization, decompaction, clogging) at shallow depths where coarse and highly permeable fluvial deposits are present. Unlike hydraulic structures continuously loaded, such as dams for which monitoring organized and regulated allows the monitoring of measurable physical quantities, fluvial protection dikes (and their foundation) still suffer from a lack of a relevant monitoring system. One of the main reasons for this gap is attributed to the random frequency of such short-lived hydraulic stresses, which only occur during floods. This specificity then induces scientific and technical locks which limit the organization of a relevant observation system (Mériaux et al., 2013), causing a lack of a physical description of the processes involved (Bonelli, 2012; 2013; Van et al., 2022). In geomechanics, the description of these soil erosion processes is mainly based on a set of conceptual models which has allowed the emergence of laboratory experiments and the development of numerical simulations (Mériaux et al., 2013; Bonelli, 2012; Van Beek et al., 2011; Takahashi et al., 2017; Robbins et al., 2015; Robbins and Griffiths; Wewer et al., 2021). However, this work lacks of in situ observations which would make it possible to capture the spatio-temporal evolution of the different processes involved at different scales. Identifying their origin, in terms of precursors and signatures, then becomes a priority. At the interface between the geomechanics, geophysics, and geomorphology communities, we deployed a multi-scale description, initiated by the acquisition of both in-situ electromagnetic and electric measurements (EMI, ERT), with the aim of overcoming the persistent locks of the literature. These observations were made on the foundation soils of the Agly river dikes (Pyrénées-Orientales). Built in the 1970s to protect proximal populations from the risks incurred by flooding events, they constitute a real natural laboratory, on which two cases of breach failures have been already recorded in 1999 and 2013 (Tourment et al., 2018).

2 CONTEXT AND MOTIVATION

Despite many assessments performed over the past 20 years, these phenomena still remain unexplained. In order to acquire a general overview of these phenomena, we seek to study them at three different scales. On large scales, i.e. on the scale of the embankment system and on the scale of the Millennium, we seek to map the paleo-environment of the river, which can constitute areas of preferential erosion. At the scale of the dike section and at the scale of the flood, we seek to observe areas mainly affected by internal erosion to study internal hydromorphodynamic processes and internal flows. At the scale of the erosion signature and at the scale of the grain erosion, we seek to reproduce these processes in the laboratory, under controlled conditions, in order to identify the physical mechanisms which control such phenomena.



Figure 1. Examples of erosion signatures observed in 2012, 2013, 2014 at the vicinity of dikes at the Agly river during floods: sand-boils (a), sinkholes (b,c), gravitational collapses (d) (Photos INRAe).

In this work, we mainly focused on the observation of the dike section, around which many erosion signatures appear during periods of floods, and based on the acquisition of a surface mapping and local vertical sections along the upward embankment system. The surface mapping of the soil conductivity measurements, averaged over the first six meters beneath the surface using slingram methods (EMI), allows us to detect the presence of an old meandering river bed (upper than 6m) near the dike toes. Analyses of sediment boreholes sampled after the major flooding event of 2013 indicate a fine to coarse sandy matrix with the presence of gravels for these permeable layers, whose granulometry increases with depth. Two-dimensional imaging performed across the dikes: from the river to the protected plains, illustrate the presence of a paleo-valley, of around 350m wide and 20m deep, incised within a sandy-marly substrate and filled with sandy-gravelly sediments. The morphology of these incurved sediment reservoir beneath the present river bed then allows the circulation of internal flows, initiated during periods of floods, along the sands-marls interface, and justifies the presence of leaks, sand-boils, and sinkholes near the dikes.

REFERENCES

- Mériaux P., Monier T., Tourment R., Mallet T., Palma-Lopes S., Maurin J., Pinhas M. (2013). L'auscultation des digues de protection contre les inondations: un concept encore à inventer. In *Digues maritimes et fluviales de protection contre les submersions*, Royet et Bonelli (eds.).
- Bonelli S. (2012) Erosion des géomatériaux, *Traité MIM, Série Risques Naturels, Hermes*, pp. 416.
- Bonelli S. (2013) Erosion in Geomechanics Applied to Dams and Levees, *Wiley/ISTE*, pp. 388.
- Van M. A, Rosenbrand E., Tourment R., Smith P., Zwanenburg C. (2022) Failure paths for levees, *International Society for Soil Mechanics and Geotechnical Engineering. (ISSMGE)*, TC201.
- Van Beek V.M., Knoeff H., Sellmeijer H. (2011). Observations on the process of backward erosion piping in small-medium-and full-scale experiments, *European Journal of Environmental and Civil Engineering*, 15(8), 1115-113, <https://doi.org/10.1080/19648189.2011.9714844>.
- Takahashi A., Horikoshi K., Maruyama T. (2017). Physical modelling of backward erosion piping in levee foundation subjected to repeated flooding, *25th Meeting European Working Group on Internal Erosion in Embankment Dams & their Foundations*, Delft, Netherlands, 4-7.
- Robbins B.A., Sharp M.K., Corcoran M.K. (2015). Laboratory tests for backward erosion piping, *Geotechnical Safety and Risk*, IOS Press: 849-854.
- Robbins B.A. and Griffiths D.V. (2021). A two-dimensional, adaptive finite element approach for simulation of backward erosion piping, *Computers and Geotechnics*, 129, 103820.
- Wewer M.J., Aguilar-Lopez P., Kok M., Bogaard T. (2021) A transient backward erosion piping model based on laminar flow transport equations, *Computers and Geotechnics*, 132, 103992.
- Tourment R., Benahmed N., Nicaise S., Mériaux P., Salmi A., Rougé M. (2018). Lessons learned on the damaged levees of the Agly River, analysis of the sand-boils phenomena, *Processing of the 26th ICOLD Congress*, Q.103 R.21, Vienna.

Underseepage analysis on the Szigetköz floodplain area

E. Koch^{1,2}, M. Maller³, R.P. Ray^{1,2}, G. Bartal³, M. Mayassah^{1,2}

1. Széchenyi István University, Győr, Hungary, koche@sze.hu

2. Vízudományi és Vízbiztonsági Nemzeti Laboratórium, Pannon Egyetem, Körforgásos Gazdaság Egyetemi Központ, Nagykanizsa (Széchenyi István University)

3. North-Transdanubian Water Directorate, Győr, Hungary, Maller.Marton@eduvizig.hu

ABSTRACT: In many parts of the world, flooding is the leading cause of losses from natural phenomena and is responsible for more damaging events than any other type of natural hazard. Hungary has one of the longest river levee systems in Europe along its two major rivers and their tributaries. Szigetköz island is located along the Danube River and is a "hotbed" of sand boil formation, mainly due to the combination of a 100-250 m thick gravel layer beneath a relatively thin blanket of poor soil with variable thickness. Sand boils have a long history in this area where they recur at the same locations and water levels; some even have names. This paper contributes to the efforts of levee vulnerability evolutions, through the demonstration of a methodology for calculation of fragility curve for failure mechanism of piping. The procedure is applied to the upper part of the River Danube levee, a site that has continuously increased water levels in recent years.

Keywords: Internal erosion; sandboil; levee; Szigetköz; fragility curve

1 STUDY AREA

The Danube reaches the Carpathian basin at Devin gate, where the upper section of the Danube ends. There, the velocity of the river reduces and creates a unique inner delta in the Szigetköz-Csallóköz region (Ács et al., 2020). The Szigetköz area is a part of the Little Hungarian Plain, which developed in the course of the Middle Miocene subsidence and the filling up of the alpine orogeny between the Eastern Alps and the Western Carpathians. The uppermost 100-250 m sedimentary sequence of the Szigetköz is characterized by sand and gravel sediments. The surface gravel, characterized by high hydraulic conductivity is underlain by fine-grained sediments with low conductivity, the sand, silt and clay deposits of the Upper Pannonian. An overburden Holocene layer of 0-6 m thickness covers the surface of the alluvial fan and is characterized by a medium permeability (Trásy et al., 2020).

In the operational area of the North-Transdanubian Water Directorate (ÉDUVIZIG), dozens of sand boils have been catalogued in the last decades. In 2013 during the latest and largest flood event, 14 sand boils were observed along the upper part of the Danube River (01.03. section). One of the sandboil is shown in Figure 1. Following the flood event, a comprehensive site investigation program was carried out. Within the study area, 24 sample boreholes were drilled on both the landside and riverside to depths of ~8m, recovering over 50 samples. Adjacent to the most extensive sand boils, 4 CPT soundings were pushed to depths of ~10m. Additionally, a total of 3km of surface geophysical measurements to depths of ~15m transected the site. Finally, bag samples of the sand boil ejecta were collected. Related to the results of the site investigations, one of the cross-sections is shown in Figure 2.

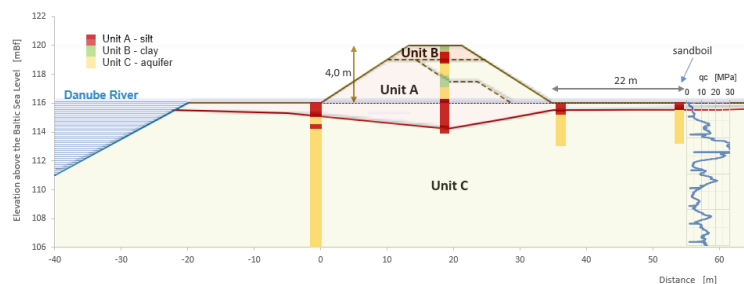


Figure 1. Sandboils along the Danube River. Figure 2. Typical cross-section.

2 METHODOLOGY AND RESULTS

The commonly used method for performing an underseepage analysis of a levee is the United States Army Corps of Engineers “blanket theory” approach (USACE 2000). Following this approach, the levee foundation can be generally subdivided into two layers: an overlying “blanket” layer and an underlying pervious foundation layer.

The underseepage/erosion failure mechanism is characterized by erosion and piping of individual soil particles, which occurs when the seepage exit gradient becomes too high relative to the weight of the soil particles. In this situation, following an effective stress approach, the associated Factor of Safety against piping failure can be determined using the following equation (USACE 200):

$$F_p = \frac{i_{cr}}{i_0} = \frac{i_{cr} \cdot z}{h_0} \quad (1)$$

where i_{cr} = the critical exit gradient, i_0 = the upward gradient through the blanket layer, z = the blanket layer thickness, and h_0 = the head beneath the blanket layer.

The probability of failure (Pf) can be calculated using various probabilistic methods. In this study, the Monte Carlo Simulation was applied (Benjasupattananan et al., 2012). A critical levee cross-section (Fig. 2) was selected for the analyses. The height of the levee is 4,0 m with 3:1 side slopes and a 6 m crest width. The mean value of the blanket permeability is $k_{blanket}=10^{-6}$ m/s, and the permeability of the aquifer is $k_{aquifer}=2,5 \cdot 10^{-5}$ m/s. The coefficient of variation (COV) of all the input variables was set to 20, 50 and 70 %. The probability of failure curves are shown in Figure 3. It can be observed that the probability of failure becomes 50% for a 2.7 m height water level and larger than 70% when the water level approaching to the crest of the levee.

The result clearly demonstrates that quantities and quality of in-situ and laboratory investigations are required to estimate the key parameters. By utilizing the USACE classification and considering the 100-year flood event, the case study levee fits into the “hazardous” performance regarding the piping mechanism.

Integrating the analysis with hazard maps focusing on failure mechanisms and historical data on levee failures offers insights for flood-risk management, streamlining maintenance, and emergency response.

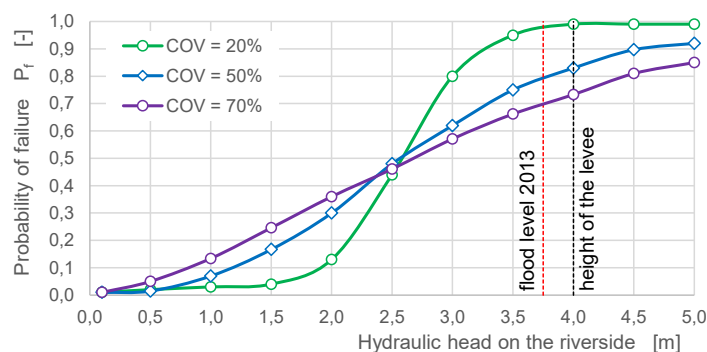


Figure 3. Probability of piping failure.

ACKNOWLEDGMENTS

The research presented in the article was carried out within the framework of the Széchenyi Plan Plus program with the support of the RRF 2.3.1 21 2022 00008 project.

REFERENCES

- Ács, É., Bíró, T., Berta, C., Duleba, M., Földi, A., Grigorszky, I., Hidas, A., Knisz, J., Korponai, J.L., Trábert, Z., Vadkerti, E., Buczkó, K. (2020). Long-Term Changes of Species Composition and Functional Traits of Epiphytic Diatoms in the Szigetköz Region (Hungary) of the Danube River. *Water* 2020, 12, 776. <https://doi.org/10.3390/w12030776>.
- Benjasupattananan, S., C. L. Meehan (2012). An Investigation of Three Probabilistic Approaches for Levee Underseepage Analysis. *GeoCongress 2012: State of the Art and Practice in Geotechnical Engineering*. Mar 25, 2012. Oakland, California, United States. <https://doi.org/10.1061/9780784412121.298>
- Trásy, B., Magyar, N., Havril, T., Kovács, J., Garamhegyi, T. (2020). "The Role of Environmental Background Processes in Determining Groundwater Level Variability—An Investigation of a Record Flood Event Using Dynamic Factor Analysis" *Water* 12, no. 9: 2336. <https://doi.org/10.3390/w12092336>
- USACE (2000). Design and Construction of Levees. Engineer Manual 1110-2- 1913.

Internal erosion within CNR earth structures: a review of field cases on the Rhône River from the 1950's to the present

F. Seblany¹, R. Fellag¹, H. Chapuis¹, C. Picault¹, R. Béguin², C. Guidoux³

1. Compagnie Nationale du Rhône, Lyon, France, f.seblany@cnr.tm.fr

2. ISL ingénierie, Lyon, France

3. GéophyConsult, Chambéry, France

ABSTRACT: The Compagnie Nationale du Rhône (CNR) is France's leading producer of exclusively renewable energy. As concession-holder and developer of the Rhône River since 1933, CNR operates 18 hydroelectric facilities, each comprising approximately 20 kilometers of dikes. Internal erosion is one of the most common causes of instabilities within hydraulic earth structures such as dams, dikes or levees. This communication is an opportunity to provide some statistics and feedback on the disorders induced by internal erosion and occurring on the CNR dikes.

Keywords: Embankments; Erosion mechanisms; Surveillance; dam failure; Hazard studies.

1 INTRODUCTION

The Rhône River developments operated by CNR include about 400 kilometers of embankments located between Switzerland and the city of Arles just before the Mediterranean Sea. Each CNR development includes generally an hydroelectric plant, locks, a gated dam and about 20 km of embankment dams. CNR's dikes were built between 1950 and the end of the 1980's using the materials (silts, and sand and gravels) found on site during the digging of the diversion channel. They are 10 to 15 metres high, permeable and under a permanent hydraulic load.

Due to their material composition, the main mechanism that affect CNR embankments is internal erosion. Four main types of internal erosion mechanisms can be distinguished: suffusion, soil contact erosion, backward erosion, and concentrated leak erosion (Fell and Fry, 2007; ICOLD Technical Bulletin No. 164 2015; ERINOH guides).

In hydraulic structures, internal erosion develops through four stages: initiation, continuation, progression, and failure. A safe operation of earth dams requires to quickly identify degradation processes that affect their structural components and to understand their main causes and possible effects and study the ways to prevent serious accidents and/or failures.

The detection of internal erosion within CNR dams relies mainly on visual indicators (seepage, checking whether particles are removed with water...) and piezometric monitoring data.

Since the filling stage and during different operation conditions including historic floods, visual inspection was conducted to early detect any changes or anomalous zones along the entire length of the CNR dikes and to obtain reliable information about the current state of these structures. Well documented case histories and observations occurred on CNR's embankment dams were thus compiled into a database. This incidents database provides insightful feedback information about field cases and the first signs of degradation ("Precursor Events for Hydraulic Safety" in application of the French ministerial decree of 21 May 2010) based on experience gained over the functional lifetime of these earthen structures.

To ensure hydraulic safety and meet the requirements of French regulations, CNR is responsible for establishing hazard studies for its dike systems. The main objective is to justify the performance of these earthen structures based on a risk analysis considering different failure scenarios. In this context, the inquiry on past incidents and observations can provide an appropriate starting point for risk assessment studies (Béguin et al., 2024).

2 CNR INCIDENTS REPORT

This chapter provides, based on the CNR incidents database, reports on the filling and available flood reports, a brief statistical framework of incidents induced by internal erosion and occurring on CNR dikes.

94 incidents with internal flow involved were recorded on CNR earth dams and no breaches were reported. Half of these incidents were not directly associated with internal erosion mechanisms (appearance of water resurgences without eroded soil particles, which illustrates the fact that CNR embankments are not perfectly watertight). An initiation of internal erosion is suspected for 49 incidents. 2/3 of these incidents occurred under normal operating conditions, 1/3 during the filling stage (and the next 3 years) and only 2 cases during flood periods, despite the 100-year flood which affected almost the entire CNR earth dams. Under flood conditions and depending on the location of the dike along the river, the Rhône

water level can increase by around 20 cm to 3 m, causing an overflow of the upstream facing area clogged by fine sediments from the river, thus leading to significant changes in the seepage flow rate within the earth structure, compared to normal hydraulic conditions.

Based on historical data, the probability of occurrence of incidents during and just after the impounding is of the order: 1 incident involving slow erosion kinetics per development, i.e. every 20 km (leakage with solid transport, settlement, sinkhole, sliding...), and 0.3 incident involving rapid kinetics of erosion per development (incidents linked to backward erosion at the downstream face, combining small local sliding and leakages with particles transport, which required emergency repair).

For the CNR dikes, the most probable internal erosion mechanisms are suffusion and contact erosion (slow kinetic of erosion processes). The analysis of granulometric data indicates that contact erosion between silty and gravel materials constituting CNR dams is often geometrically possible and that the sandy gravel is often internally instable. However, the initiation of such erosion mechanisms has been observed only in specific zones (approximately one incident every 15 km of the embankment). No case of erosion along a pipe crossing the earthen structure has been identified, even though hundreds of crossing rigid structures are present. This is probably related to the significant width of the CNR embankments and the presence of antiseep collars around the rigid structures.

Since construction, the number of incidents per km is of the order of 0.1 regardless of the type of materials constituting the earth dams. Regarding the age of dams, 1.5 incidents per development occurred over the first decade then 0.5 incident per development every 10 years.



Figure 1. Leakage and fine particles erosion at the earth dam toe (Bourg-lès-Valence, 2007).



Figure 2. Sinkhole development on the dam crest (Brégner-Cordon, 1991).

3 CONCLUSION

The records of incidents and defects observed on CNR dikes due to internal erosion provide a comprehensive guideline to better understand the behaviour of such earthen dams and to assess the risks of internal erosion. The incidents database for CNR dams permits to provides a general overview of different erosion kinetics and degradation symptoms based on case histories and observations: leakage, deposits of eroded materials, sinkholes, settlement, increase of piezometric levels at the toe of the structure... It also serves as a feedback mechanism for the whole process of dam monitoring and surveillance: increasing monitoring and inspection frequencies, adding instrumentation (piezometric, temperature or leakage flow rates measurements...) and finally permits to provide efficient and suitable maintenance solutions (cut-off wall...). This helps ensure that the dams continue to operate as intended. In addition, and as part of the hazard studies required by French regulations, the inquiry on past incidents is an essential step in risk assessment; it permits to determine potential failure scenarios and calibrate probabilistic risk assessment methods.

REFERENCES

- Béguin, R., Fellag, R., Chapuis, H., and Picault, C. (2024). Méthodologie d'évaluation du risque d'érosion interne des barrages latéraux du Rhône. *Colloque Dignes 2024 - Systèmes et ouvrages de protection contre les inondations d'origines maritimes et fluviales. État des lieux, avancées, innovations et perspectives*, Aix-en-Provence (in French).
- Deroo L. and Fry J.J. (2014). *Projet National ERINOH (Erosion Interne dans les Ouvrages hydrauliques)* vol. 3: Guide ingénierie (in French).
- Fell, R. and Fry, J. J. (2007). The state of the art of assessing the likelihood of internal erosion of embankment dams, water retaining structures and their foundations. *Internal erosion of dams and their foundations*, 9-32.
- ICOLD (2015). *Internal Erosion of Existing Dams, Levees and Dikes, and their Foundations*. Volume 1: Internal Erosion Processes and Engineering Assessment. Technical Bulletin 164. CIGB-ICOLD, Paris.

On the triggering mechanism and evolution of concentrated erosion causing the failure of the levee of Panaro River (Italy) on the 6th December 2020

F. Ceccato¹, P. Simonini²

1. University of Padova, Department ICEA, Padova, Italy, francesca.ceccato.1@unipd.it

2. University of Padova, Department ICEA, Padova, Italy, paolo.simonini@unipd.it

ABSTRACT: The paper presents and discusses the cause of the levee failure that occurred on 6th December 2020 at Castelfranco Emilia, near Modena (Italy), in the levee embankment of the Panaro River, that was probably due to the presence of a small cavity or poorly repaired animal burrow, in hydraulic communication with the river and buried at shallow depth. On the basis of collapse analysis, a new analytical expression for levee factor of safety calculation is proposed as well as an evaluation of the time required by the internal erosion to open a breach in to the levee embankment. This approach is very simple and easily applicable, for example, to the assessment of levee vulnerability to animal burrows at a large scale.

Keywords: Levee collapse, concentrated erosion, soil heterogeneity, animal burrow.

1 INTRODUCTION

The existence of local defects in levee embankments may significantly reduce their stability by altering its structural integrity leading to a local collapse that can evolve into catastrophic failure. This could be, for example, an inclusion of low-strength material, due to an unsatisfactory reconstruction of a levee already collapsed in the past, or even a cavity, such as those excavated by animals (Bayoumi & Meguid, 2011, Ceccato et al. 2022). These inclusions may alter the pore pressure distribution in the soil, thus reducing its shear strength and creating preferential flow paths that favor internal erosion mechanisms. The local increase in water pressure within the cavity can trigger local failure of the landside slope, thus starting concentrated erosion (Bonelli & Nicot, 2013). The cavity expands at a rate that depends on the erodibility of the material, the path length, and the pressure difference between the entrance and exit (Bonelli et al., 2007).

2 CASE STUDY

A significant number of flood events have been recorded in the last centuries along the Panaro river. In some cases, they have been attributed to overflow and internal erosion, but for most of the events the causes are unknown. Moreover, in the last decade, two erosion phenomena were observed very close to the new breach (Figure 1a), namely sand boils (in 2019) and concentrated erosion due to animal burrows (in 2014) (Figure 1b) (Orlandini et al., 2015).



Figure 1. (a) Location at regional scale, (b) previous observed erosion phenomena and burrow presence.

To investigate the cause of collapse, which is clearly not due to overtopping, an extensive geophysical and geotechnical investigation was carried out, as well as careful observation of the breach fan, where several pieces of brick and stone elements as well as large *Arundo Donax* were observed. Evidences of past animal burrows repaired a few years before the breach and new active burrows were present (Figure 1b).

By comparing possible levee failure mechanisms, such as landside slope instability, backward erosion and piping through foundation soil, landside failure due to uplift water pressure, concentrated erosion through the embankment body, the latter appeared to be the unique possible mode of failure consistent with the sandy and silty nature of the soil forming the levee and very rapid evolution of the breach (Ceccato et al., 2022). However, to explain the observed type of failure, it was necessary to hypothesize the presence of a local defect, necessary to trigger the concentrated erosion. This may consist in the presence of a small cavity close to the landside slope in hydraulic communication with the river, namely an animal burrow poorly repaired in the past and therefore not appearing on the embankment landside slope. The pressure inside the cavity increases as the water level increases and this has a double effect of (i) increasing the pressure load on the small soil cover and (ii) reducing the soil shear strength, that depends on the effective stress, by increasing the pore pressure in the vicinity of the cavity, as shown in Figure 2a. The evolution of breach formation is shown in Figure 2b and 2c.

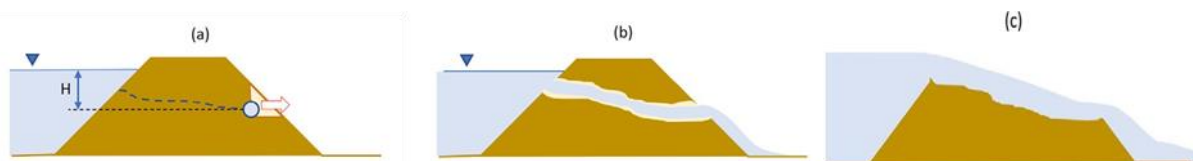


Figure 2. Hypothesized failure mechanism: (a) failure of the soil wedge, (b) progression of concentrated erosion, and (c) opening of the breach.

The trigger mechanism shown in Figure 2a was modelled by both analytical block wedge equilibrium analysis and by the finite element method. The analytical approach allows to obtain a relatively simple equation than can be applied, for example, to assessment levee vulnerability to animal burrows at a large scale.

This superficial local failure can start a concentrated erosion leading very rapidly to the opening of the breach, as illustrated in Figure 2. When the contact shear stress generated by the flow through the pipe exceeds the critical soil shear stress, particles are eroded and the size of the conduct increases leading to failure.

Considering the subsequent formation of a circular pipe, the temporal evolution of the cavity radius was calculated according to Bonelli et al. (2007), that allowed to estimate the time needed for the opening of the breach in less than 1.5 hours, which was consistent with the observations of local people.

REFERENCES

- Bayoumi, A., & Meguid, M. A. (2011). Wildlife and safety of earthen structures: A review. *Journal of Failure Analysis and Prevention*, 11(4), 295–319. <https://doi.org/10.1007/s11668-011-9439-y>
- Bonelli, S., Brivois, O., & Lachouette, D. (2007). The scaling law of piping erosion. *18ème Congrès Français de Mécanique, 18ème Congrès Français de Mécanique Grenoble, 27–31 Août 2007*, 1–6.
- Bonelli, S., & Nicot, F. (2013). Erosion in geomechanics applied to dams and levees. *In Erosion in geomechanics applied to dams and levees*. ISTE Ltd and John Wiley & Sons, Inc. <https://doi.org/10.1002/9781118577165>
- Ceccato, F., Malvestio, S., & Simonini, P. (2022). Effect of animal burrows on the vulnerability of levees to concentrated erosion. *Water (Switzerland)*, 14(18), 2777. <https://doi.org/10.3390/w14182777>
- Orlandini, S., Moretti, G., & Albertson, J. D. (2015). Evidence of an emerging levee failure mechanism causing disastrous floods in Italy. *Water Resources Research*, 51, 7995–8011. <https://doi.org/10.1002/2015WR017426>.

A forward simulation and data driven approach in fusing geophysical data for subsurface characterization

Chris Bremmer¹, Jude King, Edwin Obando Hernandez, Eline Leentvaar, Joeri van Engelen, Ane Wiersma (from same institution), Marios Karaoulis²

1. Deltares, Netherlands, chris.bremmer@deltares.nl

2. Aristotle University of Thessaloniki, Geophysics department, school of Geology, Greece, mkaoulis@geo.auth.gr

ABSTRACT: In this paper we present the results of a simulation approach enabling optimising geophysical survey parameters for characterizing subsurface conditions relevant to internal erosion and of a data fusion approach capable of fusing geophysical measurements with CPT's and borings. The simulation of geophysical measurements has been applied to two synthetic cases. The data fusion approach has been applied to generate a stochastic model of heave based on real world case.

Keywords: shallow subsurface geophysics; EM; MASW; data fusion; stochastic modelling; heave.

1 INTRODUCTION, CONTEXT, MOTIVATION

Accurate soil models are a prerequisite to estimate the probability of failure due to internal erosion. Due to the fact that the subsurface properties and parameters are variable and heterogeneously distributed, point measurements will result in an incomplete model of the subsurface. Since dike failure due to internal erosion is determined by local conditions, incomplete sampling will have to be corrected for by a statistical correction factor. Geophysical surveying offers the opportunity to provide for a continuous surface- or volume-image, thus supporting interpolation between sampling points. However, geophysical measurements almost without exception measure a property that is correlated with the primary property in which geotechnicians, and hydrologists are interested instead of the primary parameter of interest itself. In addition, most geophysical measurements need to be inverted which in general leads to a non-unique solution. These aspects can lead to uncertainty about the applicability of a geophysical measurement. Simulating the possible measurements signal beforehand offers the opportunity to test its value of information beforehand. Next to that, geophysical measurements need to be incorporated alongside observations from CPT's and borings. This asks for a method that can combine different data sources and where the model can be updated when new data from soil research or monitoring become available.

In this paper we present an approach to simulate geophysical measurements in order to optimize the surveying approach and generate results which can be included in a soil model by applying a data fusion routine based on a Random Forest algorithm (Zuada Coelho and Karaoulis (2022)). The geophysical simulations have been applied to two geophysical measurement techniques that are frequently used, namely Electro-magnetic induction measurements (Auken et al., (2015), King, J., et al. (2018)) and Multichannel Analysis of Surface Waves – MASW (Park et al., (2007)). Modeling has been carried out for two profiles, a synthetic profile, which represents a sand lens at different depths in a cover layer, and a profile from the geological model from the Netherlands, which is illustrative of a real structure of a cover layer. The settings of the field measurements were varied, such as distance between sensors or electrodes, frequencies, and distance from the EM coils to the ground. For the inversion, the application of a probabilistic inversion algorithm, the Markov-chain Monte Carlo algorithm, was examined. The advantage of this is that insight can be provided into the variation of possible, equally likely outcomes of the inversion. The results of the modeling are indicative and an example of how such an approach can help in making choices in measurement design and interpreting the results.

The application of the synthetic case gives a good idea of the sensitivity of a geophysical survey for lithological contrasts on the one hand and survey parameters on the other (see fig. 1(a) and 1(b)). The synthetic case actually demonstrates various configurations of sand lenses which are a determining factor for piping. For both the EM-survey as well as the MASW the model results show how resolution and accuracy are influenced by contrast in properties and survey parameters. We see the best result for the shallow sand lens. In the EM-model the deeper sand lenses are still discernible but begin to merge in the below lying sand layer, which is a result of the dependence of the sensitivity of penetration depth and resolving power of the EM-method as a function of frequency. The MASW method is specifically suitable for imaging continuous interfaces which can be seen in the synthetic profile. Though the sand lenses can be located, the inversion shows some shadowing and amplification effects which would make an interpretation non-trivial.

A data-driven approach has been developed which merges geophysical data with CPT's and soil sampling for modeling the subsurface to determine the piping risk along flood defenses with a foreland. This has been applied to real world case for which observations of heave were available. An important condition is that the subsurface modeling takes into account the influence of the geological history of the area. This determines the spatial distribution of lithological units in the subsurface. The subsurface was therefore modeled in two steps. In a first step, a lithofacies model was created of the different deposit types in the area and on this basis the lithological model was created, which is a refined model of the soil types. An Image Inpainting algorithm (Guillemot et al. (2014)) was used to interpolate the layer surfaces of the lithofacies model. This lithofacies model was then used as a parameter to create a 3D voxel grid based on a Random Forest algorithm (Zuada Coelho and Karaoulis (2022). The approach is applied in a stochastic modeling of the occurrence of heave during high water. The stochastic model produces a large number (100) of equally probable realizations of groundwater pressure and the onset of heave. The advantage of the chosen approach is flexibility. The model can be easily updated with new drillings, soundings and geophysical measurements. Also, more 'soft' information can be added relatively easily and assessed based on the degree in which it improves the estimation of the spatial distribution of relevant properties. Figure 2(a) and 2(b) show the results of 100 realizations for the hydrological model and the resulting modelled probability of heave during high river stand. The validation of the subsurface model has shown that an accurate estimate can be obtained from the spatial distribution of the lithology.

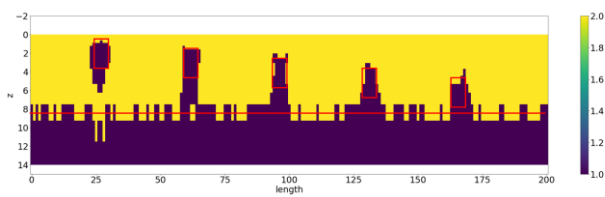


Figure 1(a). The lithological prediction based on the inversion of the DULAEM 842s system. Purple (lithology value of 1) is predicted sand lens. Red outlines show the contacts between sand and clay from the synthetic model.

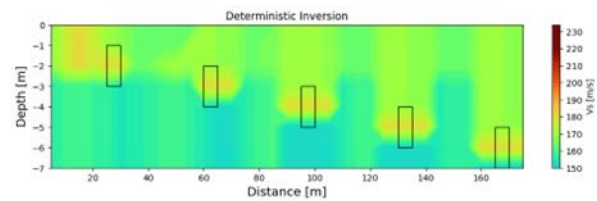


Figure 1(b). 2D S-wave velocity for the synthetic model.

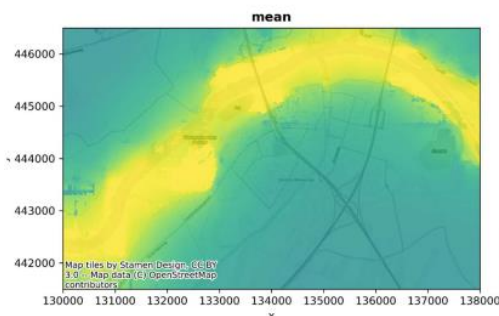


Figure 2(a). Groundwater head at high river stage, averaged over 100 realizations

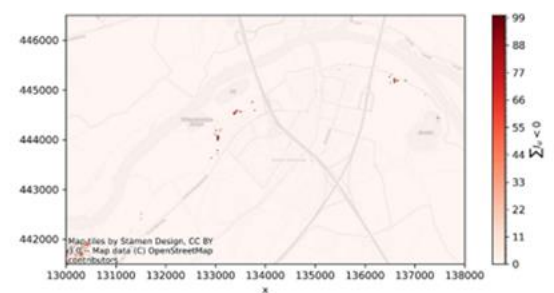


Figure 2(b). Probability of heave during high water based on 100 realizations and including EM-survey data.

ACKNOWLEDGMENTS

This work has received funding under the project Kennis voor Keringen from Rijkswaterstaat SITO-PS-funding.

REFERENCES

- Auken, E., et al., An overview of a highly versatile forward and stable inverse algorithm for airborne, ground-based and borehole electromagnetic and electric data. *J Exploration Geophysics*, 2015. 46(3): p. 223-235.
- Guillemot, C. and Olivier Le Meur (2014); Image Inpainting: Overview and Recent Advances. *IEEE Signal Processing Magazine* · January 2014. DOI: 10.1109/MSP.2013.2273004
- King, J., et al., Quantifying geophysical inversion uncertainty using airborne frequency domain electromagnetic data—applied at the province of Zeeland, the Netherlands. *J Water Resources Research*, 2018. 54(10): p. 8420-8441.
- Zuada Coelho, B. and Karaoulis, M. (2022); Data fusion of geotechnical and geophysical data for three-dimensional subsoil schematisations. *Advanced Engineering Informatics* 53 (2022) <https://doi.org/10.1016/j.aei.2022.101671>

Analysis of case studies of canal embankment failures

J.R Courivaud¹, O. Bory¹, A. Vogel², K. Jarecka²

1. EDF-CIH, La Motte Servolex, France, jean-robot.courivaud@edf.fr

2. Risk Assessment International, Vienna, Austria, rai@chello.at

ABSTRACT: The lessons learned from canal embankment failures are an important element in the regulatory safety justification analyses for structures of this type operated by EDF. In order to be able to draw lessons from these failures, EDF has initiated work to collect and analyse this data. To date, data from 25 case studies have been collected and their analysis is presented in this communication.

Keywords: canal, embankment, breach, failure, internal erosion, overflowing erosion

1 INTRODUCTION

EDF owns and operates about 500km of canal embankments in France. These canals are headrace or tailrace canals of hydroelectric schemes mainly located on the Rhine River (North-East of France), the Durance River (South-East of France) and the Garonne River (South-West of France). These canal embankments are classified as dams according to the French regulations on dams and EDF must provide risk assessment analysis of these structures to the dam safety authority every 10 years for classified A dams and every 15 years for classified B dams. The French regulation on dams defines classified A dams as dams which height (H in metres) above the natural ground is 20m or higher and $H^2 V^{1/2} \geq 1500$ (V being the volume of water retained in the canal or the reservoir, in Millions of m^3). Classified B dams are defined as dams which are not A dams and their height (H) above the natural ground is 10m or higher and $H^2 V^{1/2} \geq 200$. The justification of the safety margins of these canal embankments with regard to their potential failure modes, includes in particular feedback on the case studies of failure of these structures. It has therefore become necessary for EDF to collect and analyse available data on canal embankment failures. The task of collecting data on canal embankment failures worldwide is colossal and probably never-ending. In a first step, data collection has focused on cases where a complete breach has occurred in the canal embankment. Cases of canal embankment failure due to overflow from flooding of the plain into the canal have not been taken into account in this analysis, as these failures do not present any safety issues. To date, data has been collected on 25 cases of canal embankment where complete breaches occurred. The data collected can be considered virtually exhaustive for France, thanks to the study (CETMEF, 2010), but represent only a small proportion of canal embankment failures in Europe and worldwide. In the UK alone, the publication [Dun and Wicks, 2013] counted 380 cases of canal failures between 1770 and 2012, with an average of 4 to 5 failures per year between 2004 and 2011. So, there are certainly several hundred, and potentially several thousand, cases of canal embankment failures around the world. The conclusions drawn from this initial analysis, based on a set of 25 cases of failure, must therefore be put into perspective in view of the very large number of cases for which data has not yet been collected and analysed.

2 DATA COLLECTED FOR A SET OF 25 CASE STUDIES

The 25 cases of failure can be divided into two main categories:

- canals built before 1920: the embankments were built with low levels of compaction, due to the absence, at the time, of heavy earth compaction equipment. 12 case studies fall into this category.
- canals built from 1950 onwards, which benefited from heavy compaction equipment. 12 case studies fall into this category.

For the case study of the Murcia canal in Spain, which breached in 2019, the date of construction is not yet known.

The list of case studies of canal embankments constructed before 1920 is shown on Table 1. The list of case studies of canal embankments constructed from 1950 onwards is shown on Table 2.

The completeness of the data collected for these 25 case studies varies greatly, ranging from very limited data (just a video or press article) to in-depth technical reports.

Table 1. Case studies of canal embankments built before 1920

Canal embankment name	Country	Date of construction	Date of failure
Briare canal	France	1642	2002-2016
Bridgewater canal	UK	1761	1971
Llangolen canal	UK	1809	2004
Columbia canal	USA	1824	2015
Rhône to Rhine canal	France	1833	2005
Roanne to Digouin canal	France	1836	2007
Loire lateral canal	France	1838	2000
Berry canal	France	1841	2011-2021
Arroux canal	France	1869	2001
Dortmund EMS canal	Germany	1899	2005
Canal de Aragon y Cataluña	Spain	1906	2019
Truckee canal	USA	1906	2008

Table 2. Case studies of canal embankments built from 1950 onwards

Canal embankment name	Country	Date of construction	Date of failure
Nagajunasagar canal	India	1950	2022
Swift N°2 canal	USA	1959	2002
Main Danube canal	Germany	1960	1979
North canal	France	1965	2003
Elbe lateral canal	Germany	1976	1976
Formin canal	Slovenia	1978	2012
Ruahihi canal	New Zealand	1981	1981
Wilnis dike	The Netherlands	1981	2003
Lower Quail canal	USA	1967-1981	1984
Rangatiki canal	New Zealand	1982	1982
Kutch canal	India	2016	2022
Bansagar canal	India	2017	2022



Figure 1: Murcia canal breach, Spain, September 2019



Figure 2: Swift N°2 canal breach, USA, April 2002

3 DATA ANALYSIS

The aim of analysing the data from these case studies is to gain an understanding not only of the conditions that led to these breaches, but also of the characteristics of the breaches in relation to the characteristics of the embankments of these canals. The hydraulic conditions under which these breaches occurred, i.e. initial impoundment, normal operating conditions or exceptional flood conditions, are analysed. The geometry and kinetics of breach formation are also analysed on the basis of available data on the geometry and materials constituting the embankments.

REFERENCES

- CETMEF (June 2010). *Digues et berges des voies navigables. Retour d'expériences sur les désordres et les réparations*.
 Dun R.W. and Wicks J.M. (2013). Canal breach risk assessment for improved asset management. *Proceedings of the Institution of Civil Engineers* <http://dx.doi.org/10.1680/wama.12.00060>

Commissioning of the world's first Fibre Optics monitoring system installed along a flood protection dike, in the Arles region, France: first data and setting up of the detection thresholds

C. Guidoux¹, R. Béguin^{1,2}, P. Pinettes¹, M. Boucher¹, J.-R. Courivaud³, L. Salvan⁴ and T. Mallet⁴

1. *geophyConsult, Jacou, France, pinettes@geophyconsult.com*

2. *Presently at ISL, Lyon, France, beguin@isl.fr, but at geophyConsult during the project that led to the present article*

3. *EDF-Hydro, La Motte Servolex, France, jean-robert.courivaud@edf.fr*

4. *Symadrem, Arles, France, l.salvan@symadrem.fr*

ABSTRACT: Monitoring leaks in dykes and canals using fibre optic sensors has been technically mature for several years. To achieve this, EDF and GEOPHYCONSULT, have carried out experimental test and monitoring campaigns over a deployment perimeter of around 60km. Recent efforts have focused on the development and implementation of operational monitoring, with the aim of using and continuously processing temperature measurements taken along the fibre-optic cable. New business tools have been specifically developed. This article will focus on the deployment of such a system along the new flood protection dykes owned by SYMADREM along the Rhone river, between Beaucaire and Fourques (France). First operational monitoring lessons learned from site monitoring and following exceptional events will be presented to illustrate the benefits of operational monitoring using fibre optic sensors.

Keywords: Real-Time Monitoring; Internal Erosion; Flood Protection Dykes; Leakage; Temperature Measurements

1 CONTEXT

In order to reinforce the dykes along the Rhone river at its end, a pluriannual plan was set up a decade ago. It consisted in the creation of new dykes, and included the opportunity to improve dyke safety by using fiber optics leakage detection system. The conception of such a system was awarded to EDF (Courivaud, 2017) and geophyConsult (Guidoux, 2006). The conception focused on the feasibility of the system, that was supposed to:

- detect early signs of potentially progressive leaks during flood periods and in all weather conditions;
- detect early signs of potential failure of the filter/drain complex;
- pinpoint the position of these leaks or failures along the length of the dyke surveyed;
- increase SYMADREM's response capacity
- reduce the residual risk of breach.

In order to do so, a typical section of the dyke was modelled and the soil parameters that control the flow and temperature within the section were estimated in consultation with the dyke project managers and the project owner. Two leakage scenarios previously defined in consultation with the project owner and the dike project manager were introduced into the model, and then a pseudo-3D thermal-hydraulic model representative of the section modelled was developed, by attaching the leaky sections to a few dozen typical sections without failure. The temperatures calculated by this model at the location of the optical fibre were then used as input data for the detection algorithms used by EDF, in place of actual temperature measurements, in order to check the feasibility of detecting the modelled leaks.

2 LEAKAGE DETECTION USING FIBER OPTICS

Passive methods refer to signal processing applicable to soil temperature measurements different from those of the water retention, potentially influenced by air and groundwater (Kappelmeyer, 1957). These measurements are obtained using simple optical cables; that is, not having copper wires so that they can be heated to create a temporary thermal contrast (Johansson, 1997).

The AJOUT model developed by EDF HYDRO (Khan, 2001) is mainly used for detection purposes on a short data history, typically one day (Analyse JOURnalière de Température in French, Daily Temperature Analysis). It is based on a

signal) processing method carried out in two stages: filtering of undesirable influences from a decomposition into singular values then construction of a daily thermal anomaly indicator from the sums of dissimilarities between the residues resulting from each position within the auscultated areas. The detection of thermal anomalies is carried out in two steps: in the absence of a measurement history, high values of dissimilarity index AJOUT are pointed out. Then the evolution of the time series are observed by comparing them to historical thresholds. The calculation of the AJOUT model assumes an acquisition of hourly measurements but does not require a significant measurement history: a few days are enough. It also does not use additional input data such as air temperature or water temperature. No thermohydraulic soil modeling parameters are required.

3 DEDICATED SOFTWARE

Based on AJOUT, a dedicated software was build, with fine-tuned detection threshold aiming at distinguish between :

- infiltrations to be monitored without particular vigilance;
- leaks to be monitored with particular vigilance;
- progressive leaks requiring emergency intervention, which would imply a failure of the filter/drain complex.

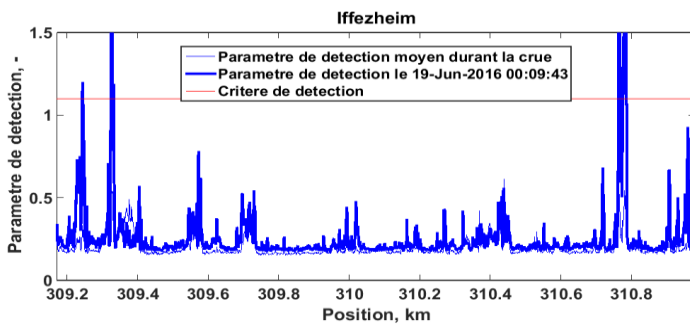


Figure 1. AJOUT Detection.



Figure 2. Software overview.

4 FIRST RESULTS

The software was successfully used during the floods of last winter. In particular, a clear detection of a seepage due to a deficient gate at the end of the equipped dyke was confirmed by field observations. Although the leakage didn't come from the dyke itself, the whole monitoring protocol proved to be effective in flood-crisis real time monitoring.

REFERENCES

Kappelmeyer O. (1957). The use of near surface temperature measurements for discovering anomalies due to causes at depths, *Geophysical Prospecting*, 5(3): 239-258, 1957

Johansson S. (1997). *Seepage monitoring in embankment dams*. Thèse de doctorat, KTH, Stockholm.

Guidoux C. (2006). *Développement et validation d'un système de détection et de localisation par fibre optique de zones de fuite dans les digues en terre*. Thèse de doctorat, université Joseph Fourier de Grenoble.

Courivaud J.-R., Lorrain N., Martinot F. Beguin R. (2017). Quantifying seepage flow velocities in embankment dams from optical fibre distributed temperature measurements. *Long-Term Behaviour and Environmentally Friendly Rehabilitation Technologies of Dams*.

Khan A.A., Vrabie V., Mars J., Girard A., D'Urso G. (2008). A source separation technique for processing of thermometric data from Fiber-Optic DTS measurements for water leakage identification in dikes. *Sensors Journal*, IEEE, 8(7):1118-1129.

Thermal and Mechanical Resistance Mapping of a Hydraulic Structure: detection and quantification of an internal flow before, during and after reinforcement work

M. Boucher¹, P. Pinettes¹ and J.-R. Courivaud²

1. *geophyConsult, Jacou, France, pinettes@geophyconsult.com*

2. *EDF Hydro, La Motte Servolex, France, jean-robert.courivaud@edf.fr*

ABSTRACT: Carrying out a thermal mapping of a zone of a hydraulic structure that is affected by abnormal internal flows has long been known as a very effective and economic way to delimit the extension of a worrisome zone. We have combined this method with the mapping of the mechanical resistance of the soil to a dike in operation where a leak had recently been detected. We repeated the measurements during and after the reinforcement work that was decided in response to the leak. Our results show that the leaking zone was located on top of the foundation and was associated with a reduction of the mechanical resistance, suggesting a mechanical weakening of the soil due to internal erosion. The inner flow velocities that we derived from the thermal monitoring enabled us to show the satisfactory impact of the remediation on the inner flow velocities.

Keywords: leakage; internal erosion; thermal mapping; inner flow velocities determination; mechanical resistance mapping

1 INTRODUCTION, CONTEXT AND MOTIVATION

In the event of the occurrence of a worrisome imbalance in a hydraulic structure (e.g. the sudden appearance of a hole in the structure, or the appearance of sudden outlets of inner flows), carrying out a thermal mapping of the abnormal zone has long been known as a very effective and economic way to delimit, if necessary in emergency, the extent of an abnormal zone (Dornstädter, 1992). Such a mapping is traditionally used to quantify the size of the expected remediation. Depending on the local thermal conditions and on the experimental configuration of the measurements that are used to build the mapping, it can also be used to deliver a first estimate of the internal flow velocities, that is required to state whether internal erosion is at risk or, on contrary, can be excluded.

We have combined this method with the mapping of the mechanical resistance of the soil to a dike in operation where a leak had recently been detected, and repeated the measurements before, during and after the reinforcement work decided in response to the leak.

Our first aim was to delimit the extension of the leaking zone. We also wanted to check whether the leaking zone was associated with a loss of mechanical resistance of the soil. We at last wanted to use the monitoring before, during and after the reinforcement to estimate the inner flow velocities and quantify the impact of the remediation on their reduction.

2 STUDIED SITE

Along one of the main French rivers, visual observations showed clear signs of a flow inlet and a flow outlet perpendicular to the axis of the right bank of an important navigation channel (see Figure 1).



Figure 1. Studied site.

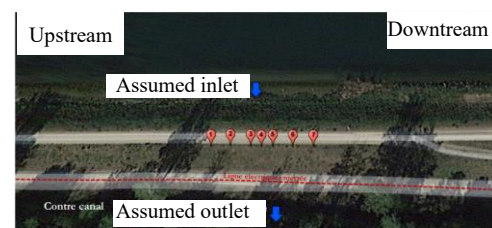


Figure 2. Drill holes that were carried out to build the thermal and mechanical mappings.

3 CARRIED OUT MEASUREMENTS

In order to delimit the extension of the zone that was potentially affected by the leakage, the structure owner ordered a thermal reconnaissance campaign that consisted in drilling in emergency 8 holes down to 10 m, below the foundation (see Figure 2), and to equip each of them with thermal resistance channels that continuously measured the temperature every meter until the thermal balance was reached. We then combined each vertical profile with their neighbours so as to deliver a thermal mapping of the leaking zone.

In parallel, we measured the mechanical resistance of the soil during the drilling operations by counting the number of shots that was requested to drill a given length, so as to deliver mechanical resistance mappings of the studied operation. We then calculated the vertical thermal profiles that would have been expected in each borehole in case the temperature had been fully controlled by thermal conduction in a 1D medium subject to top sinusoidal annual sunshine, and compared them to the actual thermal measurements (see Figure 3). After the initial reconnaissance campaign, we at last left in place three thermal channels (in boreholes 2, 4 and 6 centered on the suspected leakage flow, see Figure 2), so as to record the temperature before, during and after the remediation.

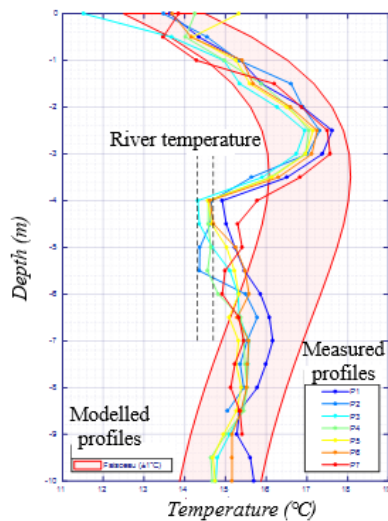
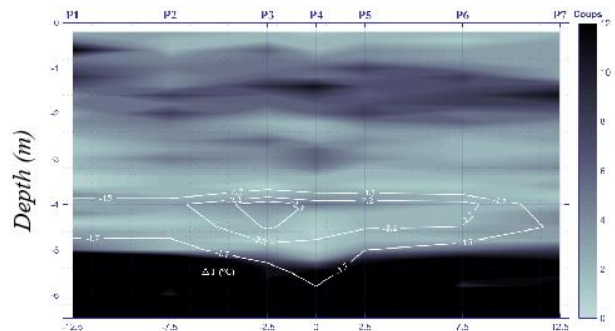


Figure 3. Measured vertical thermal profiles.



Dike axis, centered on the assumed leaking path
 Figure 4. Superposition of the mechanical resistance mapping around the leak and isotherms of the difference between the measured and the expected temperatures in the boreholes. The x-axis is centered on the assumed leaking path.

4 RESULTS

Figure 4 shows the mechanical resistance map with the isotherms of the difference between the measured and expected temperatures in the boreholes that are surrounding the suspected water path (see Figure 3).

They clearly locate the leak at the basis of the structure, just above the foundation, where a slight decrease of the mechanical resistance of the soil is detected by the mechanical resistance measurements carried out during the drilling. These results suggest a mechanical weakening of the soil due to internal erosion. The temporal phase shift that was observed between the temperature measurements carried out in the river and the same measurements carried in the 3 boreholes that were left fully equipped during the monitoring phase besides enabled us to estimate the inner flow velocities to $3 \text{ to } 5 \times 10^{-3} \text{ m} \times \text{s}^{-1}$, and to show that these velocities had been reduced by a factor of around 3 by after remediation.

5 CONCLUSION

The present measurements confirmed the key information provided by thermal mapping studies carried out in emergency to characterize the extension of a worrisome zone that appears in a hydraulic structure in operation. They also showed the interest of combining classical thermal maps with mechanical resistance maps, to study the impact of the leaking flow paths on the mechanical resistance of the structure. Finally, the monitoring carried out before, during and after the remediation enabled made it possible to estimate the inner flow velocities (which are of key importance to quantify the risk of erosion) and to show the satisfactory impact of the remediation on the inner flow velocities.

REFERENCES

Dornstädter J. (1992). Nachweis von sickerströmungen mittels bodentemperaturmessungen, *Z. dt. Geol. Ges.*, Hannover, 143, pp. 421-425.

FIBRADIKE project: Preliminary Test Results

A. Höttges^{1,2}, C. Rabaiotti¹, A. Rosso³

1. OST – Eastern Switzerland University of Applied Sciences, Oberseestrasse 10, 8640 Rapperswil, Switzerland, alessio.hoettges@ost.ch, carlo.rabaiotti@ost.ch
2. ETHZ – Swiss Federal Institute of Technology, Rämistrasse 101, 8092 Zurich, Switzerland, alessioh@ethz.ch
3. AIPo – Interregional Agency for the Po River, Strada Giuseppe Garibaldi 75, 43121 Parma, Italy, alessandro.rosso@agenziapo.to

ABSTRACT: Geohydraulic earthen structures, such as dams and river embankments, are essential for water resource management and flood risk mitigation. One of the primary failure modes for these structures is internal erosion due to seepage, which can lead to sudden collapse. Despite advances in sensor technology, traditional monitoring methods remain inadequate since they lack the spatial and temporal resolution required for effective detection.

Currently, a novel distributed pressure sensor (DPS) based on distributed fiber optic (DFO) technology has been developed at the University of Applied Sciences of Eastern Switzerland (OST). The key feature of the sensor is its unique ability to measure pore water pressure with high spatial resolution and over long distances, which is required for early detection of internal erosion phenomena. The sensor, already validated at laboratory scale, has been installed in a full-scale test basin (84 m long, 37 m wide and 4 m high) at the scientific laboratories of the Agency for the Po River (AIPo) in Boretto (Italy). This extended paper presents the results of the first preliminary test of the filling of the embankment.

Keywords: Distributed Monitoring; Distributed Pressure Sensor; Smart Dike; Distributed Fiber Optic Technology.

1 INTRODUCTION AND NEW DISTRIBUTED PRESSURE SENSOR - DPS

River dikes and dams are a major component of water resource management and flood risk protection. Their importance is heightened in the context of climate change, as flood events become more frequent and severe (Fischer et al., 2022). One of the most significant failure modes for such structures is internal erosion caused by water seepage. The main factors that trigger these phenomena are permeable layers, cracks or fissures, animal burrows, vegetation roots, and also human activities (Bonelli et al., 2012). Traditional measurement systems are limited as they have low spatial and temporal resolution, while these structures can span hundreds of kilometers and their failures can be rapid and localized. For this reason, the current most common method of detecting internal erosion relies on visual inspection.

A promising monitoring technology that meets both spatial and temporal requirements is distributed fiber optic (DFO) technique, which is currently widely used in geohydraulic applications by measuring temperature and deformation (Schenato, 2017). In this regard, a new distributed pressure sensor (DPS) based on DFO technology has been developed at the OST. This sensor can measure pore water variations with high sensitivity (on the order of centimeters water column) and a spatial resolution of decimeters over distances of several kilometers. As pointed out by Fell et al. (2003), pore water pressure within earth structures is an important parameter for monitoring anomalies due to internal erosion phenomena. The DPS consists of a helically wound fiber optic sensor attached to a cylindrical compressible central element. The pressure is obtained by measuring the constriction or expansion of the central element caused by the hydrostatic pressure of water or fluid, which induces elongation or compression of the sensing fibers. A calibration coefficient determined in a pressure chamber can be used to convert the measured deformation into pressure values. Additionally, the DPS contains a loose tube with distributed temperature sensing (DTS) fibers for temperature measurement (Höttges et al., 2023). Another important aspect is that the DPS is manufactured on an industrial scale and is now available on the market. The sensor has been validated in a 1:10 laboratory scale dike model to measure pore water pressure during dike saturation (Höttges et al., 2023) and in a wave channel to measure pressure during solitary wave propagation (Höttges et al., 2024).

2 FULL SCALE TEST EMBANKMENT

Embankment design: The test embankment is 84 m long, 37 m wide and 4 m high with a slope of 1:2 (Rabaiotti et al., 2023). The embankment is constructed of two different soil materials: silty sand according to Swiss (CH) specifications for the Rhone River and silt according to Italian (IT) specifications for the Po River. Furthermore, to ensure the applicability of the monitoring system to both new and existing structures, the experimental embankment is divided into

two parts: an "ex novo" type, where sensors were installed during construction, and an "existing" type, where sensors are installed after using horizontal directional drilling (HDD) techniques, see also *Figure 1*.

Experimental Setup: The new DPS is installed in a mesh grid (see *Figure*) at three different elevations (at 0.3 m, 1.3 m and 2.3 m above the ground level - GL) in the „ex novo“ sections in two main direction: longitudinal (in green, x-axis) and transversal (pink, y-axis). Saturable tubes are installed in various sections of the DPS, as shown in black in *Figure 2*, to protect the DPS from any earth pressure changes (e.g., erosion or sediment accumulation) and to provide only hydrostatic pressure measurements in the sections where they are installed. Conventional measuring sensors are installed to validated the DPS measurement in 4 main transversal sections (2 in the „ex novo“ and 2 in the „existing“): in total 27 piezometer, 22 tensiometer and 8 humidity sensors.



Figure 1. Overview of the test embankment in Boretto.

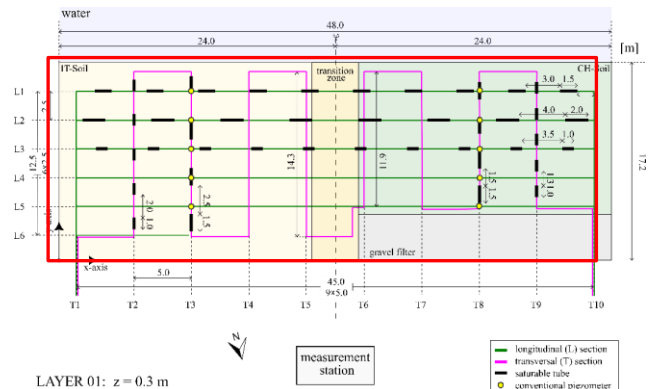


Figure 2. Installation scheme at 0.3 m – “Ex Novo”

Testing procedure: A preliminary test was conducted to verify the filling/emptying of the basin, the correct response of the measurement system, and to verify the stability of the dam at reduced water levels. The water level inside the basin was increased from 1 m (accumulated during the rain period) to 2.3 m by pumping groundwater from an existing well. It was then left to drain for a week, followed by three stages of draining to avoid rapid drawdown instability. Pressure measurements with the DPS were conducted using various DFO interrogators and were therefore performed manually about every 30 minutes, while data from conventional systems were collected automatically every 15 minutes. Temperature was measured with the temperature fibers within the DPS every 4 min.

Experimental results: in this extended paper, only the results for the Layer 01 at 0.3 m above GL are presented. *Figure 3* shows the results obtained with the temperature fibers interpolated in the two main directions at 144 h after the start of the test. *Figure 4* illustrates the pressure in cm of water column (cm wc) obtained with the DPS in the transversal direction. In the longitudinal direction, preliminary results showed significant noise due to fiber connection problems.

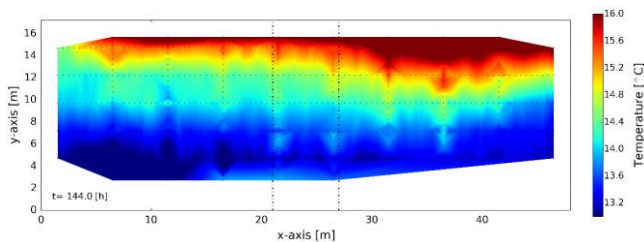


Figure 3. Temperature of Layer 01 measured with DPS temperature fibers at 144 h.

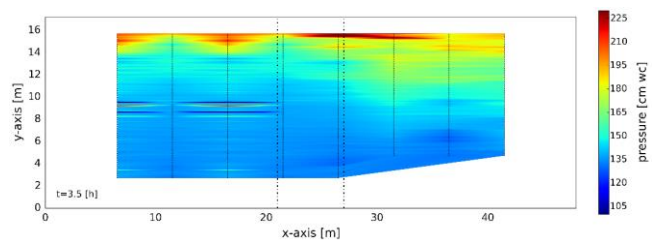


Figure 4. Pressure obtained with DPS for Layer 01 at 3.5 h.

3 CONCLUSION AND FUTURE ACTIVITIES

These preliminary results demonstrate the potential of the DPS to provide distributed information on temperature and pressure within the dike, allowing for the detection of any anomalies. During testing, there were no stability issues, the measurement system responded accurately, and the filling and emptying procedures were satisfactory. Future activities include: testing at full high capacity as the water level was only raised by 1 m, installing the sensor using horizontal directional drilling (HDD) and monitoring the animal activities.

REFERENCES

Bonelli, S., Courivaud, J., Duchesne, L., Fry, J., & Royet, P. (2012). Internal erosion on dams and dikes: Lessons from experience and modelling. 24th International Congress on Large Dams.

Internal Erosion Identification and quantification using Vadose Zone Monitoring Technologies

Aharon (Roni) Ran¹

1. Sensoil Innovations Ltd. Kibbutz Sde Boker 8499300, Israel roni@sensoils.com

ABSTRACT: The traditional piezometer-based monitoring technologies often fail to detect flows in unsaturated conditions, such as small channels where typical piping occurs. However, a pioneering Vadose Zone Monitoring System (VMS) developed at Ben Gurion University and deployed by Sensoil Innovations Ltd. now provides real-time tracking of water flow and contaminant transport across saturated and unsaturated zones*. This advanced system integrates water/moisture content and pressure changes as well as water sampling capabilities in both zones (see Fig. 1). By integrating numerical computation of the water flux, and analysis of changes in solids content- internal erosion can be identified and quantified.

* moisture or water pressure sensor will become alternatively active, according to the soil phase (saturated or unsaturated).

Keywords: Vadose zone; turbidity; water content; piping; pore water sampling; internal erosion

1 VADOSE ZONE MONITORING

Internal erosion usually takes place in episodes of erosion and discharge of muddy water interspersed with periods of clear-water discharge or no discharge at all depending on head and flow. Chemicals, salts, dissolved and suspended solids and dispersive clays can also erode unnoticed from the inside of a dam. The only way to monitor this, in the absence of visible erosion or sand boil deposits, is to send samples to a lab for testing (4). Introducing the Vadose Zone Monitoring System (VMS), brings unique solutions to both challenges: monitoring water flow in alternating conditions (saturated and unsaturated) and sampling. The breakthrough in water content sensing technology based on water dielectric constants laid the foundation for the development of specialized sensors effective in the vadose zone (1,2). This was followed by the design of sophisticated sampling ports for pore water extraction. The VMS itself is a modular system, composed of flexible sleeves, accommodating multiple monitoring units distributed along its length (refer to Fig.1, left). Each unit integrates advanced sensors and sampling ports tailored to allow real-time, continuous tracking of water percolation and contaminant transport across the entire unsaturated zone. This capability enables early detection of changes such as approaching phreatic surfaces or discrete flow pathways, even before full saturation occurs. Importantly, collecting the liquid samples for detailed laboratory analysis yields valuable insights into water chemistry, water source identification (groundwater or reservoir water), turbidity (indicative of internal erosion), and other critical parameters. The VMS incorporates also water pressure gauges to monitor pore water pressures within saturated zones. Positioned in a slanted orientation across dam structures and, the system provides continuous, real-time measurements of water content and pressure variations throughout the dam's materials. All data collected by the VMS units are relayed in real-time to a cloud-based database, ensuring accessibility for dam operators. This continuous monitoring capability spans both vadose and saturated zones enables numerical computation of the water flux. With the analysis of changes in solids content-internal erosion can be identified and quantified (3).

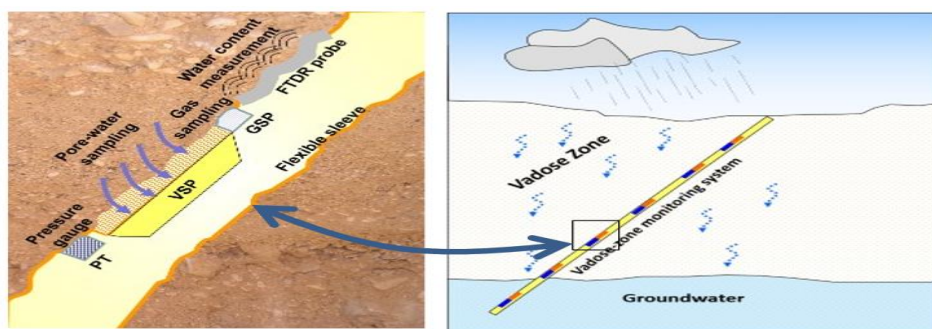


Figure 1. Schematic illustration of a monitoring sleeve installed through the vadose and saturated zones.

2 EARLY WARNING ABOUT PIPING PROCESS

A Vadose Zone Monitoring System (VMS) was installed in an earthen dam designed for flood control by Dead Sea Works Ltd., Israel (Fig.2). Following a flood, a noticeable increase in water content (before saturation) was observed ONLY in a layer located 8.0m below the dam crest. This increase began 5 days after the flood event and continued for the next 10 days until the layer reached full saturation (only then a standard piezometer would have reacted). With the VMS technology, an alarm about a potential piping process was raised a critical 10 days earlier.

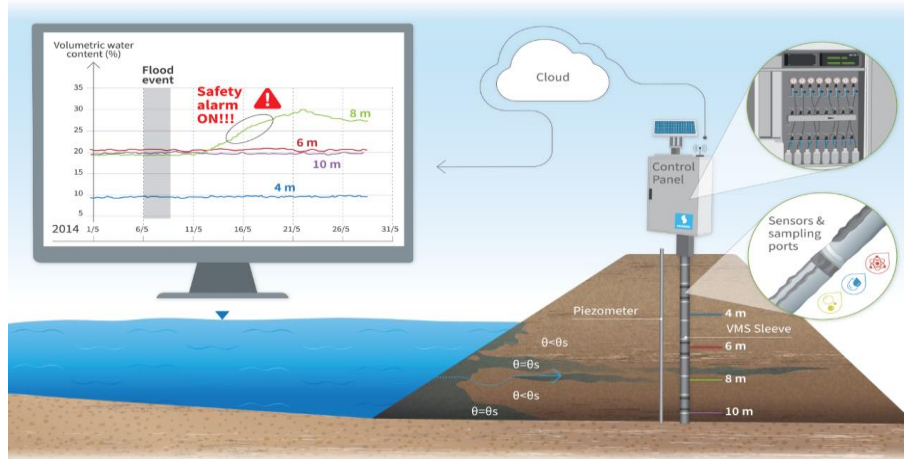


Figure 2. VMS setting for early warning of piping and dam safety.

REFERENCES

- Freeze, A. (9/7/2010) 'Influence of the Unsaturated Flow Domain on seepage Through Earth Dams', Water resources Research.
- Dahan, O., McDonald, E. and Young, M. (2003) 'Development of a flexible TDR probe for deep vadose zone monitoring', Vadose Zone Journal.
- Qun Chen, L.M. Zhang 'Three-dimensional analysis of water infiltration into Gouhou rockfill dam using saturated-unsaturated seepage theory'. Canadian Geotechnical Journal · May 2006, p.449-461
- Association of USA State Dam Safety Officials home page: [https://damsafety.org/dam-owners/internal-erosion-of-earth-dams#:~:text=Internal%20erosion%20\(called%20%E2%80%9Cpiping%E2%80%9D,or%20abutments%20of%20the%20dam](https://damsafety.org/dam-owners/internal-erosion-of-earth-dams#:~:text=Internal%20erosion%20(called%20%E2%80%9Cpiping%E2%80%9D,or%20abutments%20of%20the%20dam)

Evaluation of the Decision Support Framework on Backward Erosion Piping

V.M. van Beek¹, B.A. Robbins², E.M. van der Linde^{1,5}, W. Kanning¹, E. Rosenbrand¹, T.M. O'Leary³, A. Hill², J.G. Knoeff¹, H. van Hemert³

1. Deltares / Flood Defence Technology, Delft, The Netherlands, vera.vanbeek@deltares.nl

2. U.S. Army Corps of Engineers / Risk Management Center, Lakewood, Colorado, U.S.A., bryant.a.robbins@usace.army.mil

3. U.S. Army Corps of Engineers / Risk Management Center, Louisville, Kentucky, U.S.A., timothy.m.oleary@usace.army.mil

4. Rijkswaterstaat / Water Verkeer en Leefomgeving, Lelystad, The Netherlands, henk.van.hemert@rws.nl

5. Delft University of Technology/Hydraulic Engineering, Delft, The Netherlands, lisa.vanderlinde@deltares.nl

ABSTRACT: Backward erosion piping (BEP) poses a threat to levees and dams with sandy foundations. The current assessment and design practice for the different stages leading to failure is based on basic calculation rules in which the subsurface is schematized in a simplified manner. New insights on BEP indicate that the simplifications in models result in under- or overestimations of the failure probability. To guide practitioners to a more realistic assessment and design, we developed a decision support framework (DSF). This DSF allows for evaluation of the safety assessment in the light of influential aspects that are not inherently accounted for in prediction models. The evaluation of the DSF in Dutch and U.S. practice provided ideas for improvement and input for further research.

Keywords: Backward erosion piping; Safety assessment; Design; Decision Support

1 INTRODUCTION

Both in the Netherlands and in the U.S. BEP is considered an important failure mechanism for dams and levees. As the failure path in Figure 1 depicts, groundwater flow (node 1) caused by the high water level may induce cracking of the blanket layer (node 2), followed by the formation of shallow pipes at the interface of the sand layer and the cohesive blanket (node 3). If not intervened (node 4), ongoing erosion may lead to the connection of pipes to the outer water level (node 5), finally resulting in collapse of the levee (node 6).

In a safety assessment, calculation rules are used to assess the probability of cracking and backward erosion, using blanket theory and Sellmeijer's or Schmertmann's rules (Sellmeijer et al., 2011, Schmertmann, 2000). These calculation rules rely on geometries which are simplified to a two-dimensional geometry, characterized by homogeneous layers of sand beneath the surface, where a steady state flow is presumed.

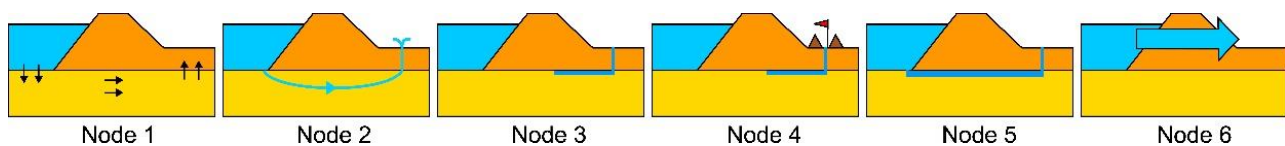


Figure 1. Nodes in the failure process for backward erosion piping.

Advancements in the understanding of BEP and the large number of infrastructure improvements required under existing guidance emphasized the need for more realistic safety assessments. However, new knowledge that emerges from research is often not yet ready to be included in safety assessments and design guidelines, because of limited theoretical understanding or lack of validation, which makes implementation of the newly developed knowledge difficult for practitioners. To assist practitioners in incorporating new knowledge, we developed a decision support framework (DSF) for BEP. The DSF is intended to guide practitioners in identifying the relative importance of influential aspects that are not inherently accounted for in prediction models, in order to evaluate the safety assessment in the light of the influential aspects. By developing such a DSF, recent findings from BEP research can readily be transitioned to aid in decision making.

2 DECISION SUPPORT FRAMEWORK

The process to assess BEP risks using the DSF consists of the steps illustrated in Figure 2. First, a baseline assessment is performed using existing guidelines and processes in step 1. Once a baseline assessment has been performed, the DSF will be used to review the nodes in the failure mode description in step 2. For each node, the DSF will guide the user to evaluate which influential aspects are either included or excluded in the present risk assessment based on factsheets. For each influential aspect, guidance to assess its relative importance and degree of available knowledge is provided in aspect sheets. Plotting the relative importance of an aspect, and degree of available knowledge in a quadrant (example in Figure 3) results in a clear overview of the influential aspects for a particular project. This allows decision makers to better inform their decisions based on the results of a risk assessment. Factsheets were made for each of the nodes in the failure path in Figure 1. The factsheets contain information regarding the node, and a list of aspects to be reviewed, with a short description. To assess the relevance of these aspects, aspect sheets are drafted that describe which site-specific parameters affect the relevance of the aspect, as well as an indication of the degree of knowledge that is available regarding the local impact on the flood risk. Each aspect sheet contains a basic description, a flow diagram for assessment of relevance, suggestions for derivations of corrections and further analyses and reference to relevant literature. The aspect sheets will guide the user to make an estimate of the relevance for the impact on flood risk and the level of available knowledge, such that the aspect can be placed in the quadrant graph.

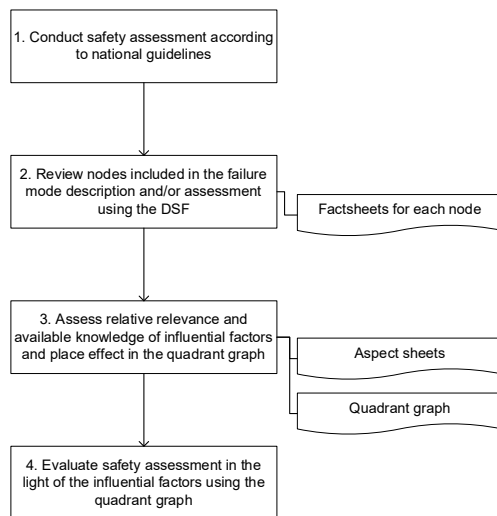


Figure 2. Illustration of envisioned risk assessment process for BEP and provided tools for guidance.

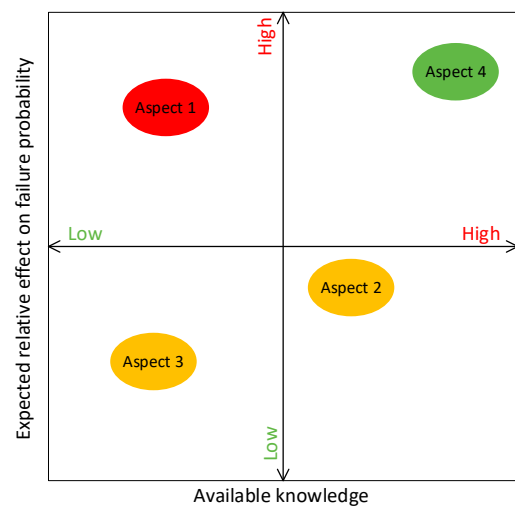


Figure 3. Quadrant graph for risk assessment, colours indicate whether the effect decreases (green) or increases (red) the flood risk.

3 EVALUATION

The DSF has been evaluated with end users from the Netherlands and the U.S. The need and usefulness for the DSF was acknowledged, but the users require more guidance on quantification of influential aspects through factors and uncertainty ranges. The implementation of the DSF in the Dutch probabilistic approach for safety assessment requires attention, while the DSF complements the U.S. Army Corps of Engineers' approach as a likelihood factor for subjective probability estimation. Finally, the users prioritized the aspects in terms of contribution to failure probability, which serves as a guidance for further research. The most significant 4 aspects in terms of frequency of occurrence and impact on risk estimates were the fine content, 3D flow, flood plains, and soil variability in the seepage path.

ACKNOWLEDGMENTS

This paper was produced as part of an international co-operation between the USACE and Rijkswaterstaat, part of the Dutch Ministry of Infrastructure and the Environment.

REFERENCES

- Schmertmann, J.H., 2000. The no filter factor of safety against piping through sands, in: Silva, F., E.Kavazanjian (Eds.), *Judgement and Innovation*. American Society of Civil Engineers, pp. 65–133.
- Sellmeijer, H., López, J., Cruz, D., Van Beek, V.M., Knoeff, H., Beek, V.M. Van, 2011. Fine-tuning of the backward erosion piping model through small-scale, medium-scale and IJkdijk experiments. *Eur. J. Environ. Civ. Eng.* 15, 1139–1154. <https://doi.org/10.3166/EJCE.15.1139-1154>.

Towards fragility curves: the case of Adige River levees

V. Mangraviti¹, L. Pinter², N. Fabbian¹, S. Cola¹

1. University of Padova, Department of Civil, Environmental and Architectural Engineering, Padova, Italy

2. University of Padova, Department of Geosciences, Padova, Italy

viviana.mangraviti@unipd.it

ABSTRACT: Evaluating the safety of river embankments is one of the most challenging problems for geotechnical engineers. Levees extend for several kilometres and the knowledge derived from in-situ testing is often limited. For this reason, probabilistic approaches are a valuable tool for schematically assessing the main criticalities of the problem and calculating the probability of failure. In this note, a preliminary study on the evaluation of fragility curves for the embankments of Adige River is presented. The formation of sand boils induced by underseepage is modelled with the finite element approach and the results are discussed in a probabilistic framework.

Keywords: levees; underseepage; fragility curve

1 INTRODUCTION

Ensuring the correct functioning of river levees in highly urbanized areas is of paramount importance. In fact, preventing flooding of the adjacent floodplain (levee collapse) by keeping the river confined to one side of the levee is the key to save an enormous amount of economic and human resources. Most Italian levees were built between the 19th and 20th century and usually extend for many kilometres. Despite the huge uncertainties behind existing levees, semi-probabilistic approaches with partial safety factors are often used in practice to evaluate both performances and safety of the system by first characterizing mechanical parameters and then adjusting resistances and loads to account for inherent uncertainties and randomness. However, for complex and diversified structures such as levees, considering random variables affecting the response of the system is particularly relevant. Consequently, probabilistic methods such as First-Order Second-Moment (FOSM) or Monte Carlo (MC) simulations are becoming increasingly widespread (Amabile et al., 2020; Gottardi et al., 2020) to estimate the probability of failure for a given flow water elevation (FWE). In this preliminary study, the probability that the exit gradient at the embankment toe exceeds the critical one is assumed to correspond to the formation of sand boils, considered a sort of pre-failure of the levee.

2 CASE STUDY

The study considers the case of an embankment of Adige River, in Trento (Italy), where several sand boils appeared near the foot of the levee during the last high-water events (Figure 1.a). These phenomena are typical evidence of active underseepage which, with time, can produce a backward erosion piping and the levee collapse.

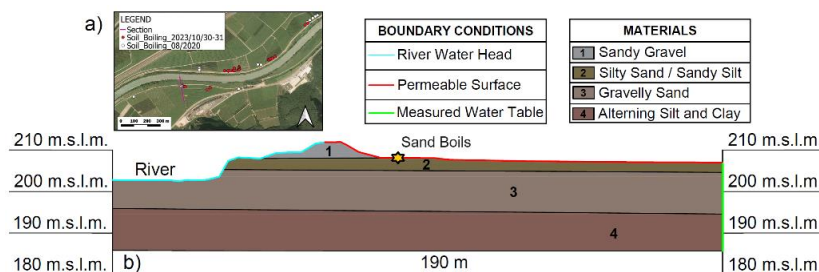


Figure 1. (a) Location of sand boils activated during the high-water events along the Adige River near Trento. (b) SEEP/W model of the studied section.

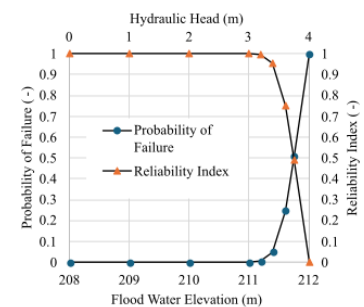


Figure 2. Fragility curve for sand boils induced by underseepage.

One representative section, along the left side levee of the Adige River, some kilometres upstream of Trento city, is modelled (Figure 1.b). As during the recent high-water events in this section several sand boils were mapped, some investigation and surveys were here conducted. For modelling purposes, the local geological sequence is simplified into

4 homogeneous layers (Figure 1.b) on the base of SPT results. Layer 1 represents the gravelly sand forming the embankment, which is based above of a relatively thin silty sand blanket (Layer 2) extending towards the country side. Layer 3 is the most permeable level extending towards the river, below confined by an impermeable layer composed of an alternation of clay and silt lenses.

3 MODELLING

The results of on-site surveys and laboratory tests are used to define a finite element model capable of reproducing underseepage. The main mechanical parameters used in the analysis (Table 1) are obtained from a statistical analysis of survey and laboratory data, or, otherwise, from scientific literature. Furthermore, a horizontal vs vertical permeability ratio of 0.1 is considered.

Steady state analyses are carried out, for different FWEs, imposing a total head boundary condition on the riverside (blue line in Fig. 1b). A groundwater total head of 205 m is imposed at the right-hand border of the model to represent the average water table level measured during the most recent survey (red line in Fig. 1b).

Table 1. Material parameters for the steady state analyses performed with SEEP/W.

Layer	Material	Horizontal permeability expected value (m/s)	Porosity
1	gravelly sand	2.5E-05	0.361
2	silty sand	1.9E-05	0.365
3	gravelly-heavily gravelly sand	2.7E-04	0.354
4	clay and silt	1.0E-09*	0.472

*data obtained from scientific literature

4 FRAGILITY CURVE

The vertical hydraulic gradient determined via FEM at the seepage exit on the landward side close to the levee toe is used for a preliminary assessment of the fragility curve in case of underseepage (Figure 2), which gives the probability of sand boils occurring, also indicated in the plot as probability of failure, p_f , for different FWEs. The Taylor series – finite difference method (Wolff, 2008) is used to evaluate the effects of three random variables: (i) the ratio between permeabilities of Layers 3 and 2; the thicknesses of both (ii) Layer 2 and (iii) Layer 3. For a first estimate of p_f , the coefficient of variation associated with each random variable is taken from the literature as 40%, 3% and 10%, respectively. A log-normal distribution is assumed for the exit gradient. The critical gradient is calculated as the ratio between the effective unit weight of soil of Layer 2 (7 kN/m^3 as estimated from lab tests) and the water unit weight (10 kN/m^3).

5 DISCUSSION

Similarly to what observed during the last high-water events, the results in terms of both p_f and reliability ($= 1 - p_f$) (Figure 2) shows that the levee is generally reliable until FWE = 211 m is reached. When the river rises to the top, high pressures generate at the base of Layer 2 and the probability of formation of sand boils for underseepage rapidly increases until reaching a unit value. However, it must be noted that a different shape of the soil layers, assumed with a constant thickness in this preliminary analysis, may affect this result. Further analyses, also for different failure mechanisms, are planned for the future.

ACKNOWLEDGMENTS

This study was carried out within the RETURN Extended Partnership and received funding from the European Union Next-GenerationEU (National Recovery and Resilience Plan – NRRP, Mission 4, Component 2, Investment 1.3 – D.D. 1243 2/8/2022, PE0000005)

REFERENCES

- Amabile, A., Pozzato, A., & Tarantino, A. (2020). Instability of flood embankments due to pore-water pressure build-up at the toe: Lesson learned from the adige river case study. *Canadian Geotechnical Journal*, 57(12).
- Gottardi G., Gagnano C. G., Ranalli M., Tonni L. (2020). Reliability analysis of riverbank stability accounting for the intrinsic variability of unsaturated soil parameters. *Structural Safety*. <https://doi.org/10.1016/j.strusafe.2020.101973>
- Wolff, T. F. (2008). Reliability of levee systems. In *Reliability-Based Design in Geotechnical Engineering: Computations and Applications*. <https://doi.org/10.1201/9781482265811-17>

Updated “Piping Toolbox” – Significant Changes to Concentrated Leak Erosion Methodology in Vertical Cracks and Impacts on Practice

Timothy M. O’Leary¹

1. U.S. Army Corps of Engineers, Risk Management Center, Louisville, Kentucky, USA, timothy.m.oleary@usace.army.mil

ABSTRACT: U.S. Army Corps of Engineers (USACE) internal erosion methodology and tools were derived from the Fell et al. (2008) “piping toolbox” that was co-authored by USACE, U.S. Bureau of Reclamation, URS Corporation, and University of New South Wales (UNSW). Since developing Fell et al. (2008), the understanding of the mechanics of internal erosion has improved, and significant experience using the “piping toolbox” has been gained. This paper examines potential impacts of the methodology updates in the updated “piping toolbox” (Fell et al. 2024) for estimating the probability of initiation of concentrated leak erosion in vertical cracks.

Keywords: internal erosion; initiation; concentrated leak erosion; cracking; quantitative risk analysis

1 INTRODUCTION

To assess the likelihood of initiation of concentrated leak erosion, hydraulic shear stresses on the surface of a vertical crack (τ) are compared to the critical shear stress (τ_c) for the embankment soil. If τ exceeds τ_c , erosion will initiate. Fell et al. (2008) compare the average hydraulic shear stress (τ_{avg}) on the surface of the vertical crack to τ_c to estimate the probabilities of initiation as a function of headwater level. Additional research on swelling potential and flow through cracks occurred since the publication of Fell et al. (2008). The methodology for initiation of concentrated leak erosion in vertical cracks resulting from differential settlement changed significantly in Fell et al. (2024).

2 HYDRAULICS OF FLOW THROUGH VERTICAL CRACKS

Fell et al. (2024) adopted the numerical modeling and laboratory testing of Peirson et al. (2023) which indicated flow in vertical cracks is controlled by the exit conditions at the downstream end of the crack, and hydraulic shear stresses are highest at the downstream end and nearer the water surface in the crack. As erosion occurs, the downstream end of the crack widens, and the water surface lowers. Peirson et al. (2023) used a numerical model to develop charts to estimate the maximum hydraulic shear stress (τ_{max}) on the walls of vertical cracks.

3 RESULTS

Fell et al. (2024) indicated the average gradient method used in Fell et al. (2008) is still appropriate for conduit-like conditions (cracks that flow full). However, the simplified graphical method of Peirson et al. (2023) better models flow in vertical cracks in the upper parts of embankments. This method is difficult to implement in practice because it requires interpreting multiple charts, with very small differences between data series of similar line types. It is iterative and labor intensive. For the purposes of this review, the raw data used to generate the charts in Peirson et al. (2023) and tables in Fell et al. (2024) were examined and incorporated into spreadsheets with interpolation techniques to improve precision and make them easier to use in practice.

Figure 1 compares τ_{avg} to τ_{max} for vertical rectangular cracks only. It illustrates how the likelihood of initiation of concentrated leak erosion based on τ_{max} will likely be grossly underestimated using τ_{avg} . In addition, the τ_{max} values from the simplified graphical method of Peirson et al. (2023) exceed the typical range of τ_c from Fell et al. (2024) except for the best and high estimates for clayey embankment soils. Therefore, the likelihood of initiation of concentrated leak erosion is high for most embankment soil types.

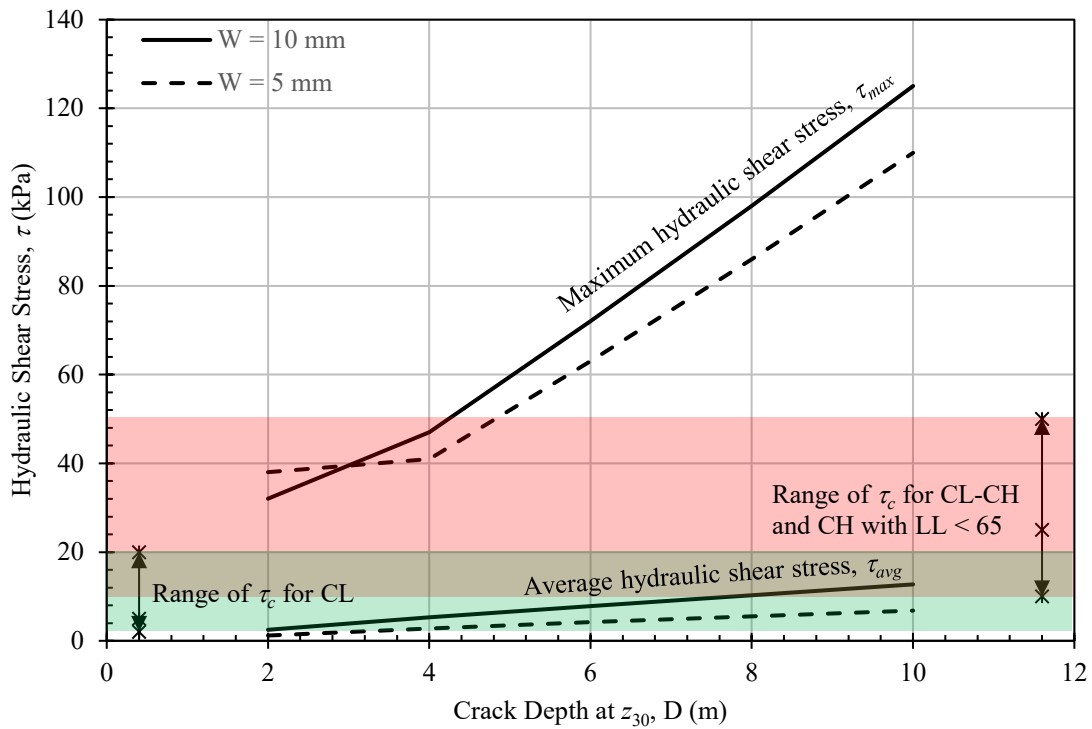


Figure 1. Comparison of hydraulic shear stresses for vertical rectangular cracks.

4 CONCLUSIONS

Based on the results of this trialing, the new methodology for estimating hydraulic shear in vertical cracks does not seem to add value to the quantitative risk analysis if concentrated leak erosion will initiate somewhere in a crack for most embankment soils. Evaluation of the likelihood of initiation, by comparing hydraulic shear stresses in the crack to critical values, becomes less important in the risk analysis because erosion will progress upstream by progressive erosion and headcutting unless swelling closes the crack or filters/transitions stop the erosion. If there is a potential for persistent open vertical cracks, with no performance history above the estimated base of the crack and no swell potential, a probability of initiation of one can be assumed for screening, and the annual probability of failure (APF) will be driven by the frequency of the loading and whether filters/transitions are present.

5 DISCLAIMER

USACE, U.S. Bureau of Reclamation, and AECOM (formerly URS Corporation) were not involved in the preparation of the draft updated “piping toolbox” (Fell et al. 2024). Trialing and review occurred from January to June 2024. The authors of Fell et al. (2024) will consider these comments and prepare a document which summarizes the feedback and provides their responses. Afterwards, they will finalize the Guidance and Support Documents and issue them as a UNSW UNICIV report, which will be free to the public. After publication, the authors recommended ceasing use of Fell et al. (2008).

REFERENCES

- Fell, R., Foster, M., Cyganiewicz, J., Davidson, R., and Sills, G.L. (2024). Methods for estimating the probability of failure of embankment dams by internal erosion and piping – AKA “The piping toolbox.” UNICIV Report No. R-XXX (Draft). School of Civil and Environmental Engineering, University of New South Wales. <https://www.dropbox.com/scl/fo/uq763qq313yv8wk2sh1ic/h?rlkey=ml6s0o2ovwqonmxsi658w3wwx&dl=0>.
- Fell, R., Foster, M., Cyganiewicz, J., Sills, G.L., Vroman, N., and Davidson, R. (2008). Risk analysis for dam safety: A unified method for estimating probabilities of failure of embankment dams by internal erosion and piping. UNICIV Report No. R-446. School of Civil and Environmental Engineering, University of New South Wales. <http://vm.civeng.unsw.edu.au/uniciv/R-446.pdf>.
- Peirson, W.L., Prapakaran, V., Fell, R., and Douglas, K. (2023). On the hydraulics of flow in cracks in embankment dam cores. *European Journal of Environmental and Civil Engineering*, 27(3): 1367-1382. <https://doi.org/10.1080/19648189.2022.2081993>.

Lessons learnt for safety analysis from internal erosion accidents and incidents on embankment dams, based on a 3000 documents database

N. Lebrun¹, J. R. Courivaud¹, A. Vogel²

1. EDF-CIH, La Motte Cervolox, France, nicolas-jean-claude.lebrun@edf.fr

2. RISK ASSESSMENT- RAI, Vienna, Austria, vogel@risk-assessment.at

ABSTRACT: Since 2013, RAI AUSTRIA and EDF have been developing a database of worldwide dam failure cases. From this database, an analysis of about a hundred cases of failure, or near failure, by internal erosion, of embankment dams has been carried out. The analysis focuses on the notion of failure scenarios. These scenarios, which aim to identify the key parameters that led to the failure of a dam from the moment it was impounded, enabled us to identify significant recurrences among the population of dams studied.

Keywords: dam failure database; embankment; internal erosion, dam safety.

1 INTRODUCTION

Since 2013, RAI AUSTRIA and EDF have been developing a database of worldwide incidents and accidents on dams. This database gathers around 500 dam failure cases, including 350 in embankments, and more than 3,000 documents. These documents include scientific publications, expert reports and newspaper articles. This article presents a synthesis of about 100 cases of internal erosion failure (or near failure) of embankment dams, based on this database. It especially focuses on long-term failures (more than 5 years after impoundment) and on the dam operator's point of view.

2 ANALYSIS OF FAILURE SCENARIOS

Each case of failure was associated with a scenario, on the basis of the following 4 parameters: age at failure since impoundment (> or < 5 years) / existence or not of a design or construction error explaining the failure / existence or not of major disorders on the dam, observed sufficiently in advance to allow an intervention / existence or not of a monitoring or maintenance deficit.

The analyses shows that:

- around 50% of cases correspond to rapid failures, shortly after impoundment, mainly due to a design or construction error,
- around 20% of cases correspond to pathological structures, having failed more than 5 years after impoundment, as a result of inadequate monitoring or maintenance,
- around 15% of cases correspond to failures, more than 5 years after impoundment, of dams that were not pathological, at least in appearance.

Regarding the operation of an embankment dam, carried out in accordance with good practices, analysis of the last category of failure cases is of particular interest.

3 ANALYSIS OF LONG-TERM FAILURES OF NON-PATHOLOGICAL STRUCTURES

This category includes 14 cases of failure, whose analysis reveals recurring characteristics:

- Foundation failure in complex geological formations: this feature appears in 5 cases (12 for all failure scenarios combined). The formations concerned may be basalts or fractured rocks intercalated with loose formations for example, and all present high mechanical or permeability contrasts, possibly leading to the development of slow, hard-to-detect mechanisms.

- Failure due to construction work: this feature appears in 5 cases (6 for all failure scenarios combined). The work may have been carried out for maintenance, operating or safety reasons, but in all cases led to the failure of a dam that was not initially pathological.
- Probable failure caused by mixed shear/internal erosion mechanisms: this feature appears in 3 to 4 cases (7 for all failure scenarios combined). Detailed analysis of the events leading to failure suggests that phenomena such as loss of suction or static liquefaction probably played a role in the failure. In particular, these failures often occurred in very loose sandy or silty embankments and/or following heavy rainfall on the dam and/or were described as a sudden collapse of the embankment.

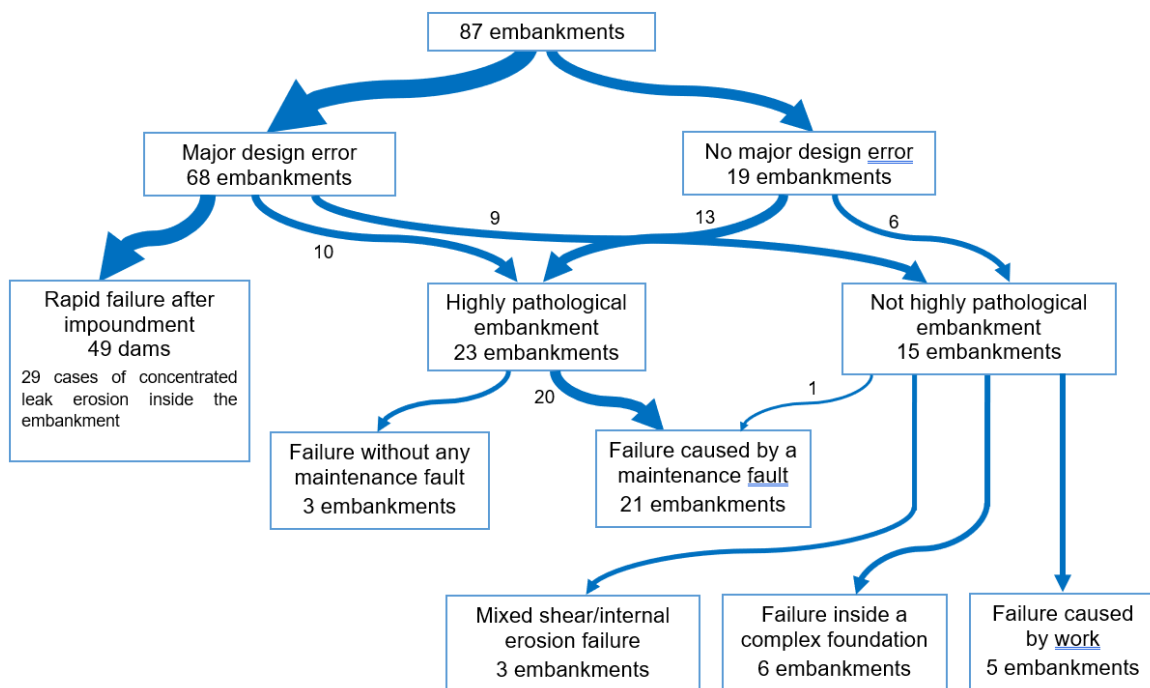
4 ADDITIONAL ANALYSES

Additional analyses were carried out, notably concerning :

- locations (30% embankment, 30% along structure crossing embankment, 20% foundation, 20% unknown) and mechanisms (concentrated leak erosion 60%, regressive erosion 20%, unknown 20%);
- rupture-initiating events: 65% impoundment (known or assumed), 20% flood and/or rain, 7% works, 4% ageing.

5 FAILURE DIAGRAM

The failure cases for which sufficient information was available (87) were distributed according to the following diagram:



6 CONCLUSION

Analysis of lessons learnt from embankment dam failures provides valuable information for the design, operation and safety studies of these structures. Analysis of internal erosion failures, based on the database developed by RAI AUSTRIA and EDF, has identified recurring scenarios and parameters that have led to the failure of most of embankment dams. Design errors play a fundamental role in short-term failures. In the longer term, maintenance plays an important role in the safety of dams, and certain specific configurations and circumstances, such as those described in paragraph 3, require particular attention.

REFERENCES

Database of dam incidents and failures. [EDF - RAI - Database of dam incidents and failures \(dfdb.eu\)](http://dfdb.eu)

USACE Levee Internal Erosion Incidents and Failures

Timothy M. O’Leary¹ and David M. Schaaf²

1. U.S. Army Corps of Engineers, Risk Management Center, Louisville, Kentucky, USA, timothy.m.oleary@usace.army.mil

2. U.S. Army Corps of Engineers, Risk Management Center, Louisville, Kentucky, USA, david.m.schaaf@usace.army.mil

ABSTRACT: Internal erosion is a primary risk driver for U.S. Army Corps of Engineers (USACE) levees. The USACE Levee Loading and Incident Database (LLID) is the result of a multi-year effort to collect and categorize historical levee performance data for USACE levees. The LLID provides probability of failure estimates and breach dimensions. The LLID is a critical component of the USACE Levee Screening Tool (LST) Version 2.0. and is used for other purposes in the USACE Levee Safety Program. This paper provides preliminary findings related to internal erosion incidents and failures for USACE levee embankments.

Keywords: Levee, internal erosion; incidents; failures; intervention; failure rate

1 INTRODUCTION

Internal erosion is a primary risk driver for the U.S. Army Corps of Engineers (USACE) levee portfolio. The USACE Levee Loading and Incident Database (LLID) is the result of a multi-year effort to collect and categorize historical USACE levee performance data. The LLID provides probability of failure estimates for multiple performance modes, tracks key contributing factors of overall levee performance, and general characteristics of breach sizes.

2 USACE LEVEE LOADING AND INCIDENT DATABASE

The USACE levee portfolio includes 2,859 levee segments for a total length of 22,800 kilometres. As part of the LLID, an initial screening of the USACE levee portfolio was performed to identify levee segments suitable for determination of failure rates. The screening process eliminated 640 of the 2,859 levee segments that did not meet the definition of a traditional coastal or riverine levee (like a spur levee), levee embankment sections less than 1 meter in loading height, and levee segments that had never been loaded above 25% of the loading height. As of June 2024, 711 (32%) of the remaining 2,219 viable levee segments were evaluated. Approximately 30,000 years of cumulative performance data was reviewed for the 711 levee segments evaluated, where both reliable performance data and reliable gage data were available. The actual number of years of service is higher, but years where the loading could not be accurately estimated and/or there was no reliable documentation of performance were excluded.

Table 1 summarizes the number of internal erosion incidents associated with levee embankments, along with the number of failures by general location of internal erosion. In the LLID, a significant internal erosion incident includes breach prior to overtopping, extensive interior flooding due to excessive seepage, flood fighting to prevent breach, or any flood damage/post-flood repair exceeding \$1 million (2020 USD values). Internal erosion failures are about equally distributed through the embankment and through the foundation.

Table 1. Summary of incidents and failures.

General Location of Internal Erosion	Total Number of	Number of	Number of
	Incidents	Significant Incidents	Failures
Through the Embankment	496	252	42
Through the Foundation	671	340	38
Total	1,167	592	80

Table 2 summarizes contributing factors for internal erosion incidents. About 36% of the breaches involved culverts/pipes or animal burrows, which could lead to concentrated leak erosion through the embankment. About 14% of the breaches involved old channel/slough crossing locations, where the foundation is more susceptible to backward erosion piping.

Table 2. Contributing factors for internal erosion incidents.

General Location of Internal Erosion	Most Common (> 20% of Incidents)	Moderately Common (10% to 20% of Incidents)	Least Common (< 10% of Incidents)
Through the Embankment	<ul style="list-style-type: none"> • Culverts/pipes through levee embankment • Encroachments 	<ul style="list-style-type: none"> • Underseepage control system • Vegetation • Design/construction deficiency • Previous damage area • Animal control 	<ul style="list-style-type: none"> • Landside culvert/pipe • Cracking • Settlement • Rutting • Other
Through the Foundation	<ul style="list-style-type: none"> • Culverts/pipes in foundation beneath levee alignment • Old channel/slough crossing location • Encroachments 	<ul style="list-style-type: none"> • Underseepage control system • Vegetation • Design/construction deficiency • Previous damage area • Animal control 	<ul style="list-style-type: none"> • Landside culvert/pipe • Cracking • Settlement • Rutting • Other

3 CONCLUSIONS

The preliminary failure rates as a function of percentage of levee height (measured from the landside embankment toe to the crest) are portrayed in *Figure 1* and *Figure 2* for the two general locations of internal erosion. For internal erosion through the embankment, the probability of failure for a loading of 90 to 100 percent of the levee height is about 2% with flood fighting and 12% without flood fighting. For internal erosion through the foundation, the probabilities of failure are about the same. For both general locations of internal erosion, the difference between probabilities of failure with and without flood fighting is about one order of magnitude. Despite many internal erosion incidents, USACE has a high rate of successful intervention. Success is due primarily to early detection of obvious signs of distress through visual inspections and the implementation of rapid remedial actions.

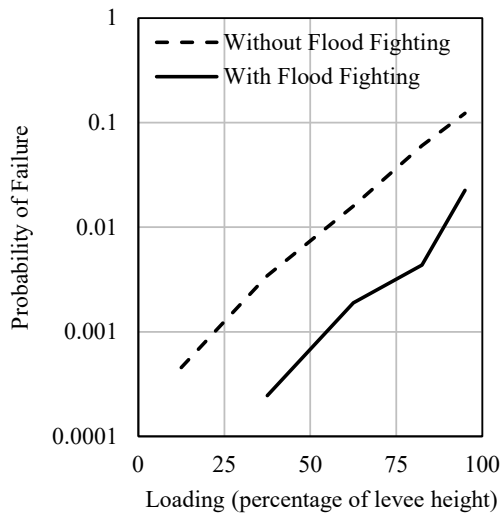


Figure 1. Probability of failure for internal erosion through the embankment.

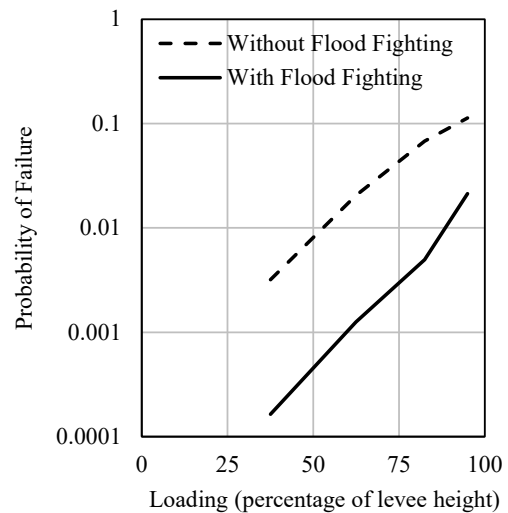


Figure 2. Probability of failure for internal erosion through the foundation.

REFERENCES

U.S Army Corps of Engineers (2023). *USACE Levee Screening Tool Application Guide and Technical Reference Manual*, Draft.

Emergency reconstruction and safety enhancement project for the Idice Torrent embankment breach – Part 1

D. Mingozi¹, M. Bentini¹, R. Paciolla¹, S. Tozzi¹, A. Zamagni¹, S. Saccà¹

1. Enser srl, Faenza (RA), Italy, ingegneria@enser.it

ABSTRACT: The flood event that occurred in Emilia Romagna between May 16th and 17th of last year 2023, caused a breach at the right bank of the Idice Torrent, leading to the collapse of the Motta Bridge on via Zenzalino Nord and the flooding of the surrounding lands, in the surroundings of La Motta (Budrio, Bologna, Italy). The breach was preceded and triggered by overtopping, a phenomenon that occurred in several points, both on the right and left sides, upstream and downstream. The embankment reconstruction project didn't only include the damaged area, but it was designed to remodel different sections, partially or totally, where erosive phenomena had resulted in an unacceptable reduction of hydraulic safety levels, aiming to restore the watercourse to its pre-event safety standard.

Typical issues of emergency works were addressed during the design phase, such as rapid execution, numerous "contractors" operating at the same time, provide minimum safety levels even during the execution phases.

Keywords: Idice, embankment breach, bank erosion, emergency intervention design, urbanized area.

1 INTRODUCTION, CONTEXT, MOTIVATION

The rainfalls during the early days of May 2023 had a significant impact on the Idice river basin area. The average daily rainfall on May 2, 2023, was of 114.15 mm and it exceeded the historical maximum of 112.12 mm, recorded in 1966. This is confirmed by the observation of the 48-hour cumulative rainfall for the first two days of May. These combined events, according to hydrological studies, have caused catastrophic consequences on the territory and may be associated with a return time of 334 years (Brath et al. 2023).

The embankment breach is estimated to be approximately 115 meters wide and caused the flooding of low-lying farmland on the right bank, affecting municipal roads and the provincial road SP6 under the jurisdiction of the Metropolitan City of Bologna, as well as residential and rural buildings.

The breach of the embankment on the right bank and the subsequent increase in water flow velocity, combined drawdown of the watercourse, resulted in partial or complete collapse of the embankment and floodplains on both the right and left banks, over a stretch of approximately 3 km upstream from the breach, up to the Bologna - Portomaggiore railway bridge. Additionally, there was erosion of the riverbed to an estimated depth of about one meter (3 meters at the breach of the embankment), as shown in *Figure 1*.

These events left the remaining levee sections extremely vulnerable, unable to contain even ordinary water levels, exposing the surrounding areas to a high risk of flooding.

The first intervention involved temporarily closing of the main breach in the embankment with a filter rockfill dam and, at the same time, the lowering of a long part of the Idice stream riverbed downstream from the breach, to enhance water flow.

The three kilometers of embankment have been classified based on the extent of damage, according to the following table and to the scheme in *Figure 2*.

Severity of instability	Color	Damage
Null	-	Minor erosion of the lower embankment
Low	Yellow	Erosion of the lower embankment
Medium	Orange	Erosion of the lower embankment, the plain, and/or the floodplain slopes, but with the embankment head intact
High	Red	Total or partial erosion of the embankment head with involvement of the countryside-facing embankment slopes

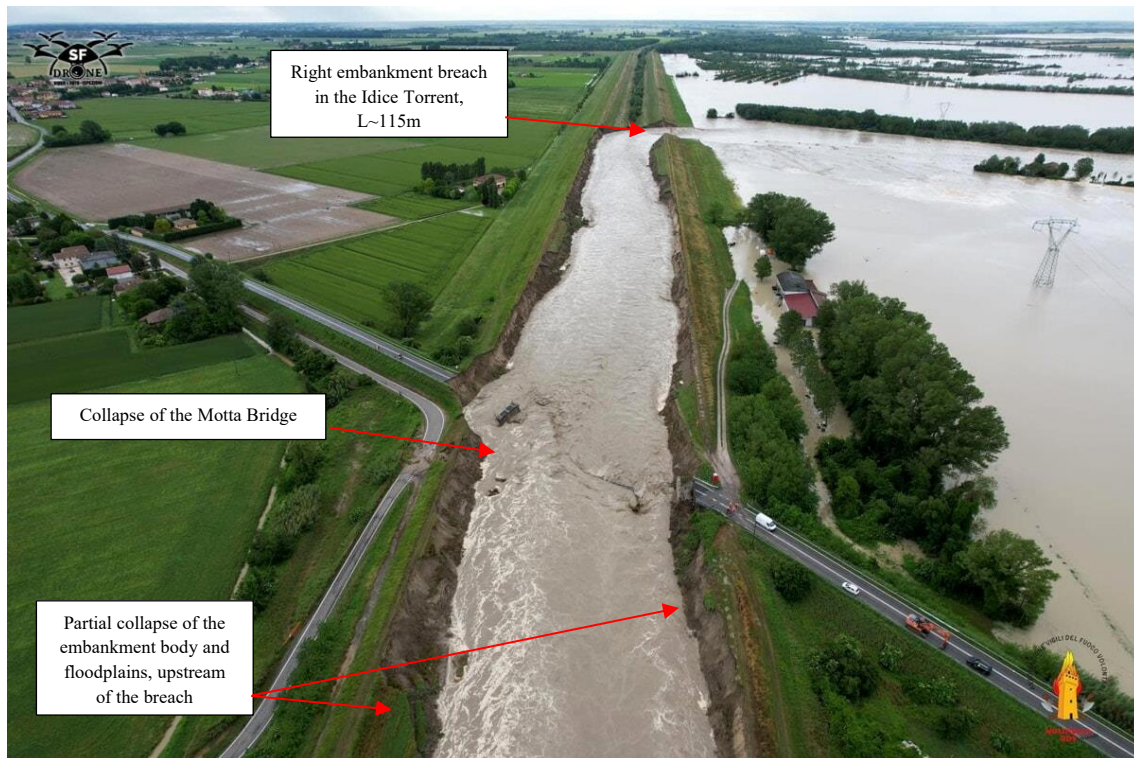


Figure 1. Aerial view of the right embankment breach in the Idice Torrent, collapse of the Motta Bridge and erosion of the riverbanks.

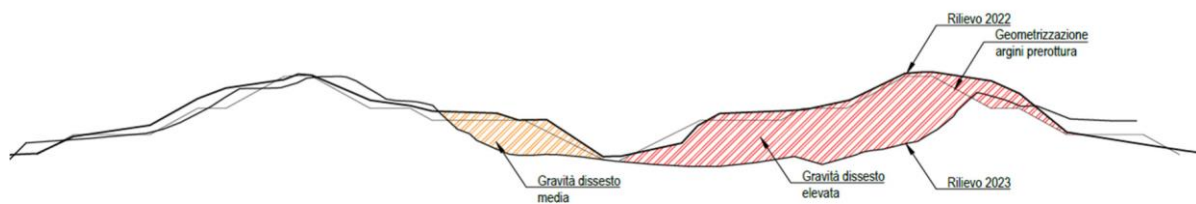


Figure 2. Example of medium (on the left) and high (on the right) severity of instability phenomena

ACKNOWLEDGMENTS

We sincerely thank the Emilia-Romagna Region and the Agency for Territorial Security and Civil Protection of the Emilia-Romagna Region for their collaboration and support.

REFERENCES

- A. Brath, N. Casagli, M. Marani, P. Mercogliano, R. Motta (2023). Rapporto della Commissione tecnico-scientifica istituita con deliberazione della Giunta Regionale n. 984/2023 e determinazione dirigenziale 14641/2023, al fine di analizzare gli eventi meteorologici estremi del mese di maggio 2023.
- GEO-SLOPE International Ltd. (2015), Stability Modeling with SLOPE/W.
- Lancellotta R. (1993). *Geotecnica*, 2nd ed, Zanichelli, Bologna.
- Raviolo P.L. (1993). *Il laboratorio geotecnico, Procedure di prova, Elaborazione, Acquisizione dati*, ed. Controls, Milano.
- Ministerial Decree of 01/17/2018: Aggiornamento delle Norme tecniche per le costruzioni, (GU n.42 del 20-02-2018 - Ordinary Supplement n. 8);
- Circular 21 January 2019, n.7 C.S.LL.PP.: Istruzioni per l'applicazione dell'Aggiornamento delle "Norme tecniche per le costruzioni" referred to in the Ministerial Decree 17 January 2018.

Emergency reconstruction and safety enhancement project for the Idice Torrent embankment breach – Part 2

D. Mingozi¹, M. Bentini¹, R. Paciolla¹, S. Tozzi¹, A. Zamagni¹, S. Saccà¹

1. Enser srl, Faenza (RA), Italy, ingegneria@enser.it

ABSTRACT: The flood event that occurred in Emilia Romagna between May 16th and 17th of last year 2023, caused a breach at the right bank of the Idice Torrent, leading to the collapse of the Motta Bridge on via Zenzalino Nord and the flooding of the surrounding lands, in the surroundings of La Motta (Budrio, Bologna, Italy). The breach was preceded and triggered by overtopping, a phenomenon that occurred in several points, both on the right and left sides, upstream and downstream. The embankment reconstruction project didn't only include the damaged area, but it was designed to remodel different sections, partially or totally, where erosive phenomena had resulted in an unacceptable reduction of hydraulic safety levels, aiming to restore the watercourse to its pre-event safety standard. Typical issues of emergency works were addressed during the design phase, such as rapid execution, numerous "contractors" operating at the same time, provide minimum safety levels even during the execution phases.

Keywords: Idice, embankment breach, bank erosion, emergency intervention design, urbanized area.

1 DESIGN OF THE INTERVENTIONS

The project includes the reconstruction of the sections predominantly classified with medium to high severity of instability, particularly in areas where erosive phenomena resulting from the embankment breach led to an unacceptable reduction in hydraulic safety levels. The sections classified as low level of damage will be included into a later phase. A survey campaign was conducted in 2023 to characterize foundation soils and those of the remaining embankment bodies.

The embankment reconstruction project had to identify implementation solutions account for multiple factors:

- Minimization of construction times;
- Minimization of the supply of materials from external or distant sites to the construction site. In this regard, it should be noted that the failure of the embankment deposited a considerable layer of silty-sandy soil (over 2m) in the surrounding area.

- compatibility with future projects for improvement of the hydraulic safety level of the watercourse.

To meet the above requirements, four types of interventions were identified:

1. **Type A:** Complete reconstruction of the embankment:

- a. Elevation to the pre-event embankment head level and outward shifting (channel widening) to maximize the use of the remaining portions;
- b. River side adopting a shape consisting of alternating terraces of 4m width and slopes of 1v/2h, compatible with maintenance requirements;
- c. Embankment head width of 5m to accommodate potential future raisings;
- d. Use of silt-sandy material from areas adjacent to the site, for sections on the landward side;
- e. Use of clayey soil for sections on the river side;
- f. Formation of a rock revetment along the lower embankment

2. **Type B:** reconstruction of the lower embankment and the first terrace;

3. **Type C:** reconstruction of the lower embankment only;

4. **Type D:** plastic diaphragm walls on existing embankment head. Filtration tests have highlighted a certain vulnerability of the old embankment bodies, constructed in the past with materials directly sourced from the watercourse containing relatively permeable sandy soils. Therefore, an impermeable barrier has been incorporated within the embankment body in the form of a suitable-length plastic diaphragm wall.

To meet the emerging needs, it was essential to establish the suitability of the available materials used and quality check for proper execution control.

The design and execution of the interventions required close collaboration among all involved parties (designers, project managers, contractor, civil protection and administrations). Only through this synergy it has been possible to ensure the reconstruction of approximately 3 km of embankments within a short timeframe (about 14 months) and solve various unforeseen issues arising from the emergency situation. This made this case an example of the efficiency and velocity required in such situations.

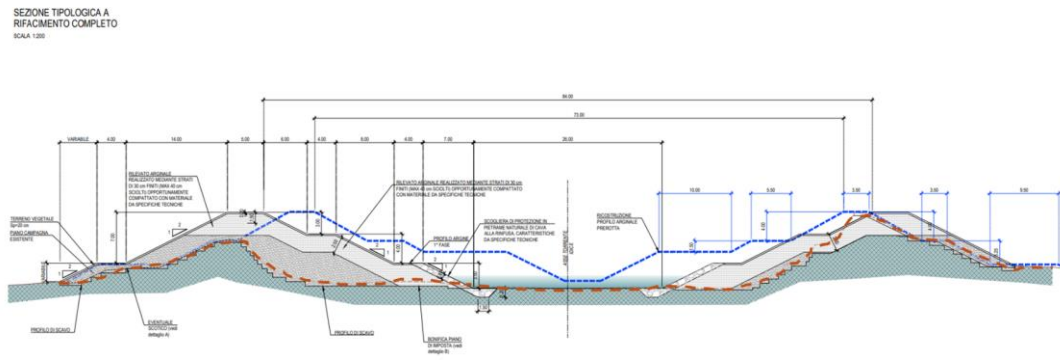


Figure 1. Type A section, complete reconstruction. In blue, the outline of the pre-event embankment; in red, the outline of the post-event embankment.

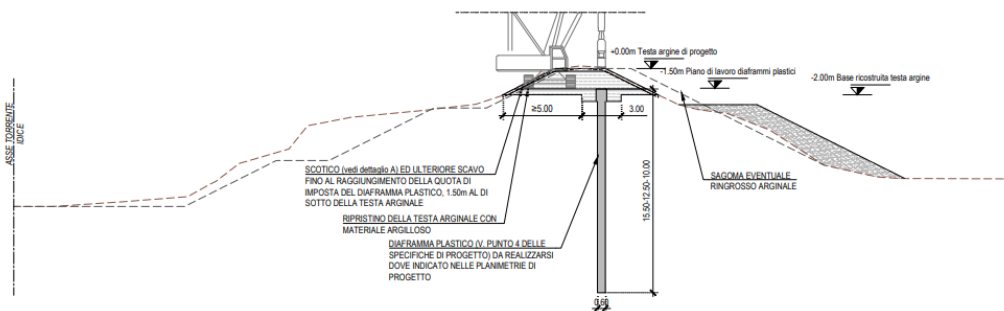


Figure 2. Type D section, plastic diaphragm wall on the pre-existing embankment head.

ACKNOWLEDGMENTS

We sincerely thank the Emilia-Romagna Region and the Agency for Territorial Security and Civil Protection of the Emilia-Romagna Region for their collaboration and support.

REFERENCES

- A. Brath, N. Casagli, M. Marani, P. Mercogliano, R. Motta (2023). Rapporto della Commissione tecnico-scientifica istituita con deliberazione della Giunta Regionale n. 984/2023 e determinazione dirigenziale 14641/2023, al fine di analizzare gli eventi meteorologici estremi del mese di maggio 2023.
- GEO-SLOPE International Ltd. (2015), Stability Modeling with SLOPE/W.
- Lancellotta R. (1993). *Geotecnica*, 2nd ed, Zanichelli, Bologna.
- Raviolo P.L. (1993). *Il laboratorio geotecnico, Procedure di prova, Elaborazione, Acquisizione dati*, ed. Controls, Milano.
- Ministerial Decree of 01/17/2018: Aggiornamento delle Norme tecniche per le costruzioni, (GU n.42 del 20-02-2018 - Ordinary Supplement n. 8);
- Circular 21 January 2019, n.7 C.S.LL.PP.: Istruzioni per l'applicazione dell'Aggiornamento delle "Norme tecniche per le costruzioni" referred to in the Ministerial Decree 17 January 2018.

A novel medium-scale experimental setup to investigate backward erosion piping

E. Dodaro¹, E. Tumedei¹, M. Marchi¹, G. Gottardi¹, L. Tonni¹

*1. University of Bologna, Department of Civil, Chemical, Environmental and Materials Engineering, Bologna, Italy,
elena.dodaro2@unibo.it, emanuele.tumedei2@unibo.it, michela.marchi@unibo.it, guido.gottardi2@unibo.it, laura.tonni@unibo.it*

ABSTRACT: Backward erosion piping (BEP) is a phenomenon that can develop in the subsoils of river embankments during intense flood events, manifesting at the ground level as emerging *sand boils*. This process affects more than 130 sections of the Po river main embankments and many major streams in Europe and worldwide. This contribution aims to illustrate the experimental setup recently developed at the University of Bologna, for the medium-scale physical modelling of the BEP process. The experimental layout and testing procedures are briefly presented, along with some preliminary results from the ongoing laboratory activities.

Keywords: Internal erosion; backward erosion piping; physical modelling; river embankments.

1 INTRODUCTION

Backward erosion piping (BEP) is a sort of internal erosion which poses a serious threat to the stability of water-retaining structures, such as dams and river embankments. This phenomenon is prone to develop under a specific stratigraphic profile, which involves the presence of a fine-grained cohesive subsoil layer, overlaying a highly permeable sandy unit. BEP process typically starts at a downstream location and works its way toward the upstream source of water, by creating pipes that can undermine the integrity of the entire earth structure, if not mitigated (van Beek et al., 2011).

Physical modelling offers a robust benchmark for studying BEP, bridging the gap between theoretical analyses and field observations. Laboratory experiments often involve prismatic boxes in which a typical stratigraphic profile, predisposed to BEP, is reproduced, along with a hydraulic system, used to impose increasing heads, thus enabling researchers to monitor the evolution of pipes in a controlled environment (Robbins et al., 2018; Pol et al., 2022).

A novel experimental setup devoted to investigating BEP has been recently developed at the Geotechnical Laboratory of the University of Bologna, as part of the activities devised in the [EU project LIFE SandBoil](#) (LIFE19 ENV/IT/000071). The aim of the laboratory investigation is to study the initiation and progression of the phenomenon, as well as to evaluate the effectiveness of a low-impact mitigation strategy against piping, i.e. the installation of a vertical permeable barrier. The present contribution focuses on the design scheme of a novel medium-size apparatus and illustrates some preliminary test results, which represent a valuable reference for the design of a large-scale prototype for the pilot site and for the validation of the previous experimental activity, carried out at a smaller scale (Gragnano et al., 2023).

2 EXPERIMENTAL SETUP AND MONITORING INSTRUMENTS

The novel medium-scale apparatus, shown in Figure 1, consists of a prismatic box, in which the sand aquifer is reconstituted, characterized by the following internal dimensions: length = 2200 mm, height = 600 mm, width = 1100 mm. A flow distribution chamber, with a filter to separate water from sand, is located on the upstream side of the box and connected to a top chimney, which is used to impose incremental hydraulic heads. A second distribution chamber positioned on the downstream side of the box and equipped with four exit holes controlling the outflow boundary conditions, allows the development of horizontal flow lines within the sample. Water used during the test is stored within an external reservoir and conveyed to the box through a hydraulic pipe system equipped with lift pumps. Water levels are kept steady by a bell-mouth shaped spillway, connected to vertical telescopic pipes, operated by external winch handles. A 50-mm thick plexiglass cover is placed on the top of the sample, to simulate the fine-grained impermeable layer, featuring an exit hole with an adjustable diameter, representing the vertical pipe. The distance between the exit hole and the upstream chamber, equivalent to the seepage length of the model, is 1800 mm. Eroded sand is collected within a 3D-printed cylinder, placed above the exit hole. The water recirculation system involves the use of a sedimentation tank, consisting of three chambers, located downstream of the box, with the aim of removing the sand particles transported by water flow. A schematic of the hydraulic system is depicted in Figure 2.

The monitoring setup includes: *i*) pore pressure transducers (PPTs), screwed in the top cover along the centreline and a middle transversal axis (Figure 3), used to monitor the hydraulic head loss associated to pipes progression. An additional

PPT (labelled as 1.1), connected to the upstream chamber, is used to record the hydraulic load sequences applied to the sample during the tests. All the PPTs are connected to a stand-alone data acquisition system; *ii*) three high-definition cameras mounted, along with four spotlights, on a support structure and oriented orthogonally to the flow direction; *iii*) two flowmeters, located downstream of the sedimentation tank, to measure the outflow rate from the exit point.

3 PRELIMINARY TEST RESULTS

To verify the functionality of the new equipment, a trial test was conducted on a poorly graded silica sand sample from the Padano aquifer, characterized by $\gamma_{d,\min}=13.7 \text{ kN/m}^3$, $\gamma_{d,\max}=16.2 \text{ kN/m}^3$, $G_s=2.68$, $D_{50}=0.34 \text{ mm}$ and a hydraulic conductivity of $5 \cdot 10^{-4} \text{ m/s}$. The aquifer model was reconstituted by water sedimentation, while maintaining a constant water head of 10 cm during deposition, which allowed achieving an average relative density equal to 30%. Denser samples will be tested in the future. The hydraulic head was progressively increased, by applying loading increments, Δh , as shown in Figure 4, while the downstream head was kept steady. Figure 4 also reports flow rates (measured by both flow meters and weightings) and pressure heads trends, as a function of time. Evidence of piping initiation (*boiling stage*) was observed at the third loading step, though without any remarkable transport of sand particles outside the vertical exit pipe. A sand volcano was formed right after. It can be noted that, as soon as the erosion process takes place and pipes develop towards a monitoring point, the corresponding pressure head tend to decrease. This tendency can be clearly observed first in the PPTs closer to the exit point (#2.4 and #1.4), then, as the erosive phenomenon progresses, even from the more distant ones. During the tip progression, as the eroded volume increases, a gradual rise in the water discharged through the exit point was measured. Finally, PPTs #2.1 and #1.2 recorded a sudden decrease of the pressure head, showing that the pipe reached the upstream chamber.

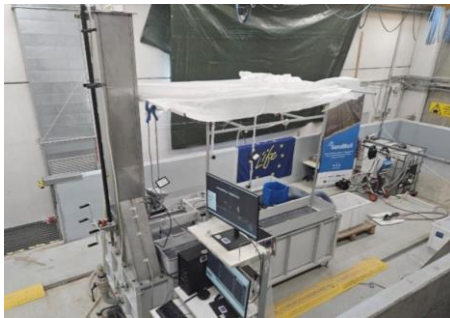


Figure 1. General view of the medium-scale experimental setup at the University of Bologna.

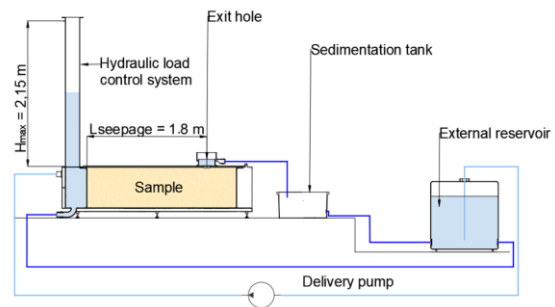


Figure 2. Schematic of the hydraulic system.

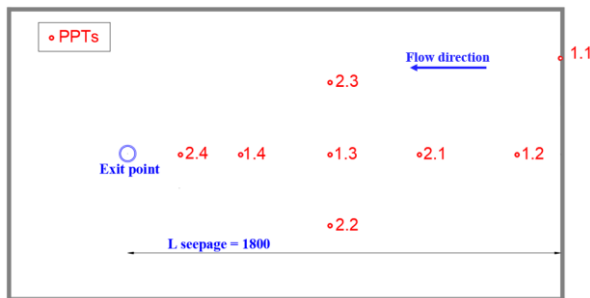


Figure 3. Pore pressure transducers (PPTs) layout.

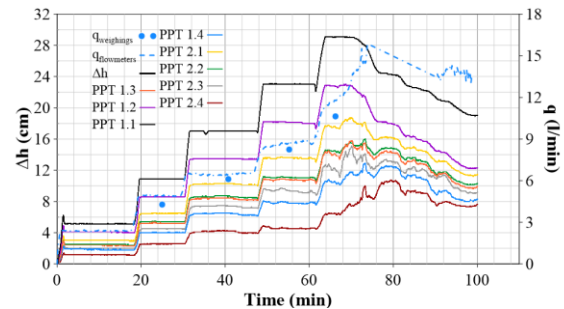


Figure 4. Water rate and pressure head trends over time.

REFERENCES

- Gragnano, C.G., Camiletti, F., Forbicini, F., Gottardi, G., Marchi, M., Tonni, L. (2023). Physical modelling of backward erosion piping for the development of natural-based mitigation strategies, *Proc. VIII Italian Conference of Researchers in Geotechnical Engineering*, Springer Series, pp. 87–94. https://doi.org/10.1007/978-3-031-34761-0_11
- Pol, J.C., Kanning, W., van Beek, V.M., Robbins, B.A., Jonkman, S.N. (2022). Temporal evolution of backward erosion piping in small-scale experiments. *Acta Geotechnica*, 17: 4555–4576. <https://doi.org/10.1007/s11440-022-01545-1>
- Robbins, B.A., Van Beek, V.M., López-Soto, J.F., Montalvo-Bartolomei, A.M., Murphy, J. (2018). A novel laboratory test for backward erosion piping. *Int. J. Phys. Model. Geotech.*, 18: 266–279. <https://doi.org/10.1680/jphmg.17.00016>.
- Van Beek, V.M., Knoeff, H., Sellmeijer, H. (2011). Observations on the process of backward erosion piping in small-, medium- and full-scale experiments. *European Journal of Environmental and Civil Engineering*, 15: 1115–1137. <https://doi.org/10.1080/19648189.2011.9714844>

Climate Change and Embankment Dam Overtopping: Lessons from the Libyan Dam Disaster in September 2023

N. Kafashan¹, M. Aufleger¹

1. University of Innsbruck, Unit of Hydraulic Engineering, Innsbruck, Austria, nima.kafashan@uibk.ac.at

ABSTRACT: On September 11, 2023, an exceptionally severe flood event in Wadi Derna, Libya, resulted in the failure of two embankment dams. The incident resulted in a considerable loss of life, with an estimated several thousand casualties. The unusually intense rainfall brought by Storm Daniel is regarded as a direct consequence of the elevated water temperatures observed in the Mediterranean during the summer of 2023. This catastrophic event offers a compelling illustration of the mounting risks to which dams are exposed in the context of climate change. A preliminary, general assessment of the Derna disaster conducted by the Unit of Hydraulic Engineering at the University of Innsbruck included an analysis of historical data, satellite images, and hydrological assessments. The findings demonstrate that the pertinent flood discharges during the incident greatly exceeded the capacity of the spillways. The excessive volume of water caused the dam to overtopping and subsequently collapse. This tragedy in Derna highlights the urgent need to review international guidelines and recommendations on dam safety and adapt them to the challenges of a rapidly changing climate.

Keywords: Embankment Dam; Overtopping; Climate Change; Storm Daniel; Dam Safety; Derna Disaster

1 IMPORTANT NOTE

The statements and information in this article about the catastrophe of September 11, 2023, in Derna have been compiled solely based on freely available information from the internet. This should be taken into account when interpreting the content. Initially, an internal report was prepared by the German Dam Committee (DTK), discussed within this body, and proposed for publication in the German professional journal "WASSERWIRTSCHAFT" due to the significance of the event. This publication forms an important basis for the present extended abstract. **IMPORTANT:** Given the severity of the disaster, with several thousand fatalities, special sensitivity is recommended when handling and interpreting the provided information.

2 INTRODUCTION

Derna is a port city in north-eastern Libya with a population of approximately 100,000. The city is situated at the confluence of the Wadi Derna with the Mediterranean Sea. Two embankment dams were constructed in this valley several decades ago with the intention of protecting the city from flooding. It is important to note that there is considerable discrepancy in the nomenclature used to refer to these dams. For this reason, the terms "large" and "small" are employed as designations in this article. On September 11, 2023, Derna experienced a catastrophic flood triggered by extreme rainfall from Storm Daniel, resulting in the failure of both dams. The event led to significant casualties, with estimates suggesting several thousand fatalities and tens of thousands displaced. This article aims to reconstruct the disaster's context using available information and imagery, emphasizing the urgent need for a thorough investigation to understand and address the calamity's aftermath effectively.

3 BRIEF OVERVIEW OF THE DAMS

The two dams in Wadi Derna were constructed between 1973 and 1977. The smaller dam is located near the coastal town, while the larger dam is approximately 13 km upstream at the confluence of a tributary valley. Both dams are rockfill embankment dams with a natural core. The larger dam stands at a height of approximately 75 m with a crown length of around 300 m and a base width of about 104 m. Its storage capacity ranges from 18,000,000 m³ to 22,500,000 m³. In contrast, the smaller dam is about 45 m high with a crown length of 130 m and a base width of 56 m, holding approximately 1,500,000 m³ of water, (Hidrotehnika, 2016). Both dams feature drop inlet (morning glory) spillways without clogging protection, with estimated capacities of 100 m³/s to 200 m³/s. However, sediment deposits had likely reduced their effective storage capacity by September 2023.

4 PREVIOUS HYDROLOGICAL ASSESSMENT

The average annual runoff load of Derna is estimated at approximately 140 million m³ per year. The average total precipitation for the entire year is 274 mm. The total area of the catchment is approximately 570 km². A subsequent comprehensive examination of the initial hydrological data of the Derna catchment, particularly with regard to the larger dam, was conducted in 2003. This investigation was aimed at identifying the fundamental characteristics of the design flood with a probability of occurrence over a 1000-year period. A variety of calculation approaches were employed in the study. In conclusion, the application of the methods resulted in significantly higher flood estimates than those considered in the original planning of the larger dam. When a probability of occurrence of 1000 years is taken into account, this results in a flood volume of 67 million m³ and a flood discharge of 2526 m³/s. These values were calculated as 14 and 855, respectively, in the original design of this dam, (Ashoor and Eladawy, 2024).



Figure 1: The smaller dam and the larger dam (MAXAR, www.crisisgroup.org, Google Earth, commons.wikimedia.org)

5 THE IMPACT OF CLIMATE CHANGE

The phenomenon of climate change is leading to an increase in the frequency and intensity of extreme precipitation and flooding events. The storm Daniel, which occurred in September, 2023, caused severe flooding in Libya. At the time of the storm, sea temperatures near the coast of Libya were three to four degrees above normal, which increased evaporation and precipitation. In Derna, Libya, 200 mm of precipitation was recorded within a few days, a frequency that would normally occur only once every 600 years, (Ashoor and Eladawy, 2024). However, the likelihood of such an event has increased significantly as a result of climate change. The resulting floods exceeded the capacity of the dams, causing considerable damage. The peak discharge was estimated to be approximately 2500 m³/s, with the total flood volume estimated to be between 70 and 100 million m³.

6 THE PROBABLE COURSE OF THE DERNA DISASTER

Prior to the flood, the reservoirs of the two embankment dams in the Wadi Derna were largely empty, but significantly reduced by sediment deposits. The bottom outlet at the larger dam was probably no longer functional. The water level rose to the top of the shaft spillway. The inflow significantly exceeded the hydraulic capacity of the spillway. The water level exceeded the crest of the dam, resulting in overtopping and subsequent erosion of the dam embankment, which ultimately led to the failure of the dam. Large volumes of water were released. The breach of the larger dam led to peak discharges of over 10,000 m³/s, which exceeded the natural inflow from the catchment area by a considerable margin. Probably the breach of the larger dam resulted in the failure of the smaller dam. The flood wave reached the city with a rapid rise in the water level of several meters, resulting in considerable destruction with thousands of fatalities.

7 CONCLUSIONS AND OUTLOOK

- The catastrophe in Derna is one of the worst dam disasters in history.
- Climate change significantly influences the maximum expected inflows to reservoirs. Uncertainty is increasing.
- Embankment dams, due to their vulnerability to overtopping, are particularly at risk in this regard.
- Hydraulically non-overloadable flood spillways (especially shafts like morning glory) are critical in this context.

REFERENCES

- Aufleger, M. and Kafashan, N. (2024). Die Talsperrenkatastrophe vom 11.09.2023 im Wadi Derna, Libyen. *Wasserwirtschaft*, 114 (4), pp. 10-17. <http://doi.org/10.1007/s35147-024-2321-0>
- Ashoor, A. and Eladawy, A. (2024). Navigating catastrophe: lessons from Derna amid intensified flash floods in the Anthropocene. *Euro-Mediterr J Environ Integr*. <https://doi.org/10.1007/s41207-024-00566-4>
- Hidrotehnika-Hidroenergetika Company. (2016). WADI DERNA. <https://www.hidrotehnika.rs/en/libya/wadi-derna/>

Estimation of breach hydrograph resulting from dam embankment failure due to internal erosion or overtopping: comparison of simplified methods with real-case break data and recommendations

L. Del Gatto¹, Y. El Badaoui¹, J.-R. Courivaud¹

1. EDF CIH, La Motte Servolex, France, laurent.del-gatto@edf.fr, yacine.el-badaoui@edf.fr, jean-robert.courivaud@edf.fr

ABSTRACT: The opening of a breach in an embankment dam, whether due to overtopping or internal erosion, is a critical failure mode for these structures. Accurately estimating the resulting breach hydrograph is essential for assessing downstream risks. While no universal physical model covers all dam types, empirical formulas are commonly used. EDF analyzed 14 such formulas, comparing them with rupture data from 32 embankment dam failures. The best formulas—Froehlich 1995, Xu & Zhang 2009, and CLF 2020—yield a “best estimate” for peak flow. However, due to variability, results should be interpreted cautiously. Consider estimating breach characteristics like width and erosion rate for better understanding and comparison.

Keywords: Breach, dam failure, internal erosion, overtopping, hydrograph

1 INTRODUCTION

The opening of a breach in an embankment dam, whether initiated by overtopping on the crest or by an internal erosion mechanism in the dam body, is the main mode of failure of these structures. Estimating the hydrograph resulting from such failure is fundamental to assessing and managing the risks downstream of the dam.

Although breaching of embankment dams has been extensively studied for several decades, there is as yet no accurate physical model of these phenomena covering all dam types. Thus, the most widely used approach, corresponding to the current state of the art, is to use empirical formulas to estimate the resulting breach hydrograph; however, the bibliography lists a large number of formulas for this purpose, often giving very different results.

EDF identified and exploited 14 formulas published on the subject, and compared them with actual rupture data from EDF's database of 351 embankment dam ruptures (32 of which had sufficient information for the present study). The aim was to identify the empirical and semi-empirical formulas giving the most likely results (by formula and/or combination of these formulas), which could then be used in the downstream consequence studies produced by EDF as part of the hazard studies for dams classified with regard to safety.

The methodology developed in this work is applicable to reservoir dams and saddle dams, but not directly to canal dike failures, where canal hydraulics play a specific role.

The main parameters involved in calculating peak flows are water head, reservoir volume, type of erosion (internal or overtopping) and the erodibility of the dam's constituent materials.

The breach hydrograph is provided in a simplified triangular form, with a rise time to reach the maximum flow also provided by formulas (or by expert opinion), and a final time corresponding to the complete emptying of the reservoir above the low level of the breach.

The study highlighted the need to test several formulas because of the possibility of significant variation in results. The best formulas selected were Froehlich 1995, Xu & Zhang 2009, and CLF 2020. The final proposed method offers a "best estimate" for peak flow by retaining the median of these three formulas, associated with a probable minimum and maximum, allowing for sensitivity analysis in modelling where necessary.

Comparison between the maximum flow rate estimated using the methodology described above and the actual flow rate observed (directly or reconstructed) on the 32 breaches used shows a confidence interval of between 0.65 and 2.05 (see graph below). These envelope interval values can be considered as the probable minimum and maximum for estimating the peak flow of the breach.

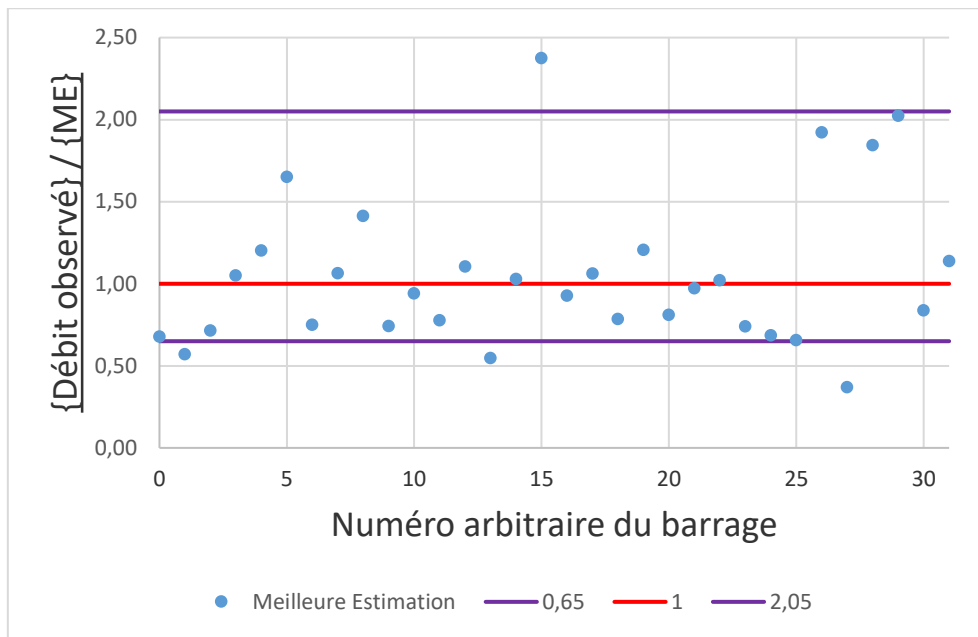


Figure 1. Observed flow to estimated flow ratio

As the range of uncertainty is wide, results must be interpreted cautiously, particularly in cases involving highly erodible or resistant materials. To this end, it may also be useful to estimate the physical characteristics of the breach, in particular its final width and erosion rate, which are important for understanding the dam failure mechanism, and for comparing the results obtained with known orders of magnitude.

USACE Levee Overtopping Incidents and Failures

T.M. O’Leary¹ and D.M. Schaaf²

1. U.S. Army Corps of Engineers, Risk Management Center, Louisville, Kentucky, USA, timothy.m.oleary@usace.army.mil
2. U.S. Army Corps of Engineers, Risk Management Center, Louisville, Kentucky, USA, david.m.schaaf@usace.army.mil

ABSTRACT: Overtopping is a primary risk driver for U.S. Army Corps of Engineers (USACE) levees. The USACE Levee Loading and Incident Database (LLID) is the result of a multi-year effort to collect and categorize historical levee performance data for USACE levees. The LLID provides probability of failure estimates and breach dimensions. The LLID is a critical component of the USACE Levee Screening Tool (LST) Version 2.0. and is used for other purposes in the USACE Levee Safety Program. This paper provides preliminary findings related to overtopping incidents and failures for USACE levee embankments.

Keywords: Levee; overtopping; incidents; failures; failure rate

1 INTRODUCTION

Overtopping is a primary risk driver for the U.S. Army Corps of Engineers (USACE) levee portfolio. The USACE Levee Loading and Incident Database (LLID) is the result of a multi-year effort to collect and categorize historical USACE levee performance data. The LLID provides probability of failure estimates for multiple performance modes, tracks key contributing factors of overall levee performance, and general characteristics of breach sizes.

2 USACE LEVEE LOADING AND INCIDENT DATABASE

The USACE levee portfolio includes 2,859 levee segments for a total length of 22,800 kilometres. As part of the LLID, an initial screening of the USACE levee portfolio was performed to identify levee segments suitable for determination of failure rates. The screening process eliminated 640 of the 2,859 levee segments that did not meet the definition of a traditional coastal or riverine levee (like a spur levee), levee embankment sections less than 1 meter in loading height, and levee segments that had never been loaded above 25% of the loading height. As of June 2024, 711 (32%) of the remaining 2,219 viable levee segments were evaluated. Approximately 30,000 years of cumulative performance data was reviewed for the 711 levee segments evaluated, where both reliable performance data and reliable stream gage data were available. The actual number of years of service is higher, but years where the loading could not be accurately estimated and/or there was no reliable documentation of performance were excluded.

The data reviewed indicates 320 documented widespread overtopping events of levee embankments, and 209 (63.5%) of these events resulted in at least one breach formation. In the LLID, only overtopping breaches (failures) resulting in an uncontrolled release of impounded water into the leveed area were considered. Erosion resistance is a key contributing factor for levee overtopping performance. The relative erosion resistance of the embankment soils was characterized in the LLID by five categories (USACE, 2023).

- Higher relative erosion resistance: Clay, clay/silt mix, clay with sand/silt, zoned embankment with impervious cover over riverside slope and crest, and clay enlargement of an existing levee embankment
- Moderate relative erosion resistance: Silt, clayey silt, silt with sand/clay, silt/clay mix with sand, silty loam, sandy clay, silty/clayey loam, sand/silt mix with clay, sand with silt/clay, and clayey sand
- Lower relative erosion resistance: Sand, silty sand, silty sand with gravel, sand/silt mix, sand/gravel mix, sand/gravel mix with silt, sandy silt, and sandy gravel
- Other relative erosion resistance: Random fill and impervious core with random fill/pervious shell
- No classification: Insufficient information to accurately characterize the embankment

The quality of construction and operation and maintenance for USACE levees was characterized in the LLID by two broad categories: 1) federally constructed and well maintained; and 2) locally constructed, operated, and maintained, or reclassified federal, but poorly maintained. There were 120 documented embankment overtopping events of federally constructed and well-maintained levees, but only 47 (39%) resulted in at least one breach. The remaining 200 embankment

overtopping events were for locally constructed, operated, and maintained, or reclassified federal, levees, and 162 (81%) resulted in at least one breach.

Overtopping depth is the height of water above the crest of the typical levee embankment section either at the time that breach occurred or the maximum overtopping depth for non-breach events. The overtopping events are characterized in the LLID by three overtopping depth ranges: 1) less than 0.3 meter; 2) 0.3 to 1 meter; and greater than 1 meter. In general, the greater the overtopping depth, the higher the likelihood of failure. Exceptions are scenarios where the leveed area quickly filled to help prevent breach and short duration overtopping events (minutes to hours) (USACE 2023).

3 CONCLUSIONS

Figure 1 shows the probability of failure for less than 0.3 meter of overtopping where sufficient data was available. Because a significant portion of the overtopping events had overtopping depth classified as “unknown,” failure rates were not developed as a function of overtopping depth. Reasons for an “unknown” classification include insufficient information to determine when the embankment breached for events that overtopped the levee by more than 0.3 m or daily stream gage data was unavailable to estimate the depth of overtopping during the event. Overtopping depths due to ice-related events was another source of uncertainty.

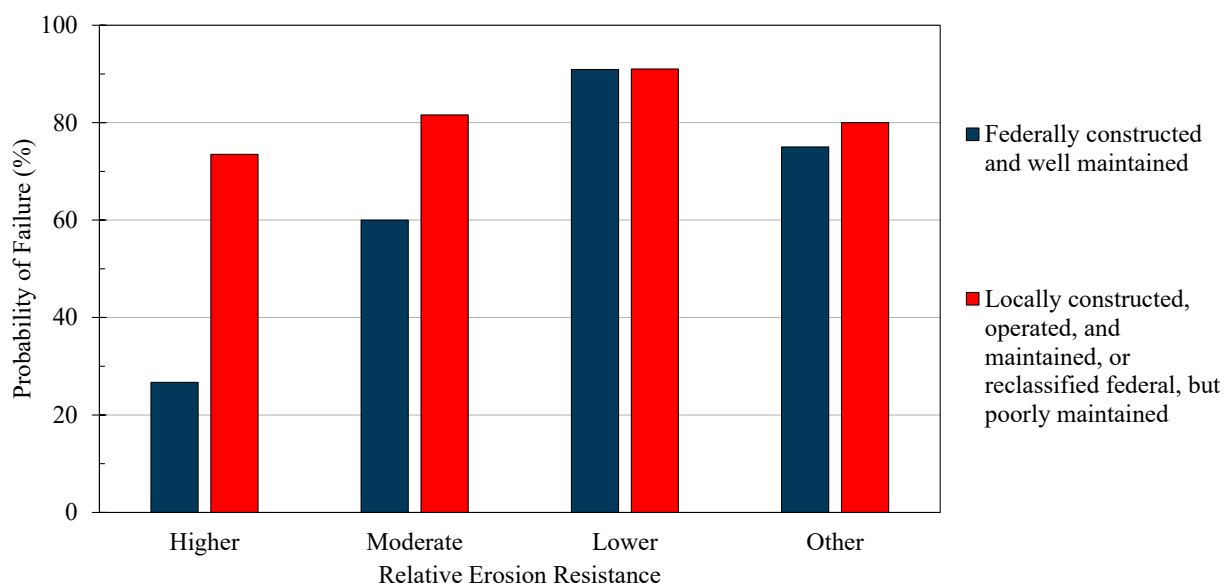


Figure 1. Probability of failure for less than 0.3 meter of overtopping as a function of relative erosion resistance and construction/maintenance quality.

Erosion resistance of the embankment soils and quality of the design, construction, and operation and maintenance were key contributing factors for overtopping performance. The likelihood of failure increased with decreasing erosion resistance. For well-maintained levees, the probability of failure was 27% for the higher erosion resistance category and nearly doubled with each decrease in relative erosion resistance category. The probability of failure was much higher than well-maintained levees (74%) for the higher erosion resistance category and increased by about 10 percent with each decrease in relative erosion resistance category.

Federally constructed levees were typically designed and constructed to much higher engineering standards than locally constructed levees. They typically used higher quality embankment soils, were compacted to higher levels, and met design specifications. Most locally constructed levees were constructed with minimal design and little to no engineering oversight. There were several well-designed, federally constructed levees that that were turned over to local entities but have since fallen into a state of disrepair typically due to a lack of local resources. Even a well-designed and constructed levee of higher erosion resistance can have a higher likelihood of failure if poorly maintained. The findings indicate higher erosion resistant embankments require a lower overtopping annual exceedance probability (AEP) for the same level of reliability if poorly constructed or maintained.

REFERENCES

U.S Army Corps of Engineers. (2023). *USACE Levee Screening Tool Application Guide and Technical Reference Manual* (Draft).

Two historical cases of dam overtopping in the Czech Republic

J. Riha¹, S. Kotaska¹

1. Brno University of Technology, Faculty of Civil engineering, Brno, Czech Republic, riha.j@vutbr.cz

ABSTRACT: Dam incidents occur mainly during extreme floods. During these events numerous incidents and total breaches of small dams were recorded in the Czech republic, few large dams were also critically endangered, however not completely breached. In the paper two cases of dam overtopping with no collapse of the structure are described and discussed. In both cases (the Pocheň and Mlýnice dams) surface erosion and scouring were the main damages at the dams.

Keywords: Dam overtopping; the Pocheň dam; the Mlýnice dam; scouring; surface erosion

1 INTRODUCTION

In addition to the benefits from dams, they also pose a potential risk if collapsed. Dam incidents occur primarily during extreme floods and are usually associated with inadequate spillway capacity or spillway blockage. Experience shows that about 2 to 10 small dams collapse due to overtopping during extreme flood events, few hazard events occurred also at large dams. In the Czech Republic (CR), large-scale regional floods were recorded at different regions in 1985, 1987, 1997, 2002, 2006, 2010 and 2013, local floods occurred in 1975, 1991, 1996, 1997, 1998, 2002, 2004, 2005, 2009 and 2010. In CR an information on dam incidents and failures, including small dams, has not yet been systematically summarized, published data are limited and scattered. This paper aims to summarize information about the overtopping incidents at two Czech dams, namely Pocheň and Mlýnice (Figure 1) which sustained the load and did not collapse.

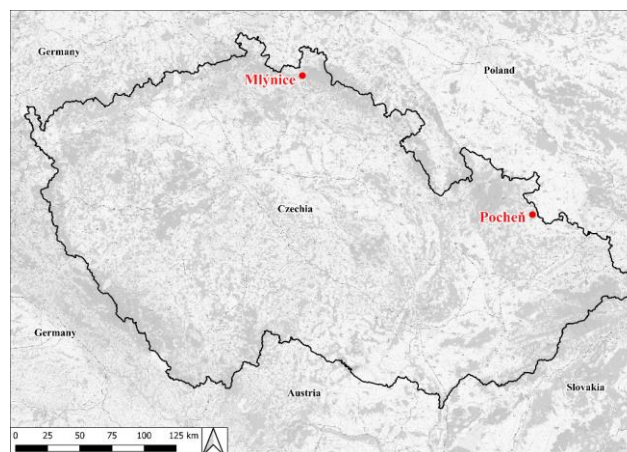


Figure 1. The location of dams Pocheň and Mlýnice

2 THE POCHENŮ DAM

The Pocheň dam is zonal nonhomogeneous embankment with a sealing clayey core and shoulders made of gravel soil. The dam was put in operation in 1975. Maximum dam height is 9.5 m, the crest length is 175 m. The lateral spillway is located at the left abutment with the weir crest 25.2 m long. The purposes of the dam are flood protection and recreation. The Pocheň dam belongs to the IIIrd category with the 100-year design flood and 1000-year check flood.

The first recorded overtopping of the dam Pocheň occurred in 1977 two years after its completion. The dam was overtopped along all its length and the downstream slope was significantly eroded. The process of overtopping was not recorded in more details. The second overtopping was in 1996 when heavy rainfall occurred in the Čížina river basin during the night from 13 to 14 May. The maximum water level at the reservoir was reached fast and dam started to be overtopped with the nappe 0.3 to 0.4 m (Figure 2), however the dam sustained this load. This resulted in 1 m deep erosion

of the downstream slope, the washed away soil volume was about 3 000 m³ (Figure 3). The spillway was damaged during the flood by undermining the bottom of the chute. In summer 1997, the regional flood occurred, and the Pocheň dam was overtopped again. The temporary channel excavated at the left abutment helped to pass the flood discharge, with no serious damage of the dam body.

Main causes of overtopping and damage of the dam were extreme floods related to extraordinary rainfall with the return period higher than 100 years. Backward analysis indicated insufficient spillway capacity. Another problem was an insufficient freeboard combined with local subsidence of the dam crest. To bring the dam into safe condition, the repair of the dam body and increase of spillway capacity were carried out in 1998.



Figure 2. Overtopping of the dam Pocheň in 1996.



Figure 3. Downstream slope after the flood in 1996.

3 THE MLÝNICE DAM

The Mlýnice is masonry dam belonging to the IIIrd category, it is 14.5 m high and 159 m long in crest. The dam was completed in 1906. The reservoir area is 4 ha with maximum depth 14 m. The purpose of the dam is the flood protection. During the rainy period in August 2010 the crest of Mlýnice dam was overtopped along the entire length with the nappe of about 16 cm which resulted in scour at the downstream toe of the dam (Figure 4). The spillway capacity was reduced by floating debris, the manipulation with the bottom outlets was difficult as the power outage of the energy occurred, subsequent manual manipulation with the gates was not possible, due to the overtopping of the crest. The crest was overtopped for about 40 minutes with the peak discharge 65 m³/s, which is about 3,6 times higher than the flood with return period 100 years and 1,5 times higher than the control flood discharge. During the overtopping, about 3 m deep scour developed along the abutments. The dam stability was not harmed due to relatively short exposure time. The securing stability of the dam rested in the stepped plain concrete slabs placed on the exposed downstream base of the dam toe. The walls of the scour were arranged into acceptable slope and provided by sprayed concrete (Figure 5). Finally, the slabs were covered with heavy rip rap with a weight of stones about 1 t a piece.



Figure 4. Overtopping of the dam Mlýnice during the flood in 2010.



Figure 5. The reconstruction of the abutments after the flood in 2010.

ACKNOWLEDGMENTS

FAST-S-24-8513, Analysis of the influence of input variables on the results of numerical models used in the safety assessment of water structures

TACR SS07010401, Water management analysis to support natural flooding and the transformation effect of the floodplain.

Testing empirical criteria for breach geometry estimation to recent embankment failure datasets

A. Domeneghetti¹, M. Vaccari¹, I. Bertolini¹, M. Marchi¹

1. Department of Civil, Chemical, Environmental and Materials Engineering, Alma Mater Studiorum, Università di Bologna, Bologna, Italy, alessio.domeneghetti@unibo.it

ABSTRACT: Considering the potential collapse of river embankment structures on riverine flood hazard assessment significantly improves the reliability of the inundation maps. Breach formations should be included in inundation modelling by defining their geometry, and in particular their length. This contribution aims at testing the application of the Zomorodi (2020)'s empirical equations for breach parameters estimation to a new and large database of breach failures occurred in Northern Italy in May 2023. In particular, the considered approach provides the breach length as a function of levee height and type of material. The comparison indicates a good accordance between the observed and estimated values, demonstrating the reliability of the prediction. Future research will delve deeper into the failure mechanisms of the collapsed embankment sections, potentially revealing additional connections between failure mechanisms and breach dimensions.

Keywords: earthen river embankments; breach databases; Emilia-Romagna flood

1 INTRODUCTION

Effective river embankment risk management requires rapid estimation of relevant breaching parameters, especially breach geometry and peak discharge, based on limited data, to support predictions of inundation zones and inform decision-making strategies. To this scope, many empirical equations have been developed, fitting data collected in databases of historical levee breaches, with the aim of correlating breach dimensions with various parameters such as levee height, water level, soil type, crest width, duration of the overtopping, longitudinal river velocity etc (e.g., Wahl, 1997). However, no widely accepted empirical equations for estimating levee breach dimensions exist. The reasons could be attributed to the quality of the datasets adopted to develop the analyses. In many cases incomplete and/or outdated datasets have been used. To address this issue, Zomorodi (2020) implemented a strict protocol for selecting reliable data, resulting in a number of carefully chosen levee failure cases for developing more accurate empirical equations.

In this study, these equations, relating the levee height (H_l) with the predicted final breach dimension (w_b), have been applied to three open-access databases and to a new and recent database that collects cases of levee breaches occurred in the Emilia-Romagna region (Italy) in May 2023, as a result of two consecutive severe flood events (Figure 1A). This new database includes, for each breach, the geometrical characteristics of the collapsed levee sections and evidences about the possible mechanisms of formation of the breaches, as deduced from field observations, carried out pre and post event. The database has been elaborated applying a rigid methodology ensuring a rare uniformity and quality of the collected data. Other peculiarities of this set of data include the fact that all monitored failures occurred in river embankments characterized by analogies in the structural features. Such similarities include construction materials and techniques, as well as geometrical characteristics. Possible relationships between the dimension of the breaches and these morphological characteristics have also been investigated.

2 EMPIRICAL BREACHING MODEL AND DATABASE CHARACTERISTICS

Many studies have underlined a significant correlation between the breach length, the levee height and soil type (Wahl, 1997). The empirical equations proposed by Zomorodi (2020) are based on 55 levee breach cases caused by high water events occurred all over the world, from Europe to USA, China and Japan. The proposed relations differ according to the soil type of the levees, which simplistically have been grouped in two categories: cohesive (clay levees typical of river levees) and non-cohesive (sand levees typical of coastal flood barriers). The considered cases have been selected within a large pool of levee failure cases according to some criteria ensuring them to fit with some "ideal" breaches. Initially, Zomorodi (2020) has correlated the breach length with the maximum water height, assuming the latter the driving force of the failure development in case of overtopping, demonstrating that breach length can be accurately predicted only with this limited piece of information. However, the water level is sometimes unknown and not easily used to define the

levee height. Thus, the distance between levee crest and the landside foot represents a more suitable parameter. Figure 1B reports in the $w_b - H_l$ plane the three proposed empirical equations for cohesive levees together with the considered breach cases by Zomorodi (2020) (black points). In this study, Zomorodi's equations have been tested on the following databases from which unrealistic cases and those lacking crucial information, such as levee height, were excluded: **a)** The Department of Water Resources (DWR) Levee Breach database that concerns levee breaches occurred in the California Central valley. From this initial dataset of 215 events, the considered cases reduce to 195. **b)** The Danka et al. (2015)'s database includes levee breaches in Hungary, Germany, China, and USA. Only 179 cases out of 1000 events were considered. **c)** The ILPD is a global database created and updated by researchers at the University of Dresden (Germany) (Ozer et al., 2020). ILPD reports more than 1500 cases, 220 of which have been selected in the present study. **d)** The last database consists of more than 60 breaches occurred in Emilia-Romagna in May 2023 and it includes data on breach location, levee geometry and possible failure mechanism. A DTM derived from LiDAR scanning has been used to obtain the missing levee height data from the database. One point of this new dataset is reported as an example in Figure 1B, for the breach shown in Figure 1A (Idice river).

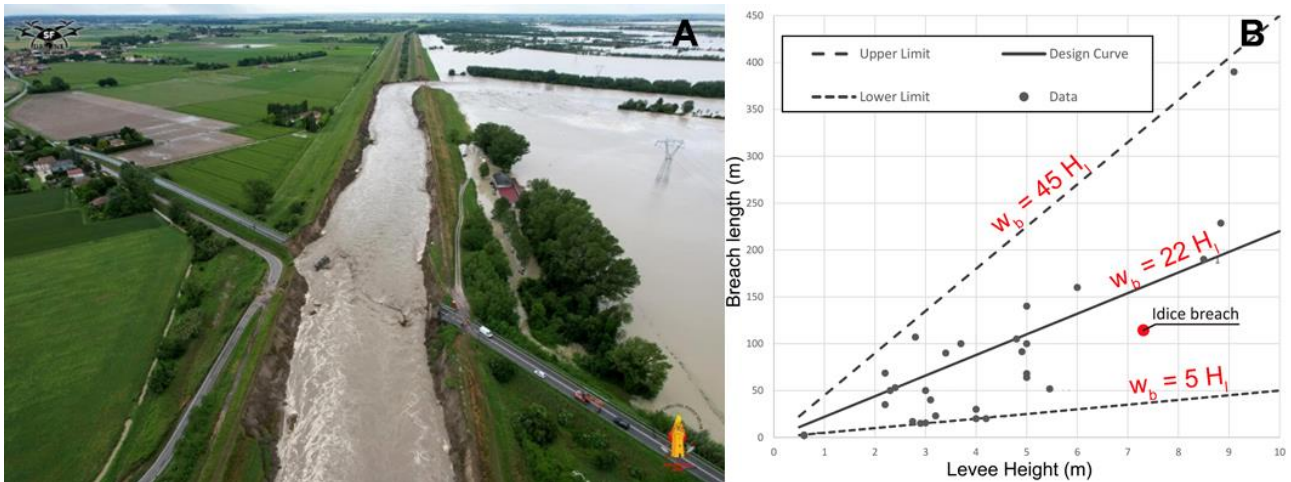


Figure 1. A) View of a breach and of a bridge failure occurred in the Idice river (Emilia-Romagna flood 2023). B) Design curves, modified after Zomorodi (2020), showing the final breach length as a function of levee height.

3 CONCLUSIVE REMARKS

While empirical equations are invaluable tools in flood risk management for their ease and rapidity in application, their accuracy and reliability strongly depend on the quality of the underlying historical data. Continuous efforts to improve data collection and validation are essential for developing better predictive models and enhancing flood preparedness and response strategies. The proposed study has tested the empirical formulations of Zomorodi (2020) for cohesive earthen embankments in the light of a new database on the breach failures occurred in the Emilia-Romagna region (Italy) in May 2023. The comparison between observed data and predictions gave encouraging results. Moreover, a statistically correlation between breach geometry and the geometric features of the embankments is currently under investigation.

ACKNOWLEDGMENTS

The authors would like to acknowledge the support of the technicians from ADBPO (Po River District Authority) and from the Agency for Territorial Security and Civil Protection of the Emilia-Romagna region in the collection of information on the river embankment failures occurred in May 2023.

REFERENCES

- Zomorodi, K. (2020). Empirical equations for levee breach parameters based on reliable international data. *Proceedings of the Dam Safety 2020 virtual conference*, 21-25 September.
- Ozer, I.E. and van Damme, M. (2020). Towards an International Levee Performance Database (ILPD) and Its Use for Macro-Scale Analysis of Levee Breaches and Failures. *Water*, 12(1), 119. <https://doi.org/10.3390/w12010119>.
- DWR. DWR Levee Breach Database. Available online: <http://www.dwr-lep.com>.
- Danka, J. and Zhang L.M. (2015). Dike Failure Mechanisms and Breaching Parameters. *Journal of Geotechnical and Geoenvironmental Engineering*, 141(9). [https://doi.org/10.1061/\(ASCE\)GT.1943-5606.0001335](https://doi.org/10.1061/(ASCE)GT.1943-5606.0001335).
- Wahl, T.L. (1997). Predicting Embankment Dam Breach Parameters - A Needs Assessment. *Proceedings of XXVII IAHR Congress*, 10-15 August, San Francisco, California.

High pressure jet testing on soil-cement

J.F. López-Soto¹, B.A. Robbins², E.R. Friend²

1. U.S Army Corps Engineers, Engineer Research and Development Center, Vicksburg MS, USA, Jamie.F.Lopez@usace.army.mil

2. U.S Army Corps Engineers Risk Management Center, Lakewood CO, USA, Bryant.A.Robbins@usace.army.mil,
Edwin.R.Friend@usace.army.mil

ABSTRACT: A high pressure jet device was developed to evaluate erodibility parameters of soil cement mixtures. The device is intended to inform material selection prior to conducting costly large scale prototype tests. A methodology of high-pressure, short time intervals is proposed using a small diameter jet for obtaining the critical shear stress. Two soil-cement mixtures subjected to variations in cement content, curing time, cement, and fly ash content were tested, and variations in critical shear stress and unconfined compression tests were measured. Only one of the soils exhibited significant variations in critical shear stress although unconfined compression test variations were observed for all soil-cement mixtures. Results indicate the proposed procedure yields critical shear stresses in agreement with standard JET procedures.

Keywords: soil-cement; erodibility; overtopping; submerged jet

1 INTRODUCTION

In embankment dam and dike designs, soil-cement mixtures are used to provide protection against erosion in the upstream face of the embankment (Choi and Hansen, 2005; Hansen, 2002; USBR, 2013). USBR(2013) provides guidance for soil-cement mixtures on upstream slopes of embankments. The use of soil-cement mixtures has been proposed for protection of the downstream face of embankments against erosion due overtopping, or also for spillway lining applications against erosion. Evaluation of soil cement- mixtures requires scale models to be tested at multiple flow velocities for extended periods of time (hours to days) to evaluate the potential for erosion of selected mixtures, see (Clopper & Chen, 1988; FHWA, 1987; Huzjak and Kadrmaz, 2016; Thornton et al., 2009). Physical modelling and scale testing prototypes require a large amount of time, effort, and cost to effectively model large scale scenarios (Powledge et al., 1989).

In lieu of scale testing that requires significant resources, space, and time, laboratory test devices have been developed or adapted to evaluate the erosion resistance and durability of the soil-cement mixtures. Results were used to inform a large-scale testing effort regarding the percentage of cement in a soil-cement mixture capable of sustaining expected hydraulic loading, due to overtopping, without affecting the integrity of the structure. A high-pressure Jet Erosion Test (JET) device was built to estimate the shear stresses at initiation of particle detachment on soil-cement mixtures at varying cement contents and was adapted to test materials that cannot be tested using traditional jet testing devices intended for soil erosion.

2 TEST DEVELOPMENT

To conduct erosion testing on soil cement mixtures, a high-pressure JET device was developed. A 30 MPa, 15 lpm pressure washer with variable nozzle diameters was selected as the basis for the JET device. The test consists of directing a submerged stream of high-pressure water directly impinging a soil-cement surface. The shear stress applied to the soil, due to the fluid discharge, is adjusted by modifying the offset distance between the soil surface and the nozzle. The test was conducted by applying low shear stresses initially and increasing the applied shear stress until erosion was apparent. A 5-second interval was selected based on the erosion experienced with preliminary trials where erosion was apparent at small intervals of time.

The critical shear stress result from using 5 second intervals were compared to a long-term erosion approach similar to the test procedure by Hanson and Cook (2004). In the short term tests the critical shear stress ranged from 10 to 37 Pa, therefore a shear stress of 48 Pa was selected as the initial shear stress for the Hanson and Cook approach, knowing that the excess shear stress would be able to begin eroding the sample. The offset was maintained, and the depth of the erosion was measured at 1 min intervals. Based on this longer interval method, the critical shear stress was calculated at 24 Pa.



Figure 1. Test setup



Figure 2. Testing being conducted

3 METHODOLOGY AND RESULTS

Two soils (SFD-Basin and CMB) were selected to create the soil-cement mixture based on vast material availability from nearby sites. The cement content (6, 8, and 10%), total curing days (7 and 28), and cement/fly ash ratio (0 and 25%) were varied, to investigate effects of these variables on the unconfined compressive strength, and erodibility of the mixtures. Soil composition played a role in the erodibility as the SFD-Basin material showed changes in critical stresses based on variation of parameters while the CMB mixture did not show significant variation in critical shear stress.

At 7 days the critical shear stress showed that for all cement contents tested erosion resistance was similar. Overall, all 28 days samples tested with SFD soil as a parent material showed an increase of erosion resistance when compared to 7-day samples. At 28 days the erosion resistance of the 10% cement sample was significantly higher than the sample at 7 days. A comparison of the soil-cement samples with SFD soil that replaced part of the cement with fly ash was evaluated based on the critical shear stress. The mixtures that contained fly ash did not show any significant erosion resistance gain due to the additive. Based on current findings to increase the erosion resistance of SFD soil-cement mixtures it is recommended the use of cement without fly ash.

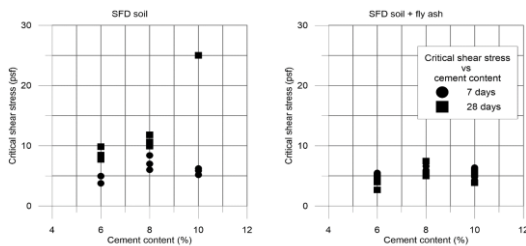


Figure 3. SFD soil test results

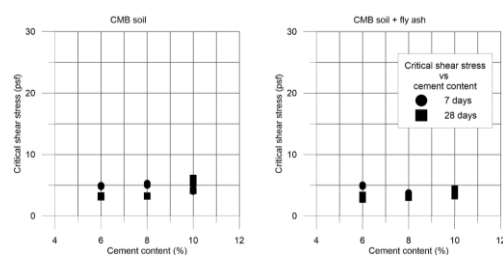


Figure 4. CMB soil test results

REFERENCES

- Choi, Y.-K., and Hansen, K. D. (2005). RCC/Soil-cement: What's the difference? *Journal of Materials in Civil Engineering*, 17(4), 371–378.
- Clopper, P. and Chen, Y.-H. (1988). *Minimizing embankment damage during overtopping flow*. Simons, Li & Associates.
- FHWA. (1987). *Development of a methodology for estimating embankment damage due to flood overtopping* (FHWA/RD-86/126). Simons, Li & Associates, Inc.
- Hansen, K.D. (2002). *Erosion and abrasion resistance of soil-cement and roller-compacted concrete* (RD126; p. 22). Portland Cement Association.
- Hanson, G.J. and Cook, K.R. (2004). Apparatus, test procedures, and analytical methods to measure soil erodibility in situ. *Applied engineering in agriculture*, 20(4), 455–462.
- Huzjak, R. and Kadrmas, K. (2016). Soil-cement for high-velocity spillway flow applications. *Protections 2016*. 2nd International Seminar on Dam Protection against Overtopping. <https://mountainscholar.org/items/da2e050a-8205-40f0-b146-5a578ac416f6>
- Powledge, G., Ralson, D., Miller, P., Chen, Y.-H., Clopper, P., & Temple, D. M. (1989). Mechanics of overflow erosion on embankments. I: Research activities. *Journal of Hydraulic Engineering*, 115(8), 1040–1055.
- Thornton, C., Scholl, B. and Turner, M. (2009). *Hydraulic performance testing and data report for soil cement*. Colorado State University.
- USBR. (2013). Chapter 17: Soil-cement slope protection. In *Design Standards No. 13 Embankment Dams*. U.S. Department of the Interior Bureau of Reclamation.

Lime treatment for erosion resistant levees in Belgium

K. Verelst¹; F. Bertola²; S. Nicaise³; B. Vandevoorde⁴

1. Flanders Hydraulics, Antwerp, Belgium, kristof.verelst@mow.vlaanderen.be

2. Lhoist, Nivelles, Belgium, federica.bertola@lhoist.com

3. INRAE, Aix Marseille Univ, RECOVER, Aix-en-Provence, France, sylvie.nicaise@inrae.fr

4. Research Institute for Nature and Forest (INBO), Brussels, Belgium, bart.vandevoorde@inbo.be

ABSTRACT: Clay cover layers for levees in Flanders (Belgium) must comply to specific criteria related to water tightness and erosion resistance. To investigate if local soils not meeting these criteria after being treated with lime can be improved and used as cover layer, an experimental test section was built in the Flood Control Area Vlassenbroek. Both a local sandy soil treated with 3 % of formulated lime and a silty soil treated with 2 % of quicklime were installed as cover layer. A 6-year monitoring program was set up to evaluate the relevant properties and their evolution, including topographical monitoring, monitoring of permeability, the mechanical resistance, the surface erosion resistance, and the vegetation development. The vegetation monitoring shows less coverage in the test strips with the grass sown directly on the lime treated soil compared to the test strips with application of a topsoil layer on the lime treated soil and compared with the vegetation of the untreated cover layer. Hole Erosion Tests performed before the installation and in-situ Jet erosion tests executed after the construction showed a significant increase in the erosion resistance of the lime treated soil compared to the untreated cover layer.

Keywords: Levee; Lime treatment; Erosion resistance; Monitoring

1 INTRODUCTION

Levees in Flanders (Belgium) consist mainly of a sandy core covered with a clay layer with vegetation. The sandy core ensures the stability of the levee, the clay layer ensures the water tightness. The clay cover layer and the vegetation must meet some specific criteria related to water tightness and erosion resistance. Finding good quality clays meeting these specific criteria is difficult. Since lime treatment is a well-known technique to improve the performance of soils, a part of the ring dike of the Flood Control Area Vlassenbroek was built by Lhoist treating the locally available soils with lime, avoiding the import of higher quality soil. This presentation shows an overview of the construction of the experimental test site, the 6-year monitoring program which was set up and some of the first results of the development level of the vegetation and the erosion resistance of the lime treated cover layer.

2 CONSTRUCTION AND MONITORING PROGRAM

At the ring dike of the Flood Control Area Vlassenbroek, an experimental test site was constructed by Lhoist in 2019. Local available soil was treated with lime and implemented as cover layer. The test site was divided into two test sections with a length of 21 m each. The cover layer of the first section consists of a sandy soil excavated from the Flood Control Area itself and treated with 3 % of formulated lime. The cover layer of the second test section consists of a silty soil treated with 2 % of quicklime. In both test sections the cover layer has a thickness of 1.10 m and was constructed in four consecutive layers, compacted along the slope of the levee (Figure 1). Details of the construction of the test site are described in Herrier et al. (2020) and Verelst and Herrier (2020). To study the influence of the lime treatment on the vegetation development, each test section was divided into three test strips where two different grass mixtures were sown, directly on the lime treated soil or after application of a topsoil layer of clay.

A 6-year monitoring program was set up to evaluate the relevant properties and their evolution in time, including topographical monitoring, monitoring of permeability, the mechanical resistance, surface erosion and vegetation development. The monitoring was performed on the six test strips of lime treated soil and on 5 reference test strips of untreated soil where the same grass mixtures were applied. After six years from the construction, large scale erosion tests, overflow tests or wave impact tests, are also planned.

3 DEVELOPMENT LEVEL OF VEGETATION AND EROSION RESISTANCE

Monitoring of the vegetation is executed once a year by the Research Institute for Nature and Forest (INBO) and includes monitoring of the vegetation cover, species diversity, the root density and biomass. The test strips with the grass directly sown on the lime treated soil have a lower vegetation coverage compared to the test strips of the untreated reference cover layer and compared to the test strips where the topsoil layer was applied on the lime treated soil.

The root density in the test strips with lime treated soil is high in the upper 7.5 cm, but then reduces to zero in the deeper layers. In the test strips with application of the topsoil layer on the lime treated soil the vegetation cover and the root density are comparable to those measured in the untreated section.

To define the appropriate lime addition before the construction of the test site, the Hole Erosion Test was used to assess the possible improvement in the erosion resistance achievable thanks to lime treatment (Peyre et al. 2022). The critical shear stress of the sandy treated soil and of the silty treated soil increased respectively from 28 Pa and 150 Pa before treatment to 175 Pa and 1000 Pa after 28 days from the lime treatment. The Fell erosion index of the sandy treated soil and of the silty treated soil slightly increased respectively from 2.5 and 3.5 before treatment to 3.7 and 3.8 after 28 days from the lime treatment.

In September 2020 and June 2022, being approximately one year and 2.5 years after the construction of the test section, in-situ JET-erosion tests were carried out by INRAE at 12 locations in the test strips with the cover layer treated with lime and during the last measurement campaign also at 4 locations on the untreated section as reference. Before the execution of the JET-erosion tests, the vegetation present was locally removed. To obtain hydraulic stresses between 600 Pa and 1900 Pa, the hydraulic feeding of the JET apparatus was adapted.

During the measurement campaign of 2020 an average value of critical shear stress of 200 Pa was measured in both the sandy and the silty treated soils. This value significantly increased during time and in the measurement campaign of 2022 average values of 728 Pa and 661 Pa were respectively measured for the sandy treated soil and the silty treated soil. These values are significantly higher than the average value measured in the untreated section (67 Pa). The Hanson erosion coefficient increased from 1.1 cm³/(sN) to 3.2 cm³/(sN) for the sandy treated soil, and from 1.8 cm³/(sN) to 7.3 cm³/(sN) for the silty treated soil, while the erosion coefficient measured in the untreated soil was around 22 cm³/(sN). Compared to other JET-erosion test results, performed by INRAE or taken from literature, the lime treated cover layer in the Vlassenbroek test section shows a significantly higher erosion resistance (Figure 2). In 2025 large scale erosion tests, overflow tests or wave impact tests, are planned to confirm this increase in erosion resistance measured through the small-scale erosion tests.

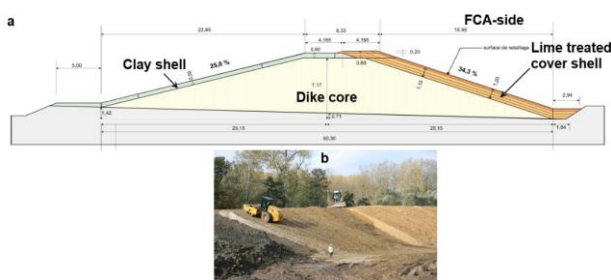


Figure 1. Scheme of the dike (a), and construction of the lime treated cover layer on the levee (b)

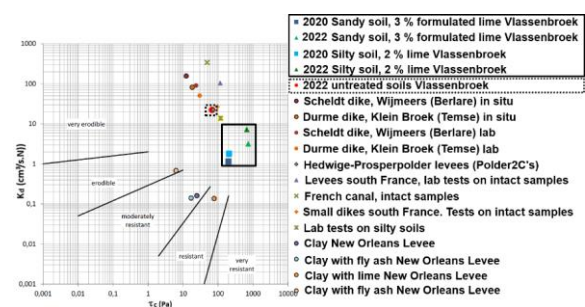


Figure 2. Overview of JET-erosion test results on lime treated soil and untreated soil

ACKNOWLEDGMENTS

The authors want to express their gratitude to The Flemish Waterway for providing the test site and admitting the tests with the lime treatment of the cover layer. Special thanks are addressed to the Geotechnical Division and the General Technical Division of the department of Mobility and Public works and the Belgian Road Research Centre for the execution of the various parts of the measurement campaign.

REFERENCES

- Herrier, G.; Bonelli, S.; Nerinx, N.; Tachker, P.; Peeters, P. and Puiatti, D. (2020). Improving dams and dikes strength and resistance to erosion by means of lime treatment. In: *Proceedings of the Fourth International Dam World Conference, Portugal, Lisbon, LNEC, September 21-25, 2020*, pp.[1-19] <https://documentatiecentrum.watlab.be/owa/imis.php?module=ref&refid=393464>
- Peyre, C.; Pellez, J.-C.; Klotz, F. (2022) Reinforcement of dikes protecting against inundations with soil treated with lime. In: *Sol Scope Mag* 21(4), J. Aubry and D. Rousseau (eds.), pp. 34-38 <https://www.calameo.com/read/0050033713b3009a9c01c> (in French)
- Verelst, K.; Herrier, G. (2020). Experimenting with lime treatment of the cover layer of dikes. In *Grond/Weg/Waterbouw Magazine* 9(06), N. Rouvrois (ed.), pp. 92-93 <https://www.gww-bouw.be/magazines/nr-06-2020/> (in Dutch)

Calcium Aluminate Concrete - a unique protective material against erosion & cavitation damages

D. Niepmann¹, A. Aboulela², C. Dowds³

1. Imerys Murg GmbH, Oberhausen, Germany, dirk.niepmann@imerys.com

2. Imerys Technology Center, Lyon, France, amr.aboulela@imerys.com

3. Imerys Aluminates Ltd., Purfleet, United Kingdom, amr.aboulela@imerys.com

ABSTRACT: For hydraulic structures, erosion and cavitation are responsible for serious damages which leads to costly rehabilitations. There are two parameters which can improve the resistance against erosion and cavitation. On the one hand we have the optimization of constructive design. On the other hand we can increase the resistance of the constructions by the use of special materials which increase the erosion and cavitation resistance. OPC based mass concrete is typically specified to improve this resistance, however this option has its limitations. Additional approved materials like steel plates or natural stone plates with high erosion resistance to protect critical areas in hydro structures are also specified. We would like to present a solution which is not widely known but has been used for over 30 years due to its improved resistance to erosion and cavitation. This is a concrete based on calcium aluminate cement (CAC) and aggregates which gives this material its unique properties.

Keywords: erosion resistance; cavitation resistance; concrete; sustainability

1 DISCUSSION

If materials with a higher erosion and cavitation resistance are specified, today, our main building material is OPC based concrete. Most developments are focused on this building material. Beside OPC, other materials with high abrasion resistance are steel plates and granite blocks. Both solutions are widely used, especially as repair solutions. Steel shows the highest abrasion and cavitation resistance of all systems, but it is not easy to install. The plates must be fixed by anchors to the substrate and the joints must be welded. Due to the thickness of the steel plates normally the geometry of the substrate is limited.

Granite blocks must be glued to the substrate and in most cases additional anchors are used to fix the blocks to the substrate. The critical point for granite blocks is the joint filling material as it has normally less erosion and cavitation resistance than granite. This oftentimes leads to the joints being washed out by erosion. In the worst case, as one consequence, further erosion can take place below the blocks, uplift pressure can occur and full blocks can be torn out.

Approximately 30 years ago a new concrete design was introduced which offers superior properties. This concrete is based on Calcium Aluminate cement and uses Calcium Aluminate aggregates. The concrete can be placed in all geometries, by the use of chess board placing method the joints can be minimized and its abrasion and cavitation properties are excellent.

For testing abrasion resistance, there are many standards and test protocols in the industry for different applications (Liu, 2024). Every test gives its own results and the results cannot be directly compared between the test methods. As a standard ASTM C 1138 (Figure 1) is established for underwater abrasion of concrete. It is known that the abrasion resistance for OPC concrete improves with the increase of compressive strength. The addition of fibres, steel or PP, have only limited effect on the abrasion resistance (Table 1). In contrast, the use of the special CAC concrete, based on calcium aluminate binder & aggregates, shows a very high abrasion resistance. There is an improvement of more than 70% when compared with OPC concrete of 90-100 MPa strength. As ASTM C 1138 is an abrasion test for concrete, there is no test data on other abrasion resistant materials such as steel or granite. C.N.R., Compagnie nationale du Rhône, developed an internal test (Figure 2). A water sand mix is projected on a sample in a 45° angle with a water velocity of 10 m/sec. for a test duration of 75 min. As a reference, glass is used (Dumas, 2024) and the abrasion resistance index for glass is set to 1. In this test different materials were tested (Table 2) including OPC concrete, CAC concrete, steel and granite, with their abrasion resistance compared. As expected, steel has an abrasion resistance of 0.04, CAC concrete (0.38-0.75) has even a comparable resistance than granite (0.4-0.8). As seen in ASTM C1138 OPC concrete has a lower abrasion resistance index of 2 than CAC concrete or granite, which was expected.

Beside the abrasion resistance, CAC concrete has an additional benefit as it also shows a high cavitation resistance. This property was tested at GEC Alstom - CERG (Cabiron, 1998). A water jet of 110 m/sec. and 54 bars was blasted at a 90° angle towards a sample for a duration of 2 min (Figure 3). Strong cavitation occurs and erodes the sample. In practice,

normally the water velocity does not exceed 10 m/sec. In this test, a high strength concrete was compared to the special CAC concrete. In Figure 4 on the left side, the OPC concrete samples are heavily damaged. Single aggregates are torn out of the concrete matrix as the forces of cavitation are higher than the bonding strength of the aggregates in the concrete matrix. In contrast, the CAC sample shows only very small defects. The sample shows a discoloration due to the high energy impact, but no large aggregates are lost. The reason is that the binder and aggregates are both reactive and form a chemical bonding during hydration which is much stronger than the bonding based on adhesion as is the case in OPC concrete. This chemical bonding is responsible for the high abrasion resistance as well as the cavitation resistance.

2 CONCLUSIONS

The special CAC concrete has

- higher abrasion resistance than OPC concrete.
- higher cavitation resistance than OPC concrete due to chemical bonded aggregates.
- can be placed without joints or minimized joints in contrast to granite.
- can be placed in every geometry like standard OPC.

With 30 years of practical experience, it is proven that the rehabilitation cycles can be prolonged which can contribute directly to an economic and sustainable benefit

Table 1. Mass lost after 72h - ASTM C 1138

Material	28d CS	Mass lost in g	reference
Special CAC concrete	80 MPa	15-40 g	Cabiron 1998
OPC with MS	90 MPa	110 g	Ojha 2021
OPC with MS plus SF	97-100 MPa	102-120 g	Ojha 2021
OPC with MS plus PF	85-90 MPa	108-110 g	Ojha 2021
OPC with MS	100 MPa	373 g	Horszczaruk 2009
OPC with MS plus SF	91-99 MPa	303-381 g	Horszczaruk 2009
OPC with MS plus PF	98 MPa	265 g	Horszczaruk 2009

Table 2. Abrasion test - C.N.R.

Material	abrasion index	reference
glass	1	Cabiron 1998
CAC concrete	0.38-0.75	Cabiron 1998
Granite	0.4-0.8	Cabiron 1998
OPC with MS	2	Cabiron 1998
Steel	0.04	Cabiron 1998

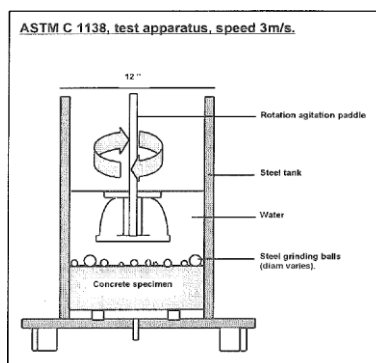


Figure 1. ASTM C 1138 test method: water velocity 3 m/sec; duration: 24h & 72h

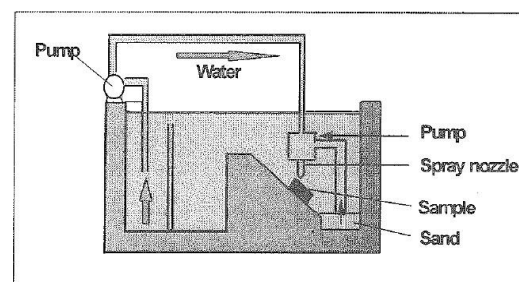


Figure 2. C.N.R. abrasion test: water velocity 10 m/sec; duration 75 min.

RCC and soil cement overtopping protection of embankments

S. Todaro¹, B.A. Robbins¹, E. Friend¹, M. Dirdal¹

1. U.S. Army Corps of Engineers Risk Management Center, Lakewood, CO 80228

ABSTRACT: Overtopping is the primary cause of embankment dam and levee failures globally. As a result, overtopping protection is often designed and constructed on embankments to mitigate the risk of failure during an overtopping event. Roller compacted concrete (RCC) and soil cement are two approaches that have been used successfully to provide overtopping protection. While the design and construction of both approaches are quite similar, the applicability, robustness, and costs are extremely different. RCC is more expensive and robust with less uncertainty in performance. Soil cement is more cost effective, but with less robustness and certainty of performance. This study describes standard RCC/soil cement overtopping protection designs and documents the considerations that should go into selecting RCC versus soil cement. Finally, research needs are identified that could reduce the uncertainty in soil cement performance, leading to broader applicability and associated cost savings.

Keywords: roller compacted concrete, soil cement, overtopping

1 INTRODUCTION

Overtopping is the leading cause of dam and levee failures worldwide. As a result, roller compacted concrete (RCC) and soil cement overtopping protection is often designed and constructed to protect embankments from overtopping induced damages and breach. A typical RCC overtopping protection design is illustrated in Figure 1. The roller compacted concrete is placed in steps up the downstream face of the embankment with appropriate measures for drainage. Soil cement designs are very similar in that rolled lifts of soil cement are placed in steps. While the designs are similar, soil cement is significantly more variable in terms of properties, typically uses less cement, and has much lower erosion resistance. As a result, it is important to carefully review design considerations when selecting soil cement over RCC.

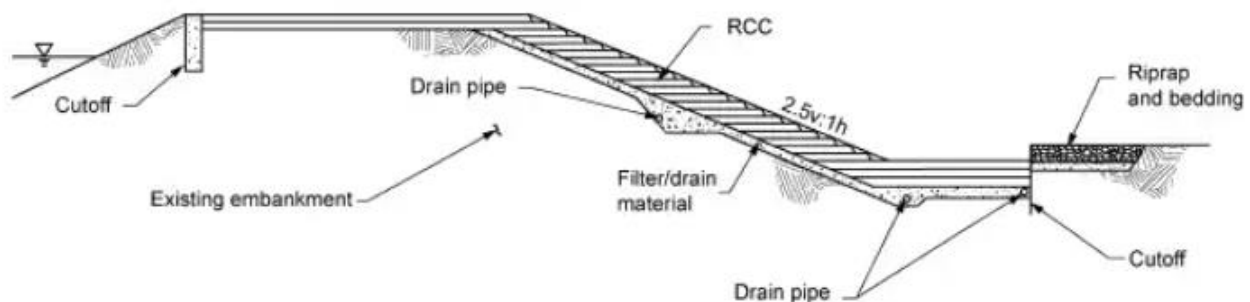


Figure 1. Typical design of RCC overtopping protection (FEMA, 2014).

2 DESIGN CONSIDERATIONS

An overview of various considerations that influence whether soil cement or RCC is the preferred alternative for a project is provided in Table 1. As RCC is more robust and expensive, it should be used for important structures that are frequently loaded with significant overtopping depths to obtain high project reliability. Additionally, soil cement should not be used in projects that significantly exceed the scale and precedence of prior soil cement applications until the behaviour is better characterized and understood. The materials available onsite are another significant factor in selecting soil cement or RCC. Sites with significant quantities of coarse aggregates may be able to readily use RCC without large increases in cost. In these cases, the additional cost of RCC may be reduced and the incremental investment is warranted for the significant increase in robustness. Soil cement may be more appropriate when coarse aggregates are not available onsite. Operation and maintenance should also be considered as frequent inspection and maintenance may be needed for designs

with more performance uncertainty such as soil cement. Additional considerations in selecting soil cement or RCC are listed in Table 1.

Table 1. Design consideration matrix for selecting soil cement or RCC.

Consideration	Soil Cement	RCC
Structure Importance	Less important	More important
Loading Frequency	Low	High
Overtopping Depth	Low	High
Onsite Materials	Finer grained	Coarser aggregates
Freeze thaw resistance	Low	Medium
Cyclic wetting/drying resistance	Low	High
Project Scale (height, discharge, etc.)	Smaller	Larger
Overtopping duration	Shorter	Longer
Longevity Requirements	Shorter	Longer
Budget	Smaller	Larger
Foundation conditions	Variable	Rigid
Toe Energy Dissipation Required	Varies*	Use with integrated energy dissipator
Maintenance	Certain O&M	Less certainty

*Occasionally used with caution, but generally advised against

3 RESEARCH NEEDS

Recent experience in the U.S. Army Corps of Engineers developing soil cement overtopping protection designs has led to the realization of numerous knowledge gaps regarding the design and long-term performance of soil cement. Research in these areas will reduce the uncertainty in the performance of soil cement overtopping protection which may make use of soil cement more reliable as a long-term overtopping protection measure. The primary areas identified needing additional research are:

- Characterization of erosion resistance of soil cement mixes for various soil types.
- Impact of debris and sediment laden overtopping flows on erosion resistance and longevity.
- Failure mechanisms of soil cement overtopping protection.
- Breach formation in soil cement armored embankments.
- Long term resistance and performance of soil cement for various soil types and mix designs.
- Necessity for air entrainment in high cement content soil cement mixes.
- Influence of fiber reinforcement on soil cement and RCC for weathering and erosion resistance.
- Allowable unit discharges for soil cement designs.

With additional research in these areas, it may become possible to reliably design soil cement overtopping protection for a broad range of soil conditions, environments, and hydraulic loads. Reliable prediction of permissible shear stresses or flow energies for various designs is essential for widespread use of soil cement overtopping protection. Additionally, the long-term overtopping performance of soil cement overtopping protection is largely unknown.

4 CONCLUSIONS

RCC and soil cement overtopping protection are commonly used to increase the reliability of embankments when overtopped. Numerous considerations should be reviewed when selecting RCC or soil cement for a design. In general, however, RCC is used for more frequently loaded, important structures due to uncertainty surrounding the performance of soil cement. Numerous research needs were identified that may improve the profession's ability to reliably design soil cement overtopping protection. Research in these areas may lead to increase soil cement use and significant cost savings.

REFERENCES

FEMA. (2014) Technical Manual: Overtopping Protection for Dams. Federal Emergency Management Agency, U.S. Department of Homeland Security. Washington, D.C.

Modelling of fractured rock erosion in open channels

P. Teng¹, J.G.I. Hellström¹, F. Johansson², C.-O. Nilsson³

1. Division of Fluid and Experimental Mechanics, Department of Engineering Sciences and Mathematics, Luleå University of Technology, SE-971 87 Luleå, Sweden, penghua.teng@ltu.se

1. Division of Fluid and Experimental Mechanics, Department of Engineering Sciences and Mathematics, Luleå University of Technology, SE-971 87 Luleå, Sweden, gunnar.hellstrom@ltu.se

2. Division of Soil and Rock Mechanics, KTH Royal Institute of Technology, SE-100 44 Stockholm, Sweden, fredrik.johansson@byv.kth.se

3. Uniper – Sydskraft Hydropower AB, Infanterigatan 28, SE-831 32 Östersund, Sweden, carl-oscar.nilsson@swe.uniper.energy

ABSTRACT: Rock erosion in river channels, especially downstream of spillways, presents considerable challenges for the stability and longevity of hydraulic structures. Previous research has primarily concentrated on the erosion processes of single rock blocks, with limited investigation into the interactions occurring in multi-block scenarios. This paper employs a resolved Computational Fluid Dynamics-Discrete Element Method (CFD-DEM) to model and analyse the multi-block erosion processes. This approach effectively simulates the interaction behaviours between flowing water and rock blocks. The simulation results visualize the multi-block erosion process and demonstrate that the interactions among blocks significantly influence the erosion dynamics. These findings point out the necessity of accounting for block interactions in predictions of the rock erosion.

Keywords: Fractured Rock; Resolved CFD-DEM; Multi-Block Erosion; Rock Erosion

1 INTRODUCTION

Rock erosion in river channels downstream of spillways is a critical concern for the safety and longevity of dams. The erosion processes can weaken the foundations and abutments of spillways, potentially leading to structural failures. Such failures compromise dam safety and pose significant risks to downstream communities and ecosystems. Therefore, understanding the mechanisms and dynamics of rock erosion is essential for designing effective protective measures and ensuring the integrity of hydraulic structures.

Numerous studies have investigated rock erosion processes, primarily focusing on single-block scenarios (George, 2015). However, research addressing multi-block erosion remains limited. Koulibaly et al. (2022) conducted a laboratory-scale physical model to determine the effects of various parameters on multi-block erosion. They studied the individual and interactive effects of several hydraulic and rock mass parameters on the erosion process. Despite these findings, there remains a gap in understanding how the interactions of neighboring blocks affect erosion dynamics. To address this gap, this study employs a resolved Computational Fluid Dynamics-Discrete Element Method (CFD-DEM) to model and visualize multi-block erosion processes.

The coupled CFD-DEM approach has emerged as a promising tool for modeling fluid-structure interactions (Teng et al., 2021). Teng et al. (2023) employed an unresolved CFD-DEM to represent the erosion process of a single rock block, demonstrating its potential for simulating rock block erosion processes by capturing the interactions of rock blocks in response to hydraulic forces. This approach provides a detailed understanding of the erosion process. Consequently, this study employs the resolved CFD-DEM approach to investigate multi-block erosion. Nine three-dimensional (3D) cuboid blocks are generated, and this approach is used to simulate their removal process. The simulation results are used to determine the onset of the blocks' incipient motion and subsequently visualize their movement trajectories. The findings of this study will not only enhance the understanding of multi-block erosion processes but also contribute to the development of more accurate and reliable predictive models for erosion assessment.

2 MODEL SETUP

Within the framework of the coupled CFD-DEM approach, fluid behaviours are described by the Navier-Stokes equations and are solved using CFD. In contrast, the dynamics of particles are described by Newton's laws of motion and are simulated using the DEM. The DEM assumes that materials such as granular matter, bulk materials, and rocks are composed of separate, discrete particles. The CFD-DEM engine facilitates the coupling process between fluids and particles, allowing for the detailed simulation of fluid-structure interactions.

Figure 1 shows rock blocks' configuration in an open channel. There are nine blocks placed in the block mold within the channel, and the block 5 is $30 \times 30 \times 35$ mm a protrusion height of 5 mm, while the remaining blocks are $30 \times 30 \times 30$ mm and flush with the bottom of the channel. The aperture size is 15 mm. Figure 2 shows the rock blocks represented by particles in DEM.

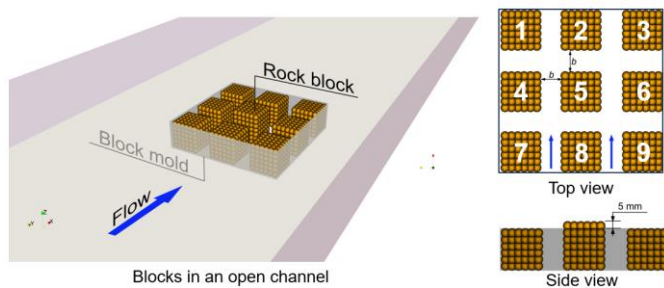


Figure 1. Blocks' configuration in an open channel

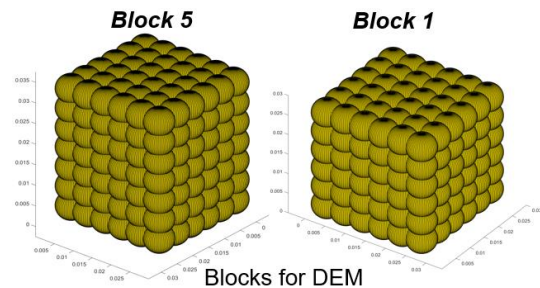


Figure 2. Blocks represented by particles

3 RESULTS

Figure 3 shows the erosion process of the blocks. Figure 3a presents the initial conditions of the simulations. As the flow velocity increases, Block 5 begins to move due to its protrusion height (Figure 3b). Subsequently, Block 5 contacts the neighbouring block and reaches a temporary state of equilibrium (Figure 3c). Finally, both Block 5 and its neighbouring block are lifted and removed from the block mold (Figure 3d).

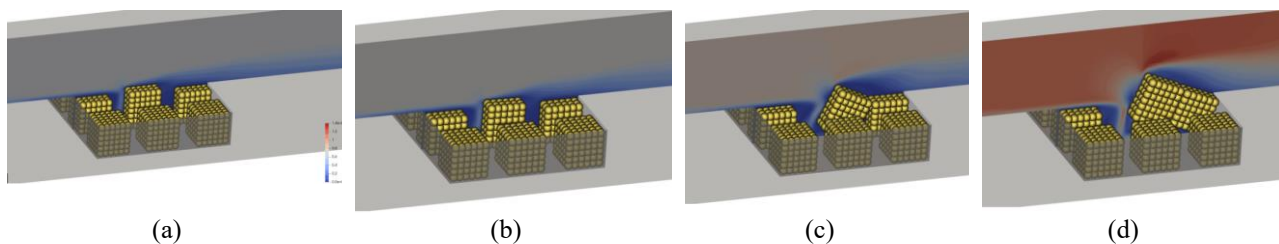


Figure 3. Erosion process of rock blocks

4 CONCLUSIONS

In this study, the resolved CFD-DEM approach is employed to investigate the effects of interactions among neighbouring blocks on the rock erosion process. The simulations visualize the multi-block erosion process, and the results demonstrate that interactions between neighbouring blocks significantly influence the erosion process. Understanding multi-block erosion is important for rock erosion prediction and its remediation, thereby enhancing the safety and longevity of hydraulic structures.

REFERENCES

- George, M.F. (2015). *3D block erodibility: dynamics of rock-water interaction in rock erosion* (Ph.D. Dissertation). UC Berkeley, California, US.
- Koulibaly, A.S., Saeidi, A., Rouleau, A. and Quirion, M. (2022). A Reduced-Scale Physical Model of a Spillway to Evaluate the Hydraulic Erodibility of a Fractured Rock Mass. *Rock Mechanics and Rock Engineering*, 1–19.
- Teng, P., Zhang, S. and Johansson, F. (2021). Numerical modelling of incipient motion of fracture infillings. *International Journal of Rock Mechanics and Mining Sciences*, 148, p.104960. <https://doi.org/10.1016/j.ijrmms.2021.104960>.
- Teng, P., Johansson, F. and Hellström, J.G.I. (2023). Modelling erosion of a single rock block using a coupled CFD-DEM approach. *Journal of Rock Mechanics and Geotechnical Engineering*, 15(9), pp. 2375–2387.

The EU Interreg BONSAI project proposal

M. van Damme¹, K. Verelst²

1. Ministry of Public Works and Water Management, Utrecht, The Netherlands, Myron.van.damme@rws.nl

2. Flanders Hydraulics, Antwerp, Belgium, Kristof.verelst@mow.vlaanderen.be

ABSTRACT: The EU Interreg North-West Europe project proposal BONSAI wants to boost flood resilience in estuarine systems anticipating shifting climate zones. The project aims to develop a transnational strategy for improved resilience against the effects of climate changes on flood defence systems in North-West Europe; develop solutions to increase flood defence robustness and resilience; enhance disaster management and set up a transnational flood defence academy to increase the capacity of flood resilience experts and disaster management organizations via training. One of the focus points of the BONSAI project proposal are levee robustness and resilience in relation to external erosion whereby the objective is to build capacity by facilitating international collaboration. Here we outline the preliminary approach envisaged within the EU Interreg BONSAI project proposal on these focus points.

Keywords: Interreg North-West Europe; Proposal; BONSAI; Levee; Erosion

1 INTRODUCTION

The EU Interreg North-West Europe programme wants to promote a green, smart, and just transition with the aim to support a balanced development and make all regions more resilient. The second main objective of the Interreg North-West Europe programme is to build capacity at organizations. The BONSAI project proposal aims to address this aim within priority 1 of the programme, being climate and environment. The overall objective of the BONSAI project is to make flood defence systems in tidal estuaries of North-West Europe more resilient against climate change by learning from sites in different climate zones over Europe and to develop and share pro-active and responsive measures (See Figure 1). The project aims to strengthen the resilience against extreme weather events via empowering organizations responsible for flood resilience and societal partners in tidal estuaries in North-West Europe, through capacity building. The BONSAI project wants to achieve this by: 1) developing a transnational strategy and action plans to improve the robustness and resilience of flood defences; 2) jointly developing piloted solutions to increase flood defence robustness and resilience, and 3) increasing the capacity of flood resilience experts via training and working in transnational communities of practice. The BONSAI project focuses on the topics Erosion, Biodiversity and Emergency management, thereby looking both at short-term robustness and long-term resilience. Here we outline the preliminary approach to align the plans for levee robustness and resilience in relation to external erosion within this project proposal.

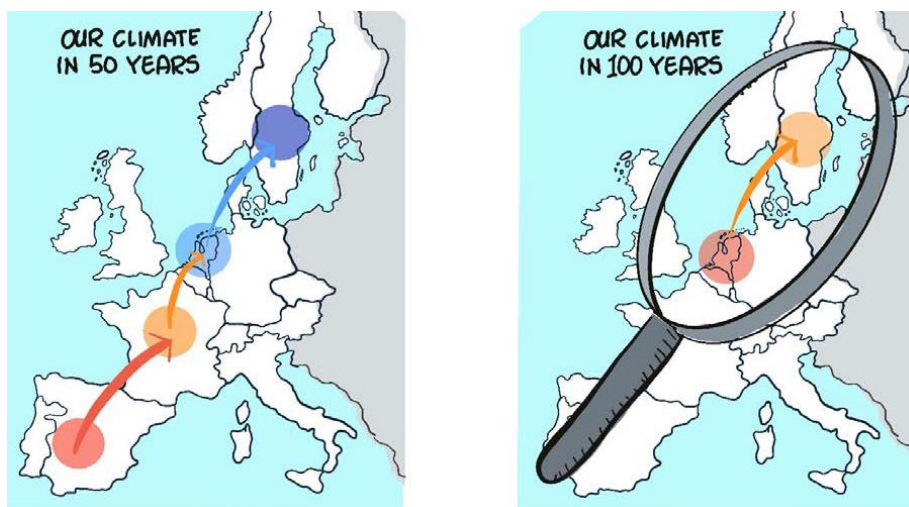


Figure 1. Main principle of the BONSAI project proposal.

2 DEVELOPMENT OF STRATEGIES

The levee cover and subsequent layers together need to offer a sufficient level of erosion resistance in order to prevent a full breach from forming during an extreme loading event. The strength of natural covers and subsequent layers could become negatively affected by long periods of drought. The strength at a specific time therefore depends on the resilience of the covers against previous conditions. The allowable amount of erosion damage to levees without the formation of a full breach is a measure of the robustness of a levee. The BONSAI project attempts to reach international agreement on an approach to quantify the resilience and robustness of levee covers. In order to optimize the level of acceptance and aid in the dissemination of the output, the ICOLD European working group on overflowing and overtopping erosion is invited to become involved in discussions on developments in the project.

2.1 *Quantifying resilience of levee covers.*

In North-West Europe the vegetated cover of a levee contributes significantly to its erosion resistance. The erosion resistance of a vegetated cover is determined by the presence and thickness of a clay cover underneath, the type of clay used and the type of vegetation and quality of the cover (Evers and Evers, 2023). The quality of grass covers is affected by periods of drought and is therefore negatively impacted by climate change. Preventing the negative impacts of droughts on the erosion resistance of vegetation results in higher maintenance costs as the probability of long drought periods increases. Other levee design techniques can also be considered which are more resilient to drought, e.g. the use of lime treatment to reinforce the cover layer. The BONSAI project believes that unifying the way in which the resilience of levee covers against drought is quantified across North-West Europe would boost the exchange of cover concepts and facilitate clear exchanges of experiences with specific covers. Therefore, experiments will be identified whereby levee cover layers have been subjected during large-scale tests to overflow, wave overtopping or wave impact. This will lead up to a select dataset containing high quality data and detailed information about the structure of the levee cover layer, the types of vegetation, but also the occurrence and magnitude of the erosion. Based on this data set, for a variety of levee covers and loading conditions identified, a method will be developed for evaluating the sensitivity of these levee covers to changes in erosion resistance due to impacts of climate change (like drought periods) and other impacts (like animal burrows). This could aid levee managers in the Northern regions of North-West Europe to learn from the Southern regions.

2.2 *Quantifying the robustness of levee covers.*

The degree of erosion that could take place over the duration of a storm is a measure for the robustness of a levee cover. Predicting erosion is a significant challenge. The erosion behaviour of soils is often represented via erosion parameters like the soil erodibility and critical shear stress, which are often determined empirically from analysing erosion tests at large, medium or small-scale. Differences in the way that stresses are predicted between models or differences in the way that data is analysed, or tests are executed cause for significant differences in the prediction of the erosion parameters. Without some form of standardization in how to interpret erosion parameters, erosion parameters derived in one way cannot be easily transferred to use in other models by other nations as it will give wrong predictions with a significant error. This translates into different definitions for levee robustness, inhibiting good communication and knowledge exchange, which in turn affect good collaboration and capacity building. The BONSAI project believes that by standardizing the way of interpreting erosion parameters, insights obtained on erosion in one nation could be translated to other nations. To arrive at a widely accepted means of deriving erosion parameters for input in erosion models, the impact of model assumptions and data interpretation is evaluated. To achieve this a dataset of high quality data is compiled consisting of experiments whereby levee soils have been subjected to prototype overflow or wave overtopping loads and for which the same soils have been tested using small-scale erosion tests. The choice in stress relations and generic approach for analysing the soil erodibility and critical shear stress will be discussed with the aim to arrive at a widely supported modelling approach. Using the outcome of the discussions the dataset will be used to derive a range of erosion parameters. Consequently, after an evaluation of the different methods, BONSAI will select a method for translating the uncertainty band following from small-scale erosion tests into an uncertainty band for large-scale tests. All these initiatives contribute to unifying the interpretation of levee robustness.

ACKNOWLEDGMENTS

The authors would like to thank the prospective partners in the BONSAI project for their contributions to this proposal.

REFERENCES

Evers, T. and Evers, M. (2023). Future Dikes Report, Thema 0, Relation between soil properties and erosion of levees (in Dutch).

Eight years of research into rockfill dams in HydroCen

F.G. Sigtryggsdóttir¹

1. NTNU, Department of Civil and Environmental Engineering, Trondheim, Norway, fiola.g.sigtryggsdottir@ntnu.no

ABSTRACT: Rockfill dams subjected to throughflow and overflow have been the main topic of the research project WP1.2 Dam construction and dam safety in the Norwegian research centre HydroCen. The project started in 2016 and concludes in 2024. Overview is provided here of 14 different physical dam model setups tested in the hydraulic laboratory as a part of this project. The research considers dams with or without riprap erosion protection, as well as with or without downstream drainage toe. In the fall 2024 it is planned to launch a website with links to videos from these experiments.

Keywords: Rockfill dams, throughflow, overtopping, experimental research

1 INTRODUCTION

Dams have been the focus of the project WP1.2 Dam construction and dam safety in the Norwegian research center HydroCen since 2016. The project is now in its final phase with HydroCen concluding in 2024. The emphasis has been on extreme loading conditions for embankment dams arising from throughflow and overtopping that may ultimately result in breaching of the dam. Most embankment dams in Norway classify as rockfill dams which has motivated selection of this dam type for the research. Rockfill dams equipped with placed riprap erosion protection on the downstream slope are further of interest since such erosion protection is a requirement in Norway for enhanced safety since 2010. However, the assumed added safety had not been investigated prior to 2010, and PhD research on the riprap protection started in 2014 (Hiller, 2017). The aim of the HydroCen WP1.2 project was to expand the research and increase knowledge relating to, firstly, robustness of rockfill dams when equipped with erosion protection comprising riprap on the downstream slope as required in Norway, secondly, the effect of different configurations of a downstream drainage toe for throughflow capacity and stability of the downstream shoulder, and thirdly, the breaching of rockfill dams. Experimental research into rockfill dams has been carried out in the Hydraulic Laboratory at NTNU as a part of the HydroCen WP1.2 project. The model setups include conceptual models of Norwegian rockfill dam as per the requirement in the Norwegian dam safety regulations. The dam models have developed from half dam models to full dam cross section (Figure 1). Altogether 14 different setups are presented in Figure 1, and include dams with and without riprap erosion protection, as well as with and without downstream drainage toe. In HydroCen, the research and analysis relating to rockfill dams spans eight years.

2 EXPERIMENTAL SETUPS AND TESTING PROCEDURE

Overview of the different physical model setups of dams employed in HydroCen are presented in Figure 1, compiled as two setup categories: (1) Half Dam Models (with aluminum core); and (2) Full Dam Models (homogeneous or with a thin central core of rubber). Additionally, models involving only the riprap layer were tested but are not discussed here. The Half Dam Model setups a)-d) in Figure 1 considered throughflow while setups e) to i) considered both throughflow and overtopping capacity. All the half dams had an aluminum core. The purpose of the Full Dam Models was to investigate breaching of rockfill dam with and without riprap erosion protection. Models in all setup categories included dumped or placed riprap erosion protection with or without support against the downstream toe stone (see models HdP, HdPi, HdD, HdDi, HdPT, FdP, FdD, FdDs in Figure 1. Dumped ripraps consist of randomly dumped stones whereas placed ripraps comprise of stones arranged in an interlocking pattern. Some of the models were not protected with riprap. (see Hd, Hdi, Hde, Hdc, FdU, FdH in Figure 1) and some of the Half Dam Models included a downstream drainage toe. (see Hdi, Hde, Hdc, HdPi, HdDi in Figure 1). The experiments were conducted in a flume measuring 25 m in length, 1 m in width, and 2 m in height. All the physical models are conceptual with a scaling of 1:10. The model dams were 1 to 1.1 m high, and 1 m long (dam length = flume width), representing about 10 m high conceptual dam in a full scale. The inclination of the dam slopes was 1:1.5). The model design considered a typical Norwegian rockfill dam. For details see Ravindra (2020), Ravindra & Sigtryggsdóttir (2021), Dezert et al. (2022); and Kiplesund et al., (2021). The testing procedure was different for the Half Dam and Full Dam Models, and for models with and without riprap erosion protection. As an example, the Full Dam Models without erosion protection were subjected to a constant discharge throughout the test until complete failure was reached. Conversely, Full Dam Models with erosion protection were subjected to flows applied progressing in incremental fixed discharge intervals until complete failure was achieved. Various instruments and

technologies have been applied to record the performance of the dams (Ravindra, 2020; Ravindra and Sigtryggisdóttir, 2021; Kiplesund et al., 2021; Kiplesund et al., 2023; Dezert and Sigtryggisdóttir, 2023 and 2024).

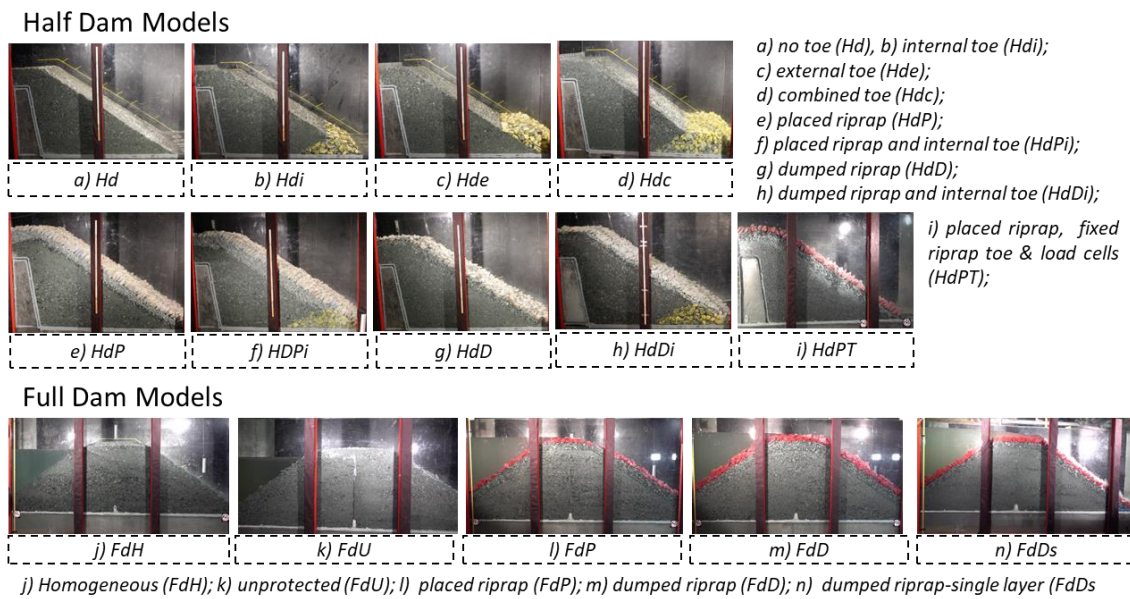


Figure 1. Experimental rockfill dam model setups investigated (1) Half Dam Models; and (2) Full Dam Models.

3 CONCLUDING REMARKS

The experimental research revealed that rockfill dams protected with riprap on the downstream shoulder, sustain much more overtopping discharges and for considerably longer time than unprotected dams (Ravindra & Sigtryggisdóttir, 2021; Dezert et al., 2022). Support at the downstream riprap toe stone enhances the capacity and changes the failure mechanics (Ravindra, 2020; Dezert and Sigtryggisdóttir, 2023 and 2024). Thus, the riprap protected dam may sustain the extreme flood situation causing the overtopping. However, in the unlikely event that the flood continues so that the riprap protected dam breaches, the breach opening is likely to be larger than for unprotected dams (Dezert et al., 2024) resulting in higher peak outflow and thus potentially higher consequences for the downstream area. This is important to consider in risk assessments and emergency preparedness and planning.

ACKNOWLEDGMENTS

The financial support by HydroCen, Norway and cooperation with Prof. Leif Lia is acknowledged. The work was carried out in project WP1.2 in HydroCen, led by the author, through the PhD studies of Ganesh H. R. Ravindra and Geir H. Kiplesund, and an associated postdoc project carried out by Dr. Théo Dezert. MSc students (14) contributed to the project.

REFERENCES

- Dezert, T., Kiplesund, G. H., & Sigtryggisdóttir, F. G. (2022). Riprap Protection Exposed to Overtopping Phenomena: A Review of Experimental Models. *Water*, 14(17), 2722 <https://doi.org/10.3390/w14172722>.
- Dezert, T.; Sigtryggisdóttir, F.G. (2024). *Stability evaluation of toe supported ripraps exposed to overtopping*. Report 12/2024, NVE. https://publikasjoner.nve.no/eksternrapport/2024/eksternrapport2024_12.pdf
- Dezert, T.; Sigtryggisdóttir, F. G. (2023). 3D Displacement and Axial Load of Placed Riprap Supported at the Toe: Use of Structure from Motion. *J. Hydraul. Eng.* <https://doi.org/10.1061/JHEND8.HYENG-13599>
- Dezert, T., Kiplesund, G. H., and Sigtryggisdóttir, F. G. (2024). Parametric breach models evaluation from laboratory rockfill dam models under overtopping conditions. *Accepted for publication in J. Hydraul. Eng.*
- Hiller, P.H. (2017). *Riprap design on the downstream slopes of rockfill dam*. Doctoral thesis, NTNU.
- Kiplesund, G.H; Sigtryggisdóttir, F.G.; Lia, L. (2023). Breach Progression Observation in Rockfill Dam Models Using Photogrammetry. *Remote Sensing*, volum 15 (6). <https://doi.org/10.3390/rs15061715>
- Kiplesund, GH., Ravindra, GHR., Rokstad, M.M., Sigtryggisdóttir, FG (2021). Effects of toe configuration on throughflow properties of rockfill dams. *J. Appl. Water Eng. Res.*, 1–16. <https://doi.org/10.1080/23249676.2021.1884615>
- Ravindra, G.H.R (2020). *Hydraulic and structural evaluation for rockfill dam behavior when exposed to throughflow and overtopping scenarios*. Doctoral thesis, NTNU
- Ravindra, G. H. R.; Sigtryggisdóttir, F.G. (2021). *Riprap protection on downstream rockfill dam shoulder & dam toe*. Report 17/2021, NVE. https://publikasjoner.nve.no/eksternrapport/2021/eksternrapport2021_17.pdf

The OVERCOME Project: Developing the Laverné Field Test Facility

M.W. Morris¹, J-R. Courivaud², C. Picault³, R. Moran⁴

1. HR Wallingford, Oxfordshire, UK; mark.morris@samuifrance.com

2. EDF-CIH, Bourget du Lac, France; jean-robot.courivaud@edf.fr

3. CNR, Lyon, France; c.picault@cnr.fr

4. UPM, Madrid, Spain; r.moran@upm.es

ABSTRACT: The Laverné Field Test Facility is being developed as part of the OVERCOME Project programme which comprises a combination of numerical, laboratory and field testing to better understand how the erosion of coarser grained materials occurs in dams and levees, leading to breach. Results from this research ultimately feed into the development of more accurate breach prediction models. By building a large scale test facility, the effects of breach modelling at different scales may be better understood.

The Laverné Field Test Facility is being developed near the Embalse de Laverné, located about 50km north of Zaragoza in Spain. The location sits within an irrigation area, managed by the Ebro Water Authority. The test facility itself is located between an irrigation canal transfer channel and a storage reservoir (Laverné Reservoir) and can benefit from water flows of up to 9m³/s. A test platform, allowing for levees up to 2.5m high and 14m wide has been designed, with the goal of providing a facility that will allow for the large-scale testing to destruction of levees constructed from different soils. A complex system of instrumentation is also being developed for the facility, including performance testing of photogrammetry and green lidar solutions. The schedule for construction depends upon financial arrangements, but it is foreseen to commence either later this year, or next.

This paper will provide an overview of the proposed facility and the design process undertaken to reach the point of construction.

Keywords: Dam and levee breach; breach modelling; surface erosion; instrumentation.

The OVERCOME Project: Advances in Experimental Research on the Macro Erosion of Coarse-Grained Embankments in Overflow Scenarios

R. Monteiro-Alves¹, R. Moran¹, M.Á. Toledo¹, M. Morris², J.R. Courivaud³, C. Picault⁴

1. Universidad Politécnica de Madrid, 28040 Madrid, Spain, ricardo.monteiro@upm.es, r.moran@upm.es, miguelangel.toledo@upm.es

2. HR Wallingford, Wallingford, United Kingdom; m.morris@hrwallingford.com

3. EDF Hydro Engineering Centre, 73290 La Motte Servolex, France, jean-robot.courivaud@edf.fr

4. Compagnie Nationale du Rhone, Lyon, France, c.picault@cnr.tm.fr

ABSTRACT: From previous flume tests, intended for investigate the effect of different soil materials, overflow discharges, soil density, and upstream face watertightness on the breaching processes, derived the need for further investigation on the real effect of the content of fines and the effect of armouring caused by the content of the coarser particles. This document presents the results of these new set of tests which have shown an impact of these variables on the breach macro erosion processes, erosion rates and breach dimensions.

Keywords: Macro erosion, Breaching; Coarse-grained soil

1 INTRODUCTION

The companies EDF and CNR are funding a research project called OVERCOME in order to investigate the macro-erosion processes observed in overflowed embankment dams and levees constructed from coarse grained soils, with the final goal of improving software capable of estimating the hydrographs resulting of the breaching processes. This work is part of an extensive series of flume tests conducted by the Technical University of Madrid (UPM) and Compagnie Nationale du Rhône (CNR), focusing on embankment dam breaching dynamics. Initial tests examined the effects of various soil materials, soil density, inflow rates, and upstream face on breaching processes. This initial set of tests comprised nine 0.55 m high embankments performed at UPM and three 2.5 m high embankments performed at CNR. Building on these insights, a new set of flume tests have been performed to specifically investigate how large and fine soil particles influence macro erosion processes. This paper specifically presents the findings from the last three tests performed at UPM, which concentrated on analyzing the impacts of fine and large particles.

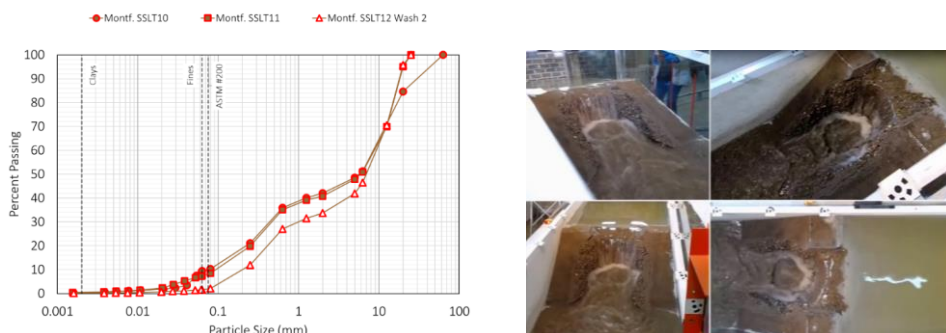


Figure 1. Grading curves used in this set of tests (left) and snapshots from the SSLT11 test (right).

2 PHYSICAL MODELLING

To achieve the objectives of this research, three embankment flume tests were performed using the same basic original soil, an alluvial soil from an existing levee (Montfaucon, Gard, France). This soil has been scalped and washed to fit our goals. These soils were used to construct 0.55 m high and 1.25 m wide embankments featuring a 0.5 m wide and 0.07 m deep central notch. The same inflow discharge was used for all three tests, 22 l/s/m. The grading curves of the soil materials and snapshots from the SSLT11 test are presented in Figure 1. SSLT10 and SSLT11 can be compared to assess the effect of the coarser particles, while SSLT11 and SSLT12 to assess the effect of the fines.

3 RESULTS

In all tests, the mechanism for soil particle detachment was consistent, involving overflow water eroding the finer materials from the downstream slope, subsequently exposing and mobilizing coarser particles which are then deposited at lower parts of the downstream slope. This process typically starts at the upper part of the downstream slope, where the transition from the crest to the downstream slope occurs. However, variations in the grading curve can influence the profile of the breach and the erodibility of the soil, leading to different erosion dynamics and breach characteristics.

For the first two tests, SSLT10 and SSLT11, the overflow initially shaped cascading steps coinciding with the compaction lifts. With time, these cascading steps were eroded off and erosion tended to be more pronounced in lower areas of the slope, forcing the formation of a single near-vertical face, starting from the crest and migrating upstream through the same soil particle detachment mechanism, without significant changes to its slope (*Figure 2*). The main differences between these two tests refer to breach dimensions and soil erodibilities, both significantly higher in SSLT11. The maximum erosion rates were approximately 5 times higher in the SSLT11 (*Table 1*) and the near vertical face was roughly 1.5 times deeper (*Figure 2*).

In the SSLT12 test, after a quite similar initiation process, i.e., erosion of the finest particles and dragging of the coarsest ones, the overflow led to the formation of gullies, deepening to create islands of uneroded soil in the middle of the slope. Given that this soil was considerably more erodible than the previous two tests, in the initial stages of erosion these gullies tended to get deeper where erosion first started, i.e., in the upper areas of the slope. As erosion progressed, the breach profile formed two steps connected by a berm, both migrating upstream at a consistent rate, with slopes which tended to be milder than in the previous tests. As the breach reached the upstream slope and outflow increased, the lower step flattened, eventually stabilizing at an equilibrium slope. The upper step also flattened, though to a lesser extent. Over time, the upper slope realigned with the downstream breach slope to form a continuous, equilibrium breach bed slope. Erodibility was substantially higher in this test, presenting maximum erosion rates 3 times higher than SSLT11 (*Table*). The same way, the final breach width was also larger but, interestingly, the final depth was lower in this test (*Figure*). These results show that both variables, content of coarse particles and content of fines, affect the breaching kinetics.

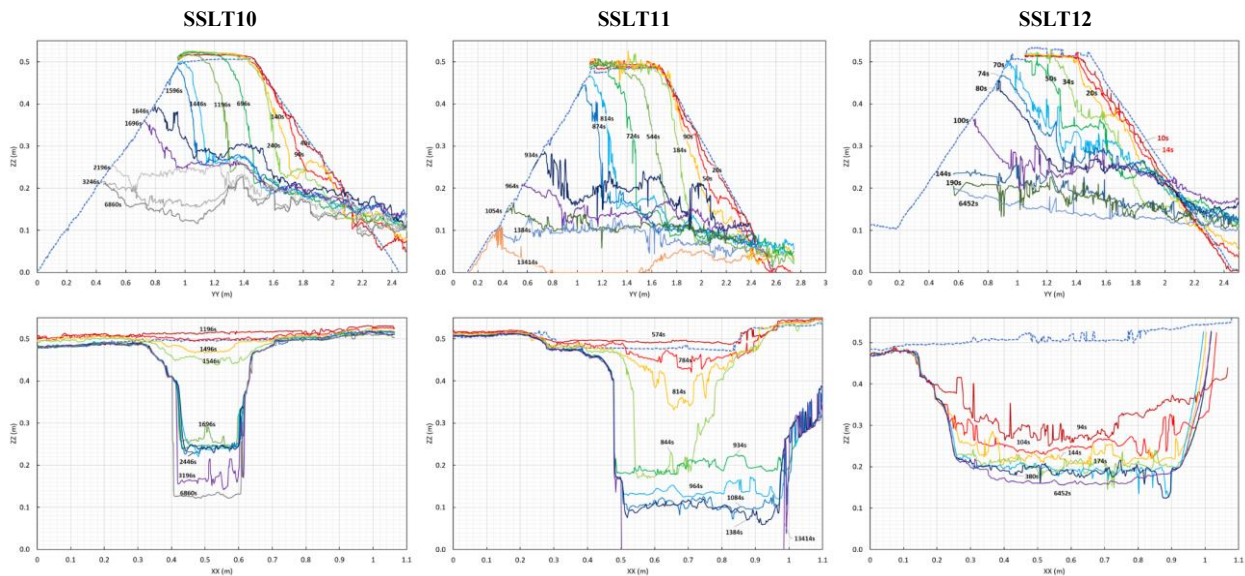


Figure 2. Breach evolution for tests SSLT10 (left), SSLT11 (middle), and SSLT12 (right). Times are all in relation to the initiation of overflow, i.e., when the reservoir level reached the notch invert elevation.

Table 1. Main soil characteristics and resulting breaching erosion rates and peak outflows.

Test	Soil	D50 (mm)	Max. Sieve Passing 100% (mm)	Percentage fines < 0.080 mm	Coefficient Uniformity (Cu)	Peak Erosion Rate (cm ³ /s)	Time to Peak (s)	Peak Outflow (l/s)
SSLT10	Original	5.7	63	10.3	132	193	1650	20.4
SSLT11	Scalped	5.9	25	8.5	90	985	940	41.8
SSLT12	Washed	7.2	25	2.0	45	3284	115	64.2

ACKNOWLEDGMENTS

The authors extend their gratitude to all members of the OVERCOME Project for their significant contributions to the discussion of our experimental test results. Special thanks are due to Électricité de France (EDF) and Compagnie Nationale du Rhône (CNR) for funding the OVERCOME Project under whose framework these tests were conducted.

Resistance to overflow of earth-fill dams: laboratory tests and numerical modelling to characterize erosion processes

H. Haddad¹, M.A.A. Hassan², L. Montabonnet¹, H. Stoter¹, C. Picault¹, M. Morris³

1. CNR-CESAME, Lyon, France, h.haddad@cnr.tm.fr

2. HR Wallingford, Oxfordshire, UK, m.hassan@hrwallingford.com

3. Samui, Oxfordshire, UK, mark.morris@samui.co.uk

ABSTRACT: The aim of the OVERCOME research project is to improve our understanding of the physical erosion processes during overtopping of coarse material embankments. Laboratory tests were conducted and provide a large dataset. Both surface and headcut geometry erosion was observed. The results highlighted that the soil density is a key parameter in the resistance of the embankment. The data obtained was used as entry and calibration data for numerical models in order to assess the performance and to improve these tools.

Keywords: OVERCOME; External erosion; Overflowing; Laboratory tests; Numerical modelling

1 INTRODUCTION

Although overtopping is identified as the dominant failure mechanism in breaches, the tools available to characterize it are limited to soils with specific and narrow characteristics. The OVERCOME research project (OVERflowing EROsion of COarse Material Embankments) was initiated in 2018 to investigate the resistance of embankments to overflowing erosion. This project brings together CNR, EDF (CIH/LNHE), UPM, HR Wallingford, and INRAE and aims to identify the main parameters that drive the erosion processes by means of laboratory tests and numerical modelling. This communication presents the insights from two laboratory tests conducted in CESAME – CNR laboratory and numerical modelling runs using the EMBREA and WINDAM C models based on the data obtained from the laboratory tests.

2 METHODS

Laboratory tests

The material used for the construction of the embankments was typical gravel and sand taken from a Rhone River levee. The material was placed in layers and compacted to obtain a target density. A notch was dug at the centre of the crest of the dike. To avoid excessive seepage, the upstream face was sealed with a layer of Kaolinite. During each test, the water level upstream of the embankment was adjusted to approx. 5 cm above the notch. Discharges, water levels and topography were monitored (Figure 1). The two tests presented differed in terms of density: 2.05 t/m³ for the first and 2.15 t/m³ for the second.

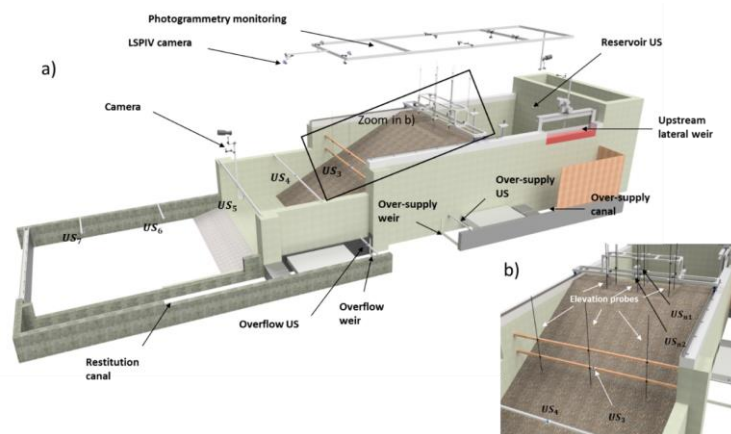


Figure 1: Embankment and its associated instrumentation. (a) 3D view and (b) zoom on the downstream face.

Numerical modelling

To assess the performance of existing numerical models, single and Monte Carlo runs have been undertaken using the EMBREA (Mohamed, 2002) and WinDAM C (Temple et al, 2006) breach models using the data from test 1. The single runs included headcut (which seems to be the dominant erosion mechanism in the two tests) and surface erosion runs whilst the Monte Carlo runs were undertaken for headcut erosion in which several parameters were varied, namely, soil erosion rate, Manning's coefficient and critical shear stress. Runs for Test 2 are currently being undertaken.

3 RESULTS AND DISCUSSION

Both tests led to similar observations with four successive phases: filling of the reservoir, surface erosion, headcut-like erosion process and breach. The peak outflow discharge measured was about 290 L/s (approx. 100 L/s/m unit discharge). The erosion was asymmetrical and the embankment ended up collapsing at the end. The duration of the surface erosion and breach phases were the same, but the headcut erosion phase was more than 4 times longer for the second test.

The numerical modelling that was undertaken using EMBREA and WinDAM C showed the following:

- The headcut migration coefficient affected the modelling results of EMBREA headcut runs. The initial estimate of this parameter, based on empirical equations, showed a slow breach development with time in comparison to what was observed in Test 1. Doubling the value of this coefficient gave better results (See *Figure 2*).
- The erodibility coefficient affected the modelling results of WINDAM C and EMBREA surface erosion runs. The initial value of this parameter that is based on laboratory experiments showed a rapid breach development with time in comparison to what was observed. Reducing the value of this coefficient gave better results.
- The results of the EMBREA Monte Carlo runs show that the model results deviation from the Test 1 data is within the expected range of uncertainty of the measured data and processes involved in the breach development.

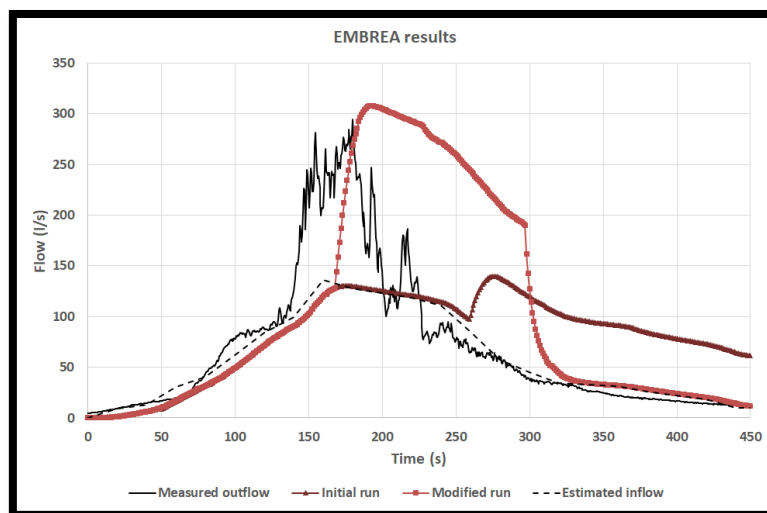


Figure 2: EMBREA headcut run results with initial and modified migration coefficients.

4 CONCLUSION

The large laboratory tests allowed us to monitor closely the erosion processes involved during the overtopping erosion of an embankment built from coarse materials. They also brought insight and valuable data to calibrate numerical models. In perspective, the two tests will be thoroughly compared via observations and numerical modelling runs.

REFERENCES

- Mohamed, M.A.A. (2002). *Embankment Breach Formation and Modelling Methods*. PhD Thesis, The Open University, England.
- Temple, D.M., Hanson, G.J. and Neilsen, M.L. (2006). *WinDAM - Analysis of overtopped earth embankment dams*, In Proc. of the ASABE Annual Conference, Paper Number 062105.

Rhone dike overflow: comparison of field test measurements with different numerical modelling results

H. Umdenstock¹, C. Picault¹, F. Golay², S. Bonelli³

1. CNR-CESAME, Lyon, France, c.picault@cnr.tm.fr

2. Institut de Mathématique de Toulon (IMATH), Toulon, France, frederic.golay@univ-tln.fr

3. Aix-Marseille Université et INRAE, Aix-en-Provence, France, stephane.bonelli@inrae.fr

ABSTRACT: Two tests were carried out in May 2022 on a dike, with increasing flows corresponding to a crest water height of 4 to 18 cm. The first test concerned intact soil, covered with natural grass: no significant erosion of the natural grass was observed; the gap graded gravel fill located at the dike toe was eroded (1.5 m³). The second test was conducted on the soil stripped of the vegetation cover: silt and clayey sand were eroded (9m³). During these tests, the following variables were measured: flow rate, flow velocity, water height and soil erosion. These measurements were compared with the results obtained by numerical modelling (shallow water equations).

Keywords: Earth dikes; Overflow; External erosion; Field tests; Numerical modelling

1 INTRODUCTION

The OVERCOME research project (OVERflowing ERosion of COarse Material Embankments) was initiated in 2018 to investigate the resistance of embankments to overflowing erosion. This project brings together CNR, EDF (CIH/LNHE), UPM, HR Wallingford, and INRAE and aims to identify the main parameters that drive the erosion processes by means of laboratory and field tests, and numerical modelling. This communication presents the insights from two field tests conducted by INRAE team and numerical modelling runs using the TELEMAC (EDF) and CERF (Toulon Univ.) softwares.

2 FIELD TESTS

As part of the OVERCOME project, launched by Compagnie Nationale du Rhône and Electricité de France to fill in some of the gaps in understanding the overflowing resistance of earthen levees, INRAE performed two tests in May 2022 on a CNR dike near Avignon (France). The dike is 6.2 m high; the core is mainly made of sandy silts (Fig. 1). The toe is covered by a gravel shoulder which forms a berm. The first test was carried out on the intact soil: the core covered by a natural grass on the upper part, and the gravel fill without grass in the lower part of the slope. The test consisted of carrying out a flow in a channel of 1 m wide and 25 m long, in 12 steps of 30 min (6 hours of flow in total). The second test was carried out on the soil stripped of the vegetation cover in order to study the soil of the upper part of the embankment, made up of compacted sandy silt and sandy gravel. The test consisted of carrying out a flow in a 60 cm wide and 20 m long channel, in 9 steps of 30 min (4.5 hours of flow in total). The test campaigns were carried out with flows ranging from 12 to 140 l/s per linear meter, corresponding to a crest water depth ranging from 4 to 18 cm (Fig. 2).

3 NUMERICAL MODELLING

Several numerical modelling runs solving shallow water equations were carried out on initial fixed background, on real measured topography (fixed) at each step and on topography modelled with an erosion law (ongoing work): 1) with the TELEMAC 2D code (EDF), 2) with the TELEMAC 2D/GAIA codes (EDF), 3) with the CERF code (Toulon Univ.). Figure 3 shows an example of a comparison between measured and modelled flow velocities using TELEMAC 2D on initial fixed background. This set of results provides evidence for the relevance of numerical modelling to represent overflows, and the possibility to use the bed shear stress to compute the bottom evolution with erosion laws.

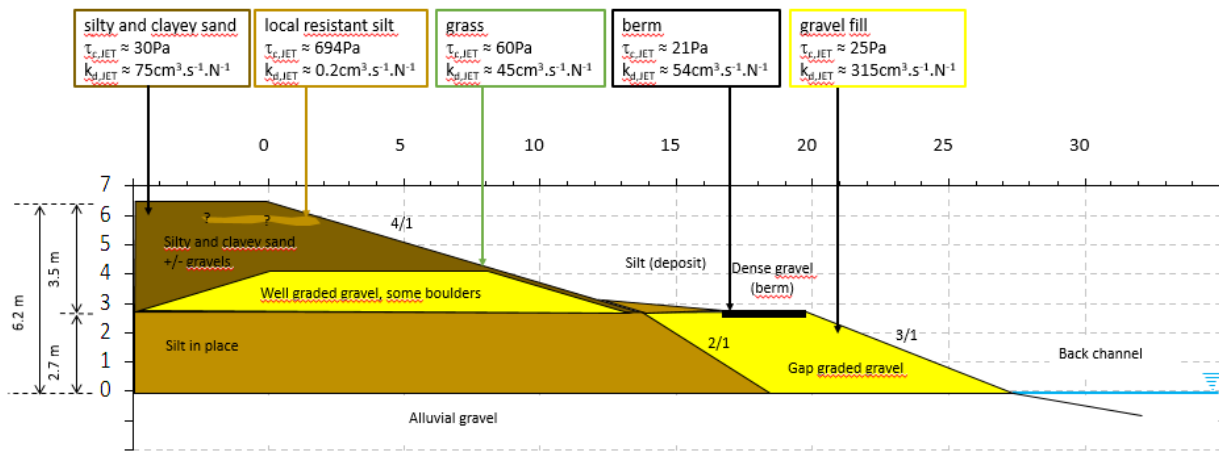


Figure 1. Cross-section of the dike, with JET characteristics measured in laboratory or on site

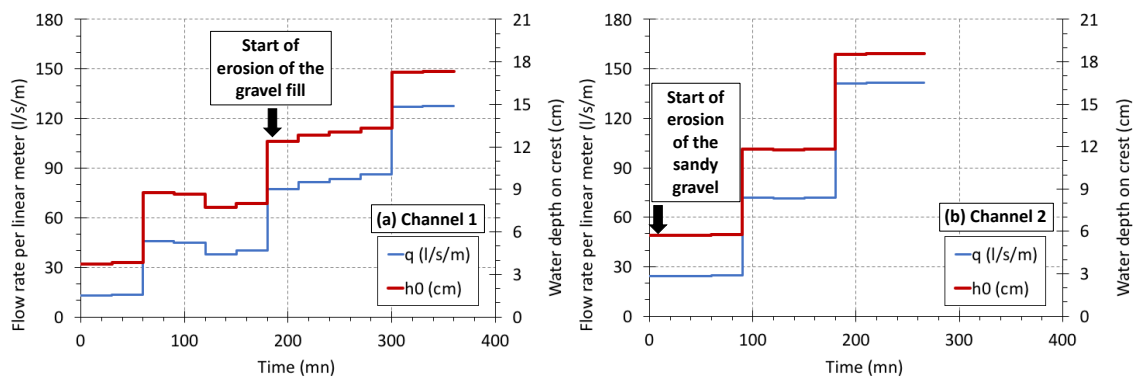


Figure 2: Flow sequence of (a) the 12 steps on Channel 1 and (b) of the 9 steps on Channel 2.

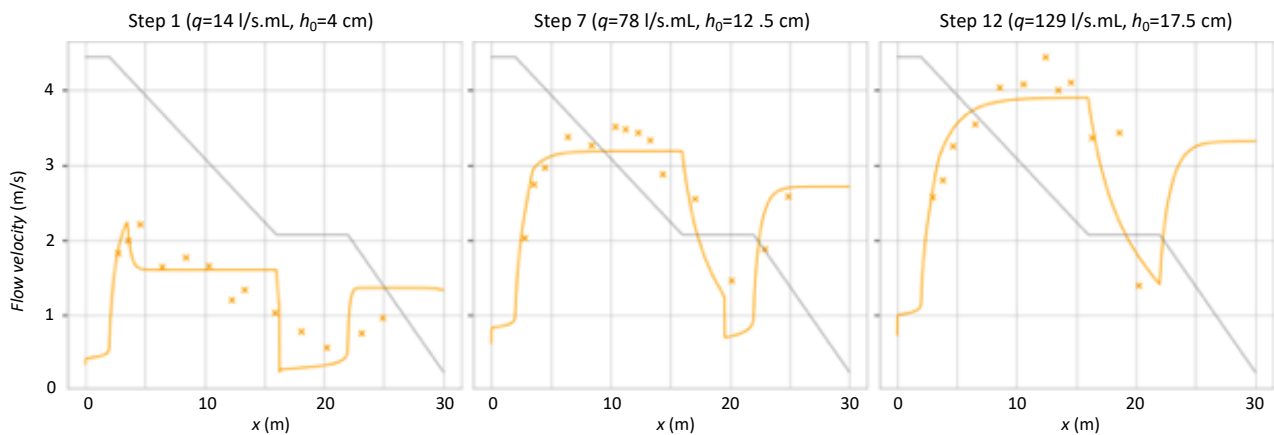


Figure 3: Comparison of measured (symbols) and modelled (continuous lines, TELEMAC 2D) flow velocities on Channel 1.

REFERENCES

- Bonelli S., Nicaise S., Charrier G., Chaouch N., Byron F., Gremeaux Y. (2018), Quantifying the erosion resistance of dikes with the overflowing simulator, 3rd Int. Conf. on Protection against Overtopping, 6-8 June 2018, UK.
- Nerinx N., Bonelli S., Mercier F., Cornacchioli F., Fry J.-J., Herrier G., Richard J.-M., Puiatti D., Tachker P. (2018), DigueElite overflow resistant lime treated soils for dikes and earthdams, 26th International Congress on Large Dam, Vienna, Austria, 4-6 July.
- Picault C., Crampette F., Bonelli S., Nicaise S., Chaouch N., Byron F., Grémeaux Y., Doghmane A., Garoui M., Herbeck J., Golay F. (2022), Field testing of the overflow erosion of Rhone river levees. 4th Int. Conf. on Protection against Overtopping, 30 Nov-12 Dec, Spain.

Simulation of headcut breach dynamics using the two-dimensional depth averaged hydraulic model TELEMAC-2D

Z. Amama^{1,2}, S.E. Bourban^{1,2}, J.R. Courivaud³, M. Morris⁴, K. El Kadi Abderrezzak^{1,2}

1. EDF R&D, LNHE, Laboratoire National d'Hydraulique et Environnement, Chatou, France, zied.amama@edf.fr, sebastien.bourban@edf.fr; kamal.el-kadi-abderrezzak@edf.fr

2. LHSV, Laboratoire d'Hydraulique Saint-Venant, Chatou, France

3. EDF CIH, Centre d'Ingénierie Hydraulique, La Motte Servolex, France, jean-robot.courivaud@edf.fr

4. HR Wallingford Ltd, Wallingford, UK, mark.morris@samui.co.uk

ABSTRACT: Dams and levees can be overtopped with a continuous flow, leading to the breach formation that may in turn cause the structure to fail. This study integrates the headcut erosion algorithm from the physically-based model WinDAM into the two-dimensional depth-averaged TELEMAC-2D software to simulate the breach expansion and the induced inundation. The model was applied to simulate a laboratory experiment, accurately reproducing the measured breach discharge.

Keywords: Headcut erosion, TELEMAC-2D, WinDAM, Breach dynamics, Embankment failure

1 INTRODUCTION

Embankment (e.g., dam, levees) failures due to headcut erosion present severe risks to downstream areas (Morris et al., 2009). Accurate modeling of headcut dynamics is crucial for predicting breach development and appropriate floodwater routing (Hunt et al., 2021). Models, such as WinDAM, provide physically based algorithms for simulating headcut processes in cohesive embankments. Integrating these algorithms into an advanced two-dimensional hydraulic models, offers enhanced capabilities for simulating breach scenario and flood propagation. This study aims to reproduce the headcut breach dynamics observed in ARS embankment overtopping Test 1 using TELEMAC-2D.

2 NUMERICAL MODELLING APPROACH

TELEMAC-2D is a widely used hydrodynamic model solving the shallow water equations with the finite element method. The model can handle complex geometries, variable grid resolutions, and diverse boundary conditions. The headcut erosion algorithm from WinDAM model was integrated into TELEMAC-2D to simulate the breaching process.

WinDAM models reservoir routing by importing inflow hydrographs and routing them using stepwise steady-state conditions (Hunt et al., 2021). The model accounts for various outflow paths, including principal, dam overtopping, reservoirs outflows and developing breach areas. It uses elevation-discharge tables and spillway properties to compute discharge, considering tailwater effects through iterative calculations. Breach discharge is determined based on unit discharge and breach area width, with erosion dynamics modeled in stages: slope protection failure, headcut formation, headcut progression, and breach widening.

The headcut erosion algorithm was implemented in TELEMAC-2D using the same equations as WinDAM. However, reservoir routing was handled differently. In TELEMAC-2D, upstream and downstream reservoir routing is automatically managed by the 2D solver. The erosion rate is calculated as follows:

$$\epsilon_r = k_d(\tau_e - \tau_c) \quad (1)$$

where ϵ_r is the erosion rate ($\text{m}^3/\text{s}/\text{m}^2$), k_d is the detachment rate coefficient ($\text{m}^3/\text{N}/\text{s}$), τ_e is the effective shear stress (Pa) and τ_c is the critical shear stress (Pa). The headcut advance rate is computed as:

$$\frac{dX}{dT} = C(qH)^{\frac{1}{3}} \quad (2)$$

where C is a material dependent constant for backward erosion, q is the unit discharge (m^2/s), and H is the headcut height (m).

TELEMAC-2D is applied to simulate the ARS embankment overtopping Test 1 (Hanson et al., 2005). The embankment was 2.3 m high, with a 4.6-m crest width and 3:1 side slope, constructed from silty sand material (70% sand; 25 % silt and 5% clay). The test section for initial overtopping was 1.8 m wide, expanding during the breach process. Soil properties and inflow hydrograph data were obtained from the original test documentation (Hanson et al., 2005).

3 RESULTS

Calibration of the headcut coefficient C , the detachment rate coefficient k_d and the critical shear stress τ_c was necessary to achieve good results for the breach hydrograph. The calibrated values obtained using the Nelder Mead optimisation algorithm (Nelder and Mead, 1965), were $C = 0.006$, $k_d = 5.2 \text{ cm}^3/\text{N}/\text{s}$ and $\tau_c = 19 \text{ Pa}$. The model accurately reproduces the breach hydrograph, as shown in Figure 1, but had limitations in predicting breach widening and backward erosion. The Root Mean Square Error (RMSE) between the simulated and observed discharge was around $0.31 \text{ m}^3/\text{s}$ and the relative error was around $0.037 \text{ m}^3/\text{s}$, indicating a reasonable match.

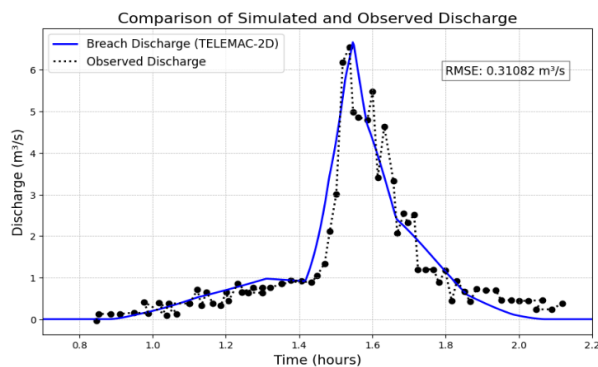


Figure 1. Simulated breach discharge and observed data from USDA ARS#1 test case

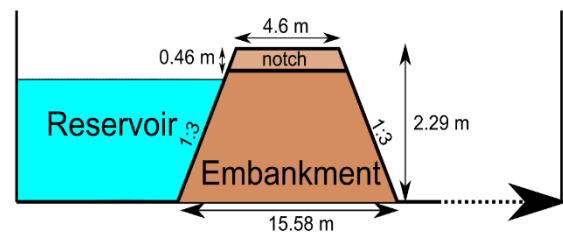


Figure 2. Geometry of USDA ARS#1 embankment

4 DISCUSSION

The results demonstrated that the TELEMAC-2D model with the integrated headcut erosion algorithm could effectively simulate the headcut breach process and the breach outflow. However, the calibration highlighted significant uncertainties in the parameters, affecting the model's ability to predict breach widening and backward erosion accurately. Backward migration of the headcut was overestimated, while the widening of the breach was underestimated. This discrepancy indicates that while the overall hydrograph was well reproduced, the detailed breach progression dynamics were less accurately modeled. Among the calibration parameters, the headcut coefficient (C) and the detachment rate coefficient (k_d) were found to be the most sensitive. Small changes in these parameters significantly affected the simulation results, highlighting their importance in accurately modeling headcut erosion. The critical shear stress (τ_c) had a lesser impact on the overall results but was still crucial for defining the onset of erosion. Integrating the headcut erosion algorithm from WinDAM into TELEMAC-2D significantly enhances its capability to simulate breach dynamics.

REFERENCES

- Hanson, G., Cook, K. R., & Hunt, S. (2005). Physical modeling of overtopping erosion and breach formation of cohesive embankments. *Transactions of the ASABE*, 48, 1783–1794. <https://doi.org/10.13031/2013.20012>
- Hunt, S. L., Temple, D. M., Neilsen, M. L., Ali, A., & Tejral, R. D. (2021). WinDAM C: Analysis tool for predicting breach erosion processes of embankment dams due to overtopping or internal erosion. *Applied Engineering in Agriculture*, 37(3), 523-534.
- Morris, M., Hassan, M., Kortenhaus, A., & Visser, P. (2009). Breaching Processes: A state of the art review. *FLOODsite Publications*, 70.
- Nelder, J. A., & Mead, R. (1965). Iterative method for nonlinear optimization. *Comp J*, 7, 308.

A dataset on the breaches caused by the flood events that affected Emilia-Romagna in May 2023

M. Marchi¹, I. Bertolini¹, A. Colombo², G. Gottardi¹, L. Morreale², T. Simonelli², L. Tonni¹

1. University of Bologna, Department of Civil, Chemical, Environmental and Materials Engineering, Bologna, Italy, michela.marchi@unibo.it

2. Flood Risk Management Office, Po River District Authority, Strada Garibaldi, 75, 43121, Parma, Italy

ABSTRACT: This contribution describes the methodology adopted for the systematic collection of data on the main breaches experienced by the embankment systems affected by the exceptional flood events occurred in May 2023 in Emilia-Romagna. To this purpose, all main observed failures and their characteristics have been catalogued and extensive visual evidence collected in the field. Additionally, a GIS-based tool has been implemented to synthesize the collected information. By analysing the entire dataset, managers and scientists can identify the primary fragility factors of the embankment systems, providing robust indicators for increasing their resilience.

Keywords: Emilia-Romagna flood events; river embankments; breaches; database; GIS

1 CONTEXT AND MOTIVATION

The exceptionally intense meteorological events that impacted the Emilia-Romagna region between May 2-3, 2023, and subsequently on May 16-17 (Brath et al., 2023), caused severe damage to all structures and infrastructures in the area, including the embankments of rivers and streams. The first event featured intense rainfall, with over 200 mm of precipitation in central-eastern Emilia-Romagna, making it the most severe 48-hour event since 1997 and the most intense spring event since 1961. The second event, on May 16-17, brought even higher rainfall, exceeding 240 mm in some areas. The cumulative effect of these events led to significant flooding and damage. The embankment systems that experienced the main failures were located in the provinces of Bologna, Ravenna, and Forli-Cesena. The affected watercourses were: Gaiana, Quaderna, Idice, Santerno, Sillaro, Senio, Lamone, Marzeno, Montone, Ronco, Savio, Rabbi, and, to a lesser extent, Lavino, Rio Casalecchio, Uso, and Marano (Fig. 1).

Recent studies demonstrated that climate change had a limited net role in the specific heavy rainfall event (World Weather Attribution, 2023). While heavy rainfall was the immediate cause, this event should be contextualized within broader climatic trends and regional vulnerabilities.



Figure 1. Map, exported from GIS, of the main watercourses affected by the flood of May 2023 in Emilia-Romagna.

2 DATA COLLECTION

The information collection began with selecting the river embankment sections that suffered the most critical failures (Fig. 1). During the flood, over a hundred failures were registered. Among them, about 60 breaches from both the first and second events were selected. The main criteria adopted for their identification were the severity of the damage produced, their location within the basins, and the presence of peculiar conditions, such as interference between the embankment and other structures. An extensive survey was carried out from June 2023 to December 2024. For each breach, data were systematically collected. The main pieces of information included: location of the collapsed section and photographic material; evidence of erosion processes (internal erosion, overflow erosion at the crest or toe of the embankments, etc.); evidence of slope instabilities, on both the land side and riverside; hydrograph of the flood event; time of breaching (from testimonials) and breach dimensions; morphological features of the river in the area of the breach; collection of samples for the identification of soil types constituting the embankment; type of vegetation on the embankments; other relevant information.



Figure 2. Aerial view of a breach occurred in the Lamone river (near Boncellino, Ravenna Province) during the 2023 flood event in Emilia-Romagna.

3 MAIN FINDINGS AND FUTURE DEVELOPMENTS

The data collection has provided a valuable overview, on a territorial scale, of the main breaches that occurred in May 2023 in Emilia-Romagna. Overall, the flood events generated more than 60 significant breaches, with the total number of breaches exceeding one hundred. In the observed breaches, predisposing elements were typically related to the fluvial morphology at the breach point or to the presence of structures within the embankment body, local discontinuities, peculiar geometric elements or other factors. The synthesis of the collected data is currently under development.

This study is to be considered as a preliminary collection of valuable information from dramatic and almost unique events—a sort of full-scale test of the response of an entire embankment system at a territorial level—and thus requires further integration and potential developments. In the future, the dataset could serve as a valuable tool to support flood risk assessment and decision-making processes for the implementation of long-term mitigation strategies.

ACKNOWLEDGMENTS

The authors would like to acknowledge the support of the Agency for Territorial Security and Civil Protection of the Emilia-Romagna region in the collection of the provided information.

REFERENCES

- Brath A., Casagli N., Marani M., Mercogliano P., Motta R. (2023). Rapporto della Commissione tecnico-scientifica istituita con deliberazione della Giunta Regionale n. 984/2023 e determinazione dirigenziale 14641/2023, al fine di analizzare gli eventi meteorologici estremi del mese di maggio 2023. *In Italian*
- World Weather Attribution (2023). Limited net role for climate change in heavy spring rainfall in Emilia-Romagna. *Retrieved from World Weather Attribution.*

